Summer 2023

Comparison Marker-Based and Markerless Motion Capture Systems in Gait Biomechanics During Running

Hui Tang

COMPARISON OF MARKER-BASED AND MARKERLESS MOTION CAPTURE SYSTEMS IN GAIT BIOMECHANICS DURING RUNNING

by

HUI TANG

(Under the Direction of LI LI)

ABSTRACT

Background: Markerless (ML) motion capture systems have recently become available for biomechanics applications. Evidence has indicated the potential feasibility of using an ML system to analyze lower extremity kinematics. However, no research examined ML systems' estimation of the lower extremity joint moments and powers. Objectives: This study primarily aimed to compare lower extremity joint moments and powers estimated by marker-based (MB) and ML motion capture systems during treadmill running. The secondary purpose was to investigate if movement's speed would affect the ML's performance. Methods: Sixteen volunteers ran on a treadmill for 120 s for each trial at the speed of 2.24, 2.91, and 3.58 m/s, respectively. The kinematic data were simultaneously recorded by 8 infrared cameras and 8 high-resolution video cameras. The force data were recorded via an instrumented treadmill. Results: Compared to the MB system, the ML system estimated greater increased hip and knee joint kinetics with faster speeds during the swing phase. Additionally, increased greater ankle joint moments with speed estimated by the ML system were observed at the early swing phase. In contrast, the greater ankle joint powers occurred at the initial stance phase. Conclusions: These observations indicated that inconsistent segment pose estimations (mainly the center of mass estimated by ML was farther away from the relevant distal joint center) might lead to systematic differences in joint moments and powers estimated by MB and ML systems. Despite the promising applications of the ML system in clinical settings, systematic ML overestimation requires extra attention.

INDEX WORDS: Markerless motion capture system, Gait analysis, Joint moment, Joint power, Treadmill running.

COMPARISON OF MARKER-BASED AND MARKERLESS MOTION CAPTURE SYSTEMS IN GAIT BIOMECHANICS DURING RUNNING

by

HUI TANG

B.S., Central China Normal University, P.R. China, 2015

M. Ed., Central China Normal University, P.R. China, 2019

A Thesis Submitted to the Graduate Faculty of Georgia Southern University

in Partial Fulfillment of the Requirements for the Degree

MASTER OF SCIENCE

WATER COLLEGE OF HEALTH PROFESSIONS

THIS IS AN EXAMPLE SHOWING HOW TO FORMAT THE ETD APPROVAL PAGE

by

HUI TANG

Major Professor:	Li Li
Committee:	Barry Munkasy
	Barry Joyner

Electronic Version Approved:
July 2023

DEDICATION

I dedicate this project and process to my family back in China and my mother rested in peace for their unconditional love, support, patience, encouragement, and motivation. Without their supports, I would not have had the strength to persevere and accomplish all that I have. I also would like to make a special dedication to my friend, Dr. Hang Qu. Without his influence, I would not establish interests in science, nor have the brevity to continue my academic life in the United States.

ACKNOWLEDGMENTS

I would like to thank my advisor Dr. Li Li, for his guidance, support, hard work and encouragement throughout the graduate program. I could not have wished for a better supervisor to guide me to learn biomechanics from scratch. His advice, patience, and support has contributed greatly not only to my professional development, but also to my life. The three projects I have conducted under his guidance helped me gradually fall in love with movement science. Also, due to these projects, I gained precious experience in different fields of kinesiology. Additionally, I would also like to thank my committee members, Dr. Barry Munkasy and Dr. Barry Joyner who have invested considerable time, effort and expertise to enable me to further understand this project.

I would like to thank my dearest friends, Dr. Qu Hang and Jiahao Pan. Dr. Qu has helped me to have a better understanding of the mechanisms of the equipment. Jiahao has contributed a lot to data processing. Without their help, I could not finish this without being stressed.

TABLE OF CONTENTS

Page

ACKNOWLEDGMENTS....3
LIST OF TABLES....5
LIST OF FIGURES....6
CHAPTER
1 COMPARISON OF LOWER EXTREMITY JOINT MOMENT AND JOINT POWER ESTIMATED BY MARKERLESS AND MARKER-BASED SYSTEMS DURING TREADMILL RUNNING....7
Introduction....7
Methods....9
Results....14
Discussion....23
Conclusion....28
2 RUNNING SPEED EXACERBATES LOWER EXTREMITY JOINT MOMENT AND POWER ESTIMATED BY MARKERLESS AND MARKER-BASED SYSTEM DURING TREADMILL RUNNING....32
Introduction....33
Methods....35
Results....39
Discussion....41
Conclusion....46
APPENDICES
Appendix A: EXTENDED INTRODUCTION....57
Marker-based Motion Capture Systems....58
Markerless Motion Capture Systems....62
Running Biomechanics....67
Appendix B: EXTENDED DISCUSSION....78
Pose Estimation Affect Joint Kinetics....78
Injury Prediction and Accommodation....82
Usability of ML in the Clinical Settings....87
Limitations....88
Directions for Future Research....89
Reference List....91
Appendix C: STATISTICAL ANALYSIS INFORMATION
Discrete Measurements Statistical Analysis Details....102
Spatial Parameter Mapping Statistical Analysis Details....292
Appendix D: INSTITUTIONAL REVIEW BOARD....297

LIST OF TABLES

Page

Table 1: Body mass scaled peak magnitude for joint moments and powers (3.58m/s)…………....19
Table 2: Relative Time to Peak for Joint moments and Powers……………………………………21
Table 3: Body mass scaled peak magnitude for joint moments and powers (3 speeds)....................48
Table 4: Relative Time to Peak for Joint moments and Powers..49

LIST OF FIGURES

Page

Figure 1: Illustration of critical events of the lower extremity joint moments................................13
Figure 2: Illustration of critical events of the lower extremity joint powers………......................14
Figure 3: Ensemble curve of lower extremity joint position differences.......................................17
Figure 4: Ensemble curve of lower extremity segment center of mass differences………….......18
Figure 5: Ensemble curve of lower extremity joint angle differences…..22
Figure 6: SPM analyses and ensembled curves of ankle joint kinetics under three speeds……….51
Figure 7: SPM analyses and ensembled curves of knee joint kinetics under three speeds……......52
Figure 8: SPM analyses and ensembled curves of hip joint kinetics under three speeds…………53

CHAPTER 1

COMPARSIONS OF LOWER EXTREMITY JOINT MOMENT AND POWERS ESTIMATED BY MARKERLESS AND MARKER-BASED SYSTEMS DURING TREADMILL RUNNING

Abstract: Background: Markerless (ML) motion capture systems have recently become available for biomechanics applications. Evidence has indicated the potential feasibility of using an ML system to analyze lower extremity kinematics. However, no research examined ML systems' estimation of the lower extremity joint moments and powers. This study aimed to compare lower extremity joint moments and powers estimated by marker-based (MB) and ML motion capture systems. Methods: Sixteen volunteers ran on a treadmill for 120 s at 3.58 m/s. The kinematic data were simultaneously recorded by 8 infrared cameras and 8 high-resolution video cameras. The force data were recorded via an instrumented treadmill. Results: Greater peak magnitudes for hip extension and flexion moments, knee flexion moment, and ankle plantarflexion moment, along with their joint powers, were observed in the ML system compared to an MB system ($p<0.0001$). Additionally, the ML system's estimations resulted in significantly smaller peak magnitudes for knee extension moment, along with the knee production power ($p<0.0001$). Conclusions: These observations indicate that inconsistent estimates of joint center position and segment center of mass between the two systems may cause differences in the lower extremity joint moments and powers. However, with the progression of pose estimation in the markerless system, future applications can be promising.

Keywords: Markerless motion capture system; Gait analysis; Joint moment; Joint power

1. Introduction

Inverse dynamics analysis is a fundamental tool widely used for biomechanical studies to understand human movement. The inverse dynamics method combines kinematic and kinetic data with anthropometric parameters and can estimate joint moments and powers (Winter 2009). The evaluation of joint moments and powers is critical in clinical decision-making, such as gait retraining

(Tate and Milner 2010), treatment with insoles or orthoses (Shaw, Charlton et al. 2018), and even surgery (Hart, Culvenor et al. 2016). Despite its widespread use, the inaccuracy of inverse dynamic analysis stemming from kinematic/kinetic/anthropometric data is well recognized (Riemer, Hsiao-Wecksler et al. 2008). Currently, most kinematic data are provided by marker-based (MB) motion capture systems (McLean, Walker et al. 2005). However, inaccuracies derived from marker placements, including the center of mass locations (Pearsall and Costigan 1999, Ganley and Powers 2004), joint centers (Schwartz and Rozumalski 2005), the noise due to surface marker movement (Richards 1999), and skin artifacts (Cappozzo, Catani et al. 1995, Stagni, Fantozzi et al. 2005), can be significant barriers. Using marker-based systems requires highly trained personnel (Simon 2004), intensive time commitment for marker placements, and a controlled environment (Buckley, Alcock et al. 2019), which can be challenging in some clinical settings with clinical populations (Whittle 1996).

As a critical advancement in vision-based motion capture, a markerless (ML) system offers an alternative approach to measuring kinematic data. Studies have shown the applicability of the deep learning algorithm-based markerless system in gait analysis. Kanko et al. reported excellent agreement with the MB system on spatial parameters (e.g., step length, stride width, and gait speed) and slight differences in temporal parameters (swing time and double support time) (Kanko, Laende et al. 2021). In two follow-up studies, they assessed the lower extremity joint center positions and joint angles. One study emphasized the inter-session variability of joint angles. They reported that the average inter-session variability across all joint angles was 2.8°in the ML system, which is less than all previously reported values (3.0-3.6°) for the MB system (Kanko, Laende et al. 2021). Their other study presented the average systematic root-mean-square joint center differences of 2.5 cm except for the hip joint, which was 3.6 cm. The average systematic root-mean-square for all segment angle differences was 5.5°, except for the rotation angle about the longitudinal axis (Kanko, Laende et al. 2021). These strong results are approaching or superior to the accuracy of MB systems.

However, we did not find any lower extremity joint moments and powers in comparison between the two types of systems in the literature.

Due to marker-based systems' weakness, markerless systems might introduce new possibilities for inverse dynamic analysis. Therefore, the purpose of the current study was to compare inverse dynamic outcomes of lower extremity joint moments and powers based on ML and MB motion capture systems.

2. Materials and Methods

2.1. Participants

Recreationally active young adults were recruited for the current study. Inclusion criteria were: (Hanavan) free of musculoskeletal injuries and operations of the lower extremity at least 6 months before the data collection and (2) experience with treadmill running. Participants were asked to be free from any intensive exercise within the 24 hours before data collection. Participants signed consent forms approved by the Ethics Committee of Georgia Southern University (Approval Number: H22327) before data collection.

2.2. Experimental setup and Procedure

Two camera systems were used in the motion capture procedure: 8 infrared cameras (Vicon Bonita, Oxford, UK) for the MB system to record marker trajectories; and 8 high-resolution video cameras (Vicon Vue, Oxford, UK) for the ML system to record movements. The resolutions of Bonita and Vue cameras are 1 megapixel (1024×1024) and 2.1 megapixels (1920×1080). Cameras were aimed at the instrumented treadmill (AMTI force-sensing tandem treadmill, MA, USA) within a 15.5 m long by 7.6 m wide by 2.4 m tall laboratory space. Camera systems and the instrumented treadmill were synchronized using Vicon Lock+ (Vicon, Oxford, UK), where kinematics were recorded at 100 Hz, and the ground reaction forces were recorded at 1000 Hz.

Before data collection, the cameras were calibrated using an Active Wand (V1, Oxford, UK). Calibration for the Bonita cameras of the MB system and the Vue cameras of the ML system included more than 1000 frames of valid wand data and 600 frames of valid wand data, respectively. The tolerance of image error for MB and ML systems was set as 0.2 and 0.4, respectively. The three-marker option, with an origin marker and two markers for the X- and Y-axis, was used to set the MB system's global coordinate system (GCS). An MTD-3 device and CalTester software (CalTester, Motion Lab Systems Inc., Baton Rouge, USA) were used to examine the spatial synchronization between the force plates and cameras, following the manufacturer's recommended protocol.

When participants arrived at the laboratory, each was introduced to the test protocol. Then each participant changed into tight shirts and shorts provided by the lab and wore their running shoes. The investigator measured their heights and body mass. Five-minute warm-up exercise and familiarization with treadmill running followed. Following standard VICON procedure, twenty-six 14 mm retro-reflective markers were attached to the participant's anterior superior iliac spine, posterior superior iliac spine, most lateral prominence of the greater trochanter, lateral prominence of the lateral femoral epicondyle, medial prominence of the medial femoral epicondyle, proximal tip of the head of the fibula, anterior border of the tibial tuberosity, lateral prominence of the lateral malleolus, medial prominence of the medial malleolus, dorsal margin of the first, second and fifth metatarsal head, and aspect of the Achilles tendon insertion on the calcaneus at both sides. A static trial for the MB system was recorded in advance while the participants stood on the treadmill with an anatomical posture. Each participant started walking at an initial speed of 1.12 m/s and then gradually transitioned to running at the target speed of 3.58 m/s. The participants ran on the treadmill for 120 seconds at 3.58 m/s, and the last 30 s running were recorded for further analysis.

2.3. Data analysis

2.3.1. Pre-processing

Raw marker trajectories were interpolated using Woltring gap filling (Woltring 1991) by Nexus (Vicon Nexus, Oxford, UK). Raw markerless video data were pre-processed by Theia3D (Theia3Dv2022.1.0.2309, Theia Markerless, Inc., Kingston, ON, Canada), where the default IK solution was used to estimate the 3-D pose (Kanko, Laende et al. 2021). The lower body kinematic chain has six degree-of-freedom (DOF) at the pelvis, three DOF at the hip, three DOF at the knee, and six DOF at the ankle. The kinematic and ground reaction force data were filtered through Nexus using a low-pass, zero-lag, 4-order Butterworth filter with cut-off frequencies of 10 Hz and 50 Hz (Gruber, Zhang et al. 2021), respectively.

2.3.2. Visual3D analyses

The pre-processed right lower extremity data were further analyzed using Visual3D (Preview v2022.06.02, C-Motion, Inc., Germantown, MD, USA).

The same Visual3D 6DOF algorithms and IK constraints for segments were adapted for both systems. IK constraints were set as six DOF at the pelvis, three at the hip, three at the knee, and six at the ankle. For the MB data, the human body was modeled by four linked segments (foot, leg, thigh, pelvis), in which a second kinematic-only foot was created as a virtual foot for kinematic estimations (Documentation 2020). The segment mass estimations were based on Dempster's regression equation (Dempster 1955), and inertia properties were computed based on segments as geometrical shapes (Hanavan 1964). The hip joint center was estimated using the method proposed by Bell et al. (Bell, Brand et al. 1989). Still, the knee and ankle joint centers were estimated using midpoints between external landmarks of the corresponding segment. The anatomical coordinate systems of segments were determined from the static calibration trial. The vertical axis was defined in the direction from distal to proximal joint center, while the anterior-posterior axis was defined perpendicular to the vertical axis with no mediolateral component. The third axis was the cross product of the vertical and anterior-posterior axis (Kristianslund, Krosshaug et al. 2012). The model was automatically created for the ML data based on the deep learning algorithm and segment properties such as segment mass, location of the center of mass, and joint center positions were generated accordingly (Kanko, Laende et al. 2021).

Resolved into the proximal coordinate system for both MB and ML data, joint angles and kinetic parameters in the extension/flexion plane were further calculated. The proximal segment was used as the reference when calculating joint moment and power. Internal joint moments and powers were obtained by applying Newton-Euler methods (Winter 2009, Robertson, Caldwell et al. 2013), where hip and knee extensor and ankle plantar-flexor moments were assigned to be positive. Positive power values indicated energy production through concentric muscular contractions (Winter 2009).

Force-based gait events were used to identify stride cycles, in which the force threshold was set at 50 N (Zhang, Pan et al. 2018). The stride cycle was defined as two consecutive right heel contacts. The duration of each stride cycle was scaled to 101 data points.

2.3.3. Discrete measurements

The dependent variables were extracted from the last 10 strides from both MB and ML systems. Within each stride, various positive and negative peak values (depending on joint action) in the extension/flexion plane were identified on moment and power profiles of the hip, knee, and ankle joints, and the relative times to the peak values were included. Presented in Fig.1, peak moments of the hip (top panel) were: extension moment in the early stance phase (HM1), flexion moment in the stance-swing transition phase (HM2), and extension moment at the end of the swing phase (HM3); for the knee (middle panel), extension moment in the early stance phase (KM1), and flexion moment at the end of the swing phase (KM2); for the ankle (bottom panel), extension moment in the stance phase (AM1). Presented in Fig 2., peak powers of the hip (top panel) were: absorption power in the middle of the stance phase (HP1), the production powers in the early swing phase (HP2), and at the end of the swing phase (HP3); for the knee (middle panel), absorption powers in the early stance phase (KP1), in the early swing phase (KP3), and at the end of the swing phase (KP4), and production power in the middle of the stance phase (KP2); for the ankle (bottom panel), absorption power in the early stance phase (AP1), and the production power at the end of the stance phase (AP2).

2.4. Statistical analysis

Means and standard deviations of the differences in kinematic parameters were estimated based on individual measurements between systems. All dependent variables were assessed for normality using a one-sample Kolmogorov-Smirnov test (α=0.05). Two-tailed paired t-test was used to test the differences between the two systems. The effect size was assessed using Cohen's d (Cohen 2013). An alpha level of 0.05 was used for statistical analysis. SPSS (22.0, IBM Inc.; Chicago, IL, USA) was used to conduct all statistical analyses. The alpha level was adjusted by 30 dependent variables using the Bonferroni correction to reduce the chances of type I error ($\alpha = 0.05/30 = 0.0017$).

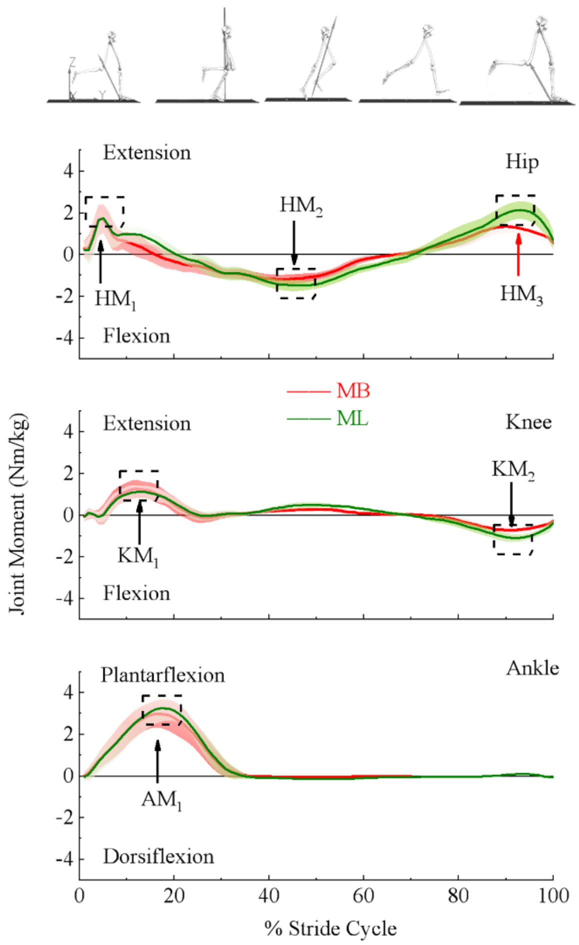

Figure 1. Illustration of critical events of the lower extremity joint moments of the hip (top panel), knee (middle panel), and ankle (bottom panel) (denoted under the ensemble moment curve measured by marker-based (MB) (red) and markerless (ML) (green) motion capture systems. Joint moments were normalized to participants' body mass.

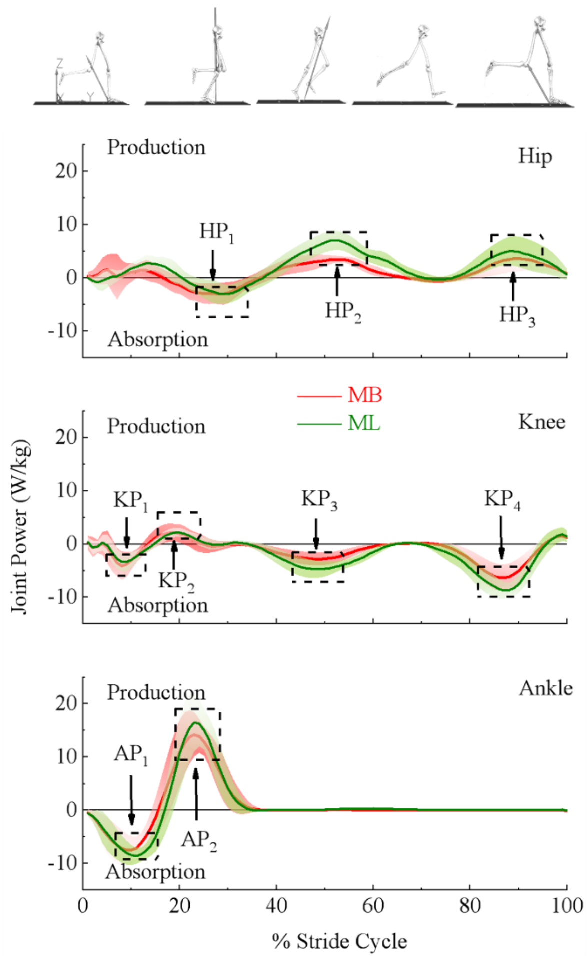

Figure 2. Illustration of critical events of the lower extremity joint powers of the hip (top panel), knee (middle panel), and ankle (bottom panel) (denoted under the ensemble power curve measured by marker-based (MB) (red) and markerless (ML) (green) motion capture systems). Joint powers were normalized to participants' body mass.

3. Results

Sixteen participants (9 males and 7 females) participated. The participants' ages, body mass, and height were 23.44±2.31 years, 69.72±9.82 kg, and 1.73±0.08 m, respectively.

3.1. Lower extremity joint moments and powers

Ensemble curves of lower extremity extension/flexion plane moments and powers estimated using MB and ML are presented in Figs. 1 and 2, respectively. Scaled (by body mass) peak magnitudes and relative timing to the peak are presented in Tables 1 and 2, respectively.

Compared to the MB system, the ML system showed significantly greater peak joint moment magnitudes at HM_2 (ML: -1.73±0.27, MB: -1.38±0.29), HM_3 (ML: 2.27±0.45, MB: 1.42±0.29), KM_2 (ML: -1.17±0.24, MB: -0.74±0.13), and AM_1 (ML: 3.32±0.55, MB: 3.14±0.51), but less peak magnitude at KM_1 (ML: 1.28±0.32, MB: 1.40±0.42). For the joint powers, significantly less peak magnitudes were at KP_1 (ML: -4.05±1.79, MB: -5.0±2.77), KP_2 (ML: 2.64±1.09, MB: 3.15±1.41), but greater at HP_2 (ML: 8.07±2.11, MB: 4.29±1.14), HP_3 (ML: 5.68±2.71, MB: 3.99±2.13), KP_3 (ML: -5.42±1.61, MB: -3.45±1.29), KP_4 (ML: -9.65±2.10, MB: -7.15±1.83), AP_1 (ML: -9.44±1.81, MB:-8.38±2.48), as well as AP_2 (ML: 18.40±4.91, MB: 16.07±3.60). In addition, the relative timing to the peak was detected to be significantly different between the MB and ML systems. To be specific, ML system took longer than the MB system to reach the HM_1 (ML: 6.74±3.40, MB: 5.16±1.27), HM_2 (ML: 43.59±7.00, MB: 40.26±6.90), HM_3 (ML: 92.73±3.00, MB: 90.58±3.39), KM_1 (ML: 13.53±3.89, MB: 12.98±2.18), KM_2 (ML: 92.19±2.51, MB: 90.93±2.21), HP_1 (ML: 28.30±3.68, MB: 26.16±4.45), and KP_1 (ML: 8.73±3.01, MB: 8.19±2.21). Besides, the ML system took less time than the MB system to reach the HP_3 (ML: 89.63±4.15, MB: 91.23±3.47). See Tables 1 and 2 for more details.

3.2. Lower extremity joint center and segment center of mass

Joint moments could be significantly affected by joint center position and segment center of mass. Figs 3 and 4 demonstrated the ensemble curves of differences in joint center positions (hip, knee, ankle) and segment center of mass (thigh, leg, foot) between MB and ML.

In the mediolateral direction (Fig. 3 top panel), the ankle (left) and knee (middle) joints center were biased toward the lateral direction in the ML than the MB throughout the stride cycle. The hip joint center showed the same trend except during initial contact and the late swing phase. In the anterior-posterior direction (Fig 3 middle panel), ML showed a posterior biased hip joint center during the stride cycle, whereas the ankle and knee joint centers varied within the stride cycle. The ML was posteriorly biased compared to the MB at initial contact for both ankle and knee joints. For the rest of the stance phase, the ML for the ankle joint was slightly more posterior, and the knee was more anterior. While the ML for the ankle joint continued in the posterior direction in the swing phase, the ML knee continued in the anterior direction in the early swing phase but turned to the posterior direction for the rest of the swing phase. In the vertical direction (Fig.3 bottom panel), the ML of the ankle varied during the stride cycle. In the early stance and mid-swing phase, the estimated bias was toward the superior direction, while in the mid-stance and early swing, it turned to the inferior direction. The ML showed inferior biased knee and hip joint center in the early stance. When the ML knee joint turned to the superior direction for the rest of the stride cycle, the hip joint showed superior in the mid-stance and early swing phase but toward the inferior direction in the rest of the swing phase. See figure 3 for more details.

In the mediolateral direction (Fig. 4 top panel), the center of mass of the foot, leg, and thigh was more lateral in the ML than in the MB systems throughout the stride cycle. In the anterior-posterior direction (Fig. 4 middle panel), the foot center of mass was more anterior in the ML than in the MB system during the stride cycle. For the leg center of mass, ML showed posterior biases than MB during the stance and swing phases except in different directions at the end of the swing phase. The thigh center of mass was mainly posterior throughout the stride cycle but briefly anterior in the swing-stance transition phase. In the vertical direction, the foot center of mass showed a higher position in the ML than in the MB system during most stance and late swing phases but lower during the stance-swing transition and early swing phase. For the leg center of mass, the ML demonstrated lower than the MB system during about 85% of the stride cycle but briefly higher during the early swing phase. The thigh center of mass from the ML showed a higher position than the MB system over the whole stride cycle.

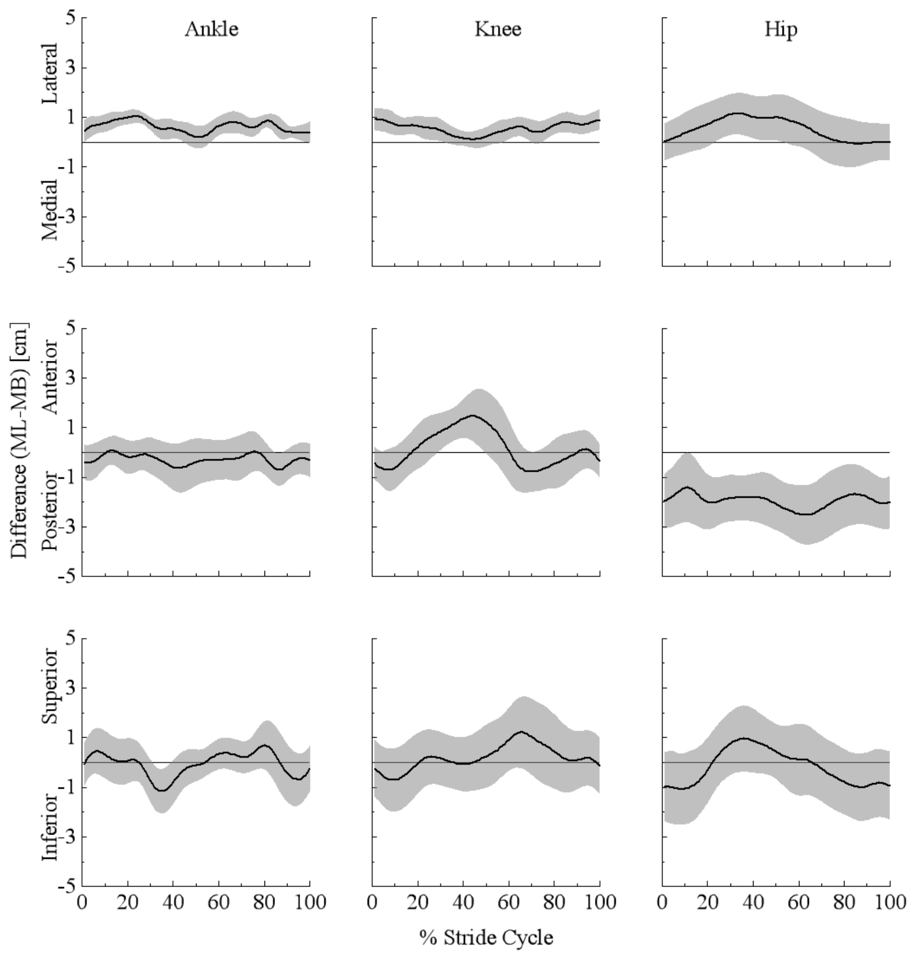

Figure 3. Ensemble curve of lower extremity joint position differences between marker-based and markerless motion capture systems across the average 10 stride cycles for 16 participants. Differences were estimated as markerless (ML) joint position – marker-based joint (MB) position.

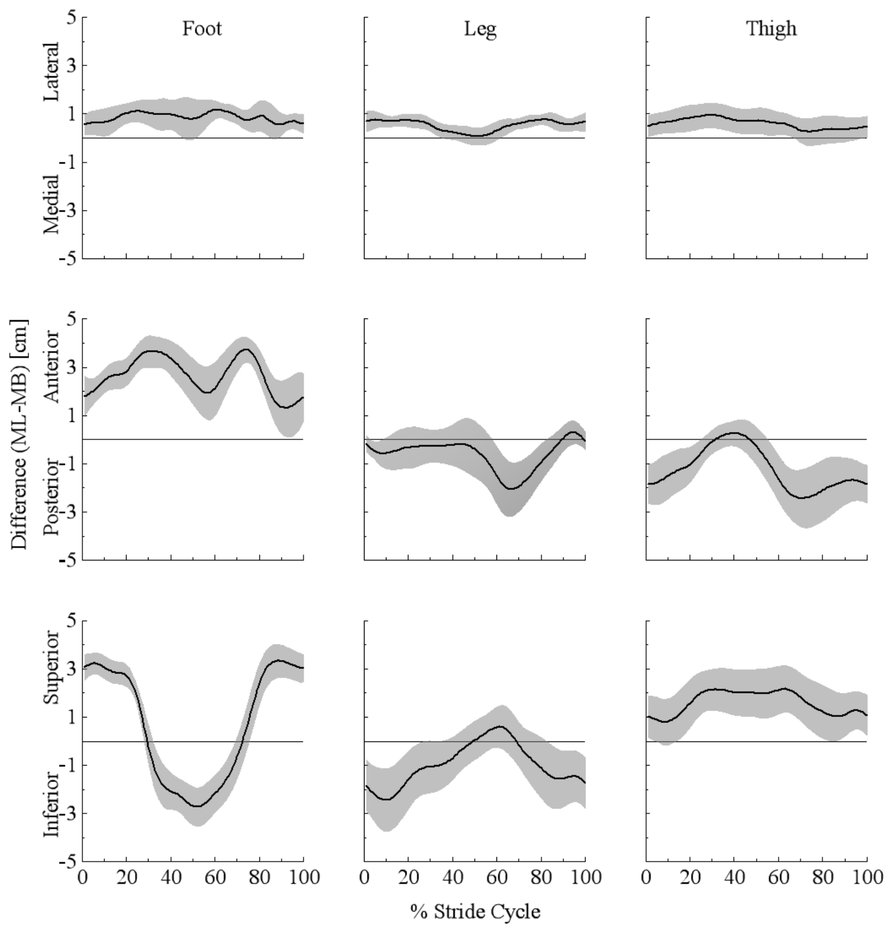

Figure 4. Ensemble curve of lower extremity segment center of mass differences between marker-based and markerless motion capture systems across the average 10 stride cycles for 16 participants. Differences were estimated as markerless (ML) center of mass position – marker-based (MB) center of mass position.

Table 1. Body mass scaled peak magnitude (Mean, SD) for joint moments and powers for the marker-based (MB) and Markerless (ML) systems.

	Parameters	MB		ML		T & P-value	Cohen's d
		Mean	SD	Mean	SD		
Moment (Nm/kg)	Hip first peak	2.09	0.66	2.05	0.73	t_{159}= -1.42, p< 0.2832	0.1
	Hip second peak	*-1.38*	*0.23*	*-1.73*	*0.27*	*t_{159}= -22.99, p< 0.0001**	*1.8*
	Hip third peak	1.42	0.29	2.27	0.45	t_{159}= 39.612, p< 0.0001	3.1
	Knee first peak	**1.40**	**0.42**	**1.28**	**0.32**	**t_{159}= 5.907, p< 0.0001***	**0.5**
	Knee second peak	-0.74	0.13	-1.17	0.24	t_{159}= 40.804, p< 0.0001*	3.2
	Ankle first peak	**3.14**	**0.51**	**3.32**	**0.55**	**t_{159}= 10.450, p< 0.0001***	**0.8**
Power (W/kg)	**Hip first peak**	**-5.02**	**2.60**	**-4.80**	**2.37**	**t_{159}= -1.570, p= 0.118**	**0.1**
	Hip second peak	4.29	1.14	8.07	2.11	t_{159}= -27.082, p< 0.0001*	2.1
	Hip third peak	3.99	2.13	5.68	2.71	t_{159}= -13.049, p< 0.0001*	1.0
	Knee first peak	**-5.00**	**2.77**	**-4.08**	**1.79**	**t_{159}= -6.138, p= 0.0229**	**0.5**
	Knee second peak	**3.15**	**1.41**	**2.64**	**1.09**	**t_{159}= 6.628, p< 0.0001***	**0.5**
	Knee third peak	-3.45	1.29	-5.42	1.61	t_{159}= 21.188, p< 0.0001*	1.7
	Knee forth peak	-7.15	1.83	-9.65	2.10	t_{159}= 31.515, p< 0.0001*	2.5

	Ankle first peak	**-8.38**	**2.48**	**-9.44**	**1.81**	**t_{159}= 7.295, p= 0.6656**	**0.6**
	Ankle second peak	**16.07**	**3.60**	**18.40**	**4.91**	**t_{159}= -10.726, p= 0.2426**	**0.9**

*Indicate significant difference; **Bold** indicates the event was observed within the stance phase; *italic with underline* indicates the event was observed during the stance-swing transition; rest of the parameters were observed within the swing phase. For joint moment data, "+" represents the extension (ankle plantar flexion) and "-" represents the flexion (ankle dorsiflexion). For joint power data, "+" represents energy production, and "-" represents energy absorption.

Table 2. Relative Time to Peak as %Stride Cycle (Mean, SD) for Joint Moments and Powers for Marker-based (MB) and Markerless (ML) Systems.

	Parameters	MB		ML		T & P-value	Cohen's d
		Mean	SD	Mean	SD		
Moment (%stride Cycle)	**Hip first peak**	**5.16**	**1.27**	**6.74**	**3.40**	**t_{159}= -5.946, p< 0.0001***	**0.5**
	Hip second peak	*40.26*	*6.90*	*43.59*	*7.00*	*t_{159}= -7.179, p < 0.0001**	*0.6*
	Hip third peak	90.58	3.39	92.73	3.00	t_{159}= -8.637, p < 0.0001*	0.7
	Knee first peak	**12.98**	**2.18**	**13.53**	**3.89**	**t_{159}= -2.008, p= 0.0015***	**0.2**
	Knee second peak	90.93	2.21	92.19	2.51	t_{159}= -10.031, p < 0.0001*	0.8
	Ankle first peak	**18.29**	**1.90**	**18.33**	**1.82**	**t_{159}= -.569, p= 0.57**	**0.0**
Power (%Stride Cycle)	**Hip first peak**	**26.61**	**4.45**	**28.30**	**3.68**	**t_{159}= -6.983, p < 0.0001***	**0.6**
	Hip second peak	51.89	3.90	52.36	4.37	t_{159}= -1.243, p= 0.216	0.1
	Hip third peak	91.23	3.47	89.63	4.15	t_{159}= 4.458, p < 0.0001*	0.4
	Knee first peak	**8.19**	**2.21**	**8.73**	**3.01**	**t_{159}= -2.380, p= 0.0006***	**0.2**
	Knee second peak	**19.45**	**3.09**	**21.17**	**3.51**	**t_{159}= -6.606, p < 0.0001***	**0.5**
	Knee third peak	49.31	2.77	49.06	3.30	t_{159}= .860, p= 0.391	0.1
	Knee forth peak	86.59	2.18	86.83	2.31	t_{159}= -1.740, p= 0.084	0.1
	Ankle first peak	**10.58**	**2.20**	**10.82**	**2.22**	**t_{159}= -1.794, p= 0.075**	**0.6**
	Ankle second peak	**24.10**	**2.32**	**24.21**	**2.08**	**t_{159}= -.943, p= 0.347**	**0.1**

*Indicate significant difference; **Bold** indicates the event was observed within the stance phase; *italic with underline* indicates the event was observed during the stance-swing transition; rest of the parameters were observed within the swing phase.

3.3. Lower extremity joint angles

Ensemble curves of the difference in lower extremity joint angles (hip, knee, ankle joints) in the extension/flexion plane between the systems are illustrated in Fig. 5.

The hip (top panel) and knee (middle panel) joint angles were biased toward the extension in the ML than MB throughout the stride cycle except briefly for the early swing phase for the hip joint, and early stance phase for the knee joint, respectively. On the other hand, ML showed a dorsiflexion-biased ankle joint angle (bottom panel) throughout the stride cycle.

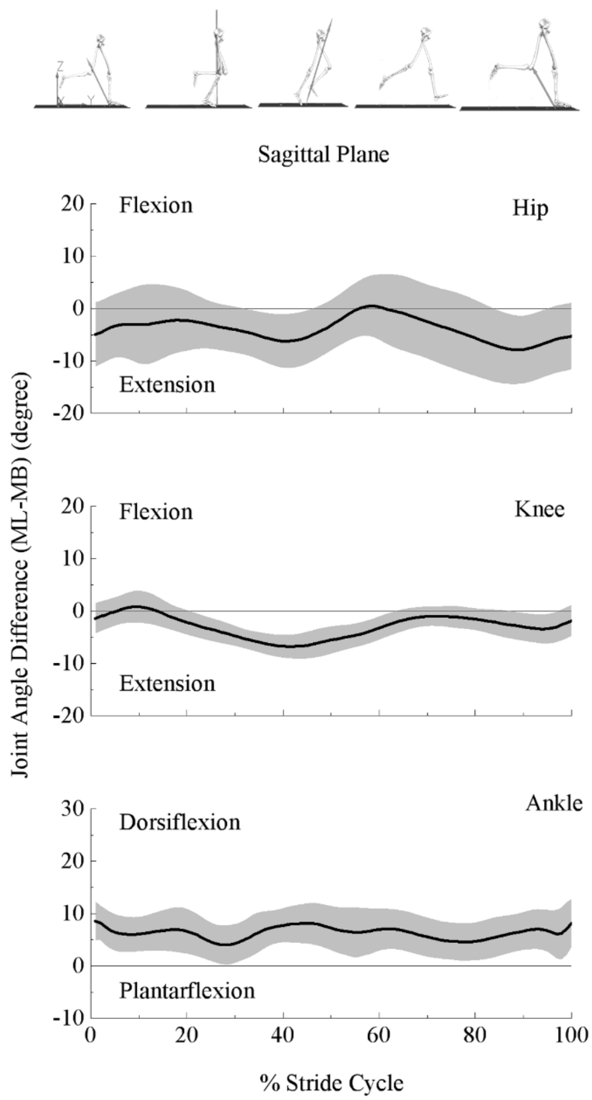

Figure 5. Ensemble curve of lower extremity joint angle differences in the flexion/extension plane between marker-based (MB) and markerless (ML) motion capture systems across the average 10 stride cycles for 16 participants. Differences were estimated as ML joint angles of each joint– MB joint angles of each joint.

4. Discussion

This study compared MB and ML systems estimated lower extremity joint moments and powers during treadmill running. Significant differences were detected in the peak magnitudes for joint moments and powers and relative timings to peak estimated by the two systems. Greater peak magnitudes for hip extension and flexion moments, knee flexion moments, and ankle plantarflexion moments, along with their joint powers, were observed in the ML system. Meanwhile, significantly smaller peak magnitudes for knee extension moments coincide with knee production power were observed.

We focused on the extension/flexion plane's joint angles, moments, and powers since running is primarily a extension/flexion plane movement (Dugan and Bhat 2005). We observed greater hip and knee flexion angles and smaller ankle dorsiflexion angles in the MB system than in the ML system. The tendency was partly consistent with Kanko et al.'s study (Kanko, Laende et al. 2021), showing that the MB system's estimation resulted in greater flexion in all three joints. One possible explanation may be the model of the virtual foot. Visual3D introduces three methods to build the virtual foot, which may affect the ankle joint angles. When we chose the heel and toe targets to define the proximal and distal ends of the foot, there was no disclosure for Kanko et al.'s foot model. Different from Kanko et al.'s results, we observed larger magnitudes of systematic differences in the knee and ankle joint angles but smaller magnitudes in the hip joint. Compared to walking in Kanko et al., running in the current project is related to greater lower extremity joint motion (Novacheck 1998). With greater joint motion, soft tissue artifacts can also be larger, leading to an additional 3° error in the joint angles. Also, inconsistent marker placement can contribute to a 5° error in the joint angles (Schwartz, Trost et al. 2004, Gorton, Hebert et al. 2009).

Compared to the MB system, the ML system's estimation resulted in greater magnitudes of peak hip flexion (MB: -1.38 vs. ML: -1.73 Nm/kg) moment in the stance-swing transition phase and extension (MB: 1.42 vs. ML: 2.27 Nm/kg) moment in the late swing phase, knee flexion moment (MB: -0.74 vs. ML: -1.17 nm/kg) in the late swing phase, and ankle plantarflexion moments (MB: 3.32 vs. ML: 3.16 Nm/kg) in the early stance phase, but smaller knee extension moments (MB: 1.40 vs. ML: 1.28 Nm/kg) in the early stance phase. Previous studies presented similar patterns of lower extremity joint moments during running estimated by MB systems. Schache et al. (2011) and Fukuchi et al. (2017) reported lower extremity joint moments at the speed of 3.5 m/s during overground and treadmill running, respectively (Schache, Blanch et al. 2011, Fukuchi, Fukuchi et al. 2017). Their results showed similar peak magnitudes of hip flexion and extension moments of -1.09 and 0.91 Nm/kg (overground) and -1.15 and 1.37 Nm/kg (treadmill); knee flexion moments of -0.53 Nm/kg (overground); as well as the ankle plantarflexion moment with the value of 2.94 Nm/kg (overground) and 2.23 Nm/kg (treadmill). Besides, they reported similar knee extension moments with the values of 3.12 Nm/kg (overground) and 3.18 Nm/kg (treadmill). Consequently, joint powers also showed the same tendency. Despite the differences between overground and treadmill running, Schache et al.'s results revealed similar systematic differences in the present study. Compared to the MB system, the estimations from the ML system may result in greater hip moments and powers in the stance-swing transition and swing phase, knee moments and powers in the swing phase, as well as the ankle moment in the early stance phase, but less in the knee moment and power in the early stance phase.

The anthropometric model affects the results of the joint moments and powers. Once rigid body equations are set, the joint centers and moment of inertia about the center of mass eventually govern the relationships between kinetics and kinematics (Derrick, van den Bogert et al. 2020). The systematic differences can be further explained by the variations of joint centers and segment mass centers.

It has been well recognized that differences in hip joint center location can propagate to hip and knee kinematic and kinetic quantities, especially the hip moments concerning flexion/extension

(Stagni, Leardini et al. 2000). Besides, the propagation of flexion/extension moments is particularly sensitive to the anteroposterior hip joint center location. We observed that hip joint centers in the ML system were about 2 cm posterior to the MB system in the stance-swing transition and late swing phase. In addition, the sensitivity of hip moments to inertial properties variations can be up to 40% (Pearsall and Costigan 1999). Supported by our results, the thigh center of mass locations was about 2 cm superior in the ML than the MB system in the stance-swing transition phase. Similar to a previous study, greater changes occurred in the swing phase (Pearsall and Costigan 1999), and the ML system showed a biased posterior (about 2 cm) and anterior (about 1 cm) center of mass. For the knee joint, joint moments are sensitive to the differences in knee joint center locations (Holden and Stanhope 1998). Previous studies have reported that tibia surface movements affected the knee joint center by 1.1 cm and resulted in the most prominent joint moment in the stance phase (Holden and Stanhope 1998). Our results exhibited that knee joint centers differed around 1 cm in all directions and greater disparities in the leg center of mass in the early stance phase, which may explain the greater knee extension moment in the MB system. Moreover, our results exhibited a greater leg center of mass in the late swing phase, which may induce greater knee flexion moments. For the ankle joint, we observed less than 1 cm differences in all three directions. Previous studies indicated that average ankle joint position differences were less than 1 cm in the anteroposterior and mediolateral direction and around 2 cm in the vertical direction (Kanko, Laende et al. 2021). Plus, the foot center of mass locations varied greatly. The ML system showed slightly biased in the lateral direction (<1 cm) with greater bias in the anterior and superior directions (almost 3 cm). Such difference may be induced by the marker placements of the first and fifth metatarsal heads. While the MB system reads the markers on the side of the first and fifth metatarsal heads, the markerless system might locate the foot center of mass based on the contour of the shoe. The different joint centers could affect moment arms, and the segment center of mass could affect the estimation of the moment of inertia. Together, they could lead to greater differences in the joint moments and powers.

The methodology differences between ML and MB systems that determine the estimation of poses (body segment positions and orientations) need further attention. The present study has guaranteed consistency in the computational algorithms for segments and inverse dynamic solutions for both systems in the Visual3D. However, the MB system depends heavily on physical marker placements over external/internal anatomical landmarks (hardware), and the ML system relies on deep learning-based algorithms to estimate joint center locations (software). The deep learning pose estimation algorithms learn to identify joint centers from the training data. ML in the current study includes over 500,000 manually labeled digital images of human body and employs biomechanically applicable training data that can identify 51 salient features of human body (Kanko, Laende et al. 2021, Kanko, Laende et al. 2021, Kanko, Laende et al. 2021). The optimization methods examined the distance between the manually labeled training data and the estimated joint centers to reduce errors. This process is repeated with the entire training data until improvements between each iteration become negligible. The pose estimation algorithm is then tested on the new image and compared to the training dataset (Wade, Needham et al. 2022). However, any omissions or biases implicit within training datasets could propagate to situations where the training was weak [19]. Note that the inverse dynamic method is very sensitive to joint center locations because the estimation of the net joint moments includes the cross product of forces and their moment arms, where the length of moment arms is largely affected by joint center locations [37]. A previous marker-based study has reported that 2 cm superior and 2 cm lateral placement of the hip joint center can decrease the moment of arms of the hip joint by about 28% [38]. Supported by our results, systematic differences in joint center positions have been observed, which might affect moment arms and lead to disparities in joint moments and powers. However, it remains unclear if the differences are caused by marker-based joint center errors induced by soft tissue artifacts (Cappozzo, Catani et al. 1995) or propagations from a weak training dataset.

While the ML system may still be considered in its infancy, evidence from previous studies demonstrated its potential for clinical applications. Since pose estimation algorithms are not dependent on markers attached to the skin, soft tissue artifact errors can be eliminated (Reinschmidt, van den Bogert et al. 1997), making human errors possible. Studies also presented that the markerless system can extract new information from old datasets (Kidziński, Yang et al. 2020, Shin, Yu et al. 2021). Therefore, the ML system can be beneficial in the streamlined monitoring of changes in disease progression (Kidziński, Yang et al. 2020), rehabilitation (Cronin, Rantalainen et al. 2019), athletic training, and competitive sports (Evans, Colyer et al. 2018). In addition, the Theia3D markerless system has shown strong results in the inter-session joint angles variability during walking with loose clothing conditions (Kanko, Laende et al. 2021). More importantly, data collection can be completed much shorter than the MB systems (Kanko, Laende et al. 2021). Such benefits could facilitate data collection in a more convenient area with less effect on people's gait (Robles-García, Corral-Bergantiños et al. 2015), when time is limited, and wearing more comfortable clothing.

However, the differences observed here could have significant implications. For example, previous studies have shown that the values of hip extension and knee flexion moments in the initial stance and late swing phase were important factors in discussing hamstrings injuries during sprinting (Liu, Garrett et al. 2012, Sun, Wei et al. 2015). The greater hip extension and knee flexion moments observed in the late swing with the ML system could impact the hamstring injury-related discussions. Like hamstrings, the biarticular rectus femoris plays an important role in the energy transfer between the hip and knee joints. Greater rectus femoris stress is associated with greater hip flexion and knee extension moments. We have observed, with the ML in comparison with the MB system, greater hip flexion moment in the stance to swing transition phase, greater hip power absorption in the late stance phase, and greater hip joint power production in the early swing phase, which could lead to a greater rectus femoris contraction estimation during the stance-swing transition. A previous study showed that greater rectus femoris contraction could lead to greater patellar tendon tension, a risk factor for patellofemoral pain during running (Lenhart, Thelen et al. 2014). Thus, joint moment/power estimated by the ML system can lead to different assessments for the risk factors of hamstring injuries, patellofemoral pain, and maybe other relevant discussions compared to the MB system. With different risk factor analyses based on the MB or ML systems, clinicians, coaches, and athletes could lead to different decisions in their practices.

The following limitations of the current work should be noted. First, our participants' pool was limited to recreationally active young adults. Different population groups may have anatomical deformities, affecting the comparison between the systems. Second, we analyzed treadmill running, where the treadmill settings may constrain the speed. Additionally, the hardware and the marker placements are unique to each lab. Despite our updated VICON high-resolution video cameras employed for markerless data, the Vicon Bonita series infrared cameras used here do not provide us with the highest resolution available on the market. Lower camera resolution may cause trajectory errors in the identifications of landmarks (Zago, Luzzago et al. 2020). Therefore, future studies should attempt to replicate the results in different populations using different speeds and hardware settings.

5. Conclusions

This study is the first to compare the inverse dynamic outcomes of lower extremity kinetics estimated by the marker-based and markerless systems. We have observed differences in joint moments and powers between the two systems, which could be partially related to the estimations of joint centers and segment center of mass (pose estimations). Although the accuracy and precision of pose estimations between the two systems require further testing, the strengths of the markerless system are apparent. The significantly less data collection and processing time contribute greatly to a more versatile application. With the progression of pose estimation software, the markerless system can be further employed in clinical biomechanics and sports medicine.

References:

Winter, D.A., Biomechanics and motor control of human movement. 2009: John Wiley & Sons.

Tate, J.J. and C.E. Milner, Real-Time Kinematic, Temporospatial, and Kinetic Biofeedback During Gait Retraining in Patients: A Systematic Review. Physical Therapy, 2010. 90(8): p. 1123-1134.

Shaw, K.E., et al., The effects of shoe-worn insoles on gait biomechanics in people with knee osteoarthritis: a systematic review and meta-analysis. British Journal of Sports Medicine, 2018. 52(4): p. 238.

Hart, H.F., et al., Knee kinematics and joint moments during gait following anterior cruciate ligament reconstruction: a systematic review and meta-analysis. British Journal of Sports Medicine, 2016. 50(10): p. 597.

Riemer, R., E.T. Hsiao-Wecksler, and X. Zhang, Uncertainties in inverse dynamics solutions: A comprehensive analysis and an application to gait. Gait & Posture, 2008. 27(4): p. 578-588.

McLean, S.G., et al., Evaluation of a two dimensional analysis method as a screening and evaluation tool for anterior cruciate ligament injury. British Journal of Sports Medicine, 2005. 39(6): p. 355.

Pearsall, D.J. and P.A. Costigan, The effect of segment parameter error on gait analysis results. Gait & Posture, 1999. 9(3): p. 173-183.

Ganley, K.J. and C.M. Powers, Determination of lower extremity anthropometric parameters using dual energy X-ray absorptiometry: the influence on net joint moments during gait. Clinical Biomechanics, 2004. 19(1): p. 50-56.

Schwartz, M.H. and A. Rozumalski, A new method for estimating joint parameters from motion data. Journal of Biomechanics, 2005. 38(1): p. 107-116.

Richards, J.G., The measurement of human motion: A comparison of commercially available systems. Human Movement Science, 1999. 18(5): p. 589-602.

Cappozzo, A., et al., Position and orientation in space of bones during movement: anatomical frame definition and determination. Clinical Biomechanics, 1995. 10(4): p. 171-178.

Stagni, R., et al., Quantification of soft tissue artefact in motion analysis by combining 3D fluoroscopy and stereophotogrammetry: a study on two subjects. Clinical Biomechanics, 2005. 20(3): p. 320-329.

Simon, S.R., Quantification of human motion: gait analysis—benefits and limitations to its application to clinical problems. Journal of Biomechanics, 2004. 37(12): p. 1869-1880.

Buckley, C., et al., The Role of Movement Analysis in Diagnosing and Monitoring Neurodegenerative Conditions: Insights from Gait and Postural Control. Brain Sciences, 2019. 9(2).

Whittle, M.W., Clinical gait analysis: A review. Human Movement Science, 1996. 15(3): p. 369-387.

Kanko, R.M., et al., Assessment of spatiotemporal gait parameters using a deep learning algorithm-based markerless motion capture system. Journal of Biomechanics, 2021. 122: p. 110414.

Kanko, R.M., et al., Inter-session repeatability of markerless motion capture gait kinematics. Journal of Biomechanics, 2021. 121: p. 110422.

Kanko, R.M., et al., Concurrent assessment of gait kinematics using marker-based and markerless motion capture. Journal of Biomechanics, 2021. 127: p. 110665.

Hanavan, E.P., A Mathematical Model of the Human Body. AMRL Technical Report, 1964: p. 64-102.

Woltring, H.J., Representation and calculation of 3-D joint movement. Human Movement Science, 1991. 10(5): p. 603-616.

Gruber, A.H., et al., Leg and Joint Stiffness Adaptations to Minimalist and Maximalist Running Shoes. Journal of Applied Biomechanics, 2021. 37(5): p. 408-414.

Documentation, C.-M.W., Tutorial: Foot and Ankle Angles. 2020.

Dempster, W.T., Space requirements of the seated operator, geometrical, kinematic, and mechanical aspects of the body with special reference to the limbs. 1955, Michigan State Univ East Lansing.
Bell, A.L., R.A. Brand, and D.R. Pedersen, Prediction of hip joint centre location from external landmarks. Human Movement Science, 1989. 8(1): p. 3-16.
Kristianslund, E., T. Krosshaug, and A.J. van den Bogert, Effect of low pass filtering on joint moments from inverse dynamics: Implications for injury prevention. Journal of Biomechanics, 2012. 45(4): p. 666-671.
Robertson, D.G.E., et al., Research methods in biomechanics. 2013: Human kinetics.
Zhang, S., J. Pan, and L. Li, Non-linear changes of lower extremity kinetics prior to gait transition. Journal of Biomechanics, 2018. 77: p. 48-54.
Cohen, J., Statistical power analysis for the behavioral sciences. 2013: Routledge.
Dugan, S.A. and K.P. Bhat, Biomechanics and Analysis of Running Gait. Physical Medicine and Rehabilitation Clinics, 2005. 16(3): p. 603-621.
Novacheck, T.F., The biomechanics of running. Gait & Posture, 1998. 7(1): p. 77-95.
Gorton, G.E., D.A. Hebert, and M.E. Gannotti, Assessment of the kinematic variability among 12 motion analysis laboratories. Gait & Posture, 2009. 29(3): p. 398-402.
Schwartz, M.H., J.P. Trost, and R.A. Wervey, Measurement and management of errors in quantitative gait data. Gait & Posture, 2004. 20(2): p. 196-203.
Fukuchi, R.K., C.A. Fukuchi, and M. Duarte, A public dataset of running biomechanics and the effects of running speed on lower extremity kinematics and kinetics. PeerJ, 2017. 5: p. e3298.
Schache, A.G., et al., Effect of running speed on lower limb joint kinetics. 2011. 43(7): p. 1260-1271.
Derrick, T.R., et al., ISB recommendations on the reporting of intersegmental forces and moments during human motion analysis. Journal of Biomechanics, 2020. 99: p. 109533.
Stagni, R., et al., Effects of hip joint centre mislocation on gait analysis results. Journal of Biomechanics, 2000. 33(11): p. 1479-1487.
Holden, J.P. and S.J. Stanhope, The effect of variation in knee center location estimates on net knee joint moments. Gait & Posture, 1998. 7(1): p. 1-6.
Wade, L., et al., Applications and limitations of current markerless motion capture methods for clinical gait biomechanics. PeerJ, 2022. 10: p. e12995.
Reinschmidt, C., et al., Effect of skin movement on the analysis of skeletal knee joint motion during running. Journal of Biomechanics, 1997. 30(7): p. 729-732.
Shin, J.H., et al., Quantitative Gait Analysis Using a Pose-Estimation Algorithm with a Single 2D-Video of Parkinson’s Disease Patients. Journal of Parkinson's Disease, 2021. 11: p. 1271-1283.
Kidziński, Ł., et al., Deep neural networks enable quantitative movement analysis using single-camera videos. Nature Communications, 2020. 11(1): p. 4054.
Cronin, N.J., et al., Markerless 2D kinematic analysis of underwater running: A deep learning approach. Journal of Biomechanics, 2019. 87: p. 75-82.
Evans, M., et al. Foot Contact Timings and Step Length for Sprint Training. in 2018 IEEE Winter Conference on Applications of Computer Vision (WACV). 2018.
Robles-García, V., et al., Spatiotemporal Gait Patterns During Overt and Covert Evaluation in Patients With Parkinson’s Disease and Healthy Subjects: Is There a Hawthorne Effect? Journal of Applied Biomechanics, 2015. 31(3): p. 189-194.
Liu, H., et al., Injury rate, mechanism, and risk factors of hamstring strain injuries in sports: A review of the literature. Journal of Sport and Health Science, 2012. 1(2): p. 92-101.
Sun, Y., et al., How joint torques affect hamstring injury risk in sprinting swing-stance transition. Medicine and science in sports and exercise, 2015. 47(2): p. 373-380.
Lenhart, R.L., et al., Increasing running step rate reduces patellofemoral joint forces. Medicine and science in sports and exercise, 2014. 46(3): p. 557-564.

Zago, M., et al., 3D tracking of human motion using visual skeletonization and stereoscopic vision. Frontiers in bioengineering and biotechnology, 2020. 8: p. 181.

CHAPTER 2

RUNNING SPEED EXACERBATES LOWER EXTREMITY JOINT MOMENT AND POWER ESTIMATED BY MARKERLESS AND MARKER-BASED SYSTEM DURING TREADMILL RUNNING

Abstract

The development of computer vision technology has enabled the use of Markerless (ML) movement tracking for biomechanical analysis. Recent research has reported the reliability of ML in motion analysis but has not yet further explored the clinical potential and limitations. The purpose of this study was to investigate the effects of speed on the comparison of estimated lower extremity joint moments and powers between ML and marker-based (MB) technologies during treadmill running. Kinematic data of both MB/ML and ground reaction force data were collected from 16 recreational young adults running on an instrumented treadmill for 120 s at three speeds: 2.24 m/s, 2.91 m/s, and 3.58 m/s. Three-dimensional moments and powers of the hip, knee, and ankle were calculated. Compared to the MB, ML estimated greater increased hip and knee joint kinetics with faster speeds during the swing. Additionally, increased greater ankle joint moments with increased speeds estimated by ML were observed during early swing. In contrast, greater ankle joint power occurred during the initial stance. Despite the promising application of ML technology in clinical settings, systematic ML overestimation requires extra attention. These observations may indicate that inconsistent segment pose estimations (mainly the center of mass estimated by ML being farther away from the relevant distal joint center) might lead to systematic differences in joint moments and powers estimated by MB versus ML.

Keywords: running speed, joint moment, joint power, Spatial Parameter Mapping.

1. Introduction

Human motion analysis plays an important role in clinical biomechanics and sports medicine for identifying, preventing and rehabilitating diseases, disabilities, and injuries (Wade, Needham, McGuigan, & Bilzon, 2022). The most frequently used biomechanical tool for three-dimensional motion analysis is the marker-based motion capture system (MB) (Mündermann, Corazza, & Andriacchi, 2006). Despite MB receiving high validity and repeatability (Collins, Ghoussayni, Ewins, & Kent, 2009), limitations including skin artifacts (Cappozzo, Catani, Della Croce, & Leardini, 1995; Fuller, Liu, Murphy, & Mann, 1997), controlled environment, human errors, and time-intensive have been summarized as shortfalls (Cappozzo, Della Croce, Leardini, & Chiari, 2005; Chiari, Croce, Leardini, & Cappozzo, 2005; Leardini, Chiari, Croce, & Cappozzo, 2005). Markerless motion capture systems (ML) that use standard video and often leverage deep-learning-based software have been slowly applied in biomechanics (Tang, Pan, Munkasy, Duffy, & Li, 2022). ML offers an attractive solution to problems associated with MB.

Supporting evidence has shown the feasibility of ML for gait analysis. For example, Kanko et al. (2021c) have concurrently compared the gait kinematics from MB/ML during treadmill walking. They reported that the average root mean square distance between corresponding lower extremity joint centers was less than 2.5 cm, except for the hip joint (3.6 cm). Differences of lower extremity joint angles for flexion/extension and abduction/adduction were from 2.6°-11° (ankle to hip), and rotation about longitudinal axis were 6.9°-13.2° (Kanko, Laende, Davis, Selbie, & Deluzio, 2021). Their pose estimation (position and orientation) results indicated that ML can be a suitable technology in kinematics studies. More recently, Tang et al. (2022)

compared lower extremity kinetics estimated by MB/ML during treadmill running. Results indicate overall significantly greater peak magnitudes of joint moments and powers estimated by ML than MB (Tang et al., 2022). Joint moments and powers are classically assessed using inverse dynamics. The accuracy of these calculations can be highly affected by the pose estimations of the body segment inertial parameters (BSIPs) expressed in the local coordinate systems (LCS), the segment kinematics, and joint center position (Valentina Camomilla et al., 2017; Timothy R. Derrick et al., 2020). Hence, Tang et al. (2022) suggested that inconsistent joint centers estimation and segment center of mass (COM) position between MB/ML might produce the joint moments and powers differences observed (Tang et al., 2022).

Noticeably, Theia3D ML used in the aforementioned studies utilizes pose estimation algorithms that can identify over 51 keypoints (joint centers and other anatomical features) (Kanko, Laende, Davis, et al., 2021). It exceeds other ML such as OpenPose (25 keypoints) using deep learning based algorithms (Wade et al., 2022). Previous studies have indicated that OpenPose pose estimation accuracy can be affected by movement speed (Nakano et al., 2020; Zago et al., 2020). As Theia3D ML is promoted as appropriate for clinical and sports settings, it is critical to investigate the effects of speed on pose estimation and further on other calculated biomechanical parameters.

Running has received accumulative attention from researchers due to its relationships to sports performance and injury (Novacheck, 1998). Effects of speed on running biomechanics have long been reported (Arampatzis, Brüggemann, & Metzler, 1999; Belli, Kyröläinen, & Komi, 2002; Dugan & Bhat, 2005; Anthony G Schache et al., 2011; Simpson & Bates, 1990; Swanson & Caldwell, 2000). For instance, Sun et al. (2015) reported that peak hip and knee joint torques during late swing might increase hamstring injuries in sprinting (Sun et al., 2015). It is noteworthy lower extremity joint kinetics, estimated using MB, increase with running speed during swing (Arampatzis et al., 1999; Sun et al., 2015)._This increase could be related to the estimation the effects of the inertial terms, which are greatly influenced by COM location estimations, dominate the moment calculation during swing (Ganley & Powers, 2004). Recalling our previous comparison study, the ensembled curves of lower extremity COM between MB/ML showed obvious differences during swing. In particular, the thigh COM locations were about 2 cm more superior and posterior while the positions of leg COM were biased inferior and posterior in ML compared to MB. These explained the significantly greater HJM and KJM and HJP and KJP estimated by ML observed during swing (Tang et al., 2022). Taken together, it is important to investigate the speed effects on the differential joint kinetic parameters estimated by MB/ML.

Therefore, the objective of this study was to investigate how running speed affects lower extremity joint moments and powers estimated by MB/ML. It was hypothesized that: (1) faster speed would generate greater differences in ML estimations of joint moments and powers compared to MB estimations; (2) the systematic differences would mostly appear during running swing phase.

2. Materials and Methods

2.1. Participants

Sixteen recreationally active college students consented (IRB Approval Number: H22327) to act as participants. Inclusion criteria were: (1) free from neuromuscular or musculoskeletal impairments that could prevent their running performance and (2) have treadmill running experience. Participants were advised to be free from any intensive exercise 24 hours before data collection.

2.2. Experimental Setup and Protocols

Experiments were carried out using the MB/ML and an instrumented treadmill (AMTI force-sensing tandem treadmill, MA, USA). MB included eight infrared cameras (Vicon Bonita, Oxford, UK). ML included 8 video cameras (Vicon Vue, Oxford, UK). Data collection from the camera systems (100 Hz) and the instrumented treadmill (1000 Hz) was internally synchronized using Vicon Lock+ (Vicon, Oxford, UK). Before data collection, the cameras were calibrated and temporally and spatially synchronized following the manufacturer's recommended protocol.

This study used a four-segment, hierarchical, biomechanical model (pelvis, thigh, leg, and foot) to capture MB data with twenty-six 14 mm retro-reflective markers (See Tang et al 2022 for more details [9]).

For testing, participants were oriented to the running protocol before they changed into lab provided tight shirts and shorts. Participant wore their own running shoes. A five-minute warm-up and treadmill running familiarization followed. Participant height and body mass were recorded before markers were placed on the participant MB static and dynamic calibration was recorded. Participants started walking at an initial speed of 1.12 m/s and then gradually transitioned to running. Participants performed three running trials at 2.24, 2.91, and 3.58 m/s with fixed order (Anthony G Schache et al., 2011). Each running trial lasted 120 s with 2 min rest in between, and the last 30 s was recorded for further analysis.

2.3. Data analysis

The kinematic and ground reaction force data were filtered through Nexus using a low-pass, zero-lag, 4th-order Butterworth filter with cut-off frequencies of 10 Hz and 50 Hz (Zhang, Pan, & Li, 2018), respectively.

Data were first processed through Nexus (Vicon Nexus, Oxford, UK), where marker trajectories were interpolated using Woltring gap filling (Woltring, 1986). ML video data were pre-processed by Theia3D (Theia3Dv2022.1.0.2309, Theia Markerless, Inc., Kingston, ON, Canada), where the inverse kinematic (IK) solution was used to estimate the 3-dimension pose in space. The lower body kinematic chain has six degrees of freedom (DOF) at the pelvis, three at the hip, three at the knee, and six at the ankle (Kanko, Laende, Selbie, & Deluzio, 2021). Both MB/ML data were then exported as 4×4 pose matrices for each frame of data for the second-level data analysis in Visual3D (Preview v2022.06.02, C-Motion, Inc., Germantown, MD, USA) (Kanko, Laende, Davis, et al., 2021).

To build the anthropometric model for MB data, the body segment inertial parameters (BSIPs) and joint centers were determined. Specifically, Dempster's regression equation for segment mass (Dempster, 1955), and segments were computed as geometrical shapes (Hanavan, 1964). The hip joint center was estimated using the method proposed by Bell et al. (Alexander L. Bell, Brand, & Pedersen, 1989). The knee and ankle joint centers were estimated using midpoints between external landmarks of the corresponding segment. The local coordinate system (LCS) was determined from the static calibration trial. The vertical axis was defined from distal to the proximal joint center, while the anterior-posterior axis was defined perpendicular to the vertical axis with no mediolateral component. The third axis was the cross-product of the vertical and anterior-posterior axis (Kristianslund, Krosshaug, & van den Bogert, 2012). On the other hand, the model was automatically created for ML data based on the deep learning algorithms. BSIPs and joint center positions were generated accordingly (Kanko, Laende, Davis, et al., 2021).

Resolved into the proximal coordinate system for both MB/ML data, lower extremity joint moments and powers in the extension/flexion plane were calculated using the proximal segment as the reference and applying Newton-Euler methods (Robertson, Caldwell, Hamill, Kamen, & Whittlesey, 2013; David A Winter, 2009). The hip and knee extensor and ankle plantar-flexor moments were assigned to be positive. Positive power values indicated energy production through concentric muscular contractions (David A Winter, 2009).

A force threshold of 50 N were used to identify stride cycles (Zhang et al., 2018) defined as two consecutive right heel contacts. The duration of each stride cycle was scaled to 101 (0 to 100%) data points.

Discrete variables were extracted from the last 10 strides of each speed for MB/ML. Tables 3 and 4, supported by figure 6-8 present the details for the identified peaks.

2.4. Statistical Analysis

Means and standard deviations of the lower extremity joint moments and powers at 2.24, 2.91, and 3.58 m/s were calculated based on individual measurements between systems.

2.4.1. Discrete parameters analysis

All discrete variables were assessed for normality using a one-sample Kolmogorov-Smirnov test (α=.05). Two-way (system×speed) within-subject repeated measure ANOVA was used to examine the outcome variables. The alpha level for all statistical tests was .05. SPSS (IBM Inc., Chicago, IL, USA) was used to perform all statistical analyses.

2.4.2. Spatial Parametric Mapping

Spatial parametric mapping (SPM) is an n-dimensional methodology for the topological analysis of smooth continuum changes associated with an experimental intervention (Pataky, 2012). SPM can present statistical results directly in the original sampling space and omit the assumptions regarding the spatiotemporal foci of signals (Pataky, 2010). Thus, SPM analyses were applied to 1D extension/flexion plane lower extremity joint moments and powers estimated by MB/ML under three speeds. A built-in function in SPM assessed the normality of data (spm1d.stats.normality.anova1rm.m). For data that followed the normal distribution, a 2×3 repeated measures ANOVA (system×speed) was performed using the built-in function (spm1d.stats.anova2rm) to compare system pairs. Then a simple linear regression was performed using speeds as the predictor variable and the difference between systems as the dependent variable. The difference between systems was calculated using MB minus ML data. The SPM built-in regression function was employed (spm1d.stats.regress).

All SPM analyses were conducted in MATLAB (The MathWorks Inc., Natick, M.A., 2022a) using the open-source package SPM1d version 0.4 (http://www.spm1d.org/) (Pataky, Robinson, & Vanrenterghem, 2013). The alpha level for all statistical tests was .05.

3. Results

Data from all 16 participants were included in the analysis. Average age, body mass, and height were 23.44±2.31 years, 69.72±9.82 kg, and 1.73±0.08 m, respectively. The discrete measurement results are presented in Tables 1 and 2 as support for the SPM results (See the table for more details).

3.1. Hip Joint

In the SPM analyses, a continuous portion of a 1D continuum can be referred to as a region-of-interest (ROI). According to the first level repeated measure ANOVA SPM analysis, significant interactions between speed and system for the HJM (F=7.908, $p<.001$) and HJP (F=7.667, $p<.001$) (top panel of Fig 6) were observed. The interactions for HJM ROIs were during the 42-52% and 88-96% of the stride cycle (Fig 6 top-left). The ROI of the HJP was around 44-62% (Fig 6 top-right). The second level SPM analysis with simple linear regression showed linear correlations between speed and differences of HJM and HJP estimated by MB/ML ($p<.05$). Correlation coefficients were presented in the second panel of Fig 6. In addition, the ensembled curves of HJM and HJP with running speed were presented in the bottom three panels of Fig 6. We observed that the ROIs of HJM at approximately 42-52% and 88-96% during early and late swing, respectively. Compared to MB estimation of HJM, ML estimation showed greater increases in the flexion HJM during early swing and extension HJM during late swing. The ROI of HJP centered around 45-62% of the stride cycle, where ML-estimated HJP production increased much faster than that of MB-estimated during early swing.

3.2. Knee Joint

The first-level SPM analysis results showed significant interactions between speed and system for KJM (F=7.512, $p<.05$) and KJP (F=7.689, $p<.05$). The ROIs of KJM were 41-60%, 68-76%, and 88-90% of stride cycle (Fig 7 top-left). The ROIs of the KJP were approximately 40-45%, 53-58%, and 68-78% of the stride cycle (Fig 7 top-right). Results from the second level SPM analysis of differences of KJM and KJP estimated by MB and ML revealed the consistency of ROIs of KJM and KJP (see second panels of Fig 7). Observed from the ensembled curves of KJM (bottom three panels of Fig 7), three ROIs of KJM showed that ML estimations changed with speed more than MB estimations. In addition, among the three ROIs of KJP, ML-estimated KJP showed an earlier and faster turn to power absorption than MB estimations in the middle of swing.

3.3. Ankle Joint

For the AJM, the first level SPM analysis revealed the statistically significant interactions at the ROI of 42-52% (F=7.627, *p*<.05) (Fig 3 top-left). Accordingly, the AJP, ROI was shown around 10-18% of early stance (F=7.908, *p*<.05) (Fig 8 top-right). The second level SPM analysis showed a significant association between speeds and differences of AJM and AJP estimated by MB/ML (*p*<.05). The corresponding correlation coefficients are shown in the second panel of Fig 8. The significant ROI of AJM was consistent with the first-level SPM analysis. Combined with ensembled curves of AJM (bottom three panels of Fig 8), we observed that ML estimated plantar flexion AJM did not increase (albeit very small) with speed as much as MB estimated during early swing. However, the ROIs of the AJP of second-level SPM analysis were detected at 10-18%, 36-42%, and 55-62% of the stride cycle (second panel of Fig 8 on the right). Observed from the ensembled curves of AJP under three speeds, the speed-related increase of plantar flexion AJM caused a faster and earlier ending of the power absorption with MB-estimated AJP but not ML-estimated.

4. Discussion

We have investigated the differential effects of running speed on lower extremity joint moments and powers estimated by marker-based (MB) and markerless (ML) systems. Time series (SPM) results, supported by discrete measurements, showed that greater increases of lower extremity joint moments and powers with running speed were observed in ML than MB, hip and knee joints at both ends of swing. Additionally, the plantarflexion AJM during stance-swing transition and the ankle absorption power during early stance were also detected with greater increases in ML with speed. These observations support our hypotheses. Lower extremity joint kinetics increase with running speed (Belli et al., 2002; Fukuchi, Fukuchi, & Duarte, 2017; Petersen, Nielsen, Rasmussen, & Sørensen, 2014; Anthony G Schache et al., 2011), especially during swing (Elizabeth S. Chumanov, Heiderscheit, & Thelen, 2007; Elizabeth S Chumanov, Heiderscheit, & Thelen, 2011; Dorn, Schache, & Pandy, 2012; Fukuchi et al., 2017; Anthony G Schache et al., 2011; Sun et al., 2015). Estimation of HJM and KJM plays an important role in clinical evaluation of running related injuries (Elizabeth S. Chumanov et al., 2007; Elizabeth S Chumanov et al., 2011; Sun et al., 2015). Greater magnitude of HJM and KJM during swing would lead to an increased hamstring injury-risks (Li & Wang, 2017). Increased HJM and KJM could be associated with greater muscle eccentric contraction speed during swing, which leads to excessive hamstring stretch and loading (Elizabeth S Chumanov et al., 2011). Meanwhile, biceps femoris loading increases more than other hamstring muscles when performing a high-speed running (Thelen et al., 2005). Hence, the runners with weak biceps femoris would have a higher risk of hamstring injuries during high-speed running. In addition, Sun et al. (2015) supported the hamstrings' maximal lengthening as injury-risk during the late swing using inter-segmental analysis. They showed that the motion dependent moments contributed significantly to the HJM and KJM at the end of swing during running. So tremendous loads on hamstring muscles are needed to counterbalance the passive torques and control rapid limb rotation during swing. Due to the large passive torques at both the knee and hip acted to lengthen hamstrings, the largest extension HJM and flexion KJM occurred at the same time and can be used as indicators for hamstring strain injuries at the end of swing phase (Sun et al., 2015).

Joint kinetics during swing are mainly determined by gravity and body segment inertia (Verheul, Sueda, & Yeo, 2022).The effects of inertial properties changes with speed on joint kinetics during swing then should be highlighted. It is noted that inertial property changes are not independent, changes in the center of mass (COM) should affect the moment of inertia based on the parallel axis theorem as well as segment mass [41]. The sensitivity of HJM to inertial property variations of thigh and leg can be up to 40%, especially during swing (Pearsall & Costigan, 1999). Supported by our previous report, greater ML estimations of HJM and KJM increased with speed during running can be explained by differences in segment COM (Tang et al., 2022). In the current study, SPM results showed the region of interest (ROI) for HJM affected by speeds during the late swing (88%-96%), which could be a direct result of leg COM estimation. We have observed that the ML estimated the leg COM were 2 cm inferior then that of the MB during late swing (Tang et al., 2022). The increased distance would increase the estimated leg inertial load on the knee joint, which can then explain the greater KJM induced by increased inertial loads during late swing. It has been reported that motion dependent moments, especially the moment due to leg acceleration, were main contributors to HJM and KJM during late swing. Greater amount of the estimated hamstring muscle loading is needed to counterbalance such motion dependent moments and control the rapid limb rotation with faster speed (Sun et al., 2015). Increased inertial loads with speed puts the lengthened hamstring muscles at risk for injury during sprinting (Elizabeth S. Chumanov et al., 2007; Elizabeth S Chumanov et al., 2011; Sun et al., 2015).

Further, it is important to note that segment COM position and components of the inertia matrix are calculated by using segment lengths which are defined by segment endpoints (Bhrigu Kumar Lahkar, Chaumeil, Dumas, Muller, & Robert, 2022). Our previously observed joint center differences during swing also help to explain the current results. The hip joint center differences in the anterior-posterior direction were particularly propagated to the extension/flexion HJM (Stagni, Leardini, Cappozzo, Grazia Benedetti, & Cappello, 2000). Reinforced by our earlier results, the hip joint center positions estimated by ML during swing were approximately 3 cm more posterior (Tang et al., 2022). It is noteworthy that gait cycles showing differences in segment center of mass and joint center matched with the current significant ROIs of HJM, KJM, HJP, and KJP. While our previous study only presented discrete single events, the current SPM results supports that such observations are aligned through temporal shifting (Honert & Pataky, 2021). Taken together, systematic differences in joint kinetics induced by inconsistent estimations of segment center of mass and joint centers can be exacerbated by the increased running speeds.

The systematic differences observed from MB/ML need to be addressed to avoid repercussions for future clinical applications. It is a common practice to apply biomechanical factors to predict running-related injury and then modify with targeted interventions (Ceyssens, Vanelderen, Barton, Malliaras, & Dingenen, 2019). For instance, researchers would use the moments, powers and work done at hip and knee joints during late swing as references to indicate hamstring muscles injuries (Elizabeth S. Chumanov et al., 2007; Elizabeth S Chumanov et al., 2011; Dorn et al., 2012; Anthony G Schache et al., 2011; Sun et al., 2015). Since we reported greater increased HJM and KJM estimation by ML, it may lead to an increased injury-risk estimation for both parallel and cross-sectional hamstring injuries (Li & Wang, 2017). Similarly, patellofemoral pain occurs at the knee joint due to excessive hip motion and overloading during running (Souza & Powers, 2009). Rectus femoris, another biarticular muscle is associated with flexion HJM and extension KJM. It has been reported that greater inertial loads to the rectus femoris during the early swing phase increased the patellar tension, leading to patellofemoral pain risks in running (Bryan C Heiderscheit, Chumanov, Michalski, Wille, & Ryan, 2011). Another example would be chronic exertional compartment syndrome induced by tibialis anterior overload (Franklyn-Miller, Roberts, Hulse, & Foster, 2014), the previous varied foot COM estimation together with the current overestimation of ankle and knee joint kinetics may result in over injury estimation. Therefore, the results from the current study indicate the overestimation from ML could be exacerbated by speeds, and could lead to over-estimated running-related injury risks if used in sports biomechanics.

ML remains worthwhile for the clinical and sports settings despite the differences between MB/ML we observed here. Advantages of ML are prominent, especially for the clinical settings. First, short preparation time is more convenient. Without putting markers on participants, less operator differences would occur. The differences caused by loose clothing reported in the spatiotemporal parameters, which were lower than typical marker placement-related differences, were smaller than the minimal changes in movement-related pathologies such as multiple sclerosis and cerebral palsy (Keller, Outerleys, Kanko, Laende, & Deluzio, 2022). Second, movements , such as, underwater running (Cronin, Rantalainen, Ahtiainen, Hynynen, & Waller, 2019), counter movement jump (Drazan, Phillips, Seethapathi, Hullfish, & Baxter, 2021), and ball throwing (Nakano et al., 2020), will not be restricted by markers. Moreover, Theia3D ML has shown to be reliable comparing inter-session joint angles during walking (Kanko, Laende, Selbie, et al., 2021). Demonstrating it can be an unobtrusive method to monitor patients in their daily lives. Prior studies have demonstrated that using monocular ML to examine gait parameters of Parkinson's disease patients can provide clinicians with an overview of disease progression and detect the minor gait disturbances that can be unnoticed by clinicians (Mathis et al., 2018; Shin et al., 2021).

The current study has several limitations. First, we only investigated the speed effects of treadmill running, and it remains unclear if ML overestimations of joint moments and powers would apply to other movements. Second, the interactions detected, using SPM, between AJM during early swing and AJP during initial stance, were not consistent with the results of discrete measurements. Further ankle joint investigations are needed to explain such inconsistency. In addition, the current study focused on joint kinetics in the extension/flexion plane. However, many lower extremity muscles have specific actions that are not limited to a single plane. For example, rectus femoris and bicep femoris muscles induce frontal hip motion (Hunter, Thelen, & Dhaher, 2009). Lower extremity motion in other planes needs to be further investigated using ML.

5. Conclusion

We have observed the differences in lower extremity joint moments and power estimated by maker-based (MB) and markerless (ML) systems during treadmill running increased with speed. Differences in joint center and center of mass estimations between the systems could partially explain the observed differences. ML is beneficial in the clinical and sports settings, it is critical to consider the overestimation issue induced by the pose estimation algorithms, especially when analyzing high speed movements.

Table 3. Body mass scaled peak magnitude (Mean±SD) for joint moments and powers for the marker-based system (MB) and Markerless system (ML).

Parameters	**MB**			**ML**			**Significant**	**Main Effect**	
	2.24 m/s	**2.91 m/s**	**3.58 m/s**	**2.24 m/s**	**2.91 m/s**	**3.58 m/s**	**Interaction**	**Speed**	**System**
	Moment (Nm/kg)								
Hip first peak	-1.39±0.48	-1.75±0.49	-2.21±0.65	-1.35±0.43	-1.61±0.49	-2.04±0.69		$p<.05$	
Hip second peak	*0.82±0.19*	*1.01±0.23*	*1.44±0.23*	*1.06±0.17*	*1.23±0.29*	*1.76±0.24*		$p<.05$	$p<.05$
Hip third peak	-0.89±0.19	-1.12±0.23	-1.42±0.29	-1.50±0.30	-1.73±0.46	-2.14±0.78		$p<.05$	$p<.05$
Knee first peak	**1.59±0.33**	**1.64±0.43**	**1.51±0.44**	**1.43±0.21**	**1.49±0.37**	**1.28±0.27**			$p<.05$
Knee second peak	-0.50±0.09	-0.61±0.10	-0.74±0.13	-0.78±0.14	-0.95±0.16	-1.17±0.23	$p<.05$		
Ankle first peak	**-2.60±0.66**	**-3.04±0.76**	**-3.41±0.85**	**-2.47±0.41**	**-2.93±0.52**	**-3.27±0.62**		$p<.05$	
	Power (W/kg)								
Hip first peak	**-2.22±1.05**	**-3.44±1.56**	**-5.59±3.30**	**-2.11±0.99**	**-3.55±1.63**	**-5.38±1.96**		$p<.05$	
Hip second peak	1.59±0.41	2.70±0.62	4.49±1.27	3.45±0.73	5.06±1.05	8.20±1.78	$p<.05$		
Hip third peak	1.33±0.50	2.24±0.94	3.96±2.26	2.27±0.85	3.43±1.21	5.65±2.54	$p<.05$		
Knee first peak	**-4.95±1.77**	**-5.56±2.12**	**-5.15±2.50**	**-4.34±1.64**	**-4.85±2.03**	**-3.98±1.69**			$p<.05$

Knee second peak	**3.17±1.45**	**3.56±1.65**	**3.34±1.36**	**2.27±1.09**	**2.79±1.50**	**2.64±0.90**			p<.05
Knee third peak	-1.15±0.32	-2.18±0.60	-3.71±1.23	-2.21±0.49	-3.48±1.03	-5.46±1.54		p<.05	p<.05
Knee forth peak	-3.37±0.70	-5.05±1.13	-7.36±1.95	-4.70±0.94	-6.69±1.23	-9.60±2.34	p<.05		
Ankle first peak	**-5.15±2.12**	**-6.82±2.76**	**-9.14±3.26**	**-4.90±1.26**	**-7.12±1.61**	**-9.40±1.54**		p<.05	
Ankle second peak	**9.61±3.05**	**13.24±4.01**	**17.28±4.66**	**9.37±2.60**	**13.96±3.39**	**18.34±4.82**		p<.05	

Bold indicates the event was observed within the stance phase; italic with underline indicates the event was observed during the stance-swing transition; otherwise, parameters were observed within the swing phase.

Table 4 Relative Time to Peak as %Stride Cycle (Mean±SD) for Joint moments and Powers for Marker-based system (MB) and Markerless system (ML).

Parameters	**MB**			**ML**			**Significant Interaction**	**Main Effect**	
	2.24 m/s	**2.91 m/s**	**3.58 m/s**	**2.24 m/s**	**2.91 m/s**	**3.58 m/s**		**Speed**	**System**
	Moment (Nm/kg)								
Hip first peak	**5.21±1.84**	**3.41±0.39**	**3.33±0.61**	**3.63±0.55**	**4.88±2.00**	**4.59±1.65**		p<.05	
Hip second peak	*27.31±4.85*	*28.29±5.65*	*26.02±3.88*	*34.55±4.67*	*32.00±4.80*	*27.91±3.46*	p<.05		

Hip third peak	68.11±6.32	64.52±6.53	59.74±6.72	69.12±5.88	65.64±5.96	60.22±5.94		p<.05	
Knee first peak	**10.38±1.54**	**9.48±1.24**	**9.55±3.33**	**10.81±1.85**	**9.89±1.72**	**9.44±2.13**			
Knee second peak	68.05±6.08	64.39±6.09	59.95±6.45	68.41±5.85	65.03±5.94	60.73±6.15		p<.05	p<.05
Ankle first peak	**14.82±1.15**	**13.34±1.42**	**12.00±1.33**	**14.89±1.33**	**13.54±1.45**	**12.11±1.48**		p<.05	
		Power (W/kg)							
Hip first peak	**19.30±3.83**	**18.18±3.66**	**17.56±4.31**	**23.28±2.84**	**20.91±2.90**	**18.76±2.67**	p<.05		
Hip second peak	38.58±4.57	36.86±4.25	34.09±5.16	38.94±3.79	37.06±4.02	34.74±4.03		p<.05	
Hip third peak	65.31±5.65	63.87±6.22	59.93±6.14	62.75±4.24	59.57±4.37	58.83±5.12		p<.05	p<.05
Knee first peak	6.78±1.25	5.63±1.42	5.35±0.84	6.67±1.87	5.89±1.01	5.82±1.31		p<.05	
Knee second peak	**14.72±1.93**	**13.84±2.03**	**12.79±1.59**	**14.92±1.88**	**14.43±1.88**	**13.88±1.73**			
Knee third peak	**39.16±3.00**	**37.08±3.24**	**34.48±3.88**	**38.63±1.88**	**36.14±2.79**	**34.21±4.00**		p<.05	
Knee forth peak	63.90±5.56	60.84±5.70	55.96±5.94	63.54±5.33	60.74±5.70	56.89±5.89		p<.05	
Ankle first peak	**8.05±1.48**	**7.62±1.38**	**7.38±2.57**	**8.73±1.30**	**7.89±1.33**	**7.28±1.53**		p<.05	
Ankle second peak	**19.87±1.72**	**17.78±1.66**	**15.80±1.94**	**19.96±1.53**	**17.83±1.58**	**15.91±1.60**		p<.05	

Bold indicates the event was observed within the stance phase; italic with underline indicates the event was observed during the stance-swing transition; otherwise, parameters were observed within the swing phase.

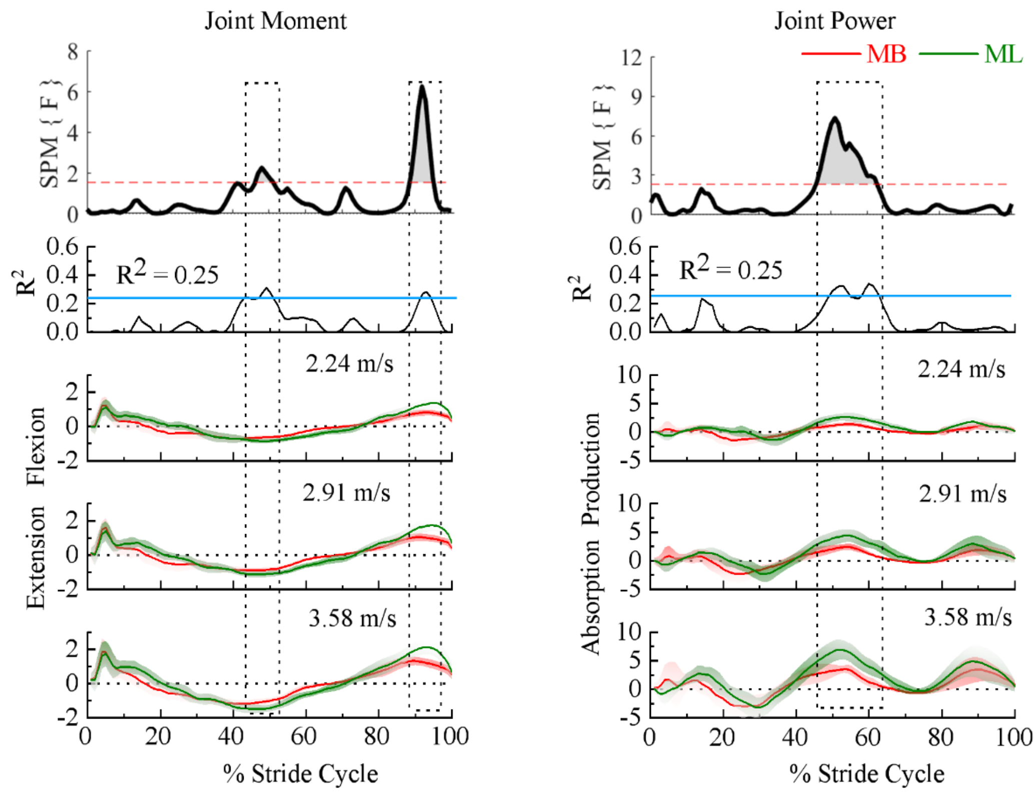

Figure 6. SPM analyses and ensembled curves of hip joint moments (left) and powers (right) under three speeds. The top panel shows the repeated measure ANOVA trajectory (SPM-F), where the horizontal red dotted line indicates the critical Random Field Theory threshold for significance (p<.05). The second panel shows the squared correlation coefficients corresponding to the SPM simple linear regression analysis of differences in hip joint moments and powers estimated by MB and ML changed with speeds. The significant squared correlation coefficient threshold was set at R^2=.25. The bottom three panels are the ensembled curves of hip joint moments and powers estimated by MB (red) and ML (green). The dotted rectangle regions represented the region of interests (ROIs).

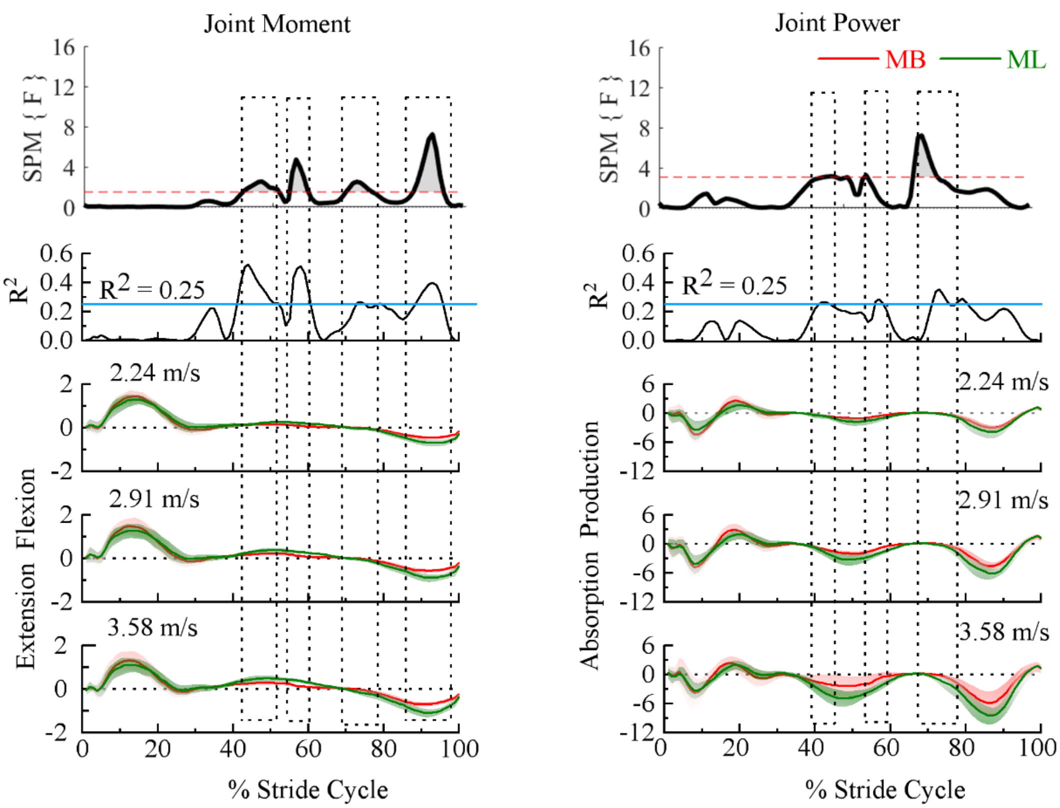

Figure 7. SPM analyses and ensembled curves of knee joint moments (left) and powers (right) under three speeds. The top panel shows the repeated measure ANOVA trajectory (SPM-F), where the horizontal red dotted line indicates the critical Random Field Theory threshold for significance (p<.05). The second panel shows the squared correlation coefficients corresponding to the results of SPM simple linear regression analysis of differences of knee joint moments and powers estimated by MB and ML and speeds. The significant squared correlation coefficient threshold was set at R^2=.25. The bottom three panels are the ensembled curves of knee joint moments and powers estimated by MB (red) and ML (green). The dotted rectangle regions represent the region of interests (ROIs).

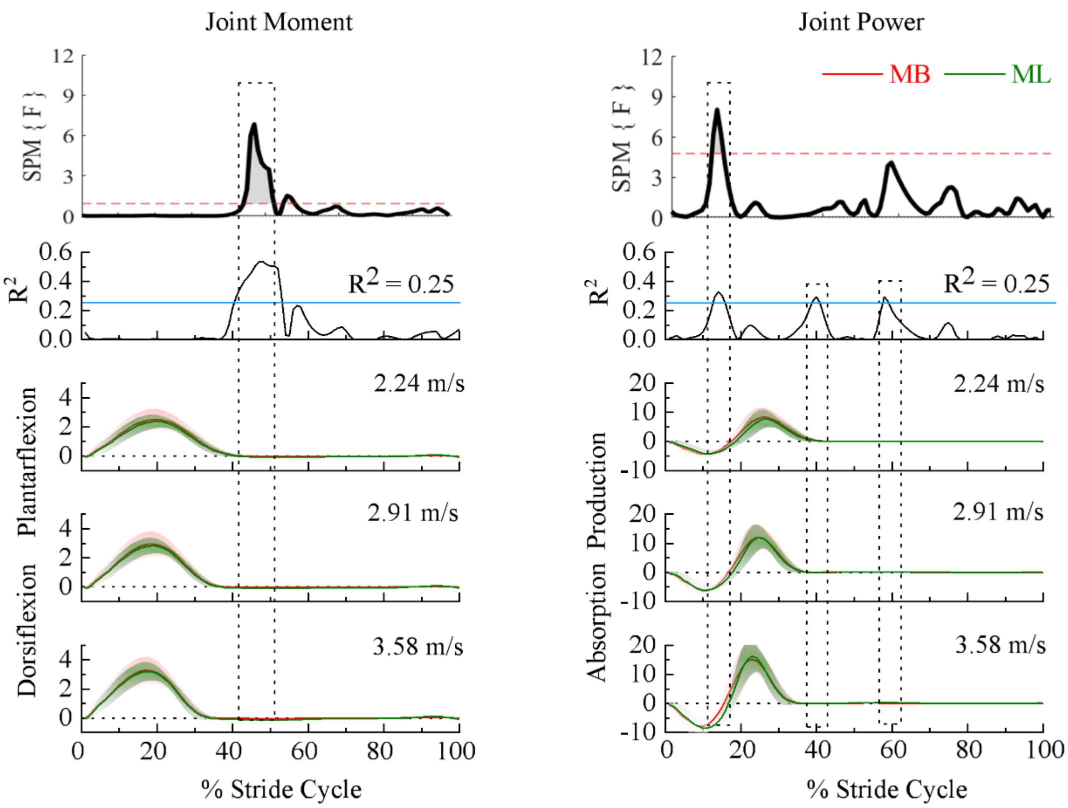

Figure 8. SPM analyses and ensembled curves of ankle joint moments (left) and powers (right) under three speeds. The top panel shows the repeated measure ANOVA trajectory (SPM-F), where the horizontal red dotted line indicates the critical Random Field Theory threshold for significance (*p*<.05). The second panel shows the squared correlation coefficients corresponding to the SPM simple linear regression analysis of differences of ankle joint moments and powers estimated by MB and ML and speeds. The significant squared correlation coefficient threshold was set at R^2=.25. The bottom three panels are the ensembled curves of ankle joint moments and powers estimated by MB (red) and ML (green). The dotted rectangle regions represent the region of interests (ROIs).

References:

Arampatzis, A., Brüggemann, G.-P., & Metzler, V., 1999. The effect of speed on leg stiffness and joint kinetics in human running. Journal of Biomechanics, 32 (12), 1349-1353.

Bell, A. L., Brand, R. A., & Pedersen, D. R., 1989. Prediction of hip joint centre location from external landmarks. Human Movement Science, 8 (1), 3-16.

Belli, A., Kyröläinen, H., & Komi, P. V., 2002. Moment and Power of Lower Limb Joints in Running. Int J Sports Med, 23 (02), 136-141.

Camomilla, V., Cereatti, A., Cutti, A. G., Fantozzi, S., Stagni, R., & Vannozzi, G., 2017. Methodological factors affecting joint moments estimation in clinical gait analysis: a systematic review. BioMedical Engineering OnLine, 16 (1), 106.

Cappozzo, A., Catani, F., Della Croce, U., & Leardini, A., 1995. Position and orientation in space of bones during movement: anatomical frame definition and determination. Clinical Biomechanics, 10 (4), 171-178.

Cappozzo, A., Della Croce, U., Leardini, A., & Chiari, L., 2005. Human movement analysis using stereophotogrammetry: Part 1: theoretical background. Gait & Posture, 21 (2), 186-196.

Ceyssens, L., Vanelderen, R., Barton, C., Malliaras, P., & Dingenen, B., 2019. Biomechanical Risk Factors Associated with Running-Related Injuries: A Systematic Review. Sports Medicine, 49 (7), 1095-1115.

Chiari, L., Croce, U. D., Leardini, A., & Cappozzo, A., 2005. Human movement analysis using stereophotogrammetry: Part 2: Instrumental errors. Gait & Posture, 21 (2), 197-211.

Chumanov, E. S., Heiderscheit, B. C., & Thelen, D. G., 2007. The effect of speed and influence of individual muscles on hamstring mechanics during the swing phase of sprinting. Journal of Biomechanics, 40 (16), 3555-3562.

Chumanov, E. S., Heiderscheit, B. C., & Thelen, D. G., 2011. Hamstring musculotendon dynamics during stance and swing phases of high speed running. Medicine and science in sports and exercise, 43 (3), 525.

Collins, T. D., Ghoussayni, S. N., Ewins, D. J., & Kent, J. A., 2009. A six degrees-of-freedom marker set for gait analysis: Repeatability and comparison with a modified Helen Hayes set. Gait & Posture, 30 (2), 173-180.

Cronin, N. J., Rantalainen, T., Ahtiainen, J. P., Hynynen, E., & Waller, B., 2019. Markerless 2D kinematic analysis of underwater running: A deep learning approach. Journal of Biomechanics, 87, 75-82.

Dempster, W. T. 1955. Space requirements of the seated operator, geometrical, kinematic, and mechanical aspects of the body with special reference to the limbs. Michigan State Univ East Lansing.

Derrick, T. R., van den Bogert, A. J., Cereatti, A., Dumas, R., Fantozzi, S., & Leardini, A., 2020. ISB recommendations on the reporting of intersegmental forces and moments during human motion analysis. Journal of Biomechanics, 99, 109533.

Dorn, T. W., Schache, A. G., & Pandy, M. G., 2012. Muscular strategy shift in human running: dependence of running speed on hip and ankle muscle performance. Journal of Experimental Biology, 215 (11), 1944-1956.

Drazan, J. F., Phillips, W. T., Seethapathi, N., Hullfish, T. J., & Baxter, J. R., 2021. Moving outside the lab: Markerless motion capture accurately quantifies extension/flexion plane kinematics during the vertical jump. Journal of Biomechanics, 125, 110547.

Dugan, S. A., & Bhat, K. P., 2005. Biomechanics and Analysis of Running Gait. Physical Medicine and Rehabilitation Clinics, 16 (3), 603-621.

Franklyn-Miller, A., Roberts, A., Hulse, D., & Foster, J., 2014. Biomechanical overload syndrome: defining a new diagnosis. British Journal of Sports Medicine, 48 (6), 415.

Fukuchi, R. K., Fukuchi, C. A., & Duarte, M., 2017. A public dataset of running biomechanics and the effects of running speed on lower extremity kinematics and kinetics. PeerJ, 5, e3298.

Fuller, J., Liu, L.-J., Murphy, M., & Mann, R., 1997. A comparison of lower-extremity skeletal kinematics measured using skin-and pin-mounted markers. Human Movement Science, 16 (2-3), 219-242.

Ganley, K. J., & Powers, C. M., 2004. Determination of lower extremity anthropometric parameters using dual energy X-ray absorptiometry: the influence on net joint moments during gait. Clinical Biomechanics, 19 (1), 50-56.

Hanavan, E. P., 1964. A Mathematical Model of the Human Body. AMRL Technical Report, 64-102.

Heiderscheit, B. C., Chumanov, E. S., Michalski, M. P., Wille, C. M., & Ryan, M. B., 2011. Effects of step rate manipulation on joint mechanics during running. Medicine and science in sports and exercise, 43 (2), 296.

Honert, E. C., & Pataky, T. C., 2021. Timing of gait events affects whole trajectory analyses: A statistical parametric mapping sensitivity analysis of lower limb biomechanics. Journal of Biomechanics, 119, 110329.

Hunter, B. V., Thelen, D. G., & Dhaher, Y. Y., 2009. A three-dimensional biomechanical evaluation of quadriceps and hamstrings function using electrical stimulation. IEEE Transactions on Neural Systems and Rehabilitation Engineering, 17 (2), 167-175.

Kanko, R. M., Laende, E., Selbie, W. S., & Deluzio, K. J., 2021. Inter-session repeatability of markerless motion capture gait kinematics. Journal of Biomechanics, 121, 110422.

Kanko, R. M., Laende, E. K., Davis, E. M., Selbie, W. S., & Deluzio, K. J., 2021. Concurrent assessment of gait kinematics using marker-based and markerless motion capture. Journal of Biomechanics, 127, 110665.

Keller, V. T., Outerleys, J. B., Kanko, R. M., Laende, E. K., & Deluzio, K. J., 2022. Clothing condition does not affect meaningful clinical interpretation in markerless motion capture. Journal of Biomechanics, 141, 111182.

Kristianslund, E., Krosshaug, T., & van den Bogert, A. J., 2012. Effect of low pass filtering on joint moments from inverse dynamics: Implications for injury prevention. Journal of Biomechanics, 45 (4), 666-671.

Lahkar, B. K., Chaumeil, A., Dumas, R., Muller, A., & Robert, T., 2022. Description, Development and Dissemination of Two Consistent Marker-based and Markerless Multibody Models. bioRxiv, 2022.2011.2008.515577.

Leardini, A., Chiari, L., Croce, U. D., & Cappozzo, A., 2005. Human movement analysis using stereophotogrammetry: Part 3. Soft tissue artifact assessment and compensation. Gait & Posture, 21 (2), 212-225.

Li, L., & Wang, D., 2017. Parallel and cross-sectional hamstring injuries in sprint running. Journal of sport and health science, 6 (2), 141.

Mathis, A., Mamidanna, P., Cury, K. M., Abe, T., Murthy, V. N., Mathis, M. W., & Bethge, M., 2018. DeepLabCut: markerless pose estimation of user-defined body parts with deep learning. Nature Neuroscience, 21 (9), 1281-1289.

Mündermann, L., Corazza, S., & Andriacchi, T. P., 2006. The evolution of methods for the capture of human movement leading to markerless motion capture for biomechanical applications. Journal of NeuroEngineering and Rehabilitation, 3 (1), 6.

Nakano, N., Sakura, T., Ueda, K., Omura, L., Kimura, A., Iino, Y., Fukashiro, S., & Yoshioka, S., 2020. Evaluation of 3D markerless motion capture accuracy using OpenPose with multiple video cameras. Frontiers in sports and active living, 2, 50.

Novacheck, T. F., 1998. The biomechanics of running. Gait & Posture, 7 (1), 77-95.

Pataky, T. C., 2010. Generalized n-dimensional biomechanical field analysis using statistical parametric mapping. Journal of Biomechanics, 43 (10), 1976-1982.

Pataky, T. C., 2012. One-dimensional statistical parametric mapping in Python. Computer Methods in Biomechanics and Biomedical Engineering, 15 (3), 295-301.

Pataky, T. C., Robinson, M. A., & Vanrenterghem, J., 2013. Vector field statistical analysis of kinematic and force trajectories. Journal of Biomechanics, 46 (14), 2394-2401.

Pearsall, D. J., & Costigan, P. A., 1999. The effect of segment parameter error on gait analysis results. Gait & Posture, 9 (3), 173-183.

Petersen, J., Nielsen, R. O., Rasmussen, S., & Sørensen, H., 2014. Comparisons of increases in knee and ankle joint moments following an increase in running speed from 8 to 12 to 16km·h−1. Clinical Biomechanics, 29 (9), 959-964.

Robertson, D. G. E., Caldwell, G. E., Hamill, J., Kamen, G., & Whittlesey, S. 2013. Research methods in biomechanics. Human kinetics.

Schache, A. G., Blanch, P. D., Dorn, T. W., Brown, N., Rosemond, D., & Pandy, M. G. J. M. S. S. E., 2011. Effect of running speed on lower limb joint kinetics. 43 (7), 1260-1271.

Shin, J. H., Yu, R., Ong, J. N., Lee, C. Y., Jeon, S. H., Park, H., Kim, H.-J., Lee, J., & Jeon, B., 2021. Quantitative Gait Analysis Using a Pose-Estimation Algorithm with a Single 2D-Video of Parkinson's Disease Patients. Journal of Parkinson's Disease, 11, 1271-1283.

Simpson, K. J., & Bates, B. T., 1990. The Effects of Running Speed on Lower Extremity Joint Moments Generated during the Support Phase. International Journal of Sport Biomechanics, 6 (3), 309-324.

Souza, R. B., & Powers, C. M., 2009. Differences in Hip Kinematics, Muscle Strength, and Muscle Activation Between Subjects With and Without Patellofemoral Pain. Journal of Orthopaedic & Sports Physical Therapy, 39 (1), 12-19.

Stagni, R., Leardini, A., Cappozzo, A., Grazia Benedetti, M., & Cappello, A., 2000. Effects of hip joint centre mislocation on gait analysis results. Journal of Biomechanics, 33 (11), 1479-1487.

Sun, Y., Wei, S., Zhong, Y., Fu, W., Li, L., & Liu, Y., 2015. How joint torques affect hamstring injury risk in sprinting swing-stance transition. Medicine and science in sports and exercise, 47 (2), 373-380.

Swanson, S. C., & Caldwell, G. E., 2000. An integrated biomechanical analysis of high speed incline and level treadmill running. Medicine and science in sports and exercise, 32 (6), 1146-1155.

Tang, H., Pan, J., Munkasy, B., Duffy, K., & Li, L., 2022. Comparison of Lower Extremity Joint Moment and Power Estimated by Markerless and Marker-Based Systems during Treadmill Running. Bioengineering, 9 (10).

Thelen, D. G., Chumanov, E. S., Hoerth, D. M., Best, T. M., Swanson, S. C., Li, L., Young, M., & Heiderscheit, B. C., 2005. Hamstring muscle kinematics during treadmill sprinting. Med Sci Sports Exerc, 37 (1), 108-114.

Verheul, J., Sueda, S., & Yeo, S.-H., 2022. Muscle Inertia During Running: A Massive Change of Moments? ISBS Proceedings Archive, 40 (1), 732.

Wade, L., Needham, L., McGuigan, P., & Bilzon, J., 2022. Applications and limitations of current markerless motion capture methods for clinical gait biomechanics. PeerJ, 10, e12995.

Winter, D. A. 2009. Biomechanics and motor control of human movement. John Wiley & Sons.

Woltring, H. J., 1986. A Fortran package for generalized, cross-validatory spline smoothing and differentiation. Advances in Engineering Software (1978), 8 (2), 104-113.

Zago, M., Luzzago, M., Marangoni, T., De Cecco, M., Tarabini, M., & Galli, M., 2020. 3D tracking of human motion using visual skeletonization and stereoscopic vision. Frontiers in bioengineering and biotechnology, 8, 181.

Zhang, S., Pan, J., & Li, L., 2018. Non-linear changes of lower extremity kinetics prior to gait transition. Journal of Biomechanics, 77, 48-54.

APPENDIX A

EXTENDED INTRODUCTION

Understanding human motion plays an important role in clinical applications and sports. Movement analysis may assist with injury prevention, identification, rehabilitation treatment and adherence in the clinical settings (Knippenberg et al., 2017). It is also important in guiding athletes' tactics and performance. (Wade et al., 2022). Analytic methods underpinned such subjects varied from traditional human observation and self-report to wearable devices, to the vision-based 3D motion capture systems. Measures that rely on observers' experiences are subjective and prone to errors (Wade et al., 2022). Wearable devices such as inertial measurement units (IMU) are portable and affordable, and can provide rich information for real-time gait analysis in both indoor and outdoor environments (Chen, Lach, Lo, & Yang, 2016). However, these devices restricted to magnetic field effects such as those generated by laboratory treadmills (de Vries, Veeger, Baten, & van der Helm, 2009) and exceed in reporting quantities such as accelerations and angular rates instead of intersegmental measures, which are beyond this thesis's scope.

Alternatively, vision-based 3D motion capture approaches are more beneficial for more biomechanical applications.

The vision-based motion analysis can be traced back to the late nineteenth century when Eadweard Muybridge developed techniques to capture image sequences of equine gait (Cappozzo, Marchetti, & Tosi, 1992). Motion analysis has evolved significantly since then in order in parallel with major technological improvements and the growing demand of more sophisticated techniques to capture movement. At present, the most common methods for accurate capture of 3D human movement require controlled labatory environment and the attachment of markers fixture on the body segments (Mündermann et al., 2006). Although bi-planar videoradiography methods such as MRI and X-ray can provide direct skeletal movements with high accuracy, these methods impede natural patterns of movements and are usually expensive to conduct (Kessler et al., 2019). The marker-based (MB) systems, on the other hand, allow errors only in the large motions such as flexion and extensions. Although the wide use of MB motion capture system in the biomechanics, there is a need for motion capture methods that are less time intensive, simpler to operate, and less impacted by human errors and marker-based errors. The markerless (ML) motion capture system that also uses videos to record human movement but relies on software to estimate poses can possibly achieve the goal.

1. Marker-based Systems

Automatic optoelectronic systems or marker-based system are the most commonly used for the study of human movement. Most of MB systems use multiple cameras emitting invisible infrared light, and passive markers that reflect this infrared back to the cameras to deduce their 3D position (Colyer, Evans, Cosker, & Salo, 2018). Commercial systems such as Vicon Motion Systems, Qualisys Motion Capture Systems, OptiTrack, and other leading motion capture companies, tracks the position of small spherical retro-reflective markers. The primary principle is that several points of interest are located in sequential images, converted to real-space coordinates and infer 3D pose of underlying skeleton. At least three non-colinear markers must be affixed to each segment to specify six DOF. Previous studies have evaluated the accuracies of some commercial MB systems. They reported that the root mean square errors were less than 2 mm when measuring the fully visible moving markers, and 1mm when measuring the stationary markers (Richards, 1999).

Noticeably, previous studies also addressed different marker sets and their influences on kinematic and kinetics assessments. For example, Cappozzo et al. (1997) presented that compared to the convenient markers, surface-marker cluster design not only minimized the error propagation from marker coordinates to bone-embedded frame position and orientation but also dealt with skin artifacts movements (Cappozzo, Cappello, Croce, & Pensalfini, 1997). Their study showed the mean radius of the cluster greater than ten times the assessed standard deviation of experimental errors. Collins et al. (2009) compared the modified Helen Hayes set and a six-degrees of freedom marker set. Although high repeatability was acquired, they still observed that kinematical differences of the lower extremity. The hip rotations showed clear differences between the two sets with indications in support of the 6DOF set. Knee coronal angles showed evidence of cross-talk in the conventional set, highlighting difficulties with anatomical identification despite control measures such as a foot alignment template. Knee transverse angles showed inconsistent patterns for both sets. At the ankle the conventional set only allowed true measurement in two planes so with high repeatability the 6DOF set is preferable (Collins et al., 2009). Ferrari et al. (2008) reported that joint flexion/extension had better correlations and smaller biases among different marker sets but not the out-of-extension/flexion rotations, especially the knee joint (Ferrari et al., 2008). A more recent study compared the six different marker sets, namely plug-in gait, ridged marker set with cluster and without cluster, six-degree of freedom, Helen Hayes, and functional approach. The authors reported the differences of kinematic and kinetics of the knee joint during landing. To be specific, the knee joint angles showed partially contradictory results in the transverse and frontal plane when using different marker sets, especially after initial ground contact. In addition, though the direction of joint moments were consistent, the amplitudes varied among different marker sets. The results of Helen Hayes and plug-in-gait differed most from the other three marker sets. This difference is once again smallest in the extension/flexion plane (Kerkhoff, Wagner, & Peikenkamp, 2020).

Although different marker sets may affect the gait analysis, the high correlations made the slight differences negligible. The needs for different technologies to be promoted in the biomechanical studies actually derived from the following inconvenience and shortcomings.

It is difficult to ensure that the precise marker placements on anatomical landmarks can directly correspond to 3D joint positions. Errors can come from various sources, including inter-operator and inter-session variability, marker placement, and skin movement artifacts (Della Croce, Leardini, Chiari, & Cappozzo, 2005; Gorton, Hebert, & Gannotti, 2009; Peters, Galna, Sangeux, Morris, & Baker, 2010). As the most prominent error source, soft tissue artefact errors as muscle, fat and skin beneath markers cause them to move independently from bone (Camomilla, Bonci, & Cappozzo, 2017; Cappozzo et al., 1995). A review reported that soft tissue artifacts reached the magnitudes of greater than 30 mm on the thigh, and up to 15 mm on the leg (Peters et al., 2010). Among reported studies, the range of soft tissue artifacts can be greater than 25 mm in some cases. To alleviate such soft tissue artifacts, different methods have been employed. For example, by using the cluster placed on each segment, the skin movement artifacts can be compensated by optimal weighting of the markers according to their degree of deformation (T. P. Andriacchi, Alexander, Toney, Dyrby, & Sum, 1998; Mündermann et al., 2006). Researchers have also tried to expand the rigid body model, imposing joint constraints and a global error compensation scheme to reduce the non-rigid body movement (Lu & O'Connor, 1999). However, these methods usually induced new limitations, leaving soft tissue errors the primary inaccuracy caused by MB systems.

In addition, optoelectronic systems are sensitive to the capture environment. In particular, sunlight, which includes a strong infrared component, can introduce undesirable noise into the measurements (Colyer et al., 2018). The MB systems are usually setup in the lab environment where lightning can be stringently controlled. Away from clinics and natural environment, the biomechanical evaluations conducted in the lab have limited utilization for treatment and intervention of movement related pathologies (Baker, 2006; Keller et al., 2022). Plus, preparations for the MB systems such as changing to tight clothes, and marker placements are time-consuming.

More than motion capture setup, the MB data processing can be labor and time intensive. Gap filling is a common procedure to obtain the position information and to perform subsequent analysis in the MB system due to the occlusion from all scenarios (Camargo, Ramanathan, Csomay-Shanklin, & Young, 2020; G. Liu & McMillan, 2006). Traditional methods of gap-filling MB data are time-intensive since the user must visually inspect each gap and decide the type of interpolation to use as well as how it should be filled with interpolation (Howarth & Callaghan, 2010). Camargo et al. proposed the automated gap-filling method that uses inverse kinematics to close the loop of an iterative process to minimize errors (Camargo et al., 2020). Although they reported that a 21% reduction in the worst-case gap-filling error and an 80% reduction in completion time, the proposed method was run through OpenSim and required the users to have some coding skills.

Taken together, although the MB system enables sub-millimeter accuracy for joint positions and joint angles calculation, limitations of MB systems would propel the advancement towards marker free motion capture technology era.

2. Markerless Systems

The investigation of using ML systems in the biomechanical studies have sprung up since the early 21st century. Markerless systems are based on four components, including a camera system (camera configuration), a body model, the image features used, and the algorithms to estimate the pose of the model (Colyer et al., 2018). Employed configurations typically range from single camera to multiple cameras (Mündermann et al., 2006).

Two major camera systems can be used for markerless motion captures, i.e., RGB-Depth camera, and standard video cameras. Compared to the standard video cameras, the RGB camera systems can be beneficial for the imperfect lightning or background condition and are more affordable. However, since in-depth camera uses technologies (time-of-flight or structured light) that have noises and trade off depth accuracy and spatial resolution (Sarbolandi, Lefloch, & Kolb, 2015), performances reported by the most common in depth camera systems were not precise enough. Microsoft Kinect is the most common in depth camera, however, based on the disclaimer by Clark et al. (Clark, Mentiplay, Hough, & Pua, 2019), the kinematic analysis required carefully chosen and validated for specific uses cases (Mentiplay et al., 2015). The validity for most of the kinematic gait parameters was restricted ($r<0.75$) (Springer & Yogev Seligmann, 2016; Tanaka, Takimoto, Yamasaki, & Higashi, 2018), as well as the substantial errors were reported as RMS error > 10°or Bland-Altman limits of agreement > 10° (Vafadar et al., 2021). Considering the limitations of in-depth camera system in capture rate, capture volume, inoperability in bright sun light, and interference between multiple sensors (Colyer et al., 2018), standard video camera systems may be better fit on markerless systems for biomechanical research.

The rapid development of artificial intelligence algorithms enabled a variety of algorithms to estimate human motion. Earlier algorithms usually relied on shape-from silhouettes and tried to match a detailed kinematic model (Slembrouck et al., 2020). More recently, deep learning-based pose estimation algorithms have become popular. Algorithms based on deep learning are the most powerful as measured by performance on human pose benchmarks (Cao, Simon, Wei, & Sheikh, 2017). The deep learning based pose estimation can often intuitively be understood as a system of an encoder that extracts important (visual) features from the frame, which are then used by the decoder to predict the body parts of interests along with their location in the image frame (Mathis, Schneider, Lauer, & Mathis, 2020).

Prior studies have examined both open sources and commercial algorithms systems. OpenPose is one of the most popular open-source pose estimation technologies (Cao et al., 2017) and is deemed easy to use for biomechanics applications. Several studies have examined multi-camera ML systems using the OpenPose algorithm. Nakano et al. compared the OpenPose based ML with the MB system during walking, countermovement jumping, and ball throwing tasks. The results demonstrated that ML system can correctly reproduce movements, but some manual adjustments were required when OpenPose incorrectly detected joints. The mean absolute errors of 47% joint positions were <20 mm, and 80% of them were <30 mm, and 10% of them were >40 mm (Nakano et al., 2020). The authors also observed that slower movements (walking) had better results compared to the fast movements (jumping and throwing). Slembrouck et al. used 2D joint detections per view from OpenPose to estimate their corresponding 3D positions while tackling the people association problem in the process to allow the tracking of multiple persons at the same time (Slembrouck et al., 2020). They reported that the differences between multi-view 3D human pose estimation and MB system were 6.6 mm- 21.3 mm. Additionally, clinical applications of the OpenPose based ML systems in patients with Parkinson's diseases have also been reported. Although Martinez et al. failed to use DARI system (ML) with OpenPose to discriminate between Off and On states of deep brain stimulation in patients with Parkinson's disease, the results of gait items showing strong negative correlations to the MDS-Unified Parkinson's Disease Rating Scale. Plus, their kinematic data obtained by ML system can discriminate between patients with Parkinson's Disease and healthy controls (Martinez, Garcia-Sarreon, Camara-Lemarroy, Salazar, & Guerrero-González, 2018). Further, another study emphasized the temporospatial measures (step length, walking velocity, step cadence) analyzed by OpenPose algorithms in Parkinson's patients also reported excellent agreement with GAITRite (ICC>0.9) (Shin et al., 2021).

Another popular open source ML algorithm is the DeepLabCut, which allows researchers to assemble a set of labeled training images and train a neural network to automatically track the position of user selected, manually identified landmarks throughout a video (Mathis et al., 2018). Flexibility is the major strength of DeepLabCut. Rather than tracking a predetermined list of external features or landmarks, it can track any feature of interest. The application of DeepLabCut in kinematic data has been reported in the underwater running study. The authors detected that high test–retest reliability of mean stride data, with between-session correlation coefficients of 0.90–0.97, indicating this method can be broadly applied in different fields (Cronin et al., 2019). Drazan et al. compared the DeepLabCut based-ML lower extremity extension/flexion kinematics during a counter movement jump with the MB system (Drazan et al., 2021). They reported that strong agreement between the ML and MB systems, with the coefficient of multiple correlations (CMC) >0.991, and root mean square errors <3.22°. Though the hip's CMC (0.853±0.23) was lower than the knee and foot, the results still indicated the DeepLabCut based- ML system has the potential for biomechanical research in the non-lab environment.

However, due to the requirements of advanced coding skills and in-depth computer science knowledge, commercial systems have developed, and enabled clinicians and researchers use this technology easier. To data, several commercial systems have been tested, including Captury, SIMI Reality, Organic Motion, and Theia3D markerless motion systems. The former three ML systems identify the silhouette of a person, which are beyond this study's scope. The Theia3D markerless, on the other hand, leverages on deep learning algorithms to estimate joint centers.

Theia3D markerless motion capture system, as a deep-learning algorithm based commercial software has been examined from different aspects. Kanko et al. reported that ML system showed excellent agreement with MB system and pressure-sensitive gait mat in spatiotemporal gait parameters. Specifically, no bias or statistical difference were observed for walking spatial measures (e.g., step length, step width, velocity) and a small difference in temporal measures (e.g., swing time and double support time) (Kanko, Laende, Strutzenberger, et al., 2021). The authors later examined the inter-session repeatability of the ML system during treadmill walking. The kinematics results have demonstrated that the average inter-session variability across all joint angles was 2.8° using the ML system, which is smaller than all previously reported values (3.0-3.6°) using the MB system (Kanko, Laende, Selbie, et al., 2021). The inter-trial joint angle variability (on average 2.5°) was larger than previously reported from the MB system (1.0°-

2.4°)(Caravaggi, Benedetti, Berti, & Leardini, 2011; Schwartz, Trost, & Wervey, 2004) but with small margins and consistency between sessions. In addition, the variability ratios were smaller than any previously reported (on average 1.1), indicating that Theia3D ML system can be reliably when measuring gait kinematics. Furthermore, a follow-up concurrent comparison study using the same data detected that the average root mean square distance between corresponding lower extremity joint centers (ML's joint positions – MB's joint position) throughout the stride across thirty participants was less than 2.5 cm, except for the hip joint (3.6 cm). Differences of lower extremity joint angles for flexion/extension and abduction/adduction were from 2.6°-11° (ankle to hip), and rotation about longitudinal axis were 6.9°-13.2°(Kanko, Laende, Davis, et al., 2021). More recently, Lahkar et al. (2022) analyzed the upper extremity kinematics during boxing using the same ML system. Compared to MB system, ML in their study showed higher differences in 3D joint centers at the elbow (more than 3 cm) compared to the shoulder and wrist (<2.5 cm). They also reported relatively weaker agreement was observed along internal/external joint angle rotation but better performance in overall segment velocities (Bhrigu K. Lahkar, Muller, Dumas, Reveret, & Robert, 2022). These strong results further indicated that Theia3D ML system can be a powerful motion capture system in the kinematical studies. Furthermore, one recent study stressed on the clothing conditions for ML system. They observed that the mean differences of segment lengths for the whole body between gym clothing and causal clothing ranged from 0.2 cm to 0.9 cm, which below the typical marker errors (1-2 cm). Although significances between clothing conditions were reported in the spatiotemporal parameters in seven out nine cases, these differences were much smaller than the minimal changes in movement-related pathologies such as multiple sclerosis and cerebral palsy (Keller et al., 2022). Thus, Theia3D ML system has the potential to be employed in the clinical settings without significantly alter the interpretations of results.

Theia3D ML system, which leverages deep-learning algorithms, has exceeded the current ML systems in the market due to its outstanding performance. It has been reported that Theia3D have labelled their own biomechanically applicable data set which identifies 51 keypoints on the body (Kanko, Laende, Davis, et al., 2021; Kanko, Laende, Strutzenberger, et al., 2021), which is superior to other deep learning-based ML systems such as OpenPose that has 25 keypoints. However, the broad application of Theia3D ML system requires more than kinematical examinations. Kinetics that employed the inverse dynamic analysis remain to be tested so that ML systems can further be promoted in the clinical and sports fields.

3. Running Biomechanics

The present study chose running to investigate for its popularity in biomechanical applications and specialty in gait analysis. Running, as one of the most worldwide popular aerobic exercise, has shown a variety of benefits. It can establish enriched cardiovascular, strength, and endurance fitness (Willick & Hansen, 2001), improve bone density, and have a positive effect on mood (Schneider et al., 2009) and cognition (Rolland, van Kan, & Vellas, 2010). However, running can also induce lower extremity injuries, such as patellofemoral pain (T. A. Dierks, Manal, Hamill, & Davis, 2008), iliotibial band syndrome (Orchard, Fricker, Abud, & Mason, 1996), and Achilles tendinopathy (Munteanu & Barton, 2011). A variety of intrinsic and extrinsic factors have been blamed for the development of running-related injuries (Novacheck, 1998). The extensive literature has assured that greater understanding of biomechanics and its applications can improve the diagnosis and counselling, rehabilitation and prevention. In addition, knowledge regarding the biomechanical function of the lower extremity across different running speeds is important in human high performance, aiding athletic training (Anthony G Schache et al., 2011). Limitations of MB motion capture have reduced the running gait analysis in applications of predicting injuries, informing interventions and improving performances. ML has fewer marker-induced problems, which might provide new insights to running gait analysis.

3.1. Running Gait

Running gait can be separated into two phases, the stance and swing phases. Subdivisions of the stance and swing phases are different among researchers. In general, the stance phase is divided into three stages (initial contact, mid support, and take-off phase) and the swing phase is divided by initial swing, mid swing and terminal swing phase (Novacheck, 1998; Õunpuu, 1994). However, during running, there are alternate periods of acceleration and deceleration occur and referred as absorption and generation. Several researchers also categorized them into the stance phase (Õunpuu, 1994). Between stance and swing phase, the transition phase is the conjunction. The stance phase accounts for less than 40% of the gait cycle and the swing phase is taken more than 60% in the running. As the running speed increases, the stance phase time decreases and swing phase increases (Dicharry, 2010). It is reported that world class sprinters toe off as early as 22% of the gait cycle (R. A. Mann & Hagy, 1980).

The primary biomechanical functions of the stance phase during running are to provide stability, and shock absorption (Perry & Burnfield, 2010). At the beginning of the foot strike, the muscle, tendon, bone, and joints of foot and lower leg function to absorb the impact of the landing (Loudon & Reiman, 2012). When the foot is flat on the ground, the mid support is reached. The lower extremity muscles reverse proximal to distal during push off, the foot begins to move from pronation to supination to prepare for take-off (Perry, 1983). The body moves forward over the stance limb represents the generation phase. The body keeps propelling forward until the foot lifts off of the ground, which signifies the take-off. During the swing phase, two double float periods occur. The first double float marks the beginning of the swing phase, which occurs immediately after the take-off (Loudon & Reiman, 2012). Once the foot leaves the ground backward momentum drives the leg posteriorly. The initial swing is achieved when the leg reaches its most posterior position and the knee reaches its maximum flexion angle. Then the limb is reversed and muscles such as rectus femoris contract to pull leg anteriorly initiating the forward swing. Finally, once the limb reaches an optimal position it descends the foot to prepare for initial foot contact, also known as the terminal swing phase. At the end of the swing phase and just prior to initial foot contact is when the second double float period occurs. Then a gait cycle begins when the initial foot contact occurs (Nicola & Jewison, 2012).

3.2. Lower Extremity Kinematics

Novacheck summarized that patterns of movement from the graphic kinematic variables are important while the peak values depend on athlete's level of training and speed are less important (Novacheck, 1998). Although motion in all three planes should be considered, the greatest degree of movement occurs within the extension/flexion plane at the lower extremity joints during running. To discern movements during running it is best to analyze kinematics by each individual joint.

Hip Joint. Extension/flexion plane hip motion is in flexed position upon the initial contact, which can be up to 65° and then extends throughout the stance phase (Õunpuu, 1994). Entering in the swing phase, the hip reaches maximum extension of 20°, which at roughly 75% of the gait cycle, then immediately the hip flexes to place the leg in position for initial contact (Õunpuu, 1994). A maximum hip flexion angle of 65° is achieved towards the end of mid swing, and then 25° of extension while the foot is ready to contact the ground again.

Knee Joint. At the initial foot contact, the knee flexes at 15° to 25°. The knee keeps flexing during the absorption stance phase and reaches the peak at mid-stance, however, sprinting takes shorter absorption period and less knee flexion (Novacheck, 1998). From midstance the knee extends through the propulsive phase of stance until peaking at 20°. During the swing phase, the knee flexes and reaches the maximum around 75% of the gait cycle before extends during terminal swing, reaching maximum extension just prior to ground contact (Novacheck, 1998; Õunpuu, 1994). The average maximum knee flexion is about 90°, highly trained athletes can move to 130° to increase energy efficiency.

Ankle Joint. (Dicharry, 2010; Novacheck, 1998). The dorsiflexion of the ankle continues until the end of the absorption phase when it reaches its peak (Langley, 2015). At toe-off, the ankle is in approximately 25°of plantarflexion. During swing phase, the ankle moves from plantarflexion to dorsiflexion in the mid swing phase, and then back to plantar flexion at the end of terminal swing and right before the next foot contact (Õunpuu, 1994). Compared to walking, net ankle mobility is higher in running.

3.3. Inverse Dynamics Analysis

Although kinematics can explain how the human move and assist the clinical research, they cannot explain the cause of the movement. Kinetics reflect the cause of movement, and therefore the forces, power and energy that affect the manner in which an individual moves. Moments acting at the skeletal joints, as correspond to resultant muscle forces and loading of passive structures (Kristianslund et al., 2012), are used as the primary measure for effort, strain, and overall healthiness of human motion (Zell & Rosenhahn, 2020). Joint power indicates the velocity of the joint moment, or the rate of the work exhibited by the muscles. Inverse dynamics is an established tool to infer joint moments from an observed motion that has been widely used in the biomechanical community. In the standard inverse dynamic method, net joint moments and powers are calculated by combining joint kinematics with measured ground reaction force (David A Winter, 2009).

Noted that the quality of inverse dynamic calculations is greatly affected by not only the biomechanical model but also the input of kinematic data (Silva & Ambrósio, 2002). The kinematic data depend on the chosen anthropometric model parameters, namely body segmental joint parameters (joint positions and orientations) and inertial parameters (masses, mass centers, and moment inertia). Variations in joint and inertial parameters' values as well as kinematic data noise alter the results of inverse dynamics analyses of gait (Reinbolt, Haftka, Chmielewski, & Fregly, 2007). Joint and inertial parameter values used in the literature are mainly based on anatomic landmarks methods from cadaver studies (Alexander L Bell, Pedersen, & Brand, 1990; Dempster, 1955; Inman, 1976). Another method is optimization methods for inertial parameter values but with limited success for plantar models of running, jumping and kicking motions (Vaughan, Andrews, & Hay, 1982). Riemer et al. presented a comprehensive analysis of the uncertainties in joint moment estimates derived through inverse dynamics (Riemer, Hsiao-Wecksler, & Zhang, 2008). Their results suggested that variations of joint and inertial parameter values in joint moments estimates derived through inverse dynamics can be substantial, with the magnitude from 2% to 232%. The more distal joints contribute smaller magnitudes. For the lower extremity, the hip exposes the most variations of joint and inertial parameter values since the anatomic landmark of hip is non-palpable. The hip joint center location errors distort the estimates of angles and resultant moments at the hip and knee joints (Stagni et al., 2000). Prior study detected the 2 cm superolateral placement of hip joint center decreased the moment arms of hip abductor muscles by 28% (Delp, Wixson, Komattu, & Kocmond, 1996). The 3 cm anterior hip joint center placement resulted in the largest propagation errors in hip flexion/extension moments with a mean of -22% (Stagni et al., 2000). Therefore, kinematic data the necessary for inverse dynamic analysis can be greatly affected by the anthropometrical model parameters.

Additionally, kinematic constraints need to be considered due to the independence of kinematic data acquisition from the biomechanical model implemented. However, in the clinical settings, three markers must be used to define each segment so that the rigid body can be considered. Six degrees of freedom in each segment can omit the kinematic constraints to model joints (Ojeda, Martínez-Reina, & Mayo, 2016). Such practice has been widely accepted in the commercial code (e.g. VICON) (Davis, Õunpuu, Tyburski, & Gage, 1991) and by many researchers, which also induce the similar joint dislocation errors due to the lack of modelling joint articulations.

Admittedly, main sources of kinematic data inaccuracies derived from the marker-based systems. The skin motion artifacts are interdependently caused by inertial effects, skin deformations from muscle contractions (Cappozzo et al., 1995). Efforts have been made to minimize the skin artifacts, including using corrective methods such as least squares methods (Alexander & Andriacchi, 2001; Söderkvist & Wedin, 1993) or cluster methods (Alexander &

Andriacchi, 2001). However, skin motion artifacts will remain a challenging in the inverse dynamic calculation unless the markers are no longer needed or the markers are attached to the bone directly or bone pin (Andersen, Benoit, Damsgaard, Ramsey, & Rasmussen, 2010).

Furthermore, the filtering is necessary before conducting the inverse dynamic analysis. The acquisition of kinematic data and ground reaction forces can induce signal noise, operator imprecision and finite precision of equipment (Silva & Ambrósio, 2002). Previous studies have shown the most common used filtering methods were Butterworth filters (David A Winter, 2009) and Fourier series with optimal regularization (Giakas & Baltzopoulos, 1997). Despite the selection of filtering remains questioning, the low-pass filter that removes random noise in the position data has been demonstrated (Chiari et al., 2005). Kristianslund et al. (2011) calculated knee and hip joint moments with four different combinations of cut off frequency for signal filtering. They used movement 10 Hz, force 10 Hz; movement 10 Hz, force 50 Hz, movement 15 Hz, force 15 Hz; and movement 15 Hz, force 50 Hz combinations. They reported the statistically differences of knee abduction moments and hip moments among different combinations (Kristianslund et al., 2012). Thus, filtering choice requires caution in the inverse dynamic analysis.

3.4. Lower Extremity Kinetics

Although kinematics can explain how the human move and assist the clinical research, they cannot explain the cause of the movement. Kinetics reflect the cause of movement, and therefore the forces, power and energy that affect the manner in which an individual moves. Moments acting at the skeletal joints, as correspond to resultant muscle forces and loading of passive structures (Kristianslund et al., 2012), are used as the primary measure for effort, strain, and overall healthiness of human motion (Zell & Rosenhahn, 2020). Joint power indicates the velocity of the joint moment, or the rate of the work exhibited by the muscles.

During running, the hip extensors are dominant at the initial foot contact. The hip extensors continue to generate power through the first half of stance phase. Then hip flexes to and decelerate backward rotating thigh in preparation of swing phase. Hip flexors continue for the first half of the swing phase. Peak hip flexion occurs in the second half of swing in both running and sprinting. After peak flexion occurs the hip extensors contract concentrically to extend the hip in preparation for initial contact.

The knee flexes following the initial contact, and quadriceps contract eccentrically to absorb the power. Then the knee extends in the second half of stance phase while the quadriceps concentrically contract to generate the power in preparation of toe-off. In the swing phase, the knee muscles need to absorb the power in order to control the swinging leg. The rectus femoris contracts eccentrically to control the knee flexion at the early swing, followed by the eccentric contraction of hamstrings during the late swing to prevent knee's hyperextension (Novacheck, 1998).

Noticeably, with each step taken during running, the lower leg and the knee can experience forces up to 11 time of the body weight. The magnitude of knee forces and moments contributes greatly to the running injuries (Scott). It has been reported that approximately 50% of running injuries occur at the knee with nearly half of those involving the patellofemoral joint (Hreljac & Ferber, 2006). The patella plays a large role in running, as its main function is to increase the mechanical advantage of the knee extensor muscles. The patella displaces the quadriceps tendon line of action away from the joint, increasing the moment arm of the quadriceps force, allowing the muscles to generate a larger torque for a given amount of muscle force (Fox, Wanivenhaus, & Rodeo, 2012). Studies have been reported that patellofemoral joint pain syndrome can be aggregated if the external knee flexion moment is increased. This moment during the stance phase must be balanced by the quadriceps to avoid the direct increase in tension in the quadriceps tendon and patellar ligament (T. Andriacchi, 1985).

The patterns of ankle moments during walking and running are similar. Initial contact is with the heel. The forefoot is lowered to the ground under the control of eccentric contraction of the anterior tibial muscles. The onset of the ankle plantarflexion moment occurs at 5–10% of the running gait cycle (Novacheck, 1998). During midstance, the ankle dorsiflexes and the ground reaction force is anterior to the ankle joint line. The GRF is imposing an external torque trying to dorsiflex the ankle, while the runner activates the plantar flexors to generate an equal and opposite internal joint torque to maintain position of the ankle at that particular point in time. Ankle plantar-flexors generate the power during the stance phase for forward propulsion. The magnitude of the ankle power generation is directly related to the athlete’s speed.

It is noteworthy that lower extremity kinetics can be used to understand the muscle functions during running. The role of ankle and knee extensors is to create high joint stiffness before and during contact phase, while the hip extensors are the primary forward movers to the body (Belli et al., 2002).

4. Significances of the Study

It is noteworthy that ML motion capture methods could be invaluable to the clinical and sports biomechanical applications. The convenience of ML systems is undeniable from many aspects. For example, ML systems requires less preparation time for participants and for the motion capture, less clothing and controlled environment restrictions. Promoting the ML systems to a wider usage would benefit more than just researchers and clinicians. It is then necessary to investigate the reliability and validity of ML system under different conditions. Although previous studies have underlined kinematic parameters using ML systems, the gap between kinematic and kinetics would be filled by the current study. Furthermore, the current study would investigate the possible reasons that contribute to the differences if any.

5. Summary and Thesis Aims

The evidence presented within this chapter highlights the dearth of information regarding:

- The development of vision-based motion capture systems.
- The lower extremity kinematics during running.
- The inverse dynamic analysis and lower extremity kinetics.
- The paucity of information relating to these areas brings into question that how markerless systems perform in lower extremity kinetic parameters during running. The application of different running speed can further investigate the relationship of movement speed and motion capture performance.

In order to address these gaps within the current literature the aims of this thesis are;

Overarching aim:

- To compare lower extremity gait biomechanics estimated by marker-based and markerless motion capture systems during treadmill running.

Secondary aims:

- To investigate how movement speed affect the performance of markerless motion capture system.

The work undertaken in line with the aims of this thesis will further develop the methodological approach for investigating lower extremity joint moments and powers estimated by marker-based and markerless systems during running. The information gathered from the comparison will supplement the current understandings of the newly proposed markerless motion capture system. The findings of the work will provide more information for clinicians and coaches if they choose to use markerless systems for injury diagnosis, prevention, and rehabilitation. Furthermore, the findings of the work undertaken to achieve the secondary aim can be advisory when the application of markerless system in the fast movement.

APPENDIX B

EXTENDED DISCUSSION

The purpose of this study was to compare lower extremity joint kinetics estimated by MB and ML systems during treadmill running. Overall, we first observed the significant differences in the peak magnitudes for joint moments and powers and relative timings to peak estimated by MB/ML. We then further verified the differences estimated by two systems were systematic as the running speed altered. To be specific, discrete measurements and time series (SPM) results showed that greater increases of lower extremity joint moments and powers with running speed were observed in the ML than the MB system during the swing phase. The prominent differences were mainly presented at hip and knee joints at both ends of the swing phase. Additionally, the ankle plantarflexion moments in the stance-swing transition phase and the ankle absorption power during the early stance phase were also detected the greater increases in the ML system with speed.

1. Pose Estimations Affect Joint Kinetics

Noted that segment kinetics are derived from these rigid body equations, where their computation requires the estimation of segment mass, the position of center of mass (COM), and its inertia tensor (moments and products of inertia) (Timothy R. Derrick et al., 2020). In most cases, the body segment inertial parameters (BSIPs) estimations using regression equations, where the COM position is consequently dependent on the estimation of joint center (JC) positions (Timothy R. Derrick et al., 2020; Wu et al., 2002).

Given JCs usually defined by regression methods from palpated external anatomical landmarks, using functional approaches or multiple body kinematic optimization techniques, the errors of segment endpoints would greatly affect the segment lengths and later contribute to errors on more than BSIPs (Valentina Camomilla et al., 2017; Timothy R. Derrick et al., 2020). Examples of JCs induced differences in joint kinetics are numerous. Hip JC is the most critical lower extremity joint because of the large distance from the palpable pelvic landmark (Timothy R. Derrick et al., 2020). Kirkwood et al. (1999) compared four non-invasive measures to radiographic systems to locate hip JC and investigated the effects of hip joint moments. According to their study, the most accurate hip JC was to take midpoint of a line connecting the antero-superior iliac spine and the symphysis pubis and moving inferiorly 2 cm, which resulted in minimal discrepancies of hip joint moments in the frontal and transverse planes in comparison to the X-ray measured true location and (Kirkwood, Culham, & Costigan, 1999). Additionally, they noticed that displacing hip JC too far laterally affected both the measures in the frontal and transverse planes, with 16%-34 % higher than those generated by using standard radiography. When displacing the hip JC too far superiorly, it would affect extension/flexion and frontal plane hip moments but not transverse plane (Kirkwood et al., 1999). Another representative study further addressed the effects of hip JC mislocations on propagation to the gait analysis. In their study, they added a constant mislocation error to the nominal hip JC local position and estimated hip and knee joint angles and moment components (Stagni et al., 2000). The results showed that hip JC did not affect hip joint angles significantly but most affected the extension/flexion plane hip joint moments, particularly with a delay of zero crossing of 26.5% when the hip JC was 3 cm posteriorly mislocated (Stagni et al., 2000).

Recalling JC variations we observed in Chapter 2 (refer to Figure 3), hip JCs differences of three axes between ML and MB were more obvious than the knee and ankle, especially in the anterio-posterior direction. Considering the aforementioned evidence from MB system, it is reasonable to induce the differences of JC estimation from MB/ML make contributions to the estimated joint kinetics' distinctions. In addition, recent comparison studies also accumulate indirect evidence to this idea. For example, Kanko et al. (2023) reported that the root mean square distance of JC between MB and ML were smaller than 3 cm of all joints, where the hip joint had the biggest variation. They also demonstrated the partially consistent results of the lower extremity joint moments during treadmill running with ours, however, their study did not explain any relationship between JC and joint kinetics (Kanko, Outerleys, Laende, Selbie, & Deluzio, 2023).

To date, no other studies using Theia3D compared the pose estimations, joint kinetics and their relationships, however, OpenPose as an open source shared similar algorithm principles as Theia3D has been well-studied. For example, Nakano et al. (2020) evaluated the joint positions estimated by OpenPose ML and MB in walking, countermovement jumping and ball throwing tasks (Nakano et al., 2020). They detected that differences of joint positions estimated by two system were presented by mean of errors, where 47% were smaller than 20 mm, and 80% were less than 30 mm. They suggested that faster movement would increase the distinctions of joint positions. Van Hoorah et al. (2023) added credits to their indications by providing differences of running kinematics at 2.78 and 3.33 m/s. They reported that OpenPose showed no statistical differences at 2.78 m/s but statistically smaller knee flexion angle during the mid-late stance phase than MB system at 3.33 m/s (Van Hooren, Pecasse, Meijer, & Essers, 2023). Additionally, Needham et al. (2021) revealed the accuracy of 3D joint centers estimated by ML (OpenPose, AlphaPose and DeepLab) and MB systems. Their results further emphasized the largest systematic JC difference occurred at the hip joint during running with a mean differences of 29 mm (Needham et al., 2021). Besides, the wider range of limb configurations and segment velocities potentially caused the lower pose estimation performance during running. Noted that their results showed systematic JC differences among three ML systems, possible reason is attributed to the training datasets exist mislocation issue then supervised learning techniques only enlarge the mislabeled locations (Needham et al., 2021).

Due to the variations of JC positions, the segment endpoints would vary, directly leading to the differences of segment COM positions. Besides, not only individual BSIP component would affect joint kinetics, the relationship between components also contributes to the accuracy of inverse dynamic calculation (Rao, Amarantini, Berton, & Favier, 2006). Although different statistical techniques or modeling the segments as geometric solids of known density also need to be considered as fundamental factors when underlining the BSIPs (Valentina Camomilla et al., 2017), these are strictly controlled in the comparison studies. Supported evidence came from Wesseling et al. (2014), who examined the BSPs perturbations (±40%) on joint moments. They not only investigated the effects of single component but also integrated compartments of BSIPs. The results showed that the single leg COM perturbation greatly influenced the hip flexion moment within the maximal -7.81 Nm, especially the COM changes occurred at the distal direction (Wesseling, de Groote, & Jonkers, 2014). In addition, Nguyen and Reynolds (2013) used Monte Carlo methods to simulate the effects of BISP variations on joint moments. They highlighted the swing phase even during slow movements such as walking, stating that variations of BISPs significantly affected the hip and knee joint moments (Nguyen & Reynolds, 2014). Recall our observed differences of segment COMs estimated by ML and MB (refer to Chapter 2, figure 4), all three segments had larger variations during the swing phase. Given the segment inertial loads dominate the swing phase, it is then reasonable to state that BSIPs also may elicit distinctions of joint kinetics estimated by the two systems.

2. Injury Prediction and Accommodation Indication

Systematic differences observed in the current study could have significant implications. Given that joint kinetics are useful indicators of various physical stress related placed on neuromuscular system (David A. Winter, 1983), it is pivotal to use such indirect mechanism to study injury and indicate accommodation strategies during running.

Hamstring muscle strain injury is common and highly prevalent especially during fast running or sprinting. Previous studies have disputed about the timing of hamstring injury occurrence. Some studies have argued that the hamstrings are more likely to be injured during the stance phase. For example, Mann and Sprague (1980) firstly reported the maximum knee flexion and hip extension moment during the early stance phase during overground sprinting, indicating the potential hamstring muscle strain injury (R. Mann & Sprague, 1980). Supported by Liu et al. (2017), they used intersegmental dynamic analysis and highlighted the early stance phase is hazardous for hamstring injury (Y. Liu, Sun, Zhu, & Yu, 2017). They observed that the dominant passive torque switched to external contact torque in the transition from late swing to initial stance phase. Hamstring muscles served to counterbalance the ground reaction forces (GRFs) that have passed anteriorly to the knee and hip and generated large knee extension and hip flexion torques. Such enormous torques are almost 8 times of the subject's body weights, making it more susceptible to injure. Additionally, Yu et al. (2008) examined the hamstring muscle-tendon kinematics and muscle activation during overground sprinting (Yu et al., 2008) and observed both late stance and late swing phase were potential for hamstring muscle strain injury. Their results showed that hamstring muscles exhibited eccentric contraction during the late stance, where peak eccentric contraction speeds were lower than late swing but hamstring muscle-tendon lengths at the peak eccentric contraction speed were greater. The hamstring muscle elongation velocity was higher during the late stance phase, indicating the strain injury may be more likely occur at the hamstring muscle-tendon junction during the late stance (Best, McElhaney, Garrett, & Myers, 1995). Noticeably, Yu et al.'s suggestions of hamstring injury was based on eccentric contraction, the function of muscle strain (Lieber & Friden, 1993). However, the results of Mann and Sprague's suggested the muscle forces were the indicators.

On the other hand, more studies have addressed the swing phase. For example, Thelen et al. (2005) conducted the hamstring kinematics exploration during treadmill sprinting and emphasized the maximum hamstring lengths occurred during the late swing before foot contact (Thelen et al., 2005). To be specific, they measured the muscle-tendon stretch, relative to muscle-tendon lengths among bicep femoris semitendinosus and semimembranosus muscles. The observed peak hamstring lengths occurred when the hip is highly flexed and knee is slightly flexed during the late swing phase. The greater hip flexion caused the greater lengthening of semitendinosus and bicep femoris while the slight knee flexion contributed to reduction in overall length of biarticular hamstrings. The combined effects would lead to greater stretch of bicep femoris is in need during sprinting, also inducing higher potential injury rate at the long head bicep femoris. Noted that Thelen et al. did not observe any significant changes of peak hamstring lengths as running speed increased, however, another study later reported that lateral hamstring loading increased significantly with speed (Elizabeth S Chumanov et al., 2011). Chumanov et al. (2011) used the whole body musculoskeletal modeling as well as EMG activities to stress on late swing phase is more hazardous to hamstring strain injury than the stance phase. In particular, their results showed that the hamstring musculotendons lengthened, with the negative work done only during swing phase. They also observed two distinct loading peaks for the hamstrings at late swing and early stance phases, however, only the peak musculotendon force during swing increased significantly with the speed. Consistent with many other studies, their results further corroborated the opinion that inertial loads put the lengthening hamstrings at risk for injury during high speed running (Elizabeth S. Chumanov et al., 2007; Bryan C. Heiderscheit et al., 2005; Anthony G. Schache, Wrigley, Baker, & Pandy, 2009).

In addition, Schache et al. (2009) underlined the biomechanical response to prior to and immediate after right hamstring strain (Anthony G. Schache et al., 2009). In their study, the pre-injury trial results showed that the increased knee extension, greater hamstring muscle tendon unit length and earlier occurrence during terminal swing. This may have resulted in larger right hamstring muscle fiber strains, the magnitude of which has been shown to relate to muscle damage (Lieber & Friden, 1993). They also reported that significant biomechanical reactions on the right hamstring strain during the proceeding swing phase in the injury trial, especially the substantial reductions in the right hip and knee joint torques and powers. Hamstrings appear to be most biomechanically exposed during the terminal swing phase. Except for the gastrocnemius's capability to stabilize the swinging leg (Li, Landin, Grodesky, & Myers, 2002), hamstrings bear the most inertial loads acting at the knee joint during the swing phase.

Recall our comparison results from Chapter 2 and 3, ML estimated greater hip and knee joint moments during the swing phase as the running speed increased, it may lead to an increased injury-risk estimation for both parallel and cross-sectional hamstring injuries (Li & Wang, 2017).

Besides hamstring injury, patellofemoral pain is another common running injury. Although a majority of studies have focused on lower extremity biomechanical responses in the frontal and transverse planes, some studies underpinned the changes of the hip and knee joints in the extension/flexion plane. (Timothy R Derrick, Dereu, & McLean, 2002; T. A. Dierks et al., 2008; Souza & Powers, 2009). In particular, Souza and Powers (2009) compared the differences of hip kinematics, hip muscle strength and hip muscle activation patterns in female with PFP and controls (Souza & Powers, 2009). They demonstrated that female with PFP showed greater hip internal rotation was accompanied by significant decrease in hip extension strength. They also observed that a 16% decrease in hip extensor torque production in PFP subjects, which might contribute to the increased hip internal rotation (Souza & Powers, 2009). Additionally, Dierks et al. (2011) compared the patellofemoral pain (PFP) runners and controls during the prolonged treadmill running. Compared to the control group, individuals with PFP exhibited reduced peak knee flexion, peak hip adduction, and eversion excursion, as well as slower peak knee flexion velocity, peak hip adduction velocity, and peak hip internal rotation velocity. Notably, there was a significant overall increase in most kinematic variables towards the end of the running task (T. Dierks, Manal, & Hamill, 2011). The reduction of knee flexion may be a protective mechanism against knee pain in PFP runners (Powers, Chen, Reischl, & Perry, 2002; Powers, Heino, Rao, & Perry, 1999). Noted that knee joint is sensitive to changes in step rate, studies have suggested that increasing step rate could reduce the magnitude of knee joint loading and hence to relieve the PFP pain (R. L. Lenhart, Thelen, Wille, Chumanov, & Heiderscheit, 2014). Specifically, as step rate increased, there was a simultaneous rise in the maximum loads experienced by the rectus femoris and hamstring muscles during early and late swing, respectively. Furthermore, the peak knee flexion during the stance phase decreased with higher step rates and was identified as the most significant predictor of the decrease in patellofemoral joint loading (R. L. Lenhart et al., 2014). Notably, rectus femoris as another biarticular muscle, is associated with hip flexion and knee extension moments. When greater inertial loads act to the rectus femoris during the early swing phase, the patellar tension would subsequently increase (R. Lenhart, Thelen, & Heiderscheit, 2014).

Recall our results showing greater hip and knee joint moments estimated by ML system during the swing phase, it would contribute to misinterpretations of potential patellofemoral pain. In addition, accommodation strategies such as increase the step rate is correlated to the decreased knee flexions during the stance phase. However, estimation of such knee flexion during stance from ML system (Chapter 2. Figure 1-middle panel) actually showed smaller magnitudes than MB. If coaches and clinicians use ML estimations as judgmental criteria, it would obfuscate the underlying issue that further jeopardize athletes' patellofemoral problems.

Last but not least, overloading issues regarding ankle and knee joint also requires some attention. Ankle plantarflexion is critical to knee and ankle stability, restrained forward rotation of the tibia on the talus during the stance phase (Gabel & Manoli, 1994). Additionally, plantarflexion moments at the ankle joint have been shown to be related to Achilles tendon loading (Fukashiro, Komi, Järvinen, & Miyashita, 1993). Greater ankle plantarflexion would indicate more Achilles tendon loading, which may contribute to Achilles tendon overuse injuries (Mahieu, Witvrouw, Stevens, Van Tiggelen, & Roget, 2006).

To sum up, the results from the current study indicate the overestimation from ML exacerbated by speeds could lead to over-estimated running-related injury risks if used in sports biomechanics. With different injury risk levels estimated by MB or ML systems, it would be challenging for clinicians to make rehabilitation plans, and for coaches and athletes to design accommodation strategies.

3. Usability of ML in the Clinical Settings

While the ML system may still be considered in its infancy, it remains worthwhile for the clinical and sports settings despite the differences between MB/ML we observed here. Advantages of ML are prominent, especially for the clinical settings. First, short preparation time is more convenient. Since pose estimation algorithms are not dependent on markers attached to the skin, soft tissue artifact errors and human errors usually induced by the MB systems can be eliminated [134]. The differences caused by loose clothing reported in the spatiotemporal parameters, which were lower than typical marker placement-related differences, were smaller than the minimal changes in movement-related pathologies such as multiple sclerosis and cerebral palsy (Keller et al., 2022). Second, movements, such as, underwater running (Cronin et al., 2019), counter movement jump (Drazan et al., 2021; Song, Hullfish, Silva, Silbernagel, & Baxter, 2023), and ball throwing (Nakano et al., 2020), will not be restricted by markers. Moreover, the Theia3D ML system has shown strong results in the inter-session joint angles variability during walking (Kanko, Laende, Selbie, et al., 2021), demonstrating it can be an unobtrusive method to monitor patients in their daily lives. For example, using ML system to monitor gait of patients with Parkinson's disease is potential. Prior studies have demonstrated that using monocular ML system to examine gait parameters of Parkinson's disease patients can provide clinicians with overview of disease progression and detect the minor gait disturbances that can be unnoticed by clinicians (Mathis et al., 2018; Shin et al., 2021).

Additionally, studies also presented that the markerless system can extract new information from old datasets (Kidziński et al., 2020; Shin et al., 2021). The development of pose estimation software may enable future ML systems to integrate both phone camera and processor to provide compact and affordable ML motion capture methods (Steinert et al., 2020). Therefore, the potential of ML system in the clinical settings is promising.

4. Limitations

The following limitations of this work should be addressed. First, our participants' pool was limited to recreationally active young adults. Different population groups may have anatomical deformities, affecting the comparison between the systems. For example, more recent studies have applied ML on overground walking gait of children with cerebral palsy and adults with chronic stroke. They reported root mean square values of joint angle variables were acceptable for ML system compared to MB (E. A. Steffensen, Magalhães, Knarr, & Kingston, 2023). However, similar drawbacks as ours. Their participants' amount was even smaller than ours.

Second, hardware constraints such as treadmill settings, cameras resolutions, and marker placements. To be specific, we analyzed treadmill running, where the treadmill settings may constrain the speed. The treadmill settings could result in altered gait mechanics that do not accurately reflect the subject's true gait, which can compromise the accuracy of the gait analysis. Additionally, despite our updated Vicon high-resolution video cameras employed for markerless data, the Vicon Bonita series infrared cameras used here do not provide us with the highest resolution available on the market. Lower camera resolution may cause trajectory errors in the identifications of landmarks (Zago et al., 2020). Marker placements could be distinguished in each lab, which could further affect the joint kinetics during running (Osis, Hettinga, Macdonald, & Ferber, 2016).

Moreover, we only investigated the speed effects of treadmill running, and hence it remains unclear if the ML overestimations of joint moments and powers would apply to other movements. Within our experimental design, we observed interactions at the ankle joint moment during the early swing phase and ankle joint power during the initial stance phase, however, these observations were not consistent with the results of discrete measurements. Further investigations on ankle joint are needed to explain such inconsistency. In addition, the current study stressed on joint kinetics in the extension/flexion plane which primarily attributes to running movements. However, many lower extremity muscles have specific actions that are not limited to a single plane. For example, rectus femoris and bicep femoris muscles induce frontal hip motion (Hunter et al., 2009), functioning as stabilizers during running (Novacheck, 1998). Therefore, to predict running injuries, improve running performance, lower extremity motion in other planes may need further investigation using the ML system.

5. Direction for Future Research

Future research is recommended to address the aforementioned limitations. The current study used SPM statistical analysis and incorporated with traditional ones, however, the ankle joint moments results mismatched. Given the Spatial Parameter Mapping analysis is a time continuous analysis, the timing variability exhibited in healthy populations can disrupt timing of biomechanical events (Honert & Pataky, 2021). Honert and Pataky (2021) demonstrated that multiple SPM tests can be performed to determine if statistical outcomes are due to temporal shifting or differences in magnitude (Honert & Pataky, 2021). Therefore, future works also need to be cautious about methodology for statistics.

Repeating the work undertaken within this thesis but expanding the scope of the study to include different movements would advance markerless (ML)'s feasibility in more biomechanical applications. Besides the lower extremity kinematic and kinetic measurements, upper extremity also requires further exploration given its importance in various sports. Additionally, future work could explore the two systems in different populations such as patients with abnormal gaits to verify the clinical adaptability. Till now, a few studies have focused on kinematics of children with cerebral palsy or adults with chronic strokes (M. Steffensen, Magalhaes PhD, Knarr PhD, & Kingston PhD, 2023). One study also discussed the participants with lower limb amputation (Song et al., 2023) but with only four men participants. Although these recent studies have reported positive results of ML in kinematic gaits, due to their small participant's pool and the lack of kinetic performance, future work remains needed.

REFERENCE LIST

Alexander, E. J., & Andriacchi, T. P. (2001). Correcting for deformation in skin-based marker systems. Journal of Biomechanics, 34(3), 355-361. doi:https://doi.org/10.1016/S0021-9290(00)00192-5

Andersen, M. S., Benoit, D. L., Damsgaard, M., Ramsey, D. K., & Rasmussen, J. (2010). Do kinematic models reduce the effects of soft tissue artefacts in skin marker-based motion analysis? An in vivo study of knee kinematics. Journal of Biomechanics, 43(2), 268-273. doi:https://doi.org/10.1016/j.jbiomech.2009.08.034

Andriacchi, T. (1985). The biomechanics of running and knee injuries. Paper presented at the Symposium on Sports Medicine: the Knee.

Andriacchi, T. P., Alexander, E. J., Toney, M. K., Dyrby, C., & Sum, J. (1998). A point cluster method for in vivo motion analysis: applied to a study of knee kinematics. J Biomech Eng, 120(6), 743-749. doi:10.1115/1.2834888

Arampatzis, A., Brüggemann, G.-P., & Metzler, V. (1999). The effect of speed on leg stiffness and joint kinetics in human running. Journal of Biomechanics, 32(12), 1349-1353. doi:https://doi.org/10.1016/S0021-9290(99)00133-5

Baker, R. (2006). Gait analysis methods in rehabilitation. Journal of NeuroEngineering and Rehabilitation, 3(1), 4. doi:10.1186/1743-0003-3-4

Bell, A. L., Brand, R. A., & Pedersen, D. R. (1989). Prediction of hip joint centre location from external landmarks. Human Movement Science, 8(1), 3-16. doi:https://doi.org/10.1016/0167-9457(89)90020-1

Bell, A. L., Pedersen, D. R., & Brand, R. A. (1990). A comparison of the accuracy of several hip center location prediction methods. Journal of Biomechanics, 23(6), 617-621.

Belli, A., Kyröläinen, H., & Komi, P. V. (2002). Moment and Power of Lower Limb Joints in Running. Int J Sports Med, 23(02), 136-141.

Best, T. M., McElhaney, J. H., Garrett, W. E., Jr., & Myers, B. S. (1995). Axial Strain Measurements in Skeletal Muscle at Various Strain Rates. Journal of Biomechanical Engineering, 117(3), 262-265. doi:10.1115/1.2794179

Camargo, J., Ramanathan, A., Csomay-Shanklin, N., & Young, A. (2020). Automated gap-filling for marker-based biomechanical motion capture data. Computer Methods in Biomechanics and Biomedical Engineering, 23(15), 1180-1189. doi:10.1080/10255842.2020.1789971

Camomilla, V., Bonci, T., & Cappozzo, A. (2017). Soft tissue displacement over pelvic anatomical landmarks during 3-D hip movements. Journal of Biomechanics, 62, 14-20. doi:https://doi.org/10.1016/j.jbiomech.2017.01.013

Camomilla, V., Cereatti, A., Cutti, A. G., Fantozzi, S., Stagni, R., & Vannozzi, G. (2017). Methodological factors affecting joint moments estimation in clinical gait analysis: a systematic review. BioMedical Engineering OnLine, 16(1), 106. doi:10.1186/s12938-017-0396-x

Cao, Z., Simon, T., Wei, S.-E., & Sheikh, Y. (2017). Realtime multi-person 2d pose estimation using part affinity fields. Paper presented at the Proceedings of the IEEE conference on computer vision and pattern recognition.

Cappozzo, A., Cappello, A., Croce, U. D., & Pensalfini, F. (1997). Surface-marker cluster design criteria for 3-D bone movement reconstruction. IEEE Transactions on Biomedical Engineering, 44(12), 1165-1174. doi:10.1109/10.649988

Cappozzo, A., Catani, F., Della Croce, U., & Leardini, A. (1995). Position and orientation in space of bones during movement: anatomical frame definition and determination. Clinical Biomechanics, 10(4), 171-178. doi:https://doi.org/10.1016/0268-0033(95)91394-T

Cappozzo, A., Della Croce, U., Leardini, A., & Chiari, L. (2005). Human movement analysis using stereophotogrammetry: Part 1: theoretical background. Gait & Posture, 21(2), 186-196. doi:https://doi.org/10.1016/j.gaitpost.2004.01.010

Cappozzo, A., Marchetti, M., & Tosi, V. (1992). Biolocomotion: a century of research using moving pictures (Vol. 1): Promograph.

Caravaggi, P., Benedetti, M. G., Berti, L., & Leardini, A. (2011). Repeatability of a multi-segment foot protocol in adult subjects. Gait & Posture, 33(1), 133-135. doi:https://doi.org/10.1016/j.gaitpost.2010.08.013

Ceyssens, L., Vanelderen, R., Barton, C., Malliaras, P., & Dingenen, B. (2019). Biomechanical Risk Factors Associated with Running-Related Injuries: A Systematic Review. Sports Medicine, 49(7), 1095-1115. doi:10.1007/s40279-019-01110-z

Chen, S., Lach, J., Lo, B., & Yang, G. Z. (2016). Toward Pervasive Gait Analysis With Wearable Sensors: A Systematic Review. IEEE Journal of Biomedical and Health Informatics, 20(6), 1521-1537. doi:10.1109/JBHI.2016.2608720

Chiari, L., Croce, U. D., Leardini, A., & Cappozzo, A. (2005). Human movement analysis using stereophotogrammetry: Part 2: Instrumental errors. Gait & Posture, 21(2), 197-211. doi:https://doi.org/10.1016/j.gaitpost.2004.04.004

Chumanov, E. S., Heiderscheit, B. C., & Thelen, D. G. (2007). The effect of speed and influence of individual muscles on hamstring mechanics during the swing phase of sprinting. Journal of Biomechanics, 40(16), 3555-3562. doi:https://doi.org/10.1016/j.jbiomech.2007.05.026

Chumanov, E. S., Heiderscheit, B. C., & Thelen, D. G. (2011). Hamstring musculotendon dynamics during stance and swing phases of high speed running. Medicine and science in sports and exercise, 43(3), 525.

Clark, R. A., Mentiplay, B. F., Hough, E., & Pua, Y. H. (2019). Three-dimensional cameras and skeleton pose tracking for physical function assessment: A review of uses, validity, current developments and Kinect alternatives. Gait & Posture, 68, 193-200. doi:https://doi.org/10.1016/j.gaitpost.2018.11.029

Collins, T. D., Ghoussayni, S. N., Ewins, D. J., & Kent, J. A. (2009). A six degrees-of-freedom marker set for gait analysis: Repeatability and comparison with a modified Helen Hayes set. Gait & Posture, 30(2), 173-180. doi:https://doi.org/10.1016/j.gaitpost.2009.04.004

Colyer, S. L., Evans, M., Cosker, D. P., & Salo, A. I. T. (2018). A Review of the Evolution of Vision-Based Motion Analysis and the Integration of Advanced Computer Vision Methods Towards Developing a Markerless System. Sports Medicine - Open, 4(1), 24. doi:10.1186/s40798-018-0139-y

Cronin, N. J., Rantalainen, T., Ahtiainen, J. P., Hynynen, E., & Waller, B. (2019). Markerless 2D kinematic analysis of underwater running: A deep learning approach. Journal of Biomechanics, 87, 75-82. doi:https://doi.org/10.1016/j.jbiomech.2019.02.021

Davis, R. B., Õunpuu, S., Tyburski, D., & Gage, J. R. (1991). A gait analysis data collection and reduction technique. Human Movement Science, 10(5), 575-587. doi:https://doi.org/10.1016/0167-9457(91)90046-Z

de Vries, W. H. K., Veeger, H. E. J., Baten, C. T. M., & van der Helm, F. C. T. (2009). Magnetic distortion in motion labs, implications for validating inertial magnetic sensors. Gait & Posture, 29(4), 535-541. doi:https://doi.org/10.1016/j.gaitpost.2008.12.004

Della Croce, U., Leardini, A., Chiari, L., & Cappozzo, A. (2005). Human movement analysis using stereophotogrammetry: Part 4: assessment of anatomical landmark misplacement and its effects on joint kinematics. Gait & Posture, 21(2), 226-237. doi:https://doi.org/10.1016/j.gaitpost.2004.05.003

Delp, S. L., Wixson, R. L., Komattu, A. V., & Kocmond, J. H. (1996). How Superior Placement of the Joint Center in Hip Arthroplasty Affects the Abductor Muscles. Clinical Orthopaedics and Related Research (1976-2007), 328. Retrieved from https://journals.lww.com/corr/Fulltext/1996/07000/How_Superior_Placement_of_the_Joint_Center_in_Hip.22.aspx

Dempster, W. T. (1955). Space requirements of the seated operator, geometrical, kinematic, and mechanical aspects of the body with special reference to the limbs. Retrieved from

Derrick, T. R., Dereu, D., & McLean, S. P. (2002). Impacts and kinematic adjustments during an exhaustive run. Medicine & Science in Sports & Exercise, 34(6), 998-1002.

Derrick, T. R., van den Bogert, A. J., Cereatti, A., Dumas, R., Fantozzi, S., & Leardini, A. (2020). ISB recommendations on the reporting of intersegmental forces and moments during human motion analysis. Journal of Biomechanics, 99, 109533. doi:https://doi.org/10.1016/j.jbiomech.2019.109533

Dicharry, J. (2010). Kinematics and Kinetics of Gait: From Lab to Clinic. Clinics in Sports Medicine, 29(3), 347-364. doi:10.1016/j.csm.2010.03.013

Dierks, T., Manal, K., & Hamill, J. (2011). Recent reviews. Medicine and science in sports and exercise, 43(4), 693-700.

Dierks, T. A., Manal, K. T., Hamill, J., & Davis, I. S. (2008). Proximal and Distal Influences on Hip and Knee Kinematics in Runners With Patellofemoral Pain During a Prolonged Run. Journal of Orthopaedic & Sports Physical Therapy, 38(8), 448-456. doi:10.2519/jospt.2008.2490

Dorn, T. W., Schache, A. G., & Pandy, M. G. (2012). Muscular strategy shift in human running: dependence of running speed on hip and ankle muscle performance. Journal of Experimental Biology, 215(11), 1944-1956. doi:10.1242/jeb.064527

Drazan, J. F., Phillips, W. T., Seethapathi, N., Hullfish, T. J., & Baxter, J. R. (2021). Moving outside the lab: Markerless motion capture accurately quantifies extension/flexion plane kinematics during the vertical jump. Journal of Biomechanics, 125, 110547. doi:https://doi.org/10.1016/j.jbiomech.2021.110547

Dugan, S. A., & Bhat, K. P. (2005). Biomechanics and Analysis of Running Gait. Physical Medicine and Rehabilitation Clinics, 16(3), 603-621. doi:10.1016/j.pmr.2005.02.007

Ferrari, A., Benedetti, M. G., Pavan, E., Frigo, C., Bettinelli, D., Rabuffetti, M., . . . Leardini, A. (2008). Quantitative comparison of five current protocols in gait analysis. Gait & Posture, 28(2), 207-216. doi:https://doi.org/10.1016/j.gaitpost.2007.11.009

Fox, A. J. S., Wanivenhaus, F., & Rodeo, S. A. (2012). The Basic Science of the Patella: Structure, Composition, and Function. J Knee Surg, 25(02), 127-142.

Franklyn-Miller, A., Roberts, A., Hulse, D., & Foster, J. (2014). Biomechanical overload syndrome: defining a new diagnosis. British Journal of Sports Medicine, 48(6), 415. doi:10.1136/bjsports-2012-091241

Fukashiro, S., Komi, P. V., Järvinen, M., & Miyashita, M. (1993). Comparison between the directly measured achilles tendon force and the tendon force calculated from the ankle joint moment during vertical jumps. Clinical Biomechanics, 8(1), 25-30. doi:https://doi.org/10.1016/S0268-0033(05)80006-3

Fukuchi, R. K., Fukuchi, C. A., & Duarte, M. (2017). A public dataset of running biomechanics and the effects of running speed on lower extremity kinematics and kinetics. PeerJ, 5, e3298.

Fuller, J., Liu, L.-J., Murphy, M., & Mann, R. (1997). A comparison of lower-extremity skeletal kinematics measured using skin-and pin-mounted markers. Human Movement Science, 16(2-3), 219-242.

Gabel, S., & Manoli, A. (1994). Neglected Rupture of the Achilles Tendon. Foot & Ankle International, 15(9), 512-517. doi:10.1177/107110079401500912

Ganley, K. J., & Powers, C. M. (2004). Determination of lower extremity anthropometric parameters using dual energy X-ray absorptiometry: the influence on net joint moments during gait. Clinical Biomechanics, 19(1), 50-56. doi:https://doi.org/10.1016/j.clinbiomech.2003.08.002

Giakas, G., & Baltzopoulos, V. (1997). A comparison of automatic filtering techniques applied to biomechanical walking data. Journal of Biomechanics, 30(8), 847-850. doi:https://doi.org/10.1016/S0021-9290(97)00042-0

Gorton, G. E., Hebert, D. A., & Gannotti, M. E. (2009). Assessment of the kinematic variability among 12 motion analysis laboratories. Gait & Posture, 29(3), 398-402. doi:https://doi.org/10.1016/j.gaitpost.2008.10.060

Hanavan, E. P. (1964). A Mathematical Model of the Human Body. AMRL Technical Report, 64-102.

Heiderscheit, B. C., Chumanov, E. S., Michalski, M. P., Wille, C. M., & Ryan, M. B. (2011). Effects of step rate manipulation on joint mechanics during running. Medicine and science in sports and exercise, 43(2), 296.

Heiderscheit, B. C., Hoerth, D. M., Chumanov, E. S., Swanson, S. C., Thelen, B. J., & Thelen, D. G. (2005). Identifying the time of occurrence of a hamstring strain injury during treadmill running: A case study. Clinical Biomechanics, 20(10), 1072-1078. doi:https://doi.org/10.1016/j.clinbiomech.2005.07.005

Honert, E. C., & Pataky, T. C. (2021). Timing of gait events affects whole trajectory analyses: A statistical parametric mapping sensitivity analysis of lower limb biomechanics. Journal of Biomechanics, 119, 110329. doi:https://doi.org/10.1016/j.jbiomech.2021.110329

Howarth, S. J., & Callaghan, J. P. (2010). Quantitative assessment of the accuracy for three interpolation techniques in kinematic analysis of human movement. Computer Methods in Biomechanics and Biomedical Engineering, 13(6), 847-855. doi:10.1080/10255841003664701

Hreljac, A., & Ferber, R. (2006). A biomechanical perspective of predicting injury risk in running : review article. International SportMed Journal, 7(2), 98-108. doi:10.10520/EJC48590

Hunter, B. V., Thelen, D. G., & Dhaher, Y. Y. (2009). A three-dimensional biomechanical evaluation of quadriceps and hamstrings function using electrical stimulation. IEEE Transactions on Neural Systems and Rehabilitation Engineering, 17(2), 167-175.

Inman, V. T. (1976). The joints of the ankle. Williams & Wilkins, Baltimore.

Kanko, R. M., Laende, E., Selbie, W. S., & Deluzio, K. J. (2021). Inter-session repeatability of markerless motion capture gait kinematics. Journal of Biomechanics, 121, 110422. doi:https://doi.org/10.1016/j.jbiomech.2021.110422

Kanko, R. M., Laende, E. K., Davis, E. M., Selbie, W. S., & Deluzio, K. J. (2021). Concurrent assessment of gait kinematics using marker-based and markerless motion capture. Journal of Biomechanics, 127, 110665. doi:https://doi.org/10.1016/j.jbiomech.2021.110665

Kanko, R. M., Laende, E. K., Strutzenberger, G., Brown, M., Selbie, W. S., DePaul, V., . . . Deluzio, K. J. (2021). Assessment of spatiotemporal gait parameters using a deep learning algorithm-based markerless motion capture system. Journal of Biomechanics, 122, 110414. doi:https://doi.org/10.1016/j.jbiomech.2021.110414

Kanko, R. M., Outerleys, J. B., Laende, E. K., Selbie, W. S., & Deluzio, K. J. (2023). Comparison of concurrent and asynchronous running kinematics and kinetics from marker-based motion capture and markerless motion capture under two clothing conditions. bioRxiv, 2023.2002.2022.529537. doi:10.1101/2023.02.22.529537

Keller, V. T., Outerleys, J. B., Kanko, R. M., Laende, E. K., & Deluzio, K. J. (2022). Clothing condition does not affect meaningful clinical interpretation in markerless motion capture. Journal of Biomechanics, 141, 111182. doi:https://doi.org/10.1016/j.jbiomech.2022.111182

Kerkhoff, A., Wagner, H., & Peikenkamp, K. (2020). Comparison of six different marker sets to analyze knee kinematics and kinetics during landings. 6(2). doi:doi:10.1515/cdbme-2020-2009

Kessler, S. E., Rainbow, M. J., Lichtwark, G. A., Cresswell, A. G., D'Andrea, S. E., Konow, N., & Kelly, L. A. (2019). A direct comparison of biplanar videoradiography and optical motion capture for foot and ankle kinematics. Frontiers in bioengineering and biotechnology, 7, 199.

Kidziński, Ł., Yang, B., Hicks, J. L., Rajagopal, A., Delp, S. L., & Schwartz, M. H. (2020). Deep neural networks enable quantitative movement analysis using single-camera videos. Nature Communications, 11(1), 4054. doi:10.1038/s41467-020-17807-z

Kirkwood, R. N., Culham, E. G., & Costigan, P. (1999). Radiographic and non-invasive determination of the hip joint center location: effect on hip joint moments. Clinical Biomechanics, 14(4), 227-235. doi:https://doi.org/10.1016/S0268-0033(98)00073-4

Knippenberg, E., Verbrugghe, J., Lamers, I., Palmaers, S., Timmermans, A., & Spooren, A. (2017). Markerless motion capture systems as training device in neurological rehabilitation: a systematic review of their use, application, target population and efficacy. Journal of NeuroEngineering and Rehabilitation, 14(1), 61. doi:10.1186/s12984-017-0270-x

Kristianslund, E., Krosshaug, T., & van den Bogert, A. J. (2012). Effect of low pass filtering on joint moments from inverse dynamics: Implications for injury prevention. Journal of Biomechanics, 45(4), 666-671. doi:https://doi.org/10.1016/j.jbiomech.2011.12.011

Lahkar, B. K., Chaumeil, A., Dumas, R., Muller, A., & Robert, T. (2022). Description, Development and Dissemination of Two Consistent Marker-based and Markerless Multibody Models. bioRxiv, 2022.2011.2008.515577. doi:10.1101/2022.11.08.515577

Lahkar, B. K., Muller, A., Dumas, R., Reveret, L., & Robert, T. (2022). Accuracy of a markerless motion capture system in estimating upper extremity kinematics during boxing. Frontiers in sports and active living, 4, 939980-939980. doi:10.3389/fspor.2022.939980

Langley, B. (2015). The Influence of Running Shoes on the Biomechanics of the Foot and Lower Limb. University of East London,

Leardini, A., Chiari, L., Croce, U. D., & Cappozzo, A. (2005). Human movement analysis using stereophotogrammetry: Part 3. Soft tissue artifact assessment and compensation. Gait & Posture, 21(2), 212-225. doi:https://doi.org/10.1016/j.gaitpost.2004.05.002

Lenhart, R., Thelen, D., & Heiderscheit, B. (2014). Hip Muscle Loads During Running at Various Step Rates. Journal of Orthopaedic & Sports Physical Therapy, 44(10), 766-A764. doi:10.2519/jospt.2014.5575

Lenhart, R. L., Thelen, D. G., Wille, C. M., Chumanov, E. S., & Heiderscheit, B. C. (2014). Increasing running step rate reduces patellofemoral joint forces. Medicine and science in sports and exercise, 46(3), 557-564. doi:10.1249/MSS.0b013e3182a78c3a

Li, L., Landin, D., Grodesky, J., & Myers, J. (2002). The function of gastrocnemius as a knee flexor at selected knee and ankle angles. Journal of Electromyography and Kinesiology, 12(5), 385-390. doi:https://doi.org/10.1016/S1050-6411(02)00049-4

Li, L., & Wang, D. (2017). Parallel and cross-sectional hamstring injuries in sprint running. Journal of Sport and Health Science, 6(2), 141.

Lieber, R. L., & Friden, J. (1993). Muscle damage is not a function of muscle force but active muscle strain. Journal of applied physiology, 74(2), 520-526. doi:10.1152/jappl.1993.74.2.520

Liu, G., & McMillan, L. (2006). Estimation of missing markers in human motion capture. The Visual Computer, 22(9), 721-728. doi:10.1007/s00371-006-0080-9

Liu, Y., Sun, Y., Zhu, W., & Yu, J. (2017). The late swing and early stance of sprinting are most hazardous for hamstring injuries. Journal of Sport and Health Science, 6(2), 133-136. doi:10.1016/j.jshs.2017.01.011

Loudon, J. K., & Reiman, M. P. (2012). Lower extremity kinematics in running athletes with and without a history of medial shin pain. International journal of sports physical therapy, 7(4), 356.

Lu, T. W., & O'Connor, J. J. (1999). Bone position estimation from skin marker co-ordinates using global optimisation with joint constraints. Journal of Biomechanics, 32(2), 129-134. doi:https://doi.org/10.1016/S0021-9290(98)00158-4

Mahieu, N. N., Witvrouw, E., Stevens, V., Van Tiggelen, D., & Roget, P. (2006). Intrinsic risk factors for the development of achilles tendon overuse injury: a prospective study. The American Journal of Sports Medicine, 34(2), 226-235.

Mann, R., & Sprague, P. (1980). A Kinetic Analysis of the Ground Leg During Sprint Running. Research Quarterly for Exercise and Sport, 51(2), 334-348. doi:10.1080/02701367.1980.10605202

Mann, R. A., & Hagy, J. (1980). Biomechanics of walking, running, and sprinting. The American Journal of Sports Medicine, 8(5), 345-350.

Martinez, H. R., Garcia-Sarreon, A., Camara-Lemarroy, C., Salazar, F., & Guerrero-González, M. L. (2018). Accuracy of Markerless 3D Motion Capture Evaluation to Differentiate between On/Off Status in Parkinson's Disease after Deep Brain Stimulation. Parkinson's Disease, 2018, 5830364. doi:10.1155/2018/5830364

Mathis, A., Mamidanna, P., Cury, K. M., Abe, T., Murthy, V. N., Mathis, M. W., & Bethge, M. (2018). DeepLabCut: markerless pose estimation of user-defined body parts with deep learning. Nature neuroscience, 21(9), 1281-1289. doi:10.1038/s41593-018-0209-y

Mathis, A., Schneider, S., Lauer, J., & Mathis, M. W. (2020). A Primer on Motion Capture with Deep Learning: Principles, Pitfalls, and Perspectives. Neuron, 108(1), 44-65. doi:https://doi.org/10.1016/j.neuron.2020.09.017

Mentiplay, B. F., Perraton, L. G., Bower, K. J., Pua, Y.-H., McGaw, R., Heywood, S., & Clark, R. A. (2015). Gait assessment using the Microsoft Xbox One Kinect: Concurrent validity and inter-day reliability of spatiotemporal and kinematic variables. Journal of Biomechanics, 48(10), 2166-2170. doi:https://doi.org/10.1016/j.jbiomech.2015.05.021

Mündermann, L., Corazza, S., & Andriacchi, T. P. (2006). The evolution of methods for the capture of human movement leading to markerless motion capture for biomechanical applications. Journal of NeuroEngineering and Rehabilitation, 3(1), 6. doi:10.1186/1743-0003-3-6

Munteanu, S. E., & Barton, C. J. (2011). Lower limb biomechanics during running in individuals with achilles tendinopathy: a systematic review. Journal of Foot and Ankle Research, 4(1), 15. doi:10.1186/1757-1146-4-15

Nakano, N., Sakura, T., Ueda, K., Omura, L., Kimura, A., Iino, Y., . . . Yoshioka, S. (2020). Evaluation of 3D markerless motion capture accuracy using OpenPose with multiple video cameras. Frontiers in sports and active living, 2, 50.

Needham, L., Evans, M., Cosker, D. P., Wade, L., McGuigan, P. M., Bilzon, J. L., & Colyer, S. L. (2021). The accuracy of several pose estimation methods for 3D joint centre localisation. Scientific Reports, 11(1), 20673. doi:10.1038/s41598-021-00212-x

Nguyen, T. C., & Reynolds, K. J. (2014). The effect of variability in body segment parameters on joint moment using Monte Carlo simulations. Gait & Posture, 39(1), 346-353. doi:https://doi.org/10.1016/j.gaitpost.2013.08.002

Nicola, T. L., & Jewison, D. J. (2012). The Anatomy and Biomechanics of Running. Clinics in Sports Medicine, 31(2), 187-201. doi:10.1016/j.csm.2011.10.001

Novacheck, T. F. (1998). The biomechanics of running. Gait & Posture, 7(1), 77-95. doi:https://doi.org/10.1016/S0966-6362(97)00038-6

Ojeda, J., Martínez-Reina, J., & Mayo, J. (2016). The effect of kinematic constraints in the inverse dynamics problem in biomechanics. Multibody System Dynamics, 37(3), 291-309. doi:10.1007/s11044-016-9508-9

Orchard, J. W., Fricker, P. A., Abud, A. T., & Mason, B. R. (1996). Biomechanics of Iliotibial Band Friction Syndrome in Runners. The American Journal of Sports Medicine, 24(3), 375-379. doi:10.1177/036354659602400321

Osis, S. T., Hettinga, B. A., Macdonald, S., & Ferber, R. (2016). Effects of Simulated Marker Placement Deviations on Running Kinematics and Evaluation of a Morphometric-Based Placement Feedback Method. PLOS ONE, 11(1), e0147111. doi:10.1371/journal.pone.0147111

Õunpuu, S. (1994). The Biomechanics Of Walking And Running. Clinics in Sports Medicine, 13(4), 843-863. doi:https://doi.org/10.1016/S0278-5919(20)30289-1

Pataky, T. C. (2010). Generalized n-dimensional biomechanical field analysis using statistical parametric mapping. Journal of Biomechanics, 43(10), 1976-1982. doi:https://doi.org/10.1016/j.jbiomech.2010.03.008

Pataky, T. C. (2012). One-dimensional statistical parametric mapping in Python. Computer Methods in Biomechanics and Biomedical Engineering, 15(3), 295-301. doi:10.1080/10255842.2010.527837

Pataky, T. C., Robinson, M. A., & Vanrenterghem, J. (2013). Vector field statistical analysis of kinematic and force trajectories. Journal of Biomechanics, 46(14), 2394-2401. doi:https://doi.org/10.1016/j.jbiomech.2013.07.031

Pearsall, D. J., & Costigan, P. A. (1999). The effect of segment parameter error on gait analysis results. Gait & Posture, 9(3), 173-183. doi:https://doi.org/10.1016/S0966-6362(99)00011-9

Perry, J. (1983). Anatomy and biomechanics of the hindfoot. Clinical orthopaedics and related research(177), 9-15.

Perry, J., & Burnfield, J. M. (2010). Gait analysis. Normal and pathological function 2nd ed. California: Slack.

Peters, A., Galna, B., Sangeux, M., Morris, M., & Baker, R. (2010). Quantification of soft tissue artifact in lower limb human motion analysis: A systematic review. Gait & Posture, 31(1), 1-8. doi:https://doi.org/10.1016/j.gaitpost.2009.09.004

Petersen, J., Nielsen, R. O., Rasmussen, S., & Sørensen, H. (2014). Comparisons of increases in knee and ankle joint moments following an increase in running speed from 8 to 12 to 16km·h−1. Clinical Biomechanics, 29(9), 959-964. doi:https://doi.org/10.1016/j.clinbiomech.2014.09.003

Powers, C. M., Chen, P.-Y., Reischl, S. F., & Perry, J. (2002). Comparison of Foot Pronation and Lower Extremity Rotation in Persons With and Without Patellofemoral Pain. Foot & Ankle International, 23(7), 634-640. doi:10.1177/107110070202300709

Powers, C. M., Heino, J. G., Rao, S., & Perry, J. (1999). The influence of patellofemoral pain on lower limb loading during gait. Clinical Biomechanics, 14(10), 722-728. doi:https://doi.org/10.1016/S0268-0033(99)00019-4

Rao, G., Amarantini, D., Berton, E., & Favier, D. (2006). Influence of body segments' parameters estimation models on inverse dynamics solutions during gait. Journal of Biomechanics, 39(8), 1531-1536. doi:https://doi.org/10.1016/j.jbiomech.2005.04.014

Reinbolt, J. A., Haftka, R. T., Chmielewski, T. L., & Fregly, B. J. (2007). Are Patient-Specific Joint and Inertial Parameters Necessary for Accurate Inverse Dynamics Analyses of

Gait? IEEE Transactions on Biomedical Engineering, 54(5), 782-793. doi:10.1109/TBME.2006.889187

Richards, J. G. (1999). The measurement of human motion: A comparison of commercially available systems. Human Movement Science, 18(5), 589-602. doi:https://doi.org/10.1016/S0167-9457(99)00023-8

Riemer, R., Hsiao-Wecksler, E. T., & Zhang, X. (2008). Uncertainties in inverse dynamics solutions: A comprehensive analysis and an application to gait. Gait & Posture, 27(4), 578-588. doi:https://doi.org/10.1016/j.gaitpost.2007.07.012

Robertson, D. G. E., Caldwell, G. E., Hamill, J., Kamen, G., & Whittlesey, S. (2013). Research methods in biomechanics: Human kinetics.

Rolland, Y., van Kan, G. A., & Vellas, B. (2010). Healthy brain aging: role of exercise and physical activity. Clinics in geriatric medicine, 26(1), 75-87.

Sarbolandi, H., Lefloch, D., & Kolb, A. (2015). Kinect range sensing: Structured-light versus Time-of-Flight Kinect. Computer Vision and Image Understanding, 139, 1-20. doi:https://doi.org/10.1016/j.cviu.2015.05.006

Schache, A. G., Blanch, P. D., Dorn, T. W., Brown, N., Rosemond, D., & Pandy, M. G. J. M. S. S. E. (2011). Effect of running speed on lower limb joint kinetics. 43(7), 1260-1271.

Schache, A. G., Wrigley, T. V., Baker, R., & Pandy, M. G. (2009). Biomechanical response to hamstring muscle strain injury. Gait & Posture, 29(2), 332-338. doi:https://doi.org/10.1016/j.gaitpost.2008.10.054

Schneider, S., Askew, C. D., Diehl, J., Mierau, A., Kleinert, J., Abel, T., . . . Strüder, H. K. (2009). EEG activity and mood in health orientated runners after different exercise intensities. Physiology & behavior, 96(4-5), 709-716.

Schwartz, M. H., Trost, J. P., & Wervey, R. A. (2004). Measurement and management of errors in quantitative gait data. Gait & Posture, 20(2), 196-203. doi:https://doi.org/10.1016/j.gaitpost.2003.09.011

Scott, S. H., Winter, DA (1990). Internal forces at chronic running injury sites. Medicine & Science in Sports & Exercise, 22(3), 357-369.

Shin, J. H., Yu, R., Ong, J. N., Lee, C. Y., Jeon, S. H., Park, H., . . . Jeon, B. (2021). Quantitative Gait Analysis Using a Pose-Estimation Algorithm with a Single 2D-Video of Parkinson’s Disease Patients. Journal of Parkinson's Disease, 11, 1271-1283. doi:10.3233/JPD-212544

Silva, M. P. T., & Ambrósio, J. A. C. (2002). Kinematic Data Consistency in the Inverse Dynamic Analysis of Biomechanical Systems. Multibody System Dynamics, 8(2), 219-239. doi:10.1023/A:1019545530737

Simpson, K. J., & Bates, B. T. (1990). The Effects of Running Speed on Lower Extremity Joint Moments Generated during the Support Phase. International Journal of Sport Biomechanics, 6(3), 309-324. doi:10.1123/ijsb.6.3.309

Slembrouck, M., Luong, H., Gerlo, J., Schütte, K., Van Cauwelaert, D., De Clercq, D., . . . Philips, W. (2020, 2020//). Multiview 3D Markerless Human Pose Estimation from OpenPose Skeletons. Paper presented at the Advanced Concepts for Intelligent Vision Systems, Cham.

Söderkvist, I., & Wedin, P.-Å. (1993). Determining the movements of the skeleton using well-configured markers. Journal of Biomechanics, 26(12), 1473-1477. doi:https://doi.org/10.1016/0021-9290(93)90098-Y

Song, K., Hullfish, T. J., Silva, R. S., Silbernagel, K. G., & Baxter, J. R. (2023). Markerless motion capture estimates of lower extremity kinematics and kinetics are comparable to marker-based across 8 movements. bioRxiv, 2023.2002.2021.526496. doi:10.1101/2023.02.21.526496

Souza, R. B., & Powers, C. M. (2009). Differences in Hip Kinematics, Muscle Strength, and Muscle Activation Between Subjects With and Without Patellofemoral Pain. Journal of Orthopaedic & Sports Physical Therapy, 39(1), 12-19. doi:10.2519/jospt.2009.2885

Springer, S., & Yogev Seligmann, G. (2016). Validity of the Kinect for Gait Assessment: A Focused Review. Sensors, 16(2). doi:10.3390/s16020194

Stagni, R., Leardini, A., Cappozzo, A., Grazia Benedetti, M., & Cappello, A. (2000). Effects of hip joint centre mislocation on gait analysis results. Journal of Biomechanics, 33(11), 1479-1487. doi:https://doi.org/10.1016/S0021-9290(00)00093-2

Steffensen, E. A., Magalhães, F., Knarr, B. A., & Kingston, D. C. (2023). Comparison of markerless and marker-based motion capture of gait kinematics in individuals with cerebral palsy and chronic stroke: A case study series.

Steffensen, M., Magalhaes PhD, F., Knarr PhD, B. A., & Kingston PhD, D. C. (2023). Comparison of markerless and marker-based motion capture in cerebral palsy and chronic stroke gait kinematics.

Steinert, A., Sattler, I., Otte, K., Röhling, H., Mansow-Model, S., & Müller-Werdan, U. (2020). Using New Camera-Based Technologies for Gait Analysis in Older Adults in Comparison to the Established GAITRite System. Sensors, 20(1). doi:10.3390/s20010125

Sun, Y., Wei, S., Zhong, Y., Fu, W., Li, L., & Liu, Y. (2015). How joint torques affect hamstring injury risk in sprinting swing-stance transition. Medicine and science in sports and exercise, 47(2), 373-380. doi:10.1249/MSS.0000000000000404

Swanson, S. C., & Caldwell, G. E. (2000). An integrated biomechanical analysis of high speed incline and level treadmill running. Medicine and science in sports and exercise, 32(6), 1146-1155.

Tanaka, R., Takimoto, H., Yamasaki, T., & Higashi, A. (2018). Validity of time series kinematical data as measured by a markerless motion capture system on a flatland for gait assessment. Journal of Biomechanics, 71, 281-285. doi:https://doi.org/10.1016/j.jbiomech.2018.01.035

Tang, H., Pan, J., Munkasy, B., Duffy, K., & Li, L. (2022). Comparison of Lower Extremity Joint Moment and Power Estimated by Markerless and Marker-Based Systems during Treadmill Running. Bioengineering, 9(10). doi:10.3390/bioengineering9100574

Thelen, D. G., Chumanov, E. S., Hoerth, D. M., Best, T. M., Swanson, S. C., Li, L., . . . Heiderscheit, B. C. (2005). Hamstring muscle kinematics during treadmill sprinting. Medicine and science in sports and exercise, 37(1), 108-114.

Vafadar, S., Skalli, W., Bonnet-Lebrun, A., Khalifé, M., Renaudin, M., Hamza, A., & Gajny, L. (2021). A novel dataset and deep learning-based approach for marker-less motion capture during gait. Gait & Posture, 86, 70-76. doi:https://doi.org/10.1016/j.gaitpost.2021.03.003

Van Hooren, B., Pecasse, N., Meijer, K., & Essers, J. M. N. (2023). The accuracy of markerless motion capture combined with computer vision techniques for measuring running kinematics. Scandinavian Journal of Medicine & Science in Sports, n/a(n/a). doi:https://doi.org/10.1111/sms.14319

Vaughan, C. L., Andrews, J. G., & Hay, J. G. (1982). Selection of Body Segment Parameters by Optimization Methods. Journal of Biomechanical Engineering, 104(1), 38-44. doi:10.1115/1.3138301

Verheul, J., Sueda, S., & Yeo, S.-H. (2022). Muscle Inertia During Running: A Massive Change of Moments? ISBS Proceedings Archive, 40(1), 732.

Wade, L., Needham, L., McGuigan, P., & Bilzon, J. (2022). Applications and limitations of current markerless motion capture methods for clinical gait biomechanics. PeerJ, 10, e12995. doi:10.7717/peerj.12995

Wesseling, M., de Groote, F., & Jonkers, I. (2014). The effect of perturbing body segment parameters on calculated joint moments and muscle forces during gait. Journal of Biomechanics, 47(2), 596-601. doi:https://doi.org/10.1016/j.jbiomech.2013.11.002

Willick, S., & Hansen, P. (2001). Running and osteoarthritis. Textbook of running medicine, 7.

Winter, D. A. (1983). Biomechanical Motor Patterns in Normal Walking. Journal of Motor Behavior, 15(4), 302-330. doi:10.1080/00222895.1983.10735302

Winter, D. A. (2009). Biomechanics and motor control of human movement: John Wiley & Sons.

Woltring, H. J. (1986). A Fortran package for generalized, cross-validatory spline smoothing and differentiation. Advances in Engineering Software (1978), 8(2), 104-113. doi:https://doi.org/10.1016/0141-1195(86)90098-7

Wu, G., Siegler, S., Allard, P., Kirtley, C., Leardini, A., Rosenbaum, D., . . . Stokes, I. (2002). ISB recommendation on definitions of joint coordinate system of various joints for the reporting of human joint motion—part I: ankle, hip, and spine. Journal of Biomechanics, 35(4), 543-548. doi:https://doi.org/10.1016/S0021-9290(01)00222-6

Yu, B., Queen, R. M., Abbey, A. N., Liu, Y., Moorman, C. T., & Garrett, W. E. (2008). Hamstring muscle kinematics and activation during overground sprinting. Journal of Biomechanics, 41(15), 3121-3126. doi:https://doi.org/10.1016/j.jbiomech.2008.09.005

Zago, M., Luzzago, M., Marangoni, T., De Cecco, M., Tarabini, M., & Galli, M. (2020). 3D tracking of human motion using visual skeletonization and stereoscopic vision. Frontiers in bioengineering and biotechnology, 8, 181.

Zell, P., & Rosenhahn, B. (2020). Learning inverse dynamics for human locomotion analysis. Neural Computing and Applications, 32(15), 11729-11743. doi:10.1007/s00521-019-04658-z

Zhang, S., Pan, J., & Li, L. (2018). Non-linear changes of lower extremity kinetics prior to gait transition. Journal of Biomechanics, 77, 48-54. doi:https://doi.org/10.1016/j.jbiomech.2018.06.022

APPENDIX C

STATISTICAL ANALYSIS INFORMATION

- Discrete Measurements Statistical Analysis Details

  Paired Sample t-test

  Two-way (system × speed) within-subject repeated measure ANOVA

- Spatial Parameter Mapping Statistical Analysis Details

  Two-way Repeated Measure ANOVA

  Simple Linear Regression

Paired Sample Test

		Paired Differences					t	df	Sig. (2-tailed)
		Mean	Std. Deviation	Std. Error Mean	95% Confidence Interval of the Difference				
					Lower	Upper			
Pair 1	MB_K_2_M - ML_K_2_M	.43290	.12620	.03155	.36565	.50015	13.721	15	.000
Pair 2	MB_K_2_M_T - ML_K_2_M_T	-.01254	.00937	.00234	-.01754	-.00755	-5.352	15	.000
Pair 3	MB_H_2_M - ML_H_2_M	-.30215	.13730	.03432	-.37531	-.22899	-8.803	15	.000
Pair 4	MB_HM_2_T - ML_HM_2_T	-.03747	.02750	.00688	-.05213	-.02282	-5.450	15	.000
Pair 5	MB_H_3_M - ML_H_3_M	.85373	.23778	.05944	.72703	.98044	14.362	15	.000
Pair 6	MB_H_3_M_T - ML_H_3_M_T	-.02168	.01829	.00457	-.03142	-.01193	-4.741	15	.000
Pair 7	MB_K_2_P - ML_K_2_P	.46318	.79091	.19773	.04173	.88462	2.342	15	.033
Pair 8	MB_KP_2_T - ML_KP_2_T	-.01838	.02440	.00610	-.03139	-.00538	-3.013	15	.009

Pair 9	MB_K_3_P - ML_K_3_P	2.05513	.82514	.20629	1.61544	2.49482	9.963	15	.000
Pair 10	MB_KP_3_T - ML_KP_3_T	-.02659	.02534	.00633	-.04009	-.01309	-4.198	15	.001
Pair 11	MB_K_4_P - ML_K_4_P	2.43989	.85466	.21366	1.98447	2.89530	11.419	15	.000
Pair 12	MB_KP_4_T - ML_KP_4_T	.00255	.02083	.00521	-.00855	.01366	.490	15	.631
Pair 13	MB_H_2_P - ML_H_2_P	-3.90006	1.49448	.37362	-4.69641	-3.10370	-10.439	15	.000
Pair 14	MB_HP_2_T - ML_HP_2_T	-.00868	.03235	.00809	-.02592	.00856	-1.073	15	.300
Pair 15	MB_H_3_P - ML_H_3_P	-1.81199	1.33089	.33272	-2.52117	-1.10280	-5.446	15	.000
Pair 16	MB_HP_3_T - ML_HP_3_T	.01534	.02770	.00692	.00058	.03010	2.216	15	.043
Pair 17	MB_AM - ML_AM	.11051	.25170	.06293	-.02361	.24464	1.756	15	.099
Pair 18	MB_AM_T - ML_AM_T	-.00174	.00434	.00108	-.00405	.00057	-1.604	15	.129
Pair 19	MB_AP_1 - ML_AP_1	1.14969	1.74399	.43600	.22038	2.07899	2.637	15	.019
Pair 20	MB_AP_1_T - ML_AP_1_T	-.00230254	.01235003	.00308751	-.00888340	.00427833	-.746	15	.467
Pair	MB_KP_1 -	-	1.6448917	.41122293	-	-	-	15	.0

21	ML_KP_1	.9035769375	27	18	1.78007787	.0270760064	2.197		44
Pair 22	MB_KP_1_T - ML_KP_1_T	-.00510810	.01693043	.00423261	-.01412969	.00391349	-1.207	15	.246
Pair 23	MB_HP_1 - ML_HP_1	-.06644	1.53755	.38439	-.88574	.75286	-.173	15	.865
Pair 24	MB_HP_1_T - ML_HP_1_T	-.01768674	.02044772	.00511193	-.02858256	-.00679092	-3.460	15	.004
Pair 25	MB_AP_2 - ML_AP_2	-2.70334269	2.43157718	.60789430	-3.99903871	-1.40764667	-4.447	15	.000
Pair 26	MB_AP_2_T - ML_AP_2_T	.00302402	.02107159	.00526790	-.00820424	.01425228	.574	15	.574
Pair 27	MB_KM_1 - ML_KM_1	.10933	.23147	.05787	-.01401	.23267	1.889	15	.078
Pair 28	MB_KM_1_T - ML_KM_1_T	-.00831040	.01623418	.00405855	-.01696098	.00034019	-2.048	15	.059
Pair 29	MB_HM_1 - ML_HM_1	-.01693	.20854	.05214	-.12806	.09419	-.325	15	.750
Pair 30	MB_HM_1_T - ML_HM_1_T	-.01572	.02535	.00634	-.02923	-.00221	-2.481	15	.025

Two-way Repeated Measure ANOVA Results

Speeds: 1—5mph; 2---6.5mph; 3---8mph

Systems: 1—marker; 2--- markerless

Ankle Joint

```
NEW FILE.
DATASET NAME DataSet1 WINDOW=FRONT.
GLM AM_M_5 AM_M_65 AM_M_8 AM_ML_5 AM_ML_65 AM_ML_8
  /WSFACTOR=System 2 Polynomial Speed 3 Polynomial
  /METHOD=SSTYPE(3)
  /PLOT=PROFILE(System*Speed)
  /EMMEANS=TABLES(OVERALL)
  /EMMEANS=TABLES(System) COMPARE ADJ(LSD)
  /EMMEANS=TABLES(Speed) COMPARE ADJ(LSD)
  /EMMEANS=TABLES(System*Speed)
  /PRINT=DESCRIPTIVE ETASQ
  /CRITERIA=ALPHA(.05)
  /WSDESIGN=System Speed System*Speed.
```

General Linear Model

[DataSet1]

Within-Subjects Factors

Measure: MEASURE_1

System	Speed	Dependent Variable
1	1	AM_M_5
	2	AM_M_65
	3	AM_M_8
2	1	AM_ML_5
	2	AM_ML_65
	3	AM_ML_8

Descriptive Statistics

	Mean	Std. Deviation	N
AM_M_5	-2.59620850	.658797571	16
AM_M_65	-3.04330956	.761981992	16
AM_M_8	-3.40620844	.854993862	16
AM_ML_5	-2.47467800	.411514988	16
AM_ML_65	-2.93496394	.521636876	16
AM_ML_8	-3.26761213	.615739198	16

Multivariate Tests[a]

Effect		Value	F	Hypothesis df	Error df	Sig.	Partial Eta Squared
System	Pillai's Trace	.074	1.191[b]	1.000	15.000	.292	.074
	Wilks' Lambda	.926	1.191[b]	1.000	15.000	.292	.074
	Hotelling's Trace	.079	1.191[b]	1.000	15.000	.292	.074
	Roy's Largest Root	.079	1.191[b]	1.000	15.000	.292	.074
Speed	Pillai's Trace	.872	47.498[b]	2.000	14.000	.000	.872
	Wilks' Lambda	.128	47.498[b]	2.000	14.000	.000	.872
	Hotelling's Trace	6.785	47.498[b]	2.000	14.000	.000	.872
	Roy's Largest Root	6.785	47.498[b]	2.000	14.000	.000	.872
System * Speed	Pillai's Trace	.013	.094[b]	2.000	14.000	.911	.013
	Wilks' Lambda	.987	.094[b]	2.000	14.000	.911	.013
	Hotelling's Trace	.013	.094[b]	2.000	14.000	.911	.013
	Roy's Largest Root	.013	.094[b]	2.000	14.000	.911	.013

a. Design: Intercept
Within Subjects Design: System + Speed + System * Speed

b. Exact statistic

Mauchly's Test of Sphericity[a]

Measure: MEASURE_1

Within Subjects Effect	Mauchly's W	Approx. Chi-Square	df	Sig.	Epsilon[b] Greenhouse-Geisser
System	1.000	.000	0	.	1.000
Speed	.638	6.289	2	.043	.734
System * Speed	.590	7.393	2	.025	.709

Mauchly's Test of Sphericity[a]

Measure: MEASURE_1

Within Subjects Effect	Epsilon[b]	
	Huynh-Feldt	Lower-bound
System	1.000	1.000
Speed	.794	.500
System * Speed	.762	.500

Tests the null hypothesis that the error covariance matrix of the orthonormalized transformed dependent variables is proportional to an identity matrix.

a. Design: Intercept
Within Subjects Design: System + Speed + System * Speed

b. May be used to adjust the degrees of freedom for the averaged tests of significance. Corrected tests are displayed in the Tests of Within-Subjects Effects table.

Tests of Within-Subjects Effects

Measure: MEASURE_1

Source		Type III Sum of Squares	df	Mean Square	F
System	Sphericity Assumed	.362	1	.362	1.191
	Greenhouse-Geisser	.362	1.000	.362	1.191
	Huynh-Feldt	.362	1.000	.362	1.191
	Lower-bound	.362	1.000	.362	1.191
Error(System)	Sphericity Assumed	4.558	15	.304	
	Greenhouse-Geisser	4.558	15.000	.304	
	Huynh-Feldt	4.558	15.000	.304	
	Lower-bound	4.558	15.000	.304	
Speed	Sphericity Assumed	10.337	2	5.169	66.753
	Greenhouse-Geisser	10.337	1.469	7.039	66.753
	Huynh-Feldt	10.337	1.589	6.507	66.753
	Lower-bound	10.337	1.000	10.337	66.753
Error(Speed)	Sphericity Assumed	2.323	30	.077	
	Greenhouse-Geisser	2.323	22.028	.105	
	Huynh-Feldt	2.323	23.830	.097	
	Lower-bound	2.323	15.000	.155	
System * Speed	Sphericity Assumed	.004	2	.002	.151
	Greenhouse-Geisser	.004	1.418	.003	.151
	Huynh-Feldt	.004	1.523	.002	.151
	Lower-bound	.004	1.000	.004	.151
Error(System*Speed)	Sphericity Assumed	.365	30	.012	
	Greenhouse-Geisser	.365	21.273	.017	
	Huynh-Feldt	.365	22.851	.016	
	Lower-bound	.365	15.000	.024	

Tests of Within-Subjects Effects

Measure: MEASURE_1

Source		Sig.	Partial Eta Squared
System	Sphericity Assumed	.292	.074
	Greenhouse-Geisser	.292	.074
	Huynh-Feldt	.292	.074
	Lower-bound	.292	.074
Error(System)	Sphericity Assumed		
	Greenhouse-Geisser		
	Huynh-Feldt		
	Lower-bound		
Speed	Sphericity Assumed	.000	.817
	Greenhouse-Geisser	.000	.817
	Huynh-Feldt	.000	.817
	Lower-bound	.000	.817
Error(Speed)	Sphericity Assumed		
	Greenhouse-Geisser		
	Huynh-Feldt		
	Lower-bound		
System * Speed	Sphericity Assumed	.860	.010
	Greenhouse-Geisser	.787	.010
	Huynh-Feldt	.803	.010
	Lower-bound	.703	.010
Error(System*Speed)	Sphericity Assumed		
	Greenhouse-Geisser		
	Huynh-Feldt		
	Lower-bound		

Tests of Within-Subjects Contrasts

Measure: MEASURE_1

Source	System	Speed	Type III Sum of Squares	df	Mean Square	F
System	Linear		.362	1	.362	1.191
Error(System)	Linear		4.558	15	.304	
Speed		Linear	10.278	1	10.278	85.353
		Quadratic	.060	1	.060	1.737
Error(Speed)		Linear	1.806	15	.120	
		Quadratic	.517	15	.034	
System * Speed	Linear	Linear	.001	1	.001	.099
		Quadratic	.003	1	.003	.201
Error(System*Speed)	Linear	Linear	.177	15	.012	
		Quadratic	.188	15	.013	

Tests of Within-Subjects Contrasts

Measure: MEASURE_1

Source	System	Speed	Sig.	Partial Eta Squared
System	Linear		.292	.074
Error(System)	Linear			
Speed		Linear	.000	.851
		Quadratic	.207	.104
Error(Speed)		Linear		
		Quadratic		
System * Speed	Linear	Linear	.758	.007
		Quadratic	.661	.013
Error(System*Speed)	Linear	Linear		
		Quadratic		

Tests of Between-Subjects Effects

Measure: MEASURE_1

Transformed Variable: Average

Source	Type III Sum of Squares	df	Mean Square	F	Sig.	Partial Eta Squared
Intercept	837.611	1	837.611	402.087	.000	.964
Error	31.247	15	2.083			

Estimated Marginal Means

1. Grand Mean

Measure: MEASURE_1

Mean	Std. Error	95% Confidence Interval	
		Lower Bound	Upper Bound
-2.954	.147	-3.268	-2.640

2. System

Estimates

Measure: MEASURE_1

System	Mean	Std. Error	95% Confidence Interval	
			Lower Bound	Upper Bound
1	-3.015	.187	-3.414	-2.616
2	-2.892	.121	-3.150	-2.634

Pairwise Comparisons

Measure: MEASURE_1

(I) System	(J) System	Mean Difference (I-J)	Std. Error	Sig.[a]	95% Confidence Interval for Difference[a]	
					Lower Bound	Upper Bound
1	2	-.123	.113	.292	-.363	.117
2	1	.123	.113	.292	-.117	.363

Based on estimated marginal means

a. Adjustment for multiple comparisons: Least Significant Difference (equivalent to no adjustments).

Multivariate Tests

	Value	F	Hypothesis df	Error df	Sig.	Partial Eta Squared
Pillai's trace	.074	1.191[a]	1.000	15.000	.292	.074
Wilks' lambda	.926	1.191[a]	1.000	15.000	.292	.074
Hotelling's trace	.079	1.191[a]	1.000	15.000	.292	.074
Roy's largest root	.079	1.191[a]	1.000	15.000	.292	.074

Each F tests the multivariate effect of System. These tests are based on the linearly independent pairwise comparisons among the estimated marginal means.

a. Exact statistic

3. Speed

Estimates

Measure: MEASURE_1

Speed	Mean	Std. Error	95% Confidence Interval Lower Bound	95% Confidence Interval Upper Bound
1	-2.535	.127	-2.806	-2.265
2	-2.989	.151	-3.311	-2.668
3	-3.337	.176	-3.713	-2.961

Pairwise Comparisons

Measure: MEASURE_1

(I) Speed	(J) Speed	Mean Difference (I-J)	Std. Error	Sig.[b]	95% Confidence Interval for Difference[b] Lower Bound	95% Confidence Interval for Difference[b] Upper Bound
1	2	.454*	.050	.000	.347	.561
	3	.801*	.087	.000	.617	.986
2	1	-.454*	.050	.000	-.561	-.347
	3	.348*	.067	.000	.205	.490
3	1	-.801*	.087	.000	-.986	-.617
	2	-.348*	.067	.000	-.490	-.205

Based on estimated marginal means

*. The mean difference is significant at the .05 level.

b. Adjustment for multiple comparisons: Least Significant Difference (equivalent to no adjustments).

Multivariate Tests

	Value	F	Hypothesis df	Error df	Sig.	Partial Eta Squared
Pillai's trace	.872	47.498[a]	2.000	14.000	.000	.872
Wilks' lambda	.128	47.498[a]	2.000	14.000	.000	.872
Hotelling's trace	6.785	47.498[a]	2.000	14.000	.000	.872
Roy's largest root	6.785	47.498[a]	2.000	14.000	.000	.872

Each F tests the multivariate effect of Speed. These tests are based on the linearly independent pairwise comparisons among the estimated marginal means.

a. Exact statistic

4. System * Speed

Measure: MEASURE_1

System	Speed	Mean	Std. Error	95% Confidence Interval Lower Bound	Upper Bound
1	1	-2.596	.165	-2.947	-2.245
	2	-3.043	.190	-3.449	-2.637
	3	-3.406	.214	-3.862	-2.951
2	1	-2.475	.103	-2.694	-2.255
	2	-2.935	.130	-3.213	-2.657
	3	-3.268	.154	-3.596	-2.940

Profile Plots

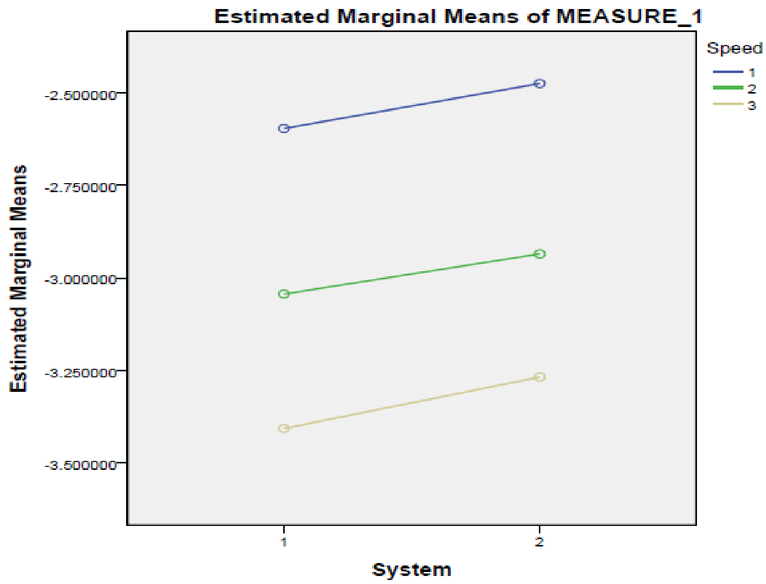


```
GLM AM_T_M_5 AM_T_M_65 AM_T_M_8 AM_T_ML_5 AM_T_ML_65 AM_T_ML_8
  /WSFACTOR=System 2 Polynomial Speed 3 Polynomial
  /METHOD=SSTYPE(3)

  /PLOT=PROFILE(System*Speed)
  /EMMEANS=TABLES(OVERALL)
  /EMMEANS=TABLES(System) COMPARE ADJ(LSD)
  /EMMEANS=TABLES(Speed) COMPARE ADJ(LSD)
  /EMMEANS=TABLES(System*Speed)
  /PRINT=DESCRIPTIVE ETASQ
  /CRITERIA=ALPHA(.05)
  /WSDESIGN=System Speed System*Speed.
```

General Linear Model

Within-Subjects Factors

Measure: MEASURE_1

System	Speed	Dependent Variable
1	1	AM_T_M_5
	2	AM_T_M_65
	3	AM_T_M_8
2	1	AM_T_ML_5
	2	AM_T_ML_65
	3	AM_T_ML_8

Descriptive Statistics

	Mean	Std. Deviation	N
AM_T_M_5	14.81875000	1.154249395	16
AM_T_M_65	13.3375	1.42215	16
AM_T_M_8	12.0000000	1.32966161	16
AM_T_ML_5	14.89375000	1.326885451	16
AM_T_ML_65	13.53750000	1.452297031	16
AM_T_ML_8	12.1125	1.48318	16

Multivariate Tests[a]

Effect		Value	F	Hypothesis df	Error df	Sig.
System	Pillai's Trace	.225	4.343[b]	1.000	15.000	.055
	Wilks' Lambda	.775	4.343[b]	1.000	15.000	.055
	Hotelling's Trace	.290	4.343[b]	1.000	15.000	.055
	Roy's Largest Root	.290	4.343[b]	1.000	15.000	.055
Speed	Pillai's Trace	.942	112.718[b]	2.000	14.000	.000
	Wilks' Lambda	.058	112.718[b]	2.000	14.000	.000
	Hotelling's Trace	16.103	112.718[b]	2.000	14.000	.000
	Roy's Largest Root	16.103	112.718[b]	2.000	14.000	.000
System * Speed	Pillai's Trace	.066	.498[b]	2.000	14.000	.618
	Wilks' Lambda	.934	.498[b]	2.000	14.000	.618
	Hotelling's Trace	.071	.498[b]	2.000	14.000	.618
	Roy's Largest Root	.071	.498[b]	2.000	14.000	.618

Multivariate Tests[a]

Effect		Partial Eta Squared
System	Pillai's Trace	.225
	Wilks' Lambda	.225
	Hotelling's Trace	.225
	Roy's Largest Root	.225
Speed	Pillai's Trace	.942
	Wilks' Lambda	.942
	Hotelling's Trace	.942
	Roy's Largest Root	.942
System * Speed	Pillai's Trace	.066
	Wilks' Lambda	.066
	Hotelling's Trace	.066
	Roy's Largest Root	.066

a. Design: Intercept
Within Subjects Design: System + Speed + System * Speed

b. Exact statistic

Mauchly's Test of Sphericity[a]

Measure: MEASURE_1

Within Subjects Effect	Mauchly's W	Approx. Chi-Square	df	Sig.	Epsilon[b] Greenhouse-Geisser
System	1.000	.000	0	.	1.000
Speed	.333	15.389	2	.000	.600
System * Speed	.871	1.931	2	.381	.886

Mauchly's Test of Sphericity[a]

Measure: MEASURE_1

Within Subjects Effect	Epsilon[b] Huynh-Feldt	Lower-bound
System	1.000	1.000
Speed	.623	.500
System * Speed	.996	.500

Tests the null hypothesis that the error covariance matrix of the orthonormalized transformed dependent variables is proportional to an identity matrix.

a. Design: Intercept
Within Subjects Design: System + Speed + System * Speed

b. May be used to adjust the degrees of freedom for the averaged tests of significance. Corrected tests are displayed in the Tests of Within-Subjects Effects table.

Tests of Within-Subjects Effects

Measure: MEASURE_1

Source		Type III Sum of Squares	df	Mean Square	F
System	Sphericity Assumed	.400	1	.400	4.343
	Greenhouse-Geisser	.400	1.000	.400	4.343
	Huynh-Feldt	.400	1.000	.400	4.343
	Lower-bound	.400	1.000	.400	4.343
Error(System)	Sphericity Assumed	1.383	15	.092	
	Greenhouse-Geisser	1.383	15.000	.092	
	Huynh-Feldt	1.383	15.000	.092	
	Lower-bound	1.383	15.000	.092	
Speed	Sphericity Assumed	125.447	2	62.724	61.282
	Greenhouse-Geisser	125.447	1.200	104.552	61.282
	Huynh-Feldt	125.447	1.246	100.664	61.282
	Lower-bound	125.447	1.000	125.447	61.282
Error(Speed)	Sphericity Assumed	30.706	30	1.024	
	Greenhouse-Geisser	30.706	17.998	1.706	
	Huynh-Feldt	30.706	18.693	1.643	
	Lower-bound	30.706	15.000	2.047	
System * Speed	Sphericity Assumed	.066	2	.033	.425
	Greenhouse-Geisser	.066	1.772	.037	.425
	Huynh-Feldt	.066	1.992	.033	.425
	Lower-bound	.066	1.000	.066	.425
Error(System*Speed)	Sphericity Assumed	2.321	30	.077	
	Greenhouse-Geisser	2.321	26.576	.087	
	Huynh-Feldt	2.321	29.877	.078	
	Lower-bound	2.321	15.000	.155	

Tests of Within-Subjects Effects

Measure: MEASURE_1

Source		Sig.	Partial Eta Squared
System	Sphericity Assumed	.055	.225
	Greenhouse-Geisser	.055	.225
	Huynh-Feldt	.055	.225
	Lower-bound	.055	.225
Error(System)	Sphericity Assumed		
	Greenhouse-Geisser		
	Huynh-Feldt		
	Lower-bound		
Speed	Sphericity Assumed	.000	.803
	Greenhouse-Geisser	.000	.803
	Huynh-Feldt	.000	.803
	Lower-bound	.000	.803
Error(Speed)	Sphericity Assumed		
	Greenhouse-Geisser		
	Huynh-Feldt		
	Lower-bound		
System * Speed	Sphericity Assumed	.657	.028
	Greenhouse-Geisser	.634	.028
	Huynh-Feldt	.657	.028
	Lower-bound	.524	.028
Error(System*Speed)	Sphericity Assumed		
	Greenhouse-Geisser		
	Huynh-Feldt		
	Lower-bound		

Tests of Within-Subjects Contrasts

Measure: MEASURE_1

Source	System	Speed	Type III Sum of Squares	df	Mean Square	F
System	Linear		.400	1	.400	4.343
Error(System)	Linear		1.383	15	.092	
Speed		Linear	125.440	1	125.440	92.010
		Quadratic	.008	1	.008	.011
Error(Speed)		Linear	20.450	15	1.363	
		Quadratic	10.256	15	.684	
System * Speed	Linear	Linear	.006	1	.006	.082
		Quadratic	.060	1	.060	.697
Error(System*Speed)	Linear	Linear	1.024	15	.068	
		Quadratic	1.296	15	.086	

Tests of Within-Subjects Contrasts

Measure: MEASURE_1

Source	System	Speed	Sig.	Partial Eta Squared
System	Linear		.055	.225
Error(System)	Linear			
Speed		Linear	.000	.860
		Quadratic	.918	.001
Error(Speed)		Linear		
		Quadratic		
System * Speed	Linear	Linear	.778	.005
		Quadratic	.417	.044
Error(System*Speed)	Linear	Linear		
		Quadratic		

Tests of Between-Subjects Effects

Measure: MEASURE_1
Transformed Variable: Average

Source	Type III Sum of Squares	df	Mean Square	F	Sig.	Partial Eta Squared
Intercept	17366.640	1	17366.640	1951.649	.000	.992
Error	133.477	15	8.898			

Estimated Marginal Means

1. Grand Mean

Measure: MEASURE_1

Mean	Std. Error	95% Confidence Interval	
		Lower Bound	Upper Bound
13.450	.304	12.801	14.099

2. System

Estimates

Measure: MEASURE_1

System	Mean	Std. Error	95% Confidence Interval	
			Lower Bound	Upper Bound
1	13.385	.297	12.752	14.018
2	13.515	.315	12.844	14.186

Pairwise Comparisons

Measure: MEASURE_1

(I) System	(J) System	Mean Difference (I-J)	Std. Error	Sig.[a]	95% Confidence Interval for Difference[a]	
					Lower Bound	Upper Bound
1	2	-.129	.062	.055	-.261	.003
2	1	.129	.062	.055	-.003	.261

Based on estimated marginal means

a. Adjustment for multiple comparisons: Least Significant Difference (equivalent to no adjustments).

Multivariate Tests

	Value	F	Hypothesis df	Error df	Sig.	Partial Eta Squared
Pillai's trace	.225	4.343[a]	1.000	15.000	.055	.225
Wilks' lambda	.775	4.343[a]	1.000	15.000	.055	.225
Hotelling's trace	.290	4.343[a]	1.000	15.000	.055	.225
Roy's largest root	.290	4.343[a]	1.000	15.000	.055	.225

Each F tests the multivariate effect of System. These tests are based on the linearly independent pairwise comparisons among the estimated marginal means.

a. Exact statistic

3. Speed

Estimates

Measure: MEASURE_1

Speed	Mean	Std. Error	95% Confidence Interval Lower Bound	95% Confidence Interval Upper Bound
1	14.856	.308	14.199	15.513
2	13.438	.353	12.685	14.190
3	12.056	.350	11.311	12.802

Pairwise Comparisons

Measure: MEASURE_1

(I) Speed	(J) Speed	Mean Difference (I-J)	Std. Error	Sig.[b]	95% Confidence Interval for Difference[b] Lower Bound	95% Confidence Interval for Difference[b] Upper Bound
1	2	1.419*	.308	.000	.763	2.075
	3	2.800*	.292	.000	2.178	3.422
2	1	-1.419*	.308	.000	-2.075	-.763
	3	1.381*	.110	.000	1.148	1.615
3	1	-2.800*	.292	.000	-3.422	-2.178
	2	-1.381*	.110	.000	-1.615	-1.148

Based on estimated marginal means

*. The mean difference is significant at the .05 level.

b. Adjustment for multiple comparisons: Least Significant Difference (equivalent to no adjustments).

Multivariate Tests

	Value	F	Hypothesis df	Error df	Sig.	Partial Eta Squared
Pillai's trace	.942	112.718[a]	2.000	14.000	.000	.942
Wilks' lambda	.058	112.718[a]	2.000	14.000	.000	.942
Hotelling's trace	16.103	112.718[a]	2.000	14.000	.000	.942
Roy's largest root	16.103	112.718[a]	2.000	14.000	.000	.942

Each F tests the multivariate effect of Speed. These tests are based on the linearly independent pairwise comparisons among the estimated marginal means.

a. Exact statistic

4. System * Speed

Measure: MEASURE_1

System	Speed	Mean	Std. Error	95% Confidence Interval Lower Bound	95% Confidence Interval Upper Bound
1	1	14.819	.289	14.204	15.434
	2	13.337	.356	12.580	14.095
	3	12.000	.332	11.291	12.709
2	1	14.894	.332	14.187	15.601
	2	13.538	.363	12.764	14.311
	3	12.113	.371	11.322	12.903

Profile Plots

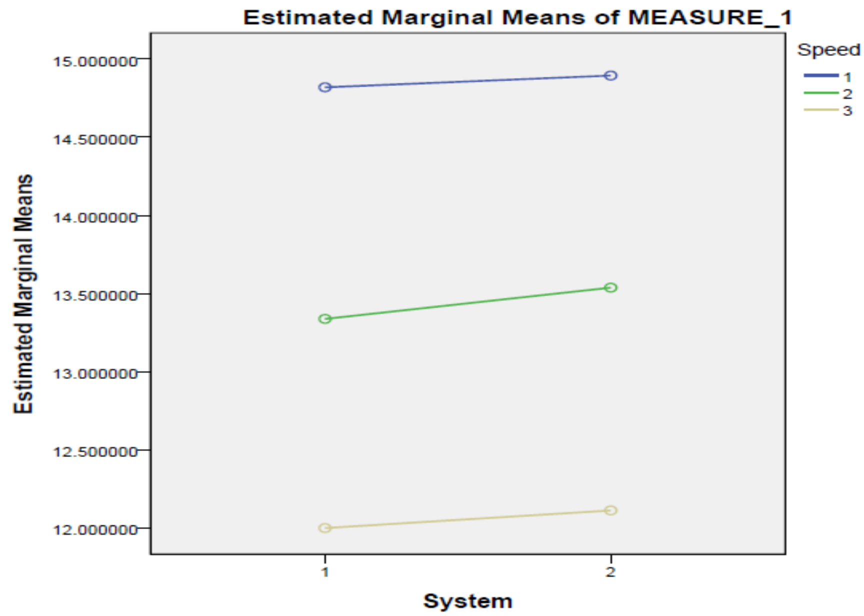


```
/PLOT=PROFILE(System*Speed)
/EMMEANS=TABLES(OVERALL)
/EMMEANS=TABLES(System) COMPARE ADJ(LSD)
/EMMEANS=TABLES(Speed) COMPARE ADJ(LSD)
/EMMEANS=TABLES(System*Speed)
/PRINT=DESCRIPTIVE ETASQ
/CRITERIA=ALPHA(.05)
/WSDESIGN=System Speed System*Speed.
```

General Linear Model

Within-Subjects Factors

Measure: MEASURE_1

System	Speed	Dependent Variable
1	1	AP_1_M_5
	2	AP_1_M_65
	3	AP_1_M_8
2	1	AP_1_ML_5
	2	AP_1_ML_65
	3	AP_1_ML_8

Descriptive Statistics

	Mean	Std. Deviation	N
AP_1_M_5	-5.1508985	2.12125606	16
AP_1_M_65	-6.81929694	2.757454406	16
AP_1_M_8	-9.13638100	3.264538413	16
AP_1_ML_5	-4.9036599	1.26381903	16
AP_1_ML_65	-7.12087806	1.614442230	16
AP_1_ML_8	-9.40180575	1.543609899	16

Multivariate Tests[a]

Effect		Value	F	Hypothesis df	Error df	Sig.
System	Pillai's Trace	.005	.072[b]	1.000	15.000	.792
	Wilks' Lambda	.995	.072[b]	1.000	15.000	.792
	Hotelling's Trace	.005	.072[b]	1.000	15.000	.792
	Roy's Largest Root	.005	.072[b]	1.000	15.000	.792
Speed	Pillai's Trace	.882	52.503[b]	2.000	14.000	.000
	Wilks' Lambda	.118	52.503[b]	2.000	14.000	.000
	Hotelling's Trace	7.500	52.503[b]	2.000	14.000	.000
	Roy's Largest Root	7.500	52.503[b]	2.000	14.000	.000
System * Speed	Pillai's Trace	.165	1.382[b]	2.000	14.000	.283
	Wilks' Lambda	.835	1.382[b]	2.000	14.000	.283
	Hotelling's Trace	.197	1.382[b]	2.000	14.000	.283
	Roy's Largest Root	.197	1.382[b]	2.000	14.000	.283

Multivariate Tests[a]

Effect		Partial Eta Squared
System	Pillai's Trace	.005
	Wilks' Lambda	.005
	Hotelling's Trace	.005
	Roy's Largest Root	.005
Speed	Pillai's Trace	.882
	Wilks' Lambda	.882
	Hotelling's Trace	.882
	Roy's Largest Root	.882
System * Speed	Pillai's Trace	.165
	Wilks' Lambda	.165
	Hotelling's Trace	.165
	Roy's Largest Root	.165

a. Design: Intercept
Within Subjects Design: System + Speed + System * Speed

b. Exact statistic

Mauchly's Test of Sphericity[a]

Measure: MEASURE_1

Within Subjects Effect	Mauchly's W	Approx. Chi-Square	df	Sig.	Epsilon[b] Greenhouse-Geisser
System	1.000	.000	0	.	1.000
Speed	.756	3.918	2	.141	.804
System * Speed	.831	2.598	2	.273	.855

Mauchly's Test of Sphericity[a]

Measure: MEASURE_1

Within Subjects Effect	Epsilon[b] Huynh-Feldt	Lower-bound
System	1.000	1.000
Speed	.886	.500
System * Speed	.954	.500

Tests the null hypothesis that the error covariance matrix of the orthonormalized transformed dependent variables is proportional to an identity matrix.

a. Design: Intercept
Within Subjects Design: System + Speed + System * Speed

b. May be used to adjust the degrees of freedom for the averaged tests of significance. Corrected tests are displayed in the Tests of Within-Subjects Effects table.

Tests of Within-Subjects Effects

Measure: MEASURE_1

Source		Type III Sum of Squares	df	Mean Square	F
System	Sphericity Assumed	.273	1	.273	.072
	Greenhouse-Geisser	.273	1.000	.273	.072
	Huynh-Feldt	.273	1.000	.273	.072
	Lower-bound	.273	1.000	.273	.072
Error(System)	Sphericity Assumed	56.981	15	3.799	
	Greenhouse-Geisser	56.981	15.000	3.799	
	Huynh-Feldt	56.981	15.000	3.799	
	Lower-bound	56.981	15.000	3.799	
Speed	Sphericity Assumed	288.564	2	144.282	83.752
	Greenhouse-Geisser	288.564	1.608	179.500	83.752
	Huynh-Feldt	288.564	1.771	162.913	83.752
	Lower-bound	288.564	1.000	288.564	83.752
Error(Speed)	Sphericity Assumed	51.682	30	1.723	
	Greenhouse-Geisser	51.682	24.114	2.143	
	Huynh-Feldt	51.682	26.569	1.945	
	Lower-bound	51.682	15.000	3.445	
System * Speed	Sphericity Assumed	1.508	2	.754	1.219
	Greenhouse-Geisser	1.508	1.710	.881	1.219
	Huynh-Feldt	1.508	1.909	.790	1.219
	Lower-bound	1.508	1.000	1.508	1.219
Error(System*Speed)	Sphericity Assumed	18.553	30	.618	
	Greenhouse-Geisser	18.553	25.654	.723	
	Huynh-Feldt	18.553	28.629	.648	
	Lower-bound	18.553	15.000	1.237	

Tests of Within-Subjects Effects

Measure: MEASURE_1

Source		Sig.	Partial Eta Squared
System	Sphericity Assumed	.792	.005
	Greenhouse-Geisser	.792	.005
	Huynh-Feldt	.792	.005
	Lower-bound	.792	.005
Error(System)	Sphericity Assumed		
	Greenhouse-Geisser		
	Huynh-Feldt		
	Lower-bound		
Speed	Sphericity Assumed	.000	.848
	Greenhouse-Geisser	.000	.848
	Huynh-Feldt	.000	.848
	Lower-bound	.000	.848
Error(Speed)	Sphericity Assumed		
	Greenhouse-Geisser		
	Huynh-Feldt		
	Lower-bound		
System * Speed	Sphericity Assumed	.310	.075
	Greenhouse-Geisser	.306	.075
	Huynh-Feldt	.309	.075
	Lower-bound	.287	.075
Error(System*Speed)	Sphericity Assumed		
	Greenhouse-Geisser		
	Huynh-Feldt		
	Lower-bound		

Tests of Within-Subjects Contrasts

Measure: MEASURE_1

Source	System	Speed	Type III Sum of Squares	df	Mean Square	F
System	Linear		.273	1	.273	.072
Error(System)	Linear		56.981	15	3.799	
Speed		Linear	287.888	1	287.888	111.853
		Quadratic	.677	1	.677	.776
Error(Speed)		Linear	38.607	15	2.574	
		Quadratic	13.075	15	.872	
System * Speed	Linear	Linear	1.051	1	1.051	1.237
		Quadratic	.456	1	.456	1.180
Error(System*Speed)	Linear	Linear	12.751	15	.850	
		Quadratic	5.802	15	.387	

Tests of Within-Subjects Contrasts

Measure: MEASURE_1

Source	System	Speed	Sig.	Partial Eta Squared
System	Linear		.792	.005
Error(System)	Linear			
Speed		Linear	.000	.882
		Quadratic	.392	.049
Error(Speed)		Linear		
		Quadratic		
System * Speed	Linear	Linear	.284	.076
		Quadratic	.295	.073
Error(System*Speed)	Linear	Linear		
		Quadratic		

Tests of Between-Subjects Effects

Measure: MEASURE_1

Transformed Variable: Average

Source	Type III Sum of Squares	df	Mean Square	F	Sig.	Partial Eta Squared
Intercept	4824.131	1	4824.131	231.198	.000	.939
Error	312.987	15	20.866			

Estimated Marginal Means

1. Grand Mean

Measure: MEASURE_1

Mean	Std. Error	95% Confidence Interval Lower Bound	95% Confidence Interval Upper Bound
-7.089	.466	-8.083	-6.095

2. System

Estimates

Measure: MEASURE_1

System	Mean	Std. Error	95% Confidence Interval Lower Bound	95% Confidence Interval Upper Bound
1	-7.036	.642	-8.404	-5.667
2	-7.142	.319	-7.822	-6.462

Pairwise Comparisons

Measure: MEASURE_1

(I) System	(J) System	Mean Difference (I-J)	Std. Error	Sig.[a]	95% Confidence Interval for Difference[a] Lower Bound	Upper Bound
1	2	.107	.398	.792	-.741	.955
2	1	-.107	.398	.792	-.955	.741

Based on estimated marginal means

a. Adjustment for multiple comparisons: Least Significant Difference (equivalent to no adjustments).

Multivariate Tests

	Value	F	Hypothesis df	Error df	Sig.	Partial Eta Squared
Pillai's trace	.005	.072[a]	1.000	15.000	.792	.005
Wilks' lambda	.995	.072[a]	1.000	15.000	.792	.005
Hotelling's trace	.005	.072[a]	1.000	15.000	.792	.005
Roy's largest root	.005	.072[a]	1.000	15.000	.792	.005

Each F tests the multivariate effect of System. These tests are based on the linearly independent pairwise comparisons among the estimated marginal means.

a. Exact statistic

3. Speed

Estimates

Measure: MEASURE_1

Speed	Mean	Std. Error	95% Confidence Interval Lower Bound	95% Confidence Interval Upper Bound
1	-5.027	.414	-5.910	-4.145
2	-6.970	.521	-8.081	-5.860
3	-9.269	.563	-10.469	-8.069

Pairwise Comparisons

Measure: MEASURE_1

(I) Speed	(J) Speed	Mean Difference (I-J)	Std. Error	Sig.[b]	95% Confidence Interval for Difference[b] Lower Bound	Upper Bound
1	2	1.943*	.284	.000	1.338	2.548
	3	4.242*	.401	.000	3.387	5.097
2	1	-1.943*	.284	.000	-2.548	-1.338
	3	2.299*	.286	.000	1.690	2.908
3	1	-4.242*	.401	.000	-5.097	-3.387
	2	-2.299*	.286	.000	-2.908	-1.690

Based on estimated marginal means

*. The mean difference is significant at the .05 level.

b. Adjustment for multiple comparisons: Least Significant Difference (equivalent to no adjustments).

Multivariate Tests

	Value	F	Hypothesis df	Error df	Sig.	Partial Eta Squared
Pillai's trace	.882	52.503[a]	2.000	14.000	.000	.882
Wilks' lambda	.118	52.503[a]	2.000	14.000	.000	.882
Hotelling's trace	7.500	52.503[a]	2.000	14.000	.000	.882
Roy's largest root	7.500	52.503[a]	2.000	14.000	.000	.882

Each F tests the multivariate effect of Speed. These tests are based on the linearly independent pairwise comparisons among the estimated marginal means.

a. Exact statistic

4. System * Speed

Measure: MEASURE_1

System	Speed	Mean	Std. Error	95% Confidence Interval	
				Lower Bound	Upper Bound
1	1	-5.151	.530	-6.281	-4.021
	2	-6.819	.689	-8.289	-5.350
	3	-9.136	.816	-10.876	-7.397
2	1	-4.904	.316	-5.577	-4.230
	2	-7.121	.404	-7.981	-6.261
	3	-9.402	.386	-10.224	-8.579

Profile Plots

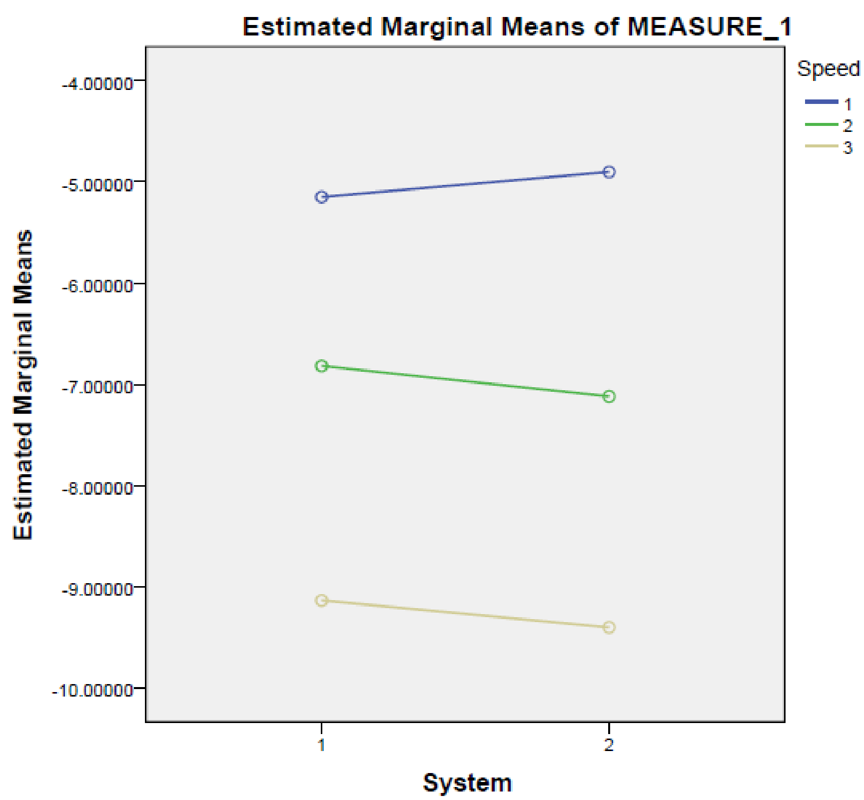

General Linear Model

Within-Subjects Factors

Measure: MEASURE_1

System	Speed	Dependent Variable
1	1	AP_1_T_M_5
	2	AP_1_T_M_65
	3	AP_1_T_M_8
2	1	AP_1_T_ML_5
	2	AP_1_T_ML_65
	3	AP_1_T_ML_8

Descriptive Statistics

	Mean	Std. Deviation	N
AP_1_T_M_5	8.05000000	1.476482306	16
AP_1_T_M_65	7.61875000	1.376090477	16
AP_1_T_M_8	7.37500000	2.566060534	16
AP_1_T_ML_5	8.73125000	1.297545760	16
AP_1_T_ML_65	7.89375000	1.331900272	16
AP_1_T_ML_8	7.2750000	1.53297097	16

Multivariate Tests[a]

Effect		Value	F	Hypothesis df	Error df	Sig.
System	Pillai's Trace	.107	1.803[b]	1.000	15.000	.199
	Wilks' Lambda	.893	1.803[b]	1.000	15.000	.199
	Hotelling's Trace	.120	1.803[b]	1.000	15.000	.199
	Roy's Largest Root	.120	1.803[b]	1.000	15.000	.199
Speed	Pillai's Trace	.295	2.926[b]	2.000	14.000	.087
	Wilks' Lambda	.705	2.926[b]	2.000	14.000	.087
	Hotelling's Trace	.418	2.926[b]	2.000	14.000	.087
	Roy's Largest Root	.418	2.926[b]	2.000	14.000	.087
System * Speed	Pillai's Trace	.202	1.777[b]	2.000	14.000	.205
	Wilks' Lambda	.798	1.777[b]	2.000	14.000	.205
	Hotelling's Trace	.254	1.777[b]	2.000	14.000	.205
	Roy's Largest Root	.254	1.777[b]	2.000	14.000	.205

Multivariate Tests[a]

Effect		Partial Eta Squared
System	Pillai's Trace	.107
	Wilks' Lambda	.107
	Hotelling's Trace	.107
	Roy's Largest Root	.107
Speed	Pillai's Trace	.295
	Wilks' Lambda	.295
	Hotelling's Trace	.295
	Roy's Largest Root	.295
System * Speed	Pillai's Trace	.202
	Wilks' Lambda	.202
	Hotelling's Trace	.202
	Roy's Largest Root	.202

a. Design: Intercept
Within Subjects Design: System + Speed + System * Speed

b. Exact statistic

Mauchly's Test of Sphericity[a]

Measure: MEASURE_1

Within Subjects Effect	Mauchly's W	Approx. Chi-Square	df	Sig.	Epsilon[b] Greenhouse-Geisser
System	1.000	.000	0	.	1.000
Speed	.240	19.965	2	.000	.568
System * Speed	.504	9.599	2	.008	.668

Mauchly's Test of Sphericity[a]

Measure: MEASURE_1

Within Subjects Effect	Epsilon[b]	
	Huynh-Feldt	Lower-bound
System	1.000	1.000
Speed	.584	.500
System * Speed	.709	.500

Tests the null hypothesis that the error covariance matrix of the orthonormalized transformed dependent variables is proportional to an identity matrix.

a. Design: Intercept
Within Subjects Design: System + Speed + System * Speed

b. May be used to adjust the degrees of freedom for the averaged tests of significance. Corrected tests are displayed in the Tests of Within-Subjects Effects table.

Tests of Within-Subjects Effects

Measure: MEASURE_1

Source		Type III Sum of Squares	df	Mean Square	F
System	Sphericity Assumed	1.955	1	1.955	1.803
	Greenhouse-Geisser	1.955	1.000	1.955	1.803
	Huynh-Feldt	1.955	1.000	1.955	1.803
	Lower-bound	1.955	1.000	1.955	1.803
Error(System)	Sphericity Assumed	16.267	15	1.084	
	Greenhouse-Geisser	16.267	15.000	1.084	
	Huynh-Feldt	16.267	15.000	1.084	
	Lower-bound	16.267	15.000	1.084	
Speed	Sphericity Assumed	18.389	2	9.194	5.750
	Greenhouse-Geisser	18.389	1.137	16.180	5.750
	Huynh-Feldt	18.389	1.167	15.752	5.750
	Lower-bound	18.389	1.000	18.389	5.750
Error(Speed)	Sphericity Assumed	47.968	30	1.599	
	Greenhouse-Geisser	47.968	17.048	2.814	
	Huynh-Feldt	47.968	17.511	2.739	
	Lower-bound	47.968	15.000	3.198	
System * Speed	Sphericity Assumed	2.443	2	1.221	2.270
	Greenhouse-Geisser	2.443	1.337	1.827	2.270
	Huynh-Feldt	2.443	1.419	1.722	2.270
	Lower-bound	2.443	1.000	2.443	2.270
Error(System*Speed)	Sphericity Assumed	16.141	30	.538	
	Greenhouse-Geisser	16.141	20.051	.805	
	Huynh-Feldt	16.141	21.284	.758	
	Lower-bound	16.141	15.000	1.076	

Tests of Within-Subjects Effects

Measure: MEASURE_1

Source		Sig.	Partial Eta Squared
System	Sphericity Assumed	.199	.107
	Greenhouse-Geisser	.199	.107
	Huynh-Feldt	.199	.107
	Lower-bound	.199	.107
Error(System)	Sphericity Assumed		
	Greenhouse-Geisser		
	Huynh-Feldt		
	Lower-bound		
Speed	Sphericity Assumed	.008	.277
	Greenhouse-Geisser	.025	.277
	Huynh-Feldt	.024	.277
	Lower-bound	.030	.277
Error(Speed)	Sphericity Assumed		
	Greenhouse-Geisser		
	Huynh-Feldt		
	Lower-bound		
System * Speed	Sphericity Assumed	.121	.131
	Greenhouse-Geisser	.142	.131
	Huynh-Feldt	.139	.131
	Lower-bound	.153	.131
Error(System*Speed)	Sphericity Assumed		
	Greenhouse-Geisser		
	Huynh-Feldt		
	Lower-bound		

Tests of Within-Subjects Contrasts

Measure: MEASURE_1

Source	System	Speed	Type III Sum of Squares	df	Mean Square	F
System	Linear		1.955	1	1.955	1.803
Error(System)	Linear		16.267	15	1.084	
Speed		Linear	18.169	1	18.169	6.100
		Quadratic	.220	1	.220	1.004
Error(Speed)		Linear	44.679	15	2.979	
		Quadratic	3.289	15	.219	
System * Speed	Linear	Linear	2.441	1	2.441	2.844
		Quadratic	.001	1	.001	.006
Error(System*Speed)	Linear	Linear	12.876	15	.858	
		Quadratic	3.265	15	.218	

Tests of Within-Subjects Contrasts

Measure: MEASURE_1

Source	System	Speed	Sig.	Partial Eta Squared
System	Linear		.199	.107
Error(System)	Linear			
Speed		Linear	.026	.289
		Quadratic	.332	.063
Error(Speed)		Linear		
		Quadratic		
System * Speed	Linear	Linear	.112	.159
		Quadratic	.939	.000
Error(System*Speed)	Linear	Linear		
		Quadratic		

Tests of Between-Subjects Effects

Measure: MEASURE_1

Transformed Variable: Average

Source	Type III Sum of Squares	df	Mean Square	F	Sig.	Partial Eta Squared
Intercept	5876.575	1	5876.575	529.061	.000	.972
Error	166.613	15	11.108			

Estimated Marginal Means

1. Grand Mean

Measure: MEASURE_1

Mean	Std. Error	95% Confidence Interval	
		Lower Bound	Upper Bound
7.824	.340	7.099	8.549

2. System

Estimates

Measure: MEASURE_1

System	Mean	Std. Error	95% Confidence Interval	
			Lower Bound	Upper Bound
1	7.681	.400	6.829	8.534
2	7.967	.307	7.313	8.620

Pairwise Comparisons

Measure: MEASURE_1

(I) System	(J) System	Mean Difference (I-J)	Std. Error	Sig.[a]	95% Confidence Interval for Difference[a]	
					Lower Bound	Upper Bound
1	2	-.285	.213	.199	-.738	.168
2	1	.285	.213	.199	-.168	.738

Based on estimated marginal means

a. Adjustment for multiple comparisons: Least Significant Difference (equivalent to no adjustments).

Multivariate Tests

	Value	F	Hypothesis df	Error df	Sig.	Partial Eta Squared
Pillai's trace	.107	1.803[a]	1.000	15.000	.199	.107
Wilks' lambda	.893	1.803[a]	1.000	15.000	.199	.107
Hotelling's trace	.120	1.803[a]	1.000	15.000	.199	.107
Roy's largest root	.120	1.803[a]	1.000	15.000	.199	.107

Each F tests the multivariate effect of System. These tests are based on the linearly independent pairwise comparisons among the estimated marginal means.

a. Exact statistic

3. Speed

Estimates

Measure: MEASURE_1

Speed	Mean	Std. Error	95% Confidence Interval	
			Lower Bound	Upper Bound
1	8.391	.326	7.696	9.086
2	7.756	.329	7.055	8.458
3	7.325	.482	6.297	8.353

Pairwise Comparisons

Measure: MEASURE_1

(I) Speed	(J) Speed	Mean Difference (I-J)	Std. Error	Sig.[b]	95% Confidence Interval for Difference[b] Lower Bound	Upper Bound
1	2	.634*	.260	.027	.081	1.188
	3	1.066*	.431	.026	.146	1.985
2	1	-.634*	.260	.027	-1.188	-.081
	3	.431	.215	.063	-.027	.889
3	1	-1.066*	.431	.026	-1.985	-.146
	2	-.431	.215	.063	-.889	.027

Based on estimated marginal means

*. The mean difference is significant at the .05 level.

b. Adjustment for multiple comparisons: Least Significant Difference (equivalent to no adjustments).

Multivariate Tests

	Value	F	Hypothesis df	Error df	Sig.	Partial Eta Squared
Pillai's trace	.295	2.926[a]	2.000	14.000	.087	.295
Wilks' lambda	.705	2.926[a]	2.000	14.000	.087	.295
Hotelling's trace	.418	2.926[a]	2.000	14.000	.087	.295
Roy's largest root	.418	2.926[a]	2.000	14.000	.087	.295

Each F tests the multivariate effect of Speed. These tests are based on the linearly independent pairwise comparisons among the estimated marginal means.

a. Exact statistic

4. System * Speed

Measure: MEASURE_1

System	Speed	Mean	Std. Error	95% Confidence Interval Lower Bound	Upper Bound
1	1	8.050	.369	7.263	8.837
	2	7.619	.344	6.885	8.352
	3	7.375	.642	6.008	8.742
2	1	8.731	.324	8.040	9.423
	2	7.894	.333	7.184	8.603
	3	7.275	.383	6.458	8.092

Profile Plots

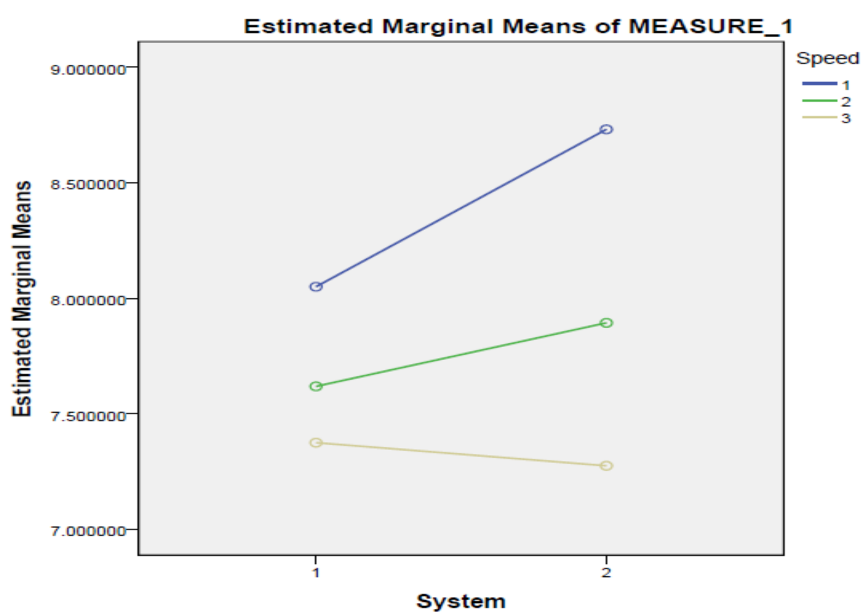

```
/PLOT=PROFILE(System*Speed)
/EMMEANS=TABLES(OVERALL)
/EMMEANS=TABLES(System) COMPARE ADJ(LSD)
/EMMEANS=TABLES(Speed) COMPARE ADJ(LSD)
/EMMEANS=TABLES(System*Speed)
/PRINT=DESCRIPTIVE ETASQ
/CRITERIA=ALPHA(.05)
/WSDESIGN=System Speed System*Speed.
```

General Linear Model

Within-Subjects Factors

Measure: MEASURE_1

System	Speed	Dependent Variable
1	1	AP_2_M_5
	2	AP_2_M_65
	3	AP_2_M_8
2	1	AP_2_ML_5
	2	AP_2_ML_65
	3	AP_2_ML_8

Descriptive Statistics

	Mean	Std. Deviation	N
AP_2_M_5	9.60511906	3.048316190	16
AP_2_M_65	13.24436406	4.014122965	16
AP_2_M_8	17.28049294	4.663550322	16
AP_2_ML_5	9.37386563	2.603606218	16
AP_2_ML_65	13.9561828	3.38924865	16
AP_2_ML_8	18.34245994	4.824582881	16

Multivariate Tests[a]

Effect		Value	F	Hypothesis df	Error df	Sig.
System	Pillai's Trace	.040	.618[b]	1.000	15.000	.444
	Wilks' Lambda	.960	.618[b]	1.000	15.000	.444
	Hotelling's Trace	.041	.618[b]	1.000	15.000	.444
	Roy's Largest Root	.041	.618[b]	1.000	15.000	.444
Speed	Pillai's Trace	.911	71.371[b]	2.000	14.000	.000
	Wilks' Lambda	.089	71.371[b]	2.000	14.000	.000
	Hotelling's Trace	10.196	71.371[b]	2.000	14.000	.000
	Roy's Largest Root	10.196	71.371[b]	2.000	14.000	.000
System * Speed	Pillai's Trace	.252	2.353[b]	2.000	14.000	.132
	Wilks' Lambda	.748	2.353[b]	2.000	14.000	.132
	Hotelling's Trace	.336	2.353[b]	2.000	14.000	.132
	Roy's Largest Root	.336	2.353[b]	2.000	14.000	.132

Multivariate Tests[a]

Effect		Partial Eta Squared
System	Pillai's Trace	.040
	Wilks' Lambda	.040
	Hotelling's Trace	.040
	Roy's Largest Root	.040
Speed	Pillai's Trace	.911
	Wilks' Lambda	.911
	Hotelling's Trace	.911
	Roy's Largest Root	.911
System * Speed	Pillai's Trace	.252
	Wilks' Lambda	.252
	Hotelling's Trace	.252
	Roy's Largest Root	.252

a. Design: Intercept
Within Subjects Design: System + Speed + System * Speed

b. Exact statistic

Mauchly's Test of Sphericity[a]

Measure: MEASURE_1

Within Subjects Effect	Mauchly's W	Approx. Chi-Square	df	Sig.	Epsilon[b] Greenhouse-Geisser
System	1.000	.000	0	.	1.000
Speed	.679	5.422	2	.066	.757
System * Speed	.991	.123	2	.940	.991

Mauchly's Test of Sphericity[a]

Measure: MEASURE_1

Within Subjects Effect	Epsilon[b] Huynh-Feldt	Lower-bound
System	1.000	1.000
Speed	.824	.500
System * Speed	1.000	.500

Tests the null hypothesis that the error covariance matrix of the orthonormalized transformed dependent variables is proportional to an identity matrix.

a. Design: Intercept
Within Subjects Design: System + Speed + System * Speed

b. May be used to adjust the degrees of freedom for the averaged tests of significance. Corrected tests are displayed in the Tests of Within-Subjects Effects table.

Tests of Within-Subjects Effects

Measure: MEASURE_1

Source		Type III Sum of Squares	df	Mean Square	F
System	Sphericity Assumed	6.345	1	6.345	.618
	Greenhouse-Geisser	6.345	1.000	6.345	.618
	Huynh-Feldt	6.345	1.000	6.345	.618
	Lower-bound	6.345	1.000	6.345	.618
Error(System)	Sphericity Assumed	154.119	15	10.275	
	Greenhouse-Geisser	154.119	15.000	10.275	
	Huynh-Feldt	154.119	15.000	10.275	
	Lower-bound	154.119	15.000	10.275	
Speed	Sphericity Assumed	1108.140	2	554.070	109.159
	Greenhouse-Geisser	1108.140	1.514	731.985	109.159
	Huynh-Feldt	1108.140	1.648	672.506	109.159
	Lower-bound	1108.140	1.000	1108.140	109.159
Error(Speed)	Sphericity Assumed	152.274	30	5.076	
	Greenhouse-Geisser	152.274	22.708	6.706	
	Huynh-Feldt	152.274	24.717	6.161	
	Lower-bound	152.274	15.000	10.152	
System * Speed	Sphericity Assumed	7.158	2	3.579	2.288
	Greenhouse-Geisser	7.158	1.983	3.611	2.288
	Huynh-Feldt	7.158	2.000	3.579	2.288
	Lower-bound	7.158	1.000	7.158	2.288
Error(System*Speed)	Sphericity Assumed	46.932	30	1.564	
	Greenhouse-Geisser	46.932	29.740	1.578	
	Huynh-Feldt	46.932	30.000	1.564	
	Lower-bound	46.932	15.000	3.129	

Tests of Within-Subjects Effects

Measure: MEASURE_1

Source		Sig.	Partial Eta Squared
System	Sphericity Assumed	.444	.040
	Greenhouse-Geisser	.444	.040
	Huynh-Feldt	.444	.040
	Lower-bound	.444	.040
Error(System)	Sphericity Assumed		
	Greenhouse-Geisser		
	Huynh-Feldt		
	Lower-bound		
Speed	Sphericity Assumed	.000	.879
	Greenhouse-Geisser	.000	.879
	Huynh-Feldt	.000	.879
	Lower-bound	.000	.879
Error(Speed)	Sphericity Assumed		
	Greenhouse-Geisser		
	Huynh-Feldt		
	Lower-bound		
System * Speed	Sphericity Assumed	.119	.132
	Greenhouse-Geisser	.119	.132
	Huynh-Feldt	.119	.132
	Lower-bound	.151	.132
Error(System*Speed)	Sphericity Assumed		
	Greenhouse-Geisser		
	Huynh-Feldt		
	Lower-bound		

Tests of Within-Subjects Contrasts

Measure: MEASURE_1

Source	System	Speed	Type III Sum of Squares	df	Mean Square	F
System	Linear		6.345	1	6.345	.618
Error(System)	Linear		154.119	15	10.275	
Speed		Linear	1108.087	1	1108.087	143.494
		Quadratic	.054	1	.054	.022
Error(Speed)		Linear	115.833	15	7.722	
		Quadratic	36.441	15	2.429	
System * Speed	Linear	Linear	6.690	1	6.690	4.608
		Quadratic	.469	1	.469	.280
Error(System*Speed)	Linear	Linear	21.778	15	1.452	
		Quadratic	25.154	15	1.677	

Tests of Within-Subjects Contrasts

Measure: MEASURE_1

Source	System	Speed	Sig.	Partial Eta Squared
System	Linear		.444	.040
Error(System)	Linear			
Speed		Linear	.000	.905
		Quadratic	.884	.001
Error(Speed)		Linear		
		Quadratic		
System * Speed	Linear	Linear	.049	.235
		Quadratic	.605	.018
Error(System*Speed)	Linear	Linear		
		Quadratic		

Tests of Between-Subjects Effects

Measure: MEASURE_1
Transformed Variable: Average

Source	Type III Sum of Squares	df	Mean Square	F	Sig.	Partial Eta Squared
Intercept	17844.391	1	17844.391	273.933	.000	.948
Error	977.123	15	65.142			

Estimated Marginal Means

1. Grand Mean

Measure: MEASURE_1

Mean	Std. Error	95% Confidence Interval	
		Lower Bound	Upper Bound
13.634	.824	11.878	15.390

2. System

Estimates

Measure: MEASURE_1

System	Mean	Std. Error	95% Confidence Interval	
			Lower Bound	Upper Bound
1	13.377	.932	11.391	15.363
2	13.891	.839	12.104	15.678

Pairwise Comparisons

Measure: MEASURE_1

(I) System	(J) System	Mean Difference (I-J)	Std. Error	Sig.[a]	95% Confidence Interval for Difference[a]	
					Lower Bound	Upper Bound
1	2	-.514	.654	.444	-1.909	.880
2	1	.514	.654	.444	-.880	1.909

Based on estimated marginal means

a. Adjustment for multiple comparisons: Least Significant Difference (equivalent to no adjustments).

Multivariate Tests

	Value	F	Hypothesis df	Error df	Sig.	Partial Eta Squared
Pillai's trace	.040	.618[a]	1.000	15.000	.444	.040
Wilks' lambda	.960	.618[a]	1.000	15.000	.444	.040
Hotelling's trace	.041	.618[a]	1.000	15.000	.444	.040
Roy's largest root	.041	.618[a]	1.000	15.000	.444	.040

Each F tests the multivariate effect of System. These tests are based on the linearly independent pairwise comparisons among the estimated marginal means.

a. Exact statistic

3. Speed

Estimates

Measure: MEASURE_1

Speed	Mean	Std. Error	95% Confidence Interval	
			Lower Bound	Upper Bound
1	9.489	.675	8.052	10.927
2	13.600	.825	11.841	15.360
3	17.811	1.103	15.461	20.162

Pairwise Comparisons

Measure: MEASURE_1

(I) Speed	(J) Speed	Mean Difference (I-J)	Std. Error	Sig.[b]	95% Confidence Interval for Difference[b]	
					Lower Bound	Upper Bound
1	2	-4.111*	.417	.000	-4.999	-3.223
	3	-8.322*	.695	.000	-9.803	-6.841
2	1	4.111*	.417	.000	3.223	4.999
	3	-4.211*	.544	.000	-5.370	-3.052
3	1	8.322*	.695	.000	6.841	9.803
	2	4.211*	.544	.000	3.052	5.370

Based on estimated marginal means

*. The mean difference is significant at the .05 level.

b. Adjustment for multiple comparisons: Least Significant Difference (equivalent to no adjustments).

Multivariate Tests

	Value	F	Hypothesis df	Error df	Sig.	Partial Eta Squared
Pillai's trace	.911	71.371[a]	2.000	14.000	.000	.911
Wilks' lambda	.089	71.371[a]	2.000	14.000	.000	.911
Hotelling's trace	10.196	71.371[a]	2.000	14.000	.000	.911
Roy's largest root	10.196	71.371[a]	2.000	14.000	.000	.911

Each F tests the multivariate effect of Speed. These tests are based on the linearly independent pairwise comparisons among the estimated marginal means.

a. Exact statistic

4. System * Speed

Measure: MEASURE_1

System	Speed	Mean	Std. Error	95% Confidence Interval	
				Lower Bound	Upper Bound
1	1	9.605	.762	7.981	11.229
	2	13.244	1.004	11.105	15.383
	3	17.280	1.166	14.795	19.766
2	1	9.374	.651	7.987	10.761
	2	13.956	.847	12.150	15.762
	3	18.342	1.206	15.772	20.913

Profile Plots

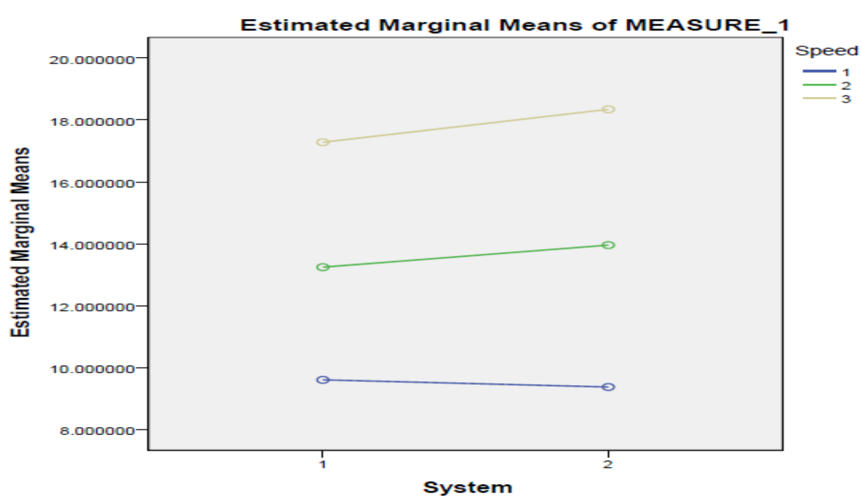

```
/PLOT=PROFILE(System*Speed)
/EMMEANS=TABLES(OVERALL)
/EMMEANS=TABLES(System) COMPARE ADJ(LSD)
/EMMEANS=TABLES(Speed) COMPARE ADJ(LSD)
/EMMEANS=TABLES(System*Speed)
/PRINT=DESCRIPTIVE ETASQ
/CRITERIA=ALPHA(.05)
/WSDESIGN=System Speed System*Speed.
```

General Linear Model

Within-Subjects Factors

Measure: MEASURE_1

System	Speed	Dependent Variable
1	1	AP_2_T_M_5
	2	AP_2_T_M_65
	3	AP_2_T_M_8
2	1	AP_2_T_ML_5
	2	AP_2_T_ML_65
	3	AP_2_T_ML_8

Descriptive Statistics

	Mean	Std. Deviation	N
AP_2_T_M_5	19.86875000	1.724226880	16
AP_2_T_M_65	17.7812500	1.65538263	16
AP_2_T_M_8	15.80000000	1.938728105	16
AP_2_T_ML_5	19.95625000	1.534913135	16
AP_2_T_ML_65	17.83125000	1.577643285	16
AP_2_T_ML_8	15.91250000	1.595357849	16

Multivariate Tests[a]

Effect		Value	F	Hypothesis df	Error df	Sig.
System	Pillai's Trace	.025	.392[b]	1.000	15.000	.540
	Wilks' Lambda	.975	.392[b]	1.000	15.000	.540
	Hotelling's Trace	.026	.392[b]	1.000	15.000	.540
	Roy's Largest Root	.026	.392[b]	1.000	15.000	.540
Speed	Pillai's Trace	.968	213.242[b]	2.000	14.000	.000
	Wilks' Lambda	.032	213.242[b]	2.000	14.000	.000
	Hotelling's Trace	30.463	213.242[b]	2.000	14.000	.000
	Roy's Largest Root	30.463	213.242[b]	2.000	14.000	.000
System * Speed	Pillai's Trace	.025	.176[b]	2.000	14.000	.840
	Wilks' Lambda	.975	.176[b]	2.000	14.000	.840
	Hotelling's Trace	.025	.176[b]	2.000	14.000	.840
	Roy's Largest Root	.025	.176[b]	2.000	14.000	.840

Multivariate Tests[a]

Effect		Partial Eta Squared
System	Pillai's Trace	.025
	Wilks' Lambda	.025
	Hotelling's Trace	.025
	Roy's Largest Root	.025
Speed	Pillai's Trace	.968
	Wilks' Lambda	.968
	Hotelling's Trace	.968
	Roy's Largest Root	.968
System * Speed	Pillai's Trace	.025
	Wilks' Lambda	.025
	Hotelling's Trace	.025
	Roy's Largest Root	.025

a. Design: Intercept
Within Subjects Design: System + Speed + System * Speed

b. Exact statistic

Mauchly's Test of Sphericity[a]

Measure: MEASURE_1

Within Subjects Effect	Mauchly's W	Approx. Chi-Square	df	Sig.	Epsilon[b] Greenhouse-Geisser
System	1.000	.000	0	.	1.000
Speed	.346	14.878	2	.001	.604
System * Speed	.692	5.156	2	.076	.764

Mauchly's Test of Sphericity[a]

Measure: MEASURE_1

Within Subjects Effect	Epsilon[b] Huynh-Feldt	Lower-bound
System	1.000	1.000
Speed	.629	.500
System * Speed	.834	.500

Tests the null hypothesis that the error covariance matrix of the orthonormalized transformed dependent variables is proportional to an identity matrix.

a. Design: Intercept
Within Subjects Design: System + Speed + System * Speed

b. May be used to adjust the degrees of freedom for the averaged tests of significance. Corrected tests are displayed in the Tests of Within-Subjects Effects table.

Tests of Within-Subjects Effects

Measure: MEASURE_1

Source		Type III Sum of Squares	df	Mean Square	F
System	Sphericity Assumed	.167	1	.167	.392
	Greenhouse-Geisser	.167	1.000	.167	.392
	Huynh-Feldt	.167	1.000	.167	.392
	Lower-bound	.167	1.000	.167	.392
Error(System)	Sphericity Assumed	6.370	15	.425	
	Greenhouse-Geisser	6.370	15.000	.425	
	Huynh-Feldt	6.370	15.000	.425	
	Lower-bound	6.370	15.000	.425	
Speed	Sphericity Assumed	263.381	2	131.690	123.566
	Greenhouse-Geisser	263.381	1.209	217.880	123.566
	Huynh-Feldt	263.381	1.257	209.460	123.566
	Lower-bound	263.381	1.000	263.381	123.566
Error(Speed)	Sphericity Assumed	31.973	30	1.066	
	Greenhouse-Geisser	31.973	18.133	1.763	
	Huynh-Feldt	31.973	18.861	1.695	
	Lower-bound	31.973	15.000	2.132	
System * Speed	Sphericity Assumed	.016	2	.008	.084
	Greenhouse-Geisser	.016	1.529	.010	.084
	Huynh-Feldt	.016	1.668	.009	.084
	Lower-bound	.016	1.000	.016	.084
Error(System*Speed)	Sphericity Assumed	2.817	30	.094	
	Greenhouse-Geisser	2.817	22.934	.123	
	Huynh-Feldt	2.817	25.013	.113	
	Lower-bound	2.817	15.000	.188	

Tests of Within-Subjects Effects

Measure: MEASURE_1

Source		Sig.	Partial Eta Squared
System	Sphericity Assumed	.540	.025
	Greenhouse-Geisser	.540	.025
	Huynh-Feldt	.540	.025
	Lower-bound	.540	.025
Error(System)	Sphericity Assumed		
	Greenhouse-Geisser		
	Huynh-Feldt		
	Lower-bound		
Speed	Sphericity Assumed	.000	.892
	Greenhouse-Geisser	.000	.892
	Huynh-Feldt	.000	.892
	Lower-bound	.000	.892
Error(Speed)	Sphericity Assumed		
	Greenhouse-Geisser		
	Huynh-Feldt		
	Lower-bound		
System * Speed	Sphericity Assumed	.919	.006
	Greenhouse-Geisser	.872	.006
	Huynh-Feldt	.888	.006
	Lower-bound	.776	.006
Error(System*Speed)	Sphericity Assumed		
	Greenhouse-Geisser		
	Huynh-Feldt		
	Lower-bound		

Tests of Within-Subjects Contrasts

Measure: MEASURE_1

Source	System	Speed	Type III Sum of Squares	df	Mean Square	F
System	Linear		.167	1	.167	.392
Error(System)	Linear		6.370	15	.425	
Speed		Linear	263.251	1	263.251	185.917
		Quadratic	.130	1	.130	.182
Error(Speed)		Linear	21.239	15	1.416	
		Quadratic	10.733	15	.716	
System * Speed	Linear	Linear	.002	1	.002	.019
		Quadratic	.013	1	.013	.250
Error(System*Speed)	Linear	Linear	2.017	15	.134	
		Quadratic	.800	15	.053	

Tests of Within-Subjects Contrasts

Measure: MEASURE_1

Source	System	Speed	Sig.	Partial Eta Squared
System	Linear		.540	.025
Error(System)	Linear			
Speed		Linear	.000	.925
		Quadratic	.676	.012
Error(Speed)		Linear		
		Quadratic		
System * Speed	Linear	Linear	.893	.001
		Quadratic	.624	.016
Error(System*Speed)	Linear	Linear		
		Quadratic		

Tests of Between-Subjects Effects

Measure: MEASURE_1
Transformed Variable: Average

Source	Type III Sum of Squares	df	Mean Square	F	Sig.	Partial Eta Squared
Intercept	30616.327	1	30616.327	2168.602	.000	.993
Error	211.770	15	14.118			

Estimated Marginal Means

1. Grand Mean

Measure: MEASURE_1

Mean	Std. Error	95% Confidence Interval	
		Lower Bound	Upper Bound
17.858	.383	17.041	18.676

2. System

Estimates

Measure: MEASURE_1

System	Mean	Std. Error	95% Confidence Interval	
			Lower Bound	Upper Bound
1	17.817	.422	16.918	18.716
2	17.900	.354	17.146	18.654

Pairwise Comparisons

Measure: MEASURE_1

(I) System	(J) System	Mean Difference (I-J)	Std. Error	Sig.[a]	95% Confidence Interval for Difference[a]	
					Lower Bound	Upper Bound
1	2	-.083	.133	.540	-.367	.200
2	1	.083	.133	.540	-.200	.367

Based on estimated marginal means

a. Adjustment for multiple comparisons: Least Significant Difference (equivalent to no adjustments).

Multivariate Tests

	Value	F	Hypothesis df	Error df	Sig.	Partial Eta Squared
Pillai's trace	.025	.392[a]	1.000	15.000	.540	.025
Wilks' lambda	.975	.392[a]	1.000	15.000	.540	.025
Hotelling's trace	.026	.392[a]	1.000	15.000	.540	.025
Roy's largest root	.026	.392[a]	1.000	15.000	.540	.025

Each F tests the multivariate effect of System. These tests are based on the linearly independent pairwise comparisons among the estimated marginal means.

a. Exact statistic

3. Speed

Estimates

Measure: MEASURE_1

Speed	Mean	Std. Error	95% Confidence Interval	
			Lower Bound	Upper Bound
1	19.913	.396	19.068	20.757
2	17.806	.399	16.957	18.656
3	15.856	.438	14.923	16.790

Pairwise Comparisons

Measure: MEASURE_1

(I) Speed	(J) Speed	Mean Difference (I-J)	Std. Error	Sig.[b]	95% Confidence Interval for Difference[b]	
					Lower Bound	Upper Bound
1	2	2.106*	.314	.000	1.438	2.775
	3	4.056*	.297	.000	3.422	4.690
2	1	-2.106*	.314	.000	-2.775	-1.438
	3	1.950*	.114	.000	1.707	2.193
3	1	-4.056*	.297	.000	-4.690	-3.422
	2	-1.950*	.114	.000	-2.193	-1.707

Based on estimated marginal means

*. The mean difference is significant at the .05 level.

b. Adjustment for multiple comparisons: Least Significant Difference (equivalent to no adjustments).

Multivariate Tests

	Value	F	Hypothesis df	Error df	Sig.	Partial Eta Squared
Pillai's trace	.968	213.242[a]	2.000	14.000	.000	.968
Wilks' lambda	.032	213.242[a]	2.000	14.000	.000	.968
Hotelling's trace	30.463	213.242[a]	2.000	14.000	.000	.968
Roy's largest root	30.463	213.242[a]	2.000	14.000	.000	.968

Each F tests the multivariate effect of Speed. These tests are based on the linearly independent pairwise comparisons among the estimated marginal means.

a. Exact statistic

4. System * Speed

Measure: MEASURE_1

System	Speed	Mean	Std. Error	95% Confidence Interval Lower Bound	95% Confidence Interval Upper Bound
1	1	19.869	.431	18.950	20.788
	2	17.781	.414	16.899	18.663
	3	15.800	.485	14.767	16.833
2	1	19.956	.384	19.138	20.774
	2	17.831	.394	16.991	18.672
	3	15.913	.399	15.062	16.763

Profile Plots

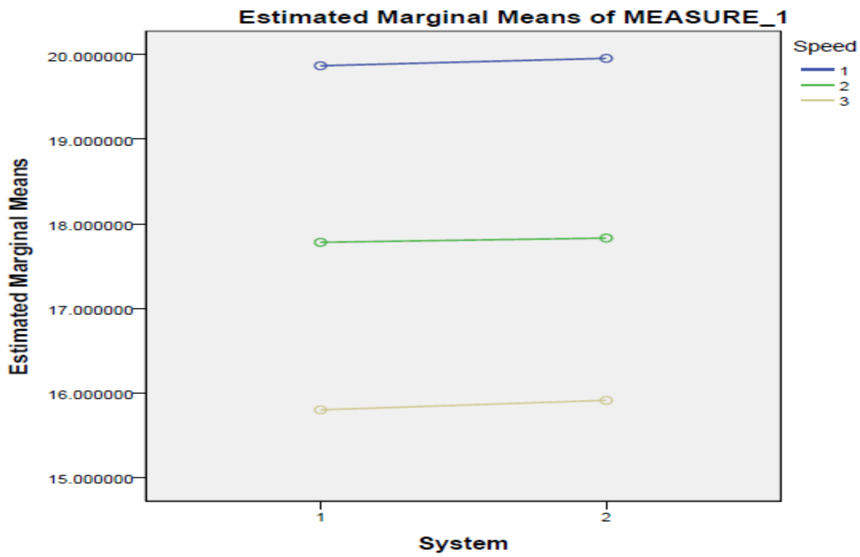

Knee Joint

```
GLM KM_1_M_5 KM_1_M_65 KM_1_M_8 KM_1_ML_5 KM_1_ML_65 KM_1_ML_8
  /WSFACTOR=System 2 Polynomial Speed 3 Polynomial
  /METHOD=SSTYPE(3)
  /PLOT=PROFILE(System*Speed)
  /EMMEANS=TABLES(OVERALL)
  /EMMEANS=TABLES(System) COMPARE ADJ(LSD)
  /EMMEANS=TABLES(Speed) COMPARE ADJ(LSD)
  /EMMEANS=TABLES(System*Speed)
  /PRINT=DESCRIPTIVE ETASQ
  /CRITERIA=ALPHA(.05)
  /WSDESIGN=System Speed System*Speed.
```

General Linear Model

Within-Subjects Factors

Measure: MEASURE_1

System	Speed	Dependent Variable
1	1	KM_1_M_5
	2	KM_1_M_65
	3	KM_1_M_8
2	1	KM_1_ML_5
	2	KM_1_ML_65
	3	KM_1_ML_8

Descriptive Statistics

	Mean	Std. Deviation	N
KM_1_M_5	1.58702381	.334964939	16
KM_1_M_65	1.63987538	.432893567	16
KM_1_M_8	1.5148198	.43991719	16
KM_1_ML_5	1.4260974	.20719512	16
KM_1_ML_65	1.48845856	.365680403	16
KM_1_ML_8	1.28396538	.274476683	16

Multivariate Tests[a]

Effect		Value	F	Hypothesis df	Error df	Sig.	Partial Eta Squared
System	Pillai's Trace	.271	5.564[b]	1.000	15.000	.032	.271
	Wilks' Lambda	.729	5.564[b]	1.000	15.000	.032	.271
	Hotelling's Trace	.371	5.564[b]	1.000	15.000	.032	.271
	Roy's Largest Root	.371	5.564[b]	1.000	15.000	.032	.271
Speed	Pillai's Trace	.306	3.092[b]	2.000	14.000	.077	.306
	Wilks' Lambda	.694	3.092[b]	2.000	14.000	.077	.306
	Hotelling's Trace	.442	3.092[b]	2.000	14.000	.077	.306
	Roy's Largest Root	.442	3.092[b]	2.000	14.000	.077	.306
System * Speed	Pillai's Trace	.219	1.968[b]	2.000	14.000	.176	.219
	Wilks' Lambda	.781	1.968[b]	2.000	14.000	.176	.219
	Hotelling's Trace	.281	1.968[b]	2.000	14.000	.176	.219
	Roy's Largest Root	.281	1.968[b]	2.000	14.000	.176	.219

a. Design: Intercept
 Within Subjects Design: System + Speed + System * Speed

b. Exact statistic

Mauchly's Test of Sphericity[a]

Measure: MEASURE_1

Within Subjects Effect	Mauchly's W	Approx. Chi-Square	df	Sig.	Epsilon[b] Greenhouse-Geisser	Huynh-Feldt	Lower-bound
System	1.000	.000	0	.	1.000	1.000	1.000
Speed	.912	1.292	2	.524	.919	1.000	.500
System * Speed	.923	1.122	2	.571	.928	1.000	.500

Tests the null hypothesis that the error covariance matrix of the orthonormalized transformed dependent variables is proportional to an identity matrix.

a. Design: Intercept
Within Subjects Design: System + Speed + System * Speed

b. May be used to adjust the degrees of freedom for the averaged tests of significance. Corrected tests are displayed in the Tests of Within-Subjects Effects table.

Tests of Within-Subjects Effects

Measure: MEASURE_1

Source		Type III Sum of Squares	df	Mean Square	F	Sig.	Partial Eta Squared
System	Sphericity Assumed	.787	1	.787	5.564	.032	.271
	Greenhouse-Geisser	.787	1.000	.787	5.564	.032	.271
	Huynh-Feldt	.787	1.000	.787	5.564	.032	.271
	Lower-bound	.787	1.000	.787	5.564	.032	.271
Error(System)	Sphericity Assumed	2.121	15	.141			
	Greenhouse-Geisser	2.121	15.000	.141			
	Huynh-Feldt	2.121	15.000	.141			
	Lower-bound	2.121	15.000	.141			
Speed	Sphericity Assumed	.448	2	.224	2.697	.084	.152
	Greenhouse-Geisser	.448	1.838	.243	2.697	.089	.152
	Huynh-Feldt	.448	2.000	.224	2.697	.084	.152
	Lower-bound	.448	1.000	.448	2.697	.121	.152
Error(Speed)	Sphericity Assumed	2.489	30	.083			
	Greenhouse-Geisser	2.489	27.569	.090			
	Huynh-Feldt	2.489	30.000	.083			
	Lower-bound	2.489	15.000	.166			
System * Speed	Sphericity Assumed	.030	2	.015	1.527	.234	.092
	Greenhouse-Geisser	.030	1.857	.016	1.527	.235	.092
	Huynh-Feldt	.030	2.000	.015	1.527	.234	.092
	Lower-bound	.030	1.000	.030	1.527	.236	.092
Error(System*Speed)	Sphericity Assumed	.296	30	.010			
	Greenhouse-Geisser	.296	27.855	.011			
	Huynh-Feldt	.296	30.000	.010			
	Lower-bound	.296	15.000	.020			

Tests of Within-Subjects Contrasts

Measure: MEASURE_1

Source	System	Speed	Type III Sum of Squares	df	Mean Square	F	Sig.	Partial Eta Squared
System	Linear		.787	1	.787	5.564	.032	.271
Error(System)	Linear		2.121	15	.141			
Speed		Linear	.184	1	.184	1.719	.210	.103
		Quadratic	.264	1	.264	4.470	.052	.230
Error(Speed)		Linear	1.604	15	.107			
		Quadratic	.885	15	.059			
System * Speed	Linear	Linear	.020	1	.020	2.247	.155	.130
		Quadratic	.011	1	.011	.958	.343	.060
Error(System*Speed)	Linear	Linear	.131	15	.009			
		Quadratic	.165	15	.011			

Tests of Between-Subjects Effects

Measure: MEASURE_1

Transformed Variable: Average

Source	Type III Sum of Squares	df	Mean Square	F	Sig.	Partial Eta Squared
Intercept	213.141	1	213.141	509.817	.000	.971
Error	6.271	15	.418			

Estimated Marginal Means

1. Grand Mean

Measure: MEASURE_1

Mean	Std. Error	95% Confidence Interval	
		Lower Bound	Upper Bound
1.490	.066	1.349	1.631

2. System

Estimates

Measure: MEASURE_1

System	Mean	Std. Error	95% Confidence Interval	
			Lower Bound	Upper Bound
1	1.581	.090	1.388	1.773
2	1.400	.059	1.273	1.526

Pairwise Comparisons

Measure: MEASURE_1

(I) System	(J) System	Mean Difference (I-J)	Std. Error	Sig.[b]	95% Confidence Interval for Difference[b] Lower Bound	Upper Bound
1	2	.181*	.077	.032	.017	.345
2	1	-.181*	.077	.032	-.345	-.017

Based on estimated marginal means

*. The mean difference is significant at the .05 level.

b. Adjustment for multiple comparisons: Least Significant Difference (equivalent to no adjustments).

Multivariate Tests

	Value	F	Hypothesis df	Error df	Sig.	Partial Eta Squared
Pillai's trace	.271	5.564[a]	1.000	15.000	.032	.271
Wilks' lambda	.729	5.564[a]	1.000	15.000	.032	.271
Hotelling's trace	.371	5.564[a]	1.000	15.000	.032	.271
Roy's largest root	.371	5.564[a]	1.000	15.000	.032	.271

Each F tests the multivariate effect of System. These tests are based on the linearly independent pairwise comparisons among the estimated marginal means.

a. Exact statistic

3. Speed

Estimates

Measure: MEASURE_1

Speed	Mean	Std. Error	95% Confidence Interval Lower Bound	Upper Bound
1	1.507	.059	1.380	1.633
2	1.564	.092	1.369	1.760
3	1.399	.080	1.230	1.569

Pairwise Comparisons

Measure: MEASURE_1

(I) Speed	(J) Speed	Mean Difference (I-J)	Std. Error	Sig.[b]	95% Confidence Interval for Difference[b] Lower Bound	Upper Bound
1	2	-.058	.069	.416	-.204	.089
	3	.107	.082	.210	-.067	.281
2	1	.058	.069	.416	-.089	.204
	3	.165*	.064	.022	.028	.302
3	1	-.107	.082	.210	-.281	.067
	2	-.165*	.064	.022	-.302	-.028

Based on estimated marginal means

*. The mean difference is significant at the .05 level.

b. Adjustment for multiple comparisons: Least Significant Difference (equivalent to no adjustments).

Multivariate Tests

	Value	F	Hypothesis df	Error df	Sig.	Partial Eta Squared
Pillai's trace	.306	3.092[a]	2.000	14.000	.077	.306
Wilks' lambda	.694	3.092[a]	2.000	14.000	.077	.306
Hotelling's trace	.442	3.092[a]	2.000	14.000	.077	.306
Roy's largest root	.442	3.092[a]	2.000	14.000	.077	.306

Each F tests the multivariate effect of Speed. These tests are based on the linearly independent pairwise comparisons among the estimated marginal means.

a. Exact statistic

4. System * Speed

Measure: MEASURE_1

System	Speed	Mean	Std. Error	95% Confidence Interval	
				Lower Bound	Upper Bound
1	1	1.587	.084	1.409	1.766
	2	1.640	.108	1.409	1.871
	3	1.515	.110	1.280	1.749
2	1	1.426	.052	1.316	1.537
	2	1.488	.091	1.294	1.683
	3	1.284	.069	1.138	1.430

Profile Plots

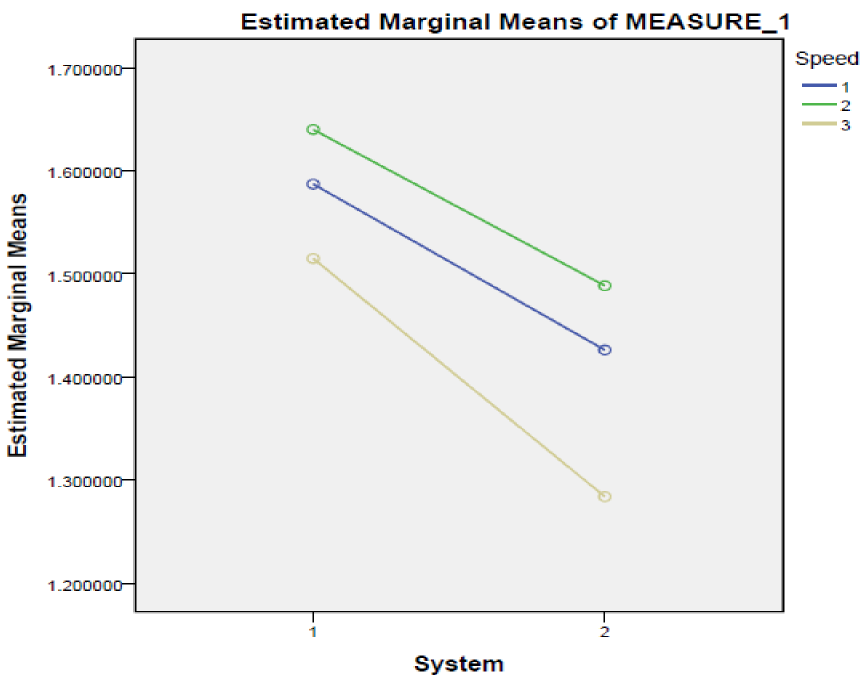

```
GLM KM_1_T_M_5 KM_1_T_M_65 KM_1_T_M_8 KM_1_T_ML_5 KM_1_T_ML_65 KM_1_T_ML_8
  /WSFACTOR=System 2 Polynomial Speed 3 Polynomial
  /METHOD=SSTYPE(3)
  /PLOT=PROFILE(System*Speed)
  /EMMEANS=TABLES(OVERALL)
  /EMMEANS=TABLES(System) COMPARE ADJ(LSD)
  /EMMEANS=TABLES(Speed) COMPARE ADJ(LSD)
  /EMMEANS=TABLES(System*Speed)
  /PRINT=DESCRIPTIVE ETASQ
  /CRITERIA=ALPHA(.05)
  /WSDESIGN=System Speed System*Speed.
```

General Linear Model

Within-Subjects Factors

Measure: MEASURE_1

System	Speed	Dependent Variable
1	1	KM_1_T_M_5
	2	KM_1_T_M_65
	3	KM_1_T_M_8
2	1	KM_1_T_ML_5
	2	KM_1_T_ML_65
	3	KM_1_T_ML_8

Descriptive Statistics

	Mean	Std. Deviation	N
KM_1_T_M_5	10.3812500	1.54152252	16
KM_1_T_M_65	9.4813	1.24484	16
KM_1_T_M_8	9.5500	3.33127	16
KM_1_T_ML_5	10.8063	1.84913	16
KM_1_T_ML_65	9.8938	1.71793	16
KM_1_T_ML_8	9.4438	2.12665	16

Multivariate Tests[a]

Effect		Value	F	Hypothesis df	Error df	Sig.	Partial Eta Squared
System	Pillai's Trace	.083	1.352[b]	1.000	15.000	.263	.083
	Wilks' Lambda	.917	1.352[b]	1.000	15.000	.263	.083
	Hotelling's Trace	.090	1.352[b]	1.000	15.000	.263	.083
	Roy's Largest Root	.090	1.352[b]	1.000	15.000	.263	.083
Speed	Pillai's Trace	.415	4.973[b]	2.000	14.000	.023	.415
	Wilks' Lambda	.585	4.973[b]	2.000	14.000	.023	.415
	Hotelling's Trace	.710	4.973[b]	2.000	14.000	.023	.415
	Roy's Largest Root	.710	4.973[b]	2.000	14.000	.023	.415
System * Speed	Pillai's Trace	.144	1.174[b]	2.000	14.000	.338	.144
	Wilks' Lambda	.856	1.174[b]	2.000	14.000	.338	.144
	Hotelling's Trace	.168	1.174[b]	2.000	14.000	.338	.144
	Roy's Largest Root	.168	1.174[b]	2.000	14.000	.338	.144

a. Design: Intercept
Within Subjects Design: System + Speed + System * Speed

b. Exact statistic

Mauchly's Test of Sphericity[a]

Measure: MEASURE_1

					Epsilon[b]		
Within Subjects Effect	Mauchly's W	Approx. Chi-Square	df	Sig.	Greenhouse-Geisser	Huynh-Feldt	Lower-bound
System	1.000	.000	0	.	1.000	1.000	1.000
Speed	.317	16.099	2	.000	.594	.616	.500
System * Speed	.564	8.010	2	.018	.697	.746	.500

Tests the null hypothesis that the error covariance matrix of the orthonormalized transformed dependent variables is proportional to an identity matrix.

a. Design: Intercept
Within Subjects Design: System + Speed + System * Speed

b. May be used to adjust the degrees of freedom for the averaged tests of significance. Corrected tests are displayed in the Tests of Within-Subjects Effects table.

Tests of Within-Subjects Effects

Measure: MEASURE_1

Source		Type III Sum of Squares	df	Mean Square	F	Sig.	Partial Eta Squared
System	Sphericity Assumed	1.426	1	1.426	1.352	.263	.083
	Greenhouse-Geisser	1.426	1.000	1.426	1.352	.263	.083
	Huynh-Feldt	1.426	1.000	1.426	1.352	.263	.083
	Lower-bound	1.426	1.000	1.426	1.352	.263	.083
Error(System)	Sphericity Assumed	15.822	15	1.055			
	Greenhouse-Geisser	15.822	15.000	1.055			
	Huynh-Feldt	15.822	15.000	1.055			
	Lower-bound	15.822	15.000	1.055			
Speed	Sphericity Assumed	21.981	2	10.991	1.468	.246	.089
	Greenhouse-Geisser	21.981	1.188	18.501	1.468	.247	.089
	Huynh-Feldt	21.981	1.232	17.849	1.468	.248	.089
	Lower-bound	21.981	1.000	21.981	1.468	.244	.089
Error(Speed)	Sphericity Assumed	224.549	30	7.485			
	Greenhouse-Geisser	224.549	17.822	12.600			
	Huynh-Feldt	224.549	18.473	12.156			
	Lower-bound	224.549	15.000	14.970			
System * Speed	Sphericity Assumed	1.471	2	.735	1.972	.157	.116
	Greenhouse-Geisser	1.471	1.393	1.056	1.972	.172	.116
	Huynh-Feldt	1.471	1.491	.986	1.972	.170	.116
	Lower-bound	1.471	1.000	1.471	1.972	.181	.116
Error(System*Speed)	Sphericity Assumed	11.186	30	.373			
	Greenhouse-Geisser	11.186	20.896	.535			
	Huynh-Feldt	11.186	22.366	.500			
	Lower-bound	11.186	15.000	.746			

Tests of Within-Subjects Contrasts

Measure: MEASURE_1

Source	System	Speed	Type III Sum of Squares	df	Mean Square	F	Sig.	Partial Eta Squared
System	Linear		1.426	1	1.426	1.352	.263	.083
Error(System)	Linear		15.822	15	1.055			
Speed		Linear	19.250	1	19.250	1.805	.199	.107
		Quadratic	2.731	1	2.731	.634	.438	.041
Error(Speed)		Linear	159.932	15	10.662			
		Quadratic	64.616	15	4.308			
System * Speed	Linear	Linear	1.129	1	1.129	2.047	.173	.120
		Quadratic	.342	1	.342	1.760	.204	.105
Error(System*Speed)	Linear	Linear	8.274	15	.552			
		Quadratic	2.912	15	.194			

Tests of Between-Subjects Effects

Measure: MEASURE_1
Transformed Variable: Average

Source	Type III Sum of Squares	df	Mean Square	F	Sig.	Partial Eta Squared
Intercept	9458.525	1	9458.525	1034.171	.000	.986
Error	137.190	15	9.146			

Estimated Marginal Means

1. Grand Mean

Measure: MEASURE_1

Mean	Std. Error	95% Confidence Interval	
		Lower Bound	Upper Bound
9.926	.309	9.268	10.584

2. System

Estimates

Measure: MEASURE_1

System	Mean	Std. Error	95% Confidence Interval	
			Lower Bound	Upper Bound
1	9.804	.305	9.154	10.454
2	10.048	.346	9.311	10.785

Pairwise Comparisons

Measure: MEASURE_1

(I) System	(J) System	Mean Difference (I-J)	Std. Error	Sig.[a]	95% Confidence Interval for Difference[a] Lower Bound	Upper Bound
1	2	-.244	.210	.263	-.691	.203
2	1	.244	.210	.263	-.203	.691

Based on estimated marginal means

a. Adjustment for multiple comparisons: Least Significant Difference (equivalent to no adjustments).

Multivariate Tests

	Value	F	Hypothesis df	Error df	Sig.	Partial Eta Squared
Pillai's trace	.083	1.352[a]	1.000	15.000	.263	.083
Wilks' lambda	.917	1.352[a]	1.000	15.000	.263	.083
Hotelling's trace	.090	1.352[a]	1.000	15.000	.263	.083
Roy's largest root	.090	1.352[a]	1.000	15.000	.263	.083

Each F tests the multivariate effect of System. These tests are based on the linearly independent pairwise comparisons among the estimated marginal means.

a. Exact statistic

3. Speed

Estimates

Measure: MEASURE_1

Speed	Mean	Std. Error	95% Confidence Interval Lower Bound	Upper Bound
1	10.594	.414	9.711	11.476
2	9.688	.363	8.914	10.461
3	9.497	.671	8.067	10.927

Pairwise Comparisons

Measure: MEASURE_1

(I) Speed	(J) Speed	Mean Difference (I-J)	Std. Error	Sig.[b]	95% Confidence Interval for Difference[b] Lower Bound	Upper Bound
1	2	.906*	.285	.006	.299	1.513
	3	1.097	.816	.199	-.643	2.837
2	1	-.906*	.285	.006	-1.513	-.299
	3	.191	.810	.817	-1.536	1.917
3	1	-1.097	.816	.199	-2.837	.643
	2	-.191	.810	.817	-1.917	1.536

Based on estimated marginal means

*. The mean difference is significant at the .05 level.

b. Adjustment for multiple comparisons: Least Significant Difference (equivalent to no adjustments).

Multivariate Tests

	Value	F	Hypothesis df	Error df	Sig.	Partial Eta Squared
Pillai's trace	.415	4.973[a]	2.000	14.000	.023	.415
Wilks' lambda	.585	4.973[a]	2.000	14.000	.023	.415
Hotelling's trace	.710	4.973[a]	2.000	14.000	.023	.415
Roy's largest root	.710	4.973[a]	2.000	14.000	.023	.415

Each F tests the multivariate effect of Speed. These tests are based on the linearly independent pairwise comparisons among the estimated marginal means.

a. Exact statistic

4. System * Speed

Measure: MEASURE_1

System	Speed	Mean	Std. Error	95% Confidence Interval Lower Bound	95% Confidence Interval Upper Bound
1	1	10.381	.385	9.560	11.203
	2	9.481	.311	8.818	10.145
	3	9.550	.833	7.775	11.325
2	1	10.806	.462	9.821	11.792
	2	9.894	.429	8.978	10.809
	3	9.444	.532	8.311	10.577

Profile Plots

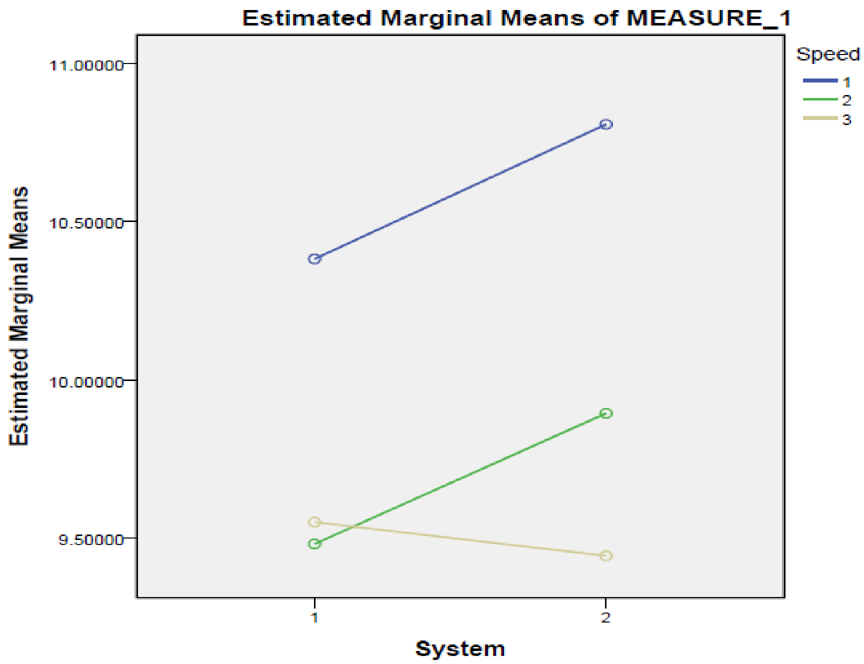

```
GLM KM_2_M_5 KM_2_M_65 KM_2_M_8 KM_2_ML_5 KM_2_ML_65 KM_2_ML_8
  /WSFACTOR=System 2 Polynomial Speed 3 Polynomial
  /METHOD=SSTYPE(3)
  /PLOT=PROFILE(System*Speed)
  /EMMEANS=TABLES(OVERALL)
  /EMMEANS=TABLES(System) COMPARE ADJ(LSD)
  /EMMEANS=TABLES(Speed) COMPARE ADJ(LSD)
  /EMMEANS=TABLES(System*Speed)
  /PRINT=DESCRIPTIVE ETASQ
  /CRITERIA=ALPHA(.05)
  /WSDESIGN=System Speed System*Speed.
```

General Linear Model

Within-Subjects Factors

Measure: MEASURE_1

System	Speed	Dependent Variable
1	1	KM_2_M_5
	2	KM_2_M_65
	3	KM_2_M_8
2	1	KM_2_ML_5
	2	KM_2_ML_65
	3	KM_2_ML_8

Descriptive Statistics

	Mean	Std. Deviation	N
KM_2_M_5	-.4952513	.09023758	16
KM_2_M_65	-.61095963	.104910014	16
KM_2_M_8	-.74133212	.125514872	16
KM_2_ML_5	-.7826791	.14230370	16
KM_2_ML_65	-.9527258	.16009008	16
KM_2_ML_8	-1.1741616	.23441179	16

Multivariate Tests[a]

Effect		Value	F	Hypothesis df	Error df	Sig.	Partial Eta Squared
System	Pillai's Trace	.958	342.120[b]	1.000	15.000	.000	.958
	Wilks' Lambda	.042	342.120[b]	1.000	15.000	.000	.958
	Hotelling's Trace	22.808	342.120[b]	1.000	15.000	.000	.958
	Roy's Largest Root	22.808	342.120[b]	1.000	15.000	.000	.958
Speed	Pillai's Trace	.940	109.005[b]	2.000	14.000	.000	.940
	Wilks' Lambda	.060	109.005[b]	2.000	14.000	.000	.940
	Hotelling's Trace	15.572	109.005[b]	2.000	14.000	.000	.940
	Roy's Largest Root	15.572	109.005[b]	2.000	14.000	.000	.940
System * Speed	Pillai's Trace	.740	19.910[b]	2.000	14.000	.000	.740
	Wilks' Lambda	.260	19.910[b]	2.000	14.000	.000	.740
	Hotelling's Trace	2.844	19.910[b]	2.000	14.000	.000	.740
	Roy's Largest Root	2.844	19.910[b]	2.000	14.000	.000	.740

a. Design: Intercept
Within Subjects Design: System + Speed + System * Speed

b. Exact statistic

Mauchly's Test of Sphericity[a]

Measure: MEASURE_1

Within Subjects Effect	Mauchly's W	Approx. Chi-Square	df	Sig.	Epsilon[b]		
					Greenhouse-Geisser	Huynh-Feldt	Lower-bound
System	1.000	.000	0	.	1.000	1.000	1.000
Speed	.628	6.504	2	.039	.729	.788	.500
System * Speed	.653	5.973	2	.050	.742	.805	.500

Tests the null hypothesis that the error covariance matrix of the orthonormalized transformed dependent variables is proportional to an identity matrix.

a. Design: Intercept
Within Subjects Design: System + Speed + System * Speed

b. May be used to adjust the degrees of freedom for the averaged tests of significance. Corrected tests are displayed in the Tests of Within-Subjects Effects table.

Tests of Within-Subjects Effects

Measure: MEASURE_1

Source		Type III Sum of Squares	df	Mean Square	F	Sig.	Partial Eta Squared
System	Sphericity Assumed	3.008	1	3.008	342.120	.000	.958
	Greenhouse-Geisser	3.008	1.000	3.008	342.120	.000	.958
	Huynh-Feldt	3.008	1.000	3.008	342.120	.000	.958
	Lower-bound	3.008	1.000	3.008	342.120	.000	.958
Error(System)	Sphericity Assumed	.132	15	.009			
	Greenhouse-Geisser	.132	15.000	.009			
	Huynh-Feldt	.132	15.000	.009			
	Lower-bound	.132	15.000	.009			
Speed	Sphericity Assumed	1.632	2	.816	87.174	.000	.853
	Greenhouse-Geisser	1.632	1.458	1.119	87.174	.000	.853
	Huynh-Feldt	1.632	1.575	1.036	87.174	.000	.853
	Lower-bound	1.632	1.000	1.632	87.174	.000	.853
Error(Speed)	Sphericity Assumed	.281	30	.009			
	Greenhouse-Geisser	.281	21.873	.013			
	Huynh-Feldt	.281	23.628	.012			
	Lower-bound	.281	15.000	.019			
System * Speed	Sphericity Assumed	.086	2	.043	9.870	.001	.397
	Greenhouse-Geisser	.086	1.484	.058	9.870	.002	.397
	Huynh-Feldt	.086	1.609	.054	9.870	.001	.397
	Lower-bound	.086	1.000	.086	9.870	.007	.397
Error(System*Speed)	Sphericity Assumed	.131	30	.004			
	Greenhouse-Geisser	.131	22.267	.006			
	Huynh-Feldt	.131	24.140	.005			
	Lower-bound	.131	15.000	.009			

Tests of Within-Subjects Contrasts

Measure: MEASURE_1

Source	System	Speed	Type III Sum of Squares	df	Mean Square	F	Sig.	Partial Eta Squared
System	Linear		3.008	1	3.008	342.120	.000	.958
Error(System)	Linear		.132	15	.009			
Speed		Linear	1.626	1	1.626	159.857	.000	.914
		Quadratic	.006	1	.006	.681	.422	.043
Error(Speed)		Linear	.153	15	.010			
		Quadratic	.128	15	.009			
System * Speed	Linear	Linear	.085	1	.085	39.793	.000	.726
		Quadratic	.002	1	.002	.271	.610	.018
Error(System*Speed)	Linear	Linear	.032	15	.002			
		Quadratic	.099	15	.007			

Tests of Between-Subjects Effects

Measure: MEASURE_1

Transformed Variable: Average

Source	Type III Sum of Squares	df	Mean Square	F	Sig.	Partial Eta Squared
Intercept	60.347	1	60.347	606.678	.000	.976
Error	1.492	15	.099			

Estimated Marginal Means

1. Grand Mean

Measure: MEASURE_1

Mean	Std. Error	95% Confidence Interval	
		Lower Bound	Upper Bound
-.793	.032	-.861	-.724

2. System

Estimates

Measure: MEASURE_1

System	Mean	Std. Error	95% Confidence Interval	
			Lower Bound	Upper Bound
1	-.616	.025	-.670	-.562
2	-.970	.040	-1.055	-.884

Pairwise Comparisons

Measure: MEASURE_1

(I) System	(J) System	Mean Difference (I-J)	Std. Error	Sig.[b]	95% Confidence Interval for Difference[b] Lower Bound	Upper Bound
1	2	.354*	.019	.000	.313	.395
2	1	-.354*	.019	.000	-.395	-.313

Based on estimated marginal means

*. The mean difference is significant at the .05 level.

b. Adjustment for multiple comparisons: Least Significant Difference (equivalent to no adjustments).

Multivariate Tests

	Value	F	Hypothesis df	Error df	Sig.	Partial Eta Squared
Pillai's trace	.958	342.120[a]	1.000	15.000	.000	.958
Wilks' lambda	.042	342.120[a]	1.000	15.000	.000	.958
Hotelling's trace	22.808	342.120[a]	1.000	15.000	.000	.958
Roy's largest root	22.808	342.120[a]	1.000	15.000	.000	.958

Each F tests the multivariate effect of System. These tests are based on the linearly independent pairwise comparisons among the estimated marginal means.

a. Exact statistic

3. Speed

Estimates

Measure: MEASURE_1

Speed	Mean	Std. Error	95% Confidence Interval Lower Bound	Upper Bound
1	-.639	.029	-.700	-.578
2	-.782	.030	-.847	-.717
3	-.958	.044	-1.052	-.863

Pairwise Comparisons

Measure: MEASURE_1

(I) Speed	(J) Speed	Mean Difference (I-J)	Std. Error	Sig.[b]	95% Confidence Interval for Difference[b] Lower Bound	Upper Bound
1	2	.143*	.016	.000	.109	.177
	3	.319*	.025	.000	.265	.373
2	1	-.143*	.016	.000	-.177	-.109
	3	.176*	.029	.000	.113	.239
3	1	-.319*	.025	.000	-.373	-.265
	2	-.176*	.029	.000	-.239	-.113

Based on estimated marginal means

*. The mean difference is significant at the .05 level.

b. Adjustment for multiple comparisons: Least Significant Difference (equivalent to no adjustments).

Multivariate Tests

	Value	F	Hypothesis df	Error df	Sig.	Partial Eta Squared
Pillai's trace	.940	109.005[a]	2.000	14.000	.000	.940
Wilks' lambda	.060	109.005[a]	2.000	14.000	.000	.940
Hotelling's trace	15.572	109.005[a]	2.000	14.000	.000	.940
Roy's largest root	15.572	109.005[a]	2.000	14.000	.000	.940

Each F tests the multivariate effect of Speed. These tests are based on the linearly independent pairwise comparisons among the estimated marginal means.

a. Exact statistic

4. System * Speed

Measure: MEASURE_1

System	Speed	Mean	Std. Error	95% Confidence Interval	
				Lower Bound	Upper Bound
1	1	-.495	.023	-.543	-.447
	2	-.611	.026	-.667	-.555
	3	-.741	.031	-.808	-.674
2	1	-.783	.036	-.859	-.707
	2	-.953	.040	-1.038	-.867
	3	-1.174	.059	-1.299	-1.049

Profile Plots

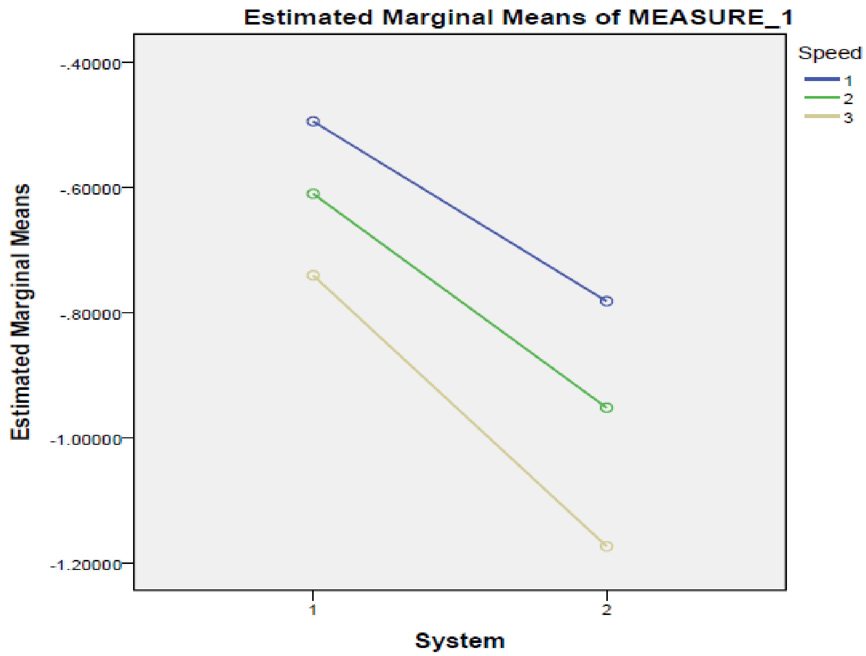


```
GLM KM_2_T_M_5 KM_2_T_M_65 KM_2_T_M_8 KM_2_T_ML_5 KM_2_T_ML_65 KM_2_T_ML_8
  /WSFACTOR=System 2 Polynomial Speed 3 Polynomial
  /METHOD=SSTYPE(3)
  /PLOT=PROFILE(System*Speed)
  /EMMEANS=TABLES(OVERALL)
  /EMMEANS=TABLES(System) COMPARE ADJ(LSD)
  /EMMEANS=TABLES(Speed) COMPARE ADJ(LSD)
  /EMMEANS=TABLES(System*Speed)
  /PRINT=DESCRIPTIVE ETASQ
  /CRITERIA=ALPHA(.05)
  /WSDESIGN=System Speed System*Speed.
```

General Linear Model

Within-Subjects Factors

Measure: MEASURE_1

System	Speed	Dependent Variable
1	1	KM_2_T_M_5
	2	KM_2_T_M_6 5
	3	KM_2_T_M_8
2	1	KM_2_T_ML_ 5
	2	KM_2_T_ML_ 65
	3	KM_2_T_ML_ 8

Descriptive Statistics

	Mean	Std. Deviation	N
KM_2_T_M_5	68.050000	6.0817761	16
KM_2_T_M_65	64.3875	6.08691	16
KM_2_T_M_8	59.9500	6.44764	16
KM_2_T_ML_5	68.4063	5.84596	16
KM_2_T_ML_65	65.0250	5.94267	16
KM_2_T_ML_8	60.7312500	6.15475088	16

Multivariate Tests[a]

Effect		Value	F	Hypothesis df	Error df	Sig.	Partial Eta Squared
System	Pillai's Trace	.321	7.095[b]	1.000	15.000	.018	.321
	Wilks' Lambda	.679	7.095[b]	1.000	15.000	.018	.321
	Hotelling's Trace	.473	7.095[b]	1.000	15.000	.018	.321
	Roy's Largest Root	.473	7.095[b]	1.000	15.000	.018	.321
Speed	Pillai's Trace	.828	33.746[b]	2.000	14.000	.000	.828
	Wilks' Lambda	.172	33.746[b]	2.000	14.000	.000	.828
	Hotelling's Trace	4.821	33.746[b]	2.000	14.000	.000	.828
	Roy's Largest Root	4.821	33.746[b]	2.000	14.000	.000	.828
System * Speed	Pillai's Trace	.100	.777[b]	2.000	14.000	.479	.100
	Wilks' Lambda	.900	.777[b]	2.000	14.000	.479	.100
	Hotelling's Trace	.111	.777[b]	2.000	14.000	.479	.100
	Roy's Largest Root	.111	.777[b]	2.000	14.000	.479	.100

a. Design: Intercept
Within Subjects Design: System + Speed + System * Speed

b. Exact statistic

Mauchly's Test of Sphericity[a]

Measure: MEASURE_1

Within Subjects Effect	Mauchly's W	Approx. Chi-Square	df	Sig.	Epsilon[b] Greenhouse-Geisser	Huynh-Feldt	Lower-bound
System	1.000	.000	0	.	1.000	1.000	1.000
Speed	.825	2.688	2	.261	.851	.949	.500
System * Speed	.733	4.355	2	.113	.789	.866	.500

Tests the null hypothesis that the error covariance matrix of the orthonormalized transformed dependent variables is proportional to an identity matrix.

a. Design: Intercept
Within Subjects Design: System + Speed + System * Speed

b. May be used to adjust the degrees of freedom for the averaged tests of significance. Corrected tests are displayed in the Tests of Within-Subjects Effects table.

Tests of Within-Subjects Effects

Measure: MEASURE_1

Source		Type III Sum of Squares	df	Mean Square	F	Sig.	Partial Eta Squared
System	Sphericity Assumed	8.402	1	8.402	7.095	.018	.321
	Greenhouse-Geisser	8.402	1.000	8.402	7.095	.018	.321
	Huynh-Feldt	8.402	1.000	8.402	7.095	.018	.321
	Lower-bound	8.402	1.000	8.402	7.095	.018	.321
Error(System)	Sphericity Assumed	17.762	15	1.184			
	Greenhouse-Geisser	17.762	15.000	1.184			
	Huynh-Feldt	17.762	15.000	1.184			
	Lower-bound	17.762	15.000	1.184			
Speed	Sphericity Assumed	999.199	2	499.600	46.460	.000	.756
	Greenhouse-Geisser	999.199	1.703	586.878	46.460	.000	.756
	Huynh-Feldt	999.199	1.898	526.396	46.460	.000	.756
	Lower-bound	999.199	1.000	999.199	46.460	.000	.756
Error(Speed)	Sphericity Assumed	322.601	30	10.753			
	Greenhouse-Geisser	322.601	25.538	12.632			
	Huynh-Feldt	322.601	28.473	11.330			
	Lower-bound	322.601	15.000	21.507			
System * Speed	Sphericity Assumed	.748	2	.374	1.064	.358	.066
	Greenhouse-Geisser	.748	1.578	.474	1.064	.346	.066
	Huynh-Feldt	.748	1.732	.432	1.064	.351	.066
	Lower-bound	.748	1.000	.748	1.064	.319	.066
Error(System*Speed)	Sphericity Assumed	10.539	30	.351			
	Greenhouse-Geisser	10.539	23.672	.445			
	Huynh-Feldt	10.539	25.984	.406			
	Lower-bound	10.539	15.000	.703			

Tests of Within-Subjects Contrasts

Measure: MEASURE_1

Source	System	Speed	Type III Sum of Squares	df	Mean Square	F	Sig.	Partial Eta Squared
System	Linear		8.402	1	8.402	7.095	.018	.321
Error(System)	Linear		17.762	15	1.184			
Speed		Linear	995.403	1	995.403	67.000	.000	.817
		Quadratic	3.797	1	3.797	.571	.462	.037
Error(Speed)		Linear	222.853	15	14.857			
		Quadratic	99.748	15	6.650			
System * Speed	Linear	Linear	.723	1	.723	1.368	.260	.084
		Quadratic	.025	1	.025	.145	.709	.010
Error(System*Speed)	Linear	Linear	7.923	15	.528			
		Quadratic	2.616	15	.174			

Tests of Between-Subjects Effects

Measure: MEASURE_1

Transformed Variable: Average

Source	Type III Sum of Squares	df	Mean Square	F	Sig.	Partial Eta Squared
Intercept	398455.740	1	398455.740	1996.385	.000	.993
Error	2993.830	15	199.589			

Estimated Marginal Means

1. Grand Mean

Measure: MEASURE_1

Mean	Std. Error	95% Confidence Interval	
		Lower Bound	Upper Bound
64.425	1.442	61.352	67.498

2. System

Estimates

Measure: MEASURE_1

System	Mean	Std. Error	95% Confidence Interval	
			Lower Bound	Upper Bound
1	64.129	1.471	60.994	67.264
2	64.721	1.421	61.692	67.749

Pairwise Comparisons

Measure: MEASURE_1

(I) System	(J) System	Mean Difference (I-J)	Std. Error	Sig.[b]	95% Confidence Interval for Difference[b] Lower Bound	Upper Bound
1	2	-.592*	.222	.018	-1.065	-.118
2	1	.592*	.222	.018	.118	1.065

Based on estimated marginal means

*. The mean difference is significant at the .05 level.

b. Adjustment for multiple comparisons: Least Significant Difference (equivalent to no adjustments).

Multivariate Tests

	Value	F	Hypothesis df	Error df	Sig.	Partial Eta Squared
Pillai's trace	.321	7.095[a]	1.000	15.000	.018	.321
Wilks' lambda	.679	7.095[a]	1.000	15.000	.018	.321
Hotelling's trace	.473	7.095[a]	1.000	15.000	.018	.321
Roy's largest root	.473	7.095[a]	1.000	15.000	.018	.321

Each F tests the multivariate effect of System. These tests are based on the linearly independent pairwise comparisons among the estimated marginal means.

a. Exact statistic

3. Speed

Estimates

Measure: MEASURE_1

Speed	Mean	Std. Error	95% Confidence Interval Lower Bound	Upper Bound
1	68.228	1.480	65.073	71.383
2	64.706	1.497	61.516	67.896
3	60.341	1.574	56.985	63.696

Pairwise Comparisons

Measure: MEASURE_1

(I) Speed	(J) Speed	Mean Difference (I-J)	Std. Error	Sig.[b]	95% Confidence Interval for Difference[b] Lower Bound	Upper Bound
1	2	3.522*	.802	.001	1.813	5.231
	3	7.888*	.964	.000	5.834	9.941
2	1	-3.522*	.802	.001	-5.231	-1.813
	3	4.366*	.667	.000	2.944	5.787
3	1	-7.888*	.964	.000	-9.941	-5.834
	2	-4.366*	.667	.000	-5.787	-2.944

Based on estimated marginal means

*. The mean difference is significant at the .05 level.

b. Adjustment for multiple comparisons: Least Significant Difference (equivalent to no adjustments).

Multivariate Tests

	Value	F	Hypothesis df	Error df	Sig.	Partial Eta Squared
Pillai's trace	.828	33.746[a]	2.000	14.000	.000	.828
Wilks' lambda	.172	33.746[a]	2.000	14.000	.000	.828
Hotelling's trace	4.821	33.746[a]	2.000	14.000	.000	.828
Roy's largest root	4.821	33.746[a]	2.000	14.000	.000	.828

Each F tests the multivariate effect of Speed. These tests are based on the linearly independent pairwise comparisons among the estimated marginal means.

a. Exact statistic

4. System * Speed

Measure: MEASURE_1

System	Speed	Mean	Std. Error	95% Confidence Interval	
				Lower Bound	Upper Bound
1	1	68.050	1.520	64.809	71.291
	2	64.388	1.522	61.144	67.631
	3	59.950	1.612	56.514	63.386
2	1	68.406	1.461	65.291	71.521
	2	65.025	1.486	61.858	68.192
	3	60.731	1.539	57.452	64.011

Profile Plots

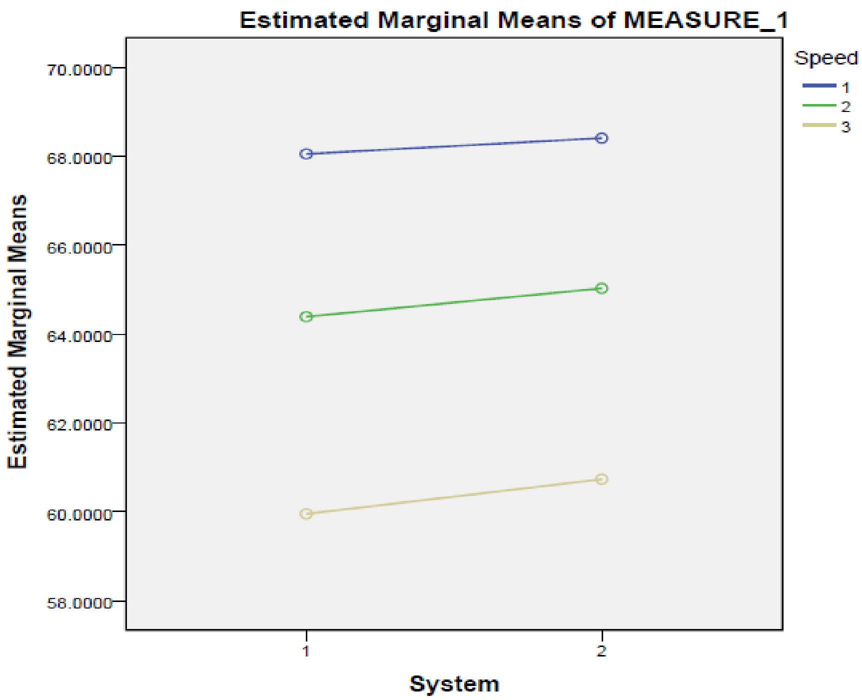

```
GLM KP_1_M_5 KP_1_M_65 KP_1_M_8 KP_1_ML_5 KP_1_ML_65 KP_1_ML_8
  /WSFACTOR=System 2 Polynomial Speed 3 Polynomial
  /METHOD=SSTYPE(3)
  /PLOT=PROFILE(System*Speed)
  /EMMEANS=TABLES(OVERALL)
  /EMMEANS=TABLES(System) COMPARE ADJ(LSD)
  /EMMEANS=TABLES(Speed) COMPARE ADJ(LSD)
  /EMMEANS=TABLES(System*Speed)
  /PRINT=DESCRIPTIVE ETASQ
  /CRITERIA=ALPHA(.05)
  /WSDESIGN=System Speed System*Speed.
```

General Linear Model

Within-Subjects Factors

Measure: MEASURE_1

System	Speed	Dependent Variable
1	1	KP_1_M_5
	2	KP_1_M_65
	3	KP_1_M_8
2	1	KP_1_ML_5
	2	KP_1_ML_65
	3	KP_1_ML_8

Descriptive Statistics

	Mean	Std. Deviation	N
KP_1_M_5	-4.9504138	1.77155653	16
KP_1_M_65	-5.5569686	2.11776880	16
KP_1_M_8	-5.1527636	2.48875630	16
KP_1_ML_5	-4.3375780	1.63828510	16
KP_1_ML_65	-4.854973	2.0299453	16
KP_1_ML_8	-3.97862162	1.688044640	16

Multivariate Tests[a]

Effect		Value	F	Hypothesis df	Error df	Sig.	Partial Eta Squared
System	Pillai's Trace	.363	8.559[b]	1.000	15.000	.010	.363
	Wilks' Lambda	.637	8.559[b]	1.000	15.000	.010	.363
	Hotelling's Trace	.571	8.559[b]	1.000	15.000	.010	.363
	Roy's Largest Root	.571	8.559[b]	1.000	15.000	.010	.363
Speed	Pillai's Trace	.278	2.690[b]	2.000	14.000	.103	.278
	Wilks' Lambda	.722	2.690[b]	2.000	14.000	.103	.278
	Hotelling's Trace	.384	2.690[b]	2.000	14.000	.103	.278
	Roy's Largest Root	.384	2.690[b]	2.000	14.000	.103	.278
System * Speed	Pillai's Trace	.156	1.291[b]	2.000	14.000	.306	.156
	Wilks' Lambda	.844	1.291[b]	2.000	14.000	.306	.156
	Hotelling's Trace	.184	1.291[b]	2.000	14.000	.306	.156
	Roy's Largest Root	.184	1.291[b]	2.000	14.000	.306	.156

a. Design: Intercept
Within Subjects Design: System + Speed + System * Speed

b. Exact statistic

Mauchly's Test of Sphericity[a]

Measure: MEASURE_1

Within Subjects Effect	Mauchly's W	Approx. Chi-Square	df	Sig.	Epsilon[b]		
					Greenhouse-Geisser	Huynh-Feldt	Lower-bound
System	1.000	.000	0	.	1.000	1.000	1.000
Speed	.877	1.844	2	.398	.890	1.000	.500
System * Speed	.700	5.001	2	.082	.769	.840	.500

Tests the null hypothesis that the error covariance matrix of the orthonormalized transformed dependent variables is proportional to an identity matrix.

a. Design: Intercept
Within Subjects Design: System + Speed + System * Speed

b. May be used to adjust the degrees of freedom for the averaged tests of significance. Corrected tests are displayed in the Tests of Within-Subjects Effects table.

Tests of Within-Subjects Effects

Measure: MEASURE_1

Source		Type III Sum of Squares	df	Mean Square	F	Sig.	Partial Eta Squared
System	Sphericity Assumed	16.520	1	16.520	8.559	.010	.363
	Greenhouse-Geisser	16.520	1.000	16.520	8.559	.010	.363
	Huynh-Feldt	16.520	1.000	16.520	8.559	.010	.363
	Lower-bound	16.520	1.000	16.520	8.559	.010	.363
Error(System)	Sphericity Assumed	28.952	15	1.930			
	Greenhouse-Geisser	28.952	15.000	1.930			
	Huynh-Feldt	28.952	15.000	1.930			
	Lower-bound	28.952	15.000	1.930			
Speed	Sphericity Assumed	7.807	2	3.903	1.881	.170	.111
	Greenhouse-Geisser	7.807	1.780	4.385	1.881	.175	.111
	Huynh-Feldt	7.807	2.000	3.903	1.881	.170	.111
	Lower-bound	7.807	1.000	7.807	1.881	.190	.111
Error(Speed)	Sphericity Assumed	62.267	30	2.076			
	Greenhouse-Geisser	62.267	26.704	2.332			
	Huynh-Feldt	62.267	30.000	2.076			
	Lower-bound	62.267	15.000	4.151			
System * Speed	Sphericity Assumed	1.456	2	.728	2.112	.139	.123
	Greenhouse-Geisser	1.456	1.538	.947	2.112	.152	.123
	Huynh-Feldt	1.456	1.679	.867	2.112	.148	.123
	Lower-bound	1.456	1.000	1.456	2.112	.167	.123
Error(System*Speed)	Sphericity Assumed	10.340	30	.345			
	Greenhouse-Geisser	10.340	23.071	.448			
	Huynh-Feldt	10.340	25.192	.410			
	Lower-bound	10.340	15.000	.689			

Tests of Within-Subjects Contrasts

Measure: MEASURE_1

Source	System	Speed	Type III Sum of Squares	df	Mean Square	F	Sig.	Partial Eta Squared
System	Linear		16.520	1	16.520	8.559	.010	.363
Error(System)	Linear		28.952	15	1.930			
Speed		Linear	.098	1	.098	.036	.852	.002
		Quadratic	7.709	1	7.709	5.445	.034	.266
Error(Speed)		Linear	41.029	15	2.735			
		Quadratic	21.238	15	1.416			
System * Speed	Linear	Linear	1.260	1	1.260	2.517	.134	.144
		Quadratic	.196	1	.196	1.037	.325	.065
Error(System*Speed)	Linear	Linear	7.512	15	.501			
		Quadratic	2.828	15	.189			

Tests of Between-Subjects Effects

Measure: MEASURE_1
Transformed Variable: Average

Source	Type III Sum of Squares	df	Mean Square	F	Sig.	Partial Eta Squared
Intercept	2216.653	1	2216.653	132.727	.000	.898
Error	250.513	15	16.701			

Estimated Marginal Means

1. Grand Mean

Measure: MEASURE_1

Mean	Std. Error	95% Confidence Interval	
		Lower Bound	Upper Bound
-4.805	.417	-5.694	-3.916

2. System

Estimates

Measure: MEASURE_1

System	Mean	Std. Error	95% Confidence Interval	
			Lower Bound	Upper Bound
1	-5.220	.482	-6.248	-4.192
2	-4.390	.394	-5.231	-3.550

Pairwise Comparisons

Measure: MEASURE_1

(I) System	(J) System	Mean Difference (I-J)	Std. Error	Sig.[b]	95% Confidence Interval for Difference[b] Lower Bound	Upper Bound
1	2	-.830*	.284	.010	-1.434	-.225
2	1	.830*	.284	.010	.225	1.434

Based on estimated marginal means

*. The mean difference is significant at the .05 level.

b. Adjustment for multiple comparisons: Least Significant Difference (equivalent to no adjustments).

Multivariate Tests

	Value	F	Hypothesis df	Error df	Sig.	Partial Eta Squared
Pillai's trace	.363	8.559[a]	1.000	15.000	.010	.363
Wilks' lambda	.637	8.559[a]	1.000	15.000	.010	.363
Hotelling's trace	.571	8.559[a]	1.000	15.000	.010	.363
Roy's largest root	.571	8.559[a]	1.000	15.000	.010	.363

Each F tests the multivariate effect of System. These tests are based on the linearly independent pairwise comparisons among the estimated marginal means.

a. Exact statistic

3. Speed

Estimates

Measure: MEASURE_1

Speed	Mean	Std. Error	95% Confidence Interval Lower Bound	Upper Bound
1	-4.644	.407	-5.511	-3.777
2	-5.206	.501	-6.274	-4.138
3	-4.566	.485	-5.599	-3.532

Pairwise Comparisons

Measure: MEASURE_1

(I) Speed	(J) Speed	Mean Difference (I-J)	Std. Error	Sig.[a]	95% Confidence Interval for Difference[a] Lower Bound	Upper Bound
1	2	.562	.355	.134	-.194	1.318
	3	-.078	.413	.852	-.960	.803
2	1	-.562	.355	.134	-1.318	.194
	3	-.640	.304	.052	-1.288	.007
3	1	.078	.413	.852	-.803	.960
	2	.640	.304	.052	-.007	1.288

Based on estimated marginal means

a. Adjustment for multiple comparisons: Least Significant Difference (equivalent to no adjustments).

Multivariate Tests

	Value	F	Hypothesis df	Error df	Sig.	Partial Eta Squared
Pillai's trace	.278	2.690[a]	2.000	14.000	.103	.278
Wilks' lambda	.722	2.690[a]	2.000	14.000	.103	.278
Hotelling's trace	.384	2.690[a]	2.000	14.000	.103	.278
Roy's largest root	.384	2.690[a]	2.000	14.000	.103	.278

Each F tests the multivariate effect of Speed. These tests are based on the linearly independent pairwise comparisons among the estimated marginal means.

a. Exact statistic

4. System * Speed

Measure: MEASURE_1

System	Speed	Mean	Std. Error	95% Confidence Interval Lower Bound	Upper Bound
1	1	-4.950	.443	-5.894	-4.006
	2	-5.557	.529	-6.685	-4.428
	3	-5.153	.622	-6.479	-3.827
2	1	-4.338	.410	-5.211	-3.465
	2	-4.855	.507	-5.937	-3.773
	3	-3.979	.422	-4.878	-3.079

Profile Plots

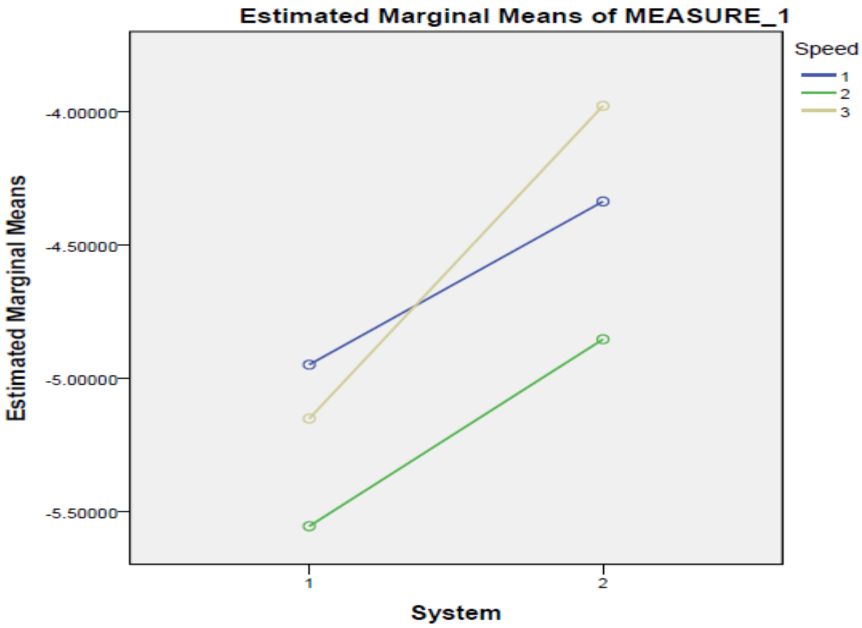


```
GLM KP_1_T_M_5 KP_1_T_M_65 KP_1_T_M_8 KP_1_T_ML_5 KP_1_T_ML_65 KP_1_T_ML_8
  /WSFACTOR=System 2 Polynomial Speed 3 Polynomial
  /METHOD=SSTYPE(3)
  /PLOT=PROFILE(System*Speed)
  /EMMEANS=TABLES(OVERALL)
  /EMMEANS=TABLES(System) COMPARE ADJ(LSD)
  /EMMEANS=TABLES(Speed) COMPARE ADJ(LSD)
  /EMMEANS=TABLES(System*Speed)
  /PRINT=DESCRIPTIVE ETASQ
  /CRITERIA=ALPHA(.05)
  /WSDESIGN=System Speed System*Speed.
```

General Linear Model

Within-Subjects Factors

Measure: MEASURE_1

System	Speed	Dependent Variable
1	1	KP_1_T_M_5
	2	KP_1_T_M_65
	3	KP_1_T_M_8
2	1	KP_1_T_ML_5
	2	KP_1_T_ML_65
	3	KP_1_T_ML_8

Descriptive Statistics

	Mean	Std. Deviation	N
KP_1_T_M_5	6.7750000	1.25299641	16
KP_1_T_M_65	5.631250	1.4220730	16
KP_1_T_M_8	5.3500000	.84380092	16
KP_1_T_ML_5	6.668750	1.8660899	16
KP_1_T_ML_65	5.8937500	1.01421152	16
KP_1_T_ML_8	5.8187500	1.30803606	16

Multivariate Tests[a]

Effect		Value	F	Hypothesis df	Error df	Sig.	Partial Eta Squared
System	Pillai's Trace	.147	2.581[b]	1.000	15.000	.129	.147
	Wilks' Lambda	.853	2.581[b]	1.000	15.000	.129	.147
	Hotelling's Trace	.172	2.581[b]	1.000	15.000	.129	.147
	Roy's Largest Root	.172	2.581[b]	1.000	15.000	.129	.147
Speed	Pillai's Trace	.368	4.076[b]	2.000	14.000	.040	.368
	Wilks' Lambda	.632	4.076[b]	2.000	14.000	.040	.368
	Hotelling's Trace	.582	4.076[b]	2.000	14.000	.040	.368
	Roy's Largest Root	.582	4.076[b]	2.000	14.000	.040	.368
System * Speed	Pillai's Trace	.143	1.168[b]	2.000	14.000	.339	.143
	Wilks' Lambda	.857	1.168[b]	2.000	14.000	.339	.143
	Hotelling's Trace	.167	1.168[b]	2.000	14.000	.339	.143
	Roy's Largest Root	.167	1.168[b]	2.000	14.000	.339	.143

a. Design: Intercept
Within Subjects Design: System + Speed + System * Speed

b. Exact statistic

Mauchly's Test of Sphericity[a]

Measure: MEASURE_1

Within Subjects Effect	Mauchly's W	Approx. Chi-Square	df	Sig.	Epsilon[b] Greenhouse-Geisser	Huynh-Feldt	Lower-bound
System	1.000	.000	0	.	1.000	1.000	1.000
Speed	.482	10.204	2	.006	.659	.698	.500
System * Speed	.864	2.049	2	.359	.880	.988	.500

Tests the null hypothesis that the error covariance matrix of the orthonormalized transformed dependent variables is proportional to an identity matrix.

a. Design: Intercept
Within Subjects Design: System + Speed + System * Speed

b. May be used to adjust the degrees of freedom for the averaged tests of significance. Corrected tests are displayed in the Tests of Within-Subjects Effects table.

Tests of Within-Subjects Effects

Measure: MEASURE_1

Source		Type III Sum of Squares	df	Mean Square	F	Sig.	Partial Eta Squared
System	Sphericity Assumed	1.042	1	1.042	2.581	.129	.147
	Greenhouse-Geisser	1.042	1.000	1.042	2.581	.129	.147
	Huynh-Feldt	1.042	1.000	1.042	2.581	.129	.147
	Lower-bound	1.042	1.000	1.042	2.581	.129	.147
Error(System)	Sphericity Assumed	6.055	15	.404			
	Greenhouse-Geisser	6.055	15.000	.404			
	Huynh-Feldt	6.055	15.000	.404			
	Lower-bound	6.055	15.000	.404			
Speed	Sphericity Assumed	23.958	2	11.979	6.322	.005	.296
	Greenhouse-Geisser	23.958	1.318	18.178	6.322	.015	.296
	Huynh-Feldt	23.958	1.395	17.174	6.322	.013	.296
	Lower-bound	23.958	1.000	23.958	6.322	.024	.296
Error(Speed)	Sphericity Assumed	56.846	30	1.895			
	Greenhouse-Geisser	56.846	19.769	2.875			
	Huynh-Feldt	56.846	20.926	2.717			
	Lower-bound	56.846	15.000	3.790			
System * Speed	Sphericity Assumed	1.358	2	.679	1.414	.259	.086
	Greenhouse-Geisser	1.358	1.760	.771	1.414	.260	.086
	Huynh-Feldt	1.358	1.976	.687	1.414	.259	.086
	Lower-bound	1.358	1.000	1.358	1.414	.253	.086
Error(System*Speed)	Sphericity Assumed	14.406	30	.480			
	Greenhouse-Geisser	14.406	26.405	.546			
	Huynh-Feldt	14.406	29.644	.486			
	Lower-bound	14.406	15.000	.960			

Tests of Within-Subjects Contrasts

Measure: MEASURE_1

Source	System	Speed	Type III Sum of Squares	df	Mean Square	F	Sig.	Partial Eta Squared
System	Linear		1.042	1	1.042	2.581	.129	.147
Error(System)	Linear		6.055	15	.404			
Speed		Linear	20.702	1	20.702	6.539	.022	.304
		Quadratic	3.255	1	3.255	5.218	.037	.258
Error(Speed)		Linear	47.487	15	3.166			
		Quadratic	9.358	15	.624			
System * Speed	Linear	Linear	1.322	1	1.322	2.432	.140	.140
		Quadratic	.035	1	.035	.085	.775	.006
Error(System*Speed)	Linear	Linear	8.157	15	.544			
		Quadratic	6.248	15	.417			

Tests of Between-Subjects Effects

Measure: MEASURE_1

Transformed Variable: Average

Source	Type III Sum of Squares	df	Mean Square	F	Sig.	Partial Eta Squared
Intercept	3482.450	1	3482.450	648.209	.000	.977
Error	80.586	15	5.372			

Estimated Marginal Means

1. Grand Mean

Measure: MEASURE_1

Mean	Std. Error	95% Confidence Interval	
		Lower Bound	Upper Bound
6.023	.237	5.519	6.527

2. System

Estimates

Measure: MEASURE_1

System	Mean	Std. Error	95% Confidence Interval	
			Lower Bound	Upper Bound
1	5.919	.225	5.438	6.399
2	6.127	.264	5.565	6.689

Pairwise Comparisons

Measure: MEASURE_1

(I) System	(J) System	Mean Difference (I-J)	Std. Error	Sig.[a]	95% Confidence Interval for Difference[a]	
					Lower Bound	Upper Bound
1	2	-.208	.130	.129	-.485	.068
2	1	.208	.130	.129	-.068	.485

Based on estimated marginal means

a. Adjustment for multiple comparisons: Least Significant Difference (equivalent to no adjustments).

Multivariate Tests

	Value	F	Hypothesis df	Error df	Sig.	Partial Eta Squared
Pillai's trace	.147	2.581[a]	1.000	15.000	.129	.147
Wilks' lambda	.853	2.581[a]	1.000	15.000	.129	.147
Hotelling's trace	.172	2.581[a]	1.000	15.000	.129	.147
Roy's largest root	.172	2.581[a]	1.000	15.000	.129	.147

Each F tests the multivariate effect of System. These tests are based on the linearly independent pairwise comparisons among the estimated marginal means.

a. Exact statistic

3. Speed

Estimates

Measure: MEASURE_1

Speed	Mean	Std. Error	95% Confidence Interval	
			Lower Bound	Upper Bound
1	6.722	.380	5.912	7.532
2	5.762	.291	5.142	6.383
3	5.584	.239	5.075	6.094

Pairwise Comparisons

Measure: MEASURE_1

(I) Speed	(J) Speed	Mean Difference (I-J)	Std. Error	Sig.[b]	95% Confidence Interval for Difference[b]	
					Lower Bound	Upper Bound
1	2	.959*	.325	.010	.267	1.651
	3	1.137*	.445	.022	.189	2.086
2	1	-.959*	.325	.010	-1.651	-.267
	3	.178	.228	.447	-.308	.664
3	1	-1.137*	.445	.022	-2.086	-.189
	2	-.178	.228	.447	-.664	.308

Based on estimated marginal means

*. The mean difference is significant at the .05 level.

b. Adjustment for multiple comparisons: Least Significant Difference (equivalent to no adjustments).

Multivariate Tests

	Value	F	Hypothesis df	Error df	Sig.	Partial Eta Squared
Pillai's trace	.368	4.076[a]	2.000	14.000	.040	.368
Wilks' lambda	.632	4.076[a]	2.000	14.000	.040	.368
Hotelling's trace	.582	4.076[a]	2.000	14.000	.040	.368
Roy's largest root	.582	4.076[a]	2.000	14.000	.040	.368

Each F tests the multivariate effect of Speed. These tests are based on the linearly independent pairwise comparisons among the estimated marginal means.

a. Exact statistic

4. System * Speed

Measure: MEASURE_1

System	Speed	Mean	Std. Error	95% Confidence Interval	
				Lower Bound	Upper Bound
1	1	6.775	.313	6.107	7.443
	2	5.631	.356	4.873	6.389
	3	5.350	.211	4.900	5.800
2	1	6.669	.467	5.674	7.663
	2	5.894	.254	5.353	6.434
	3	5.819	.327	5.122	6.516

Profile Plots

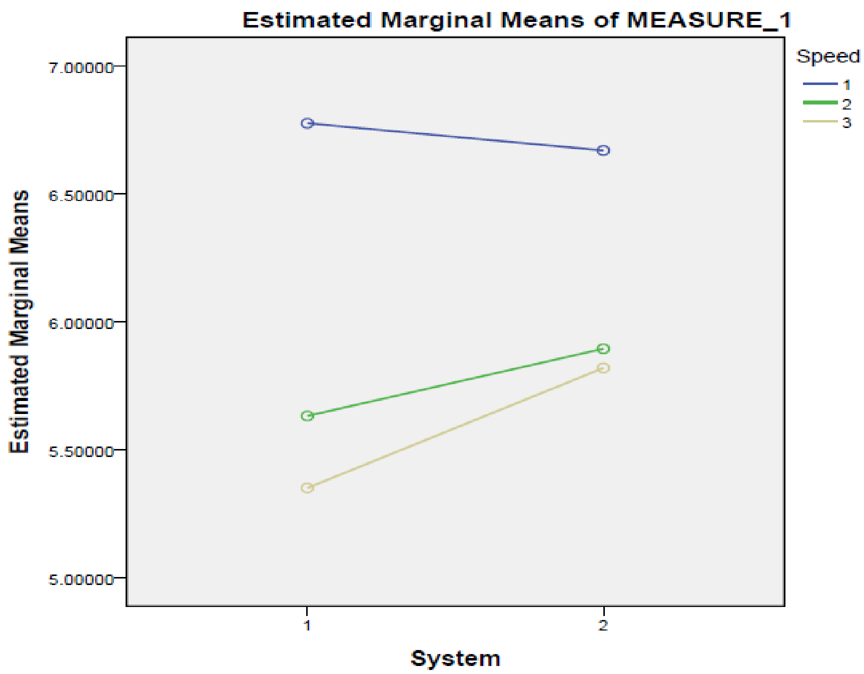


```
GLM KP_2_M_5 KP_2_M_65 KP_2_M_8 KP_2_ML_5 KP_2_ML_65 KP_2_ML_8
  /WSFACTOR=System 2 Polynomial Speed 3 Polynomial
  /METHOD=SSTYPE(3)
  /PLOT=PROFILE(System*Speed)
  /EMMEANS=TABLES(OVERALL)
  /EMMEANS=TABLES(System) COMPARE ADJ(LSD)
  /EMMEANS=TABLES(Speed) COMPARE ADJ(LSD)
  /EMMEANS=TABLES(System*Speed)
  /PRINT=DESCRIPTIVE ETASQ
  /CRITERIA=ALPHA(.05)
  /WSDESIGN=System Speed System*Speed.
```

General Linear Model

Within-Subjects Factors

Measure: MEASURE_1

System	Speed	Dependent Variable
1	1	KP_2_M_5
	2	KP_2_M_65
	3	KP_2_M_8
2	1	KP_2_ML_5
	2	KP_2_ML_65
	3	KP_2_ML_8

Descriptive Statistics

	Mean	Std. Deviation	N
KP_2_M_5	3.1679851	1.45193860	16
KP_2_M_65	3.5631638	1.64791000	16
KP_2_M_8	3.3354476	1.36440846	16
KP_2_ML_5	2.2666919	1.09154661	16
KP_2_ML_65	2.7853183	1.50068616	16
KP_2_ML_8	2.6356626	.89686008	16

Multivariate Tests[a]

Effect		Value	F	Hypothesis df	Error df	Sig.	Partial Eta Squared
System	Pillai's Trace	.628	25.338[b]	1.000	15.000	.000	.628
	Wilks' Lambda	.372	25.338[b]	1.000	15.000	.000	.628
	Hotelling's Trace	1.689	25.338[b]	1.000	15.000	.000	.628
	Roy's Largest Root	1.689	25.338[b]	1.000	15.000	.000	.628
Speed	Pillai's Trace	.233	2.127[b]	2.000	14.000	.156	.233
	Wilks' Lambda	.767	2.127[b]	2.000	14.000	.156	.233
	Hotelling's Trace	.304	2.127[b]	2.000	14.000	.156	.233
	Roy's Largest Root	.304	2.127[b]	2.000	14.000	.156	.233
System * Speed	Pillai's Trace	.099	.773[b]	2.000	14.000	.480	.099
	Wilks' Lambda	.901	.773[b]	2.000	14.000	.480	.099
	Hotelling's Trace	.110	.773[b]	2.000	14.000	.480	.099
	Roy's Largest Root	.110	.773[b]	2.000	14.000	.480	.099

a. Design: Intercept
Within Subjects Design: System + Speed + System * Speed

b. Exact statistic

Mauchly's Test of Sphericity[a]

Measure: MEASURE_1

Within Subjects Effect	Mauchly's W	Approx. Chi-Square	df	Sig.	Epsilon[b]		
					Greenhouse-Geisser	Huynh-Feldt	Lower-bound
System	1.000	.000	0	.	1.000	1.000	1.000
Speed	.985	.212	2	.899	.985	1.000	.500
System * Speed	.932	.988	2	.610	.936	1.000	.500

Tests the null hypothesis that the error covariance matrix of the orthonormalized transformed dependent variables is proportional to an identity matrix.

a. Design: Intercept
Within Subjects Design: System + Speed + System * Speed

b. May be used to adjust the degrees of freedom for the averaged tests of significance. Corrected tests are displayed in the Tests of Within-Subjects Effects table.

Tests of Within-Subjects Effects

Measure: MEASURE_1

Source		Type III Sum of Squares	df	Mean Square	F	Sig.	Partial Eta Squared
System	Sphericity Assumed	15.091	1	15.091	25.338	.000	.628
	Greenhouse-Geisser	15.091	1.000	15.091	25.338	.000	.628
	Huynh-Feldt	15.091	1.000	15.091	25.338	.000	.628
	Lower-bound	15.091	1.000	15.091	25.338	.000	.628
Error(System)	Sphericity Assumed	8.934	15	.596			
	Greenhouse-Geisser	8.934	15.000	.596			
	Huynh-Feldt	8.934	15.000	.596			
	Lower-bound	8.934	15.000	.596			
Speed	Sphericity Assumed	3.374	2	1.687	2.210	.127	.128
	Greenhouse-Geisser	3.374	1.970	1.712	2.210	.128	.128
	Huynh-Feldt	3.374	2.000	1.687	2.210	.127	.128
	Lower-bound	3.374	1.000	3.374	2.210	.158	.128
Error(Speed)	Sphericity Assumed	22.897	30	.763			
	Greenhouse-Geisser	22.897	29.555	.775			
	Huynh-Feldt	22.897	30.000	.763			
	Lower-bound	22.897	15.000	1.526			
System * Speed	Sphericity Assumed	.165	2	.083	.624	.543	.040
	Greenhouse-Geisser	.165	1.872	.088	.624	.533	.040
	Huynh-Feldt	.165	2.000	.083	.624	.543	.040
	Lower-bound	.165	1.000	.165	.624	.442	.040
Error(System*Speed)	Sphericity Assumed	3.971	30	.132			
	Greenhouse-Geisser	3.971	28.086	.141			
	Huynh-Feldt	3.971	30.000	.132			
	Lower-bound	3.971	15.000	.265			

Tests of Within-Subjects Contrasts

Measure: MEASURE_1

Source	System	Speed	Type III Sum of Squares	df	Mean Square	F	Sig.	Partial Eta Squared
System	Linear		15.091	1	15.091	25.338	.000	.628
Error(System)	Linear		8.934	15	.596			
Speed		Linear	1.151	1	1.151	1.346	.264	.082
		Quadratic	2.223	1	2.223	3.311	.089	.181
Error(Speed)		Linear	12.826	15	.855			
		Quadratic	10.071	15	.671			
System * Speed	Linear	Linear	.162	1	.162	1.652	.218	.099
		Quadratic	.003	1	.003	.017	.899	.001
Error(System*Speed)	Linear	Linear	1.475	15	.098			
		Quadratic	2.496	15	.166			

Tests of Between-Subjects Effects

Measure: MEASURE_1

Transformed Variable: Average

Source	Type III Sum of Squares	df	Mean Square	F	Sig.	Partial Eta Squared
Intercept	840.571	1	840.571	98.353	.000	.868
Error	128.197	15	8.546			

Estimated Marginal Means

1. Grand Mean

Measure: MEASURE_1

Mean	Std. Error	95% Confidence Interval Lower Bound	95% Confidence Interval Upper Bound
2.959	.298	2.323	3.595

2. System

Estimates

Measure: MEASURE_1

System	Mean	Std. Error	95% Confidence Interval Lower Bound	95% Confidence Interval Upper Bound
1	3.356	.350	2.610	4.101
2	2.563	.261	2.006	3.119

Pairwise Comparisons

Measure: MEASURE_1

(I) System	(J) System	Mean Difference (I-J)	Std. Error	Sig.[b]	95% Confidence Interval for Difference[b] Lower Bound	95% Confidence Interval for Difference[b] Upper Bound
1	2	.793*	.158	.000	.457	1.129
2	1	-.793*	.158	.000	-1.129	-.457

Based on estimated marginal means

*. The mean difference is significant at the .05 level.

b. Adjustment for multiple comparisons: Least Significant Difference (equivalent to no adjustments).

Multivariate Tests

	Value	F	Hypothesis df	Error df	Sig.	Partial Eta Squared
Pillai's trace	.628	25.338[a]	1.000	15.000	.000	.628
Wilks' lambda	.372	25.338[a]	1.000	15.000	.000	.628
Hotelling's trace	1.689	25.338[a]	1.000	15.000	.000	.628
Roy's largest root	1.689	25.338[a]	1.000	15.000	.000	.628

Each F tests the multivariate effect of System. These tests are based on the linearly independent pairwise comparisons among the estimated marginal means.

a. Exact statistic

3. Speed

Estimates

Measure: MEASURE_1

Speed	Mean	Std. Error	95% Confidence Interval	
			Lower Bound	Upper Bound
1	2.717	.310	2.056	3.379
2	3.174	.382	2.360	3.989
3	2.986	.269	2.412	3.559

Pairwise Comparisons

Measure: MEASURE_1

(I) Speed	(J) Speed	Mean Difference (I-J)	Std. Error	Sig.[b]	95% Confidence Interval for Difference[b]	
					Lower Bound	Upper Bound
1	2	-.457*	.214	.050	-.913	-.001
	3	-.268	.231	.264	-.761	.225
2	1	.457*	.214	.050	.001	.913
	3	.189	.209	.382	-.258	.635
3	1	.268	.231	.264	-.225	.761
	2	-.189	.209	.382	-.635	.258

Based on estimated marginal means

*. The mean difference is significant at the .05 level.

b. Adjustment for multiple comparisons: Least Significant Difference (equivalent to no adjustments).

Multivariate Tests

	Value	F	Hypothesis df	Error df	Sig.	Partial Eta Squared
Pillai's trace	.233	2.127[a]	2.000	14.000	.156	.233
Wilks' lambda	.767	2.127[a]	2.000	14.000	.156	.233
Hotelling's trace	.304	2.127[a]	2.000	14.000	.156	.233
Roy's largest root	.304	2.127[a]	2.000	14.000	.156	.233

Each F tests the multivariate effect of Speed. These tests are based on the linearly independent pairwise comparisons among the estimated marginal means.

a. Exact statistic

4. System * Speed

Measure: MEASURE_1

System	Speed	Mean	Std. Error	95% Confidence Interval	
				Lower Bound	Upper Bound
1	1	3.168	.363	2.394	3.942
	2	3.563	.412	2.685	4.441
	3	3.335	.341	2.608	4.062
2	1	2.267	.273	1.685	2.848
	2	2.785	.375	1.986	3.585
	3	2.636	.224	2.158	3.114

Profile Plots

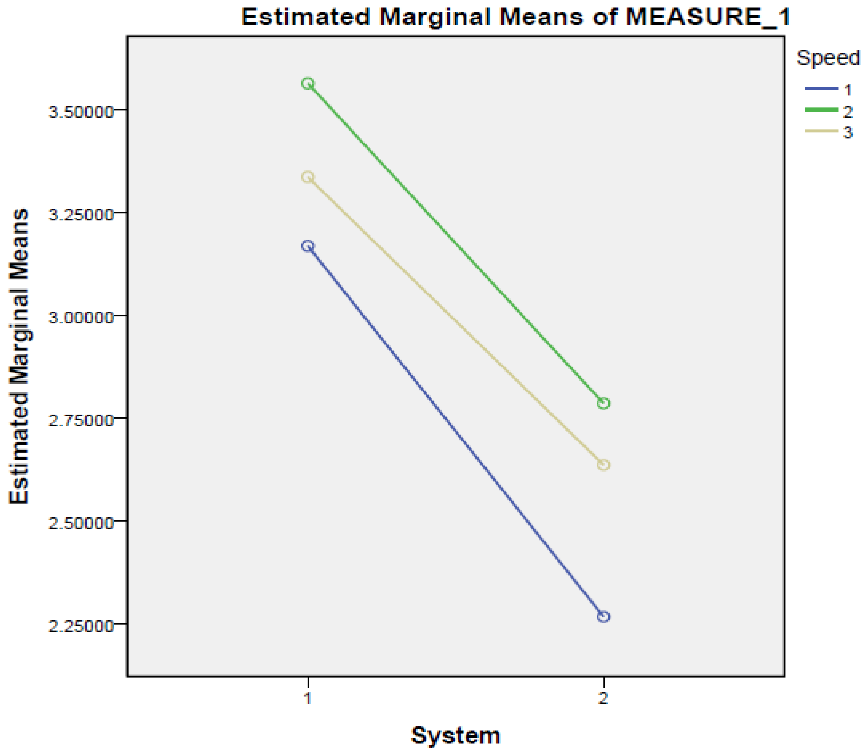
Estimated Marginal Means of MEASURE_1
Speed
1
2
3
Estimated Marginal Means
3.50000
3.25000
3.00000
2.75000
2.50000
2.25000
1
2
System

```
GLM KP_2_T_M_5 KP_2_T_M_65 KP_2_T_M_8 KP_2_T_ML_5 KP_2_T_ML_65 KP_2_T_ML_8
  /WSFACTOR=System 2 Polynomial Speed 3 Polynomial
  /METHOD=SSTYPE(3)
  /PLOT=PROFILE(System*Speed)
  /EMMEANS=TABLES(OVERALL)
  /EMMEANS=TABLES(System) COMPARE ADJ(LSD)
  /EMMEANS=TABLES(Speed) COMPARE ADJ(LSD)
  /EMMEANS=TABLES(System*Speed)
  /PRINT=DESCRIPTIVE ETASQ
  /CRITERIA=ALPHA(.05)
  /WSDESIGN=System Speed System*Speed.
```

General Linear Model

Within-Subjects Factors

Measure: MEASURE_1

System	Speed	Dependent Variable
1	1	KP_2_T_M_5
	2	KP_2_T_M_65
	3	KP_2_T_M_8
2	1	KP_2_T_ML_5
	2	KP_2_T_ML_65
	3	KP_2_T_ML_8

Descriptive Statistics

	Mean	Std. Deviation	N
KP_2_T_M_5	14.7187500	1.93329382	16
KP_2_T_M_65	13.8437500	2.02516460	16
KP_2_T_M_8	12.78750000	1.591592494	16
KP_2_T_ML_5	14.9187500	3.56972805	16
KP_2_T_ML_65	14.4312500	1.88280597	16
KP_2_T_ML_8	13.8812500	1.73059479	16

Multivariate Tests[a]

Effect		Value	F	Hypothesis df	Error df	Sig.	Partial Eta Squared
System	Pillai's Trace	.226	4.382[b]	1.000	15.000	.054	.226
	Wilks' Lambda	.774	4.382[b]	1.000	15.000	.054	.226
	Hotelling's Trace	.292	4.382[b]	1.000	15.000	.054	.226
	Roy's Largest Root	.292	4.382[b]	1.000	15.000	.054	.226
Speed	Pillai's Trace	.261	2.476[b]	2.000	14.000	.120	.261
	Wilks' Lambda	.739	2.476[b]	2.000	14.000	.120	.261
	Hotelling's Trace	.354	2.476[b]	2.000	14.000	.120	.261
	Roy's Largest Root	.354	2.476[b]	2.000	14.000	.120	.261
System * Speed	Pillai's Trace	.133	1.074[b]	2.000	14.000	.368	.133
	Wilks' Lambda	.867	1.074[b]	2.000	14.000	.368	.133
	Hotelling's Trace	.153	1.074[b]	2.000	14.000	.368	.133
	Roy's Largest Root	.153	1.074[b]	2.000	14.000	.368	.133

a. Design: Intercept
Within Subjects Design: System + Speed + System * Speed

b. Exact statistic

Mauchly's Test of Sphericity[a]

Measure: MEASURE_1

Within Subjects Effect	Mauchly's W	Approx. Chi-Square	df	Sig.	Epsilon[b]		
					Greenhouse-Geisser	Huynh-Feldt	Lower-bound
System	1.000	.000	0	.	1.000	1.000	1.000
Speed	.618	6.743	2	.034	.723	.780	.500
System * Speed	.913	1.271	2	.530	.920	1.000	.500

Tests the null hypothesis that the error covariance matrix of the orthonormalized transformed dependent variables is proportional to an identity matrix.

a. Design: Intercept
Within Subjects Design: System + Speed + System * Speed

b. May be used to adjust the degrees of freedom for the averaged tests of significance. Corrected tests are displayed in the Tests of Within-Subjects Effects table.

Tests of Within-Subjects Effects

Measure: MEASURE_1

Source		Type III Sum of Squares	df	Mean Square	F	Sig.	Partial Eta Squared
System	Sphericity Assumed	9.438	1	9.438	4.382	.054	.226
	Greenhouse-Geisser	9.438	1.000	9.438	4.382	.054	.226
	Huynh-Feldt	9.438	1.000	9.438	4.382	.054	.226
	Lower-bound	9.438	1.000	9.438	4.382	.054	.226
Error(System)	Sphericity Assumed	32.307	15	2.154			
	Greenhouse-Geisser	32.307	15.000	2.154			
	Huynh-Feldt	32.307	15.000	2.154			
	Lower-bound	32.307	15.000	2.154			
Speed	Sphericity Assumed	35.333	2	17.667	4.215	.024	.219
	Greenhouse-Geisser	35.333	1.447	24.419	4.215	.039	.219
	Huynh-Feldt	35.333	1.561	22.641	4.215	.036	.219
	Lower-bound	35.333	1.000	35.333	4.215	.058	.219
Error(Speed)	Sphericity Assumed	125.734	30	4.191			
	Greenhouse-Geisser	125.734	21.704	5.793			
	Huynh-Feldt	125.734	23.409	5.371			
	Lower-bound	125.734	15.000	8.382			
System * Speed	Sphericity Assumed	3.214	2	1.607	1.116	.341	.069
	Greenhouse-Geisser	3.214	1.840	1.746	1.116	.338	.069
	Huynh-Feldt	3.214	2.000	1.607	1.116	.341	.069
	Lower-bound	3.214	1.000	3.214	1.116	.307	.069
Error(System*Speed)	Sphericity Assumed	43.186	30	1.440			
	Greenhouse-Geisser	43.186	27.604	1.565			
	Huynh-Feldt	43.186	30.000	1.440			
	Lower-bound	43.186	15.000	2.879			

Tests of Within-Subjects Contrasts

Measure: MEASURE_1

Source	System	Speed	Type III Sum of Squares	df	Mean Square	F	Sig.	Partial Eta Squared
System	Linear		9.438	1	9.438	4.382	.054	.226
Error(System)	Linear		32.307	15	2.154			
Speed		Linear	35.254	1	35.254	5.258	.037	.260
		Quadratic	.079	1	.079	.047	.831	.003
Error(Speed)		Linear	100.569	15	6.705			
		Quadratic	25.165	15	1.678			
System * Speed	Linear	Linear	3.195	1	3.195	2.014	.176	.118
		Quadratic	.019	1	.019	.015	.906	.001
Error(System*Speed)	Linear	Linear	23.797	15	1.586			
		Quadratic	19.389	15	1.293			

Tests of Between-Subjects Effects

Measure: MEASURE_1

Transformed Variable: Average

Source	Type III Sum of Squares	df	Mean Square	F	Sig.	Partial Eta Squared
Intercept	19077.301	1	19077.301	1174.723	.000	.987
Error	243.597	15	16.240			

Estimated Marginal Means

1. Grand Mean

Measure: MEASURE_1

Mean	Std. Error	95% Confidence Interval	
		Lower Bound	Upper Bound
14.097	.411	13.220	14.974

2. System

Estimates

Measure: MEASURE_1

System	Mean	Std. Error	95% Confidence Interval	
			Lower Bound	Upper Bound
1	13.783	.377	12.980	14.587
2	14.410	.491	13.364	15.457

Pairwise Comparisons

Measure: MEASURE_1

(I) System	(J) System	Mean Difference (I-J)	Std. Error	Sig.[a]	95% Confidence Interval for Difference[a]	
					Lower Bound	Upper Bound
1	2	-.627	.300	.054	-1.266	.011
2	1	.627	.300	.054	-.011	1.266

Based on estimated marginal means

a. Adjustment for multiple comparisons: Least Significant Difference (equivalent to no adjustments).

Multivariate Tests

	Value	F	Hypothesis df	Error df	Sig.	Partial Eta Squared
Pillai's trace	.226	4.382[a]	1.000	15.000	.054	.226
Wilks' lambda	.774	4.382[a]	1.000	15.000	.054	.226
Hotelling's trace	.292	4.382[a]	1.000	15.000	.054	.226
Roy's largest root	.292	4.382[a]	1.000	15.000	.054	.226

Each F tests the multivariate effect of System. These tests are based on the linearly independent pairwise comparisons among the estimated marginal means.

a. Exact statistic

3. Speed

Estimates

Measure: MEASURE_1

Speed	Mean	Std. Error	95% Confidence Interval	
			Lower Bound	Upper Bound
1	14.819	.644	13.446	16.192
2	14.138	.467	13.142	15.133
3	13.334	.369	12.548	14.121

Pairwise Comparisons

Measure: MEASURE_1

(I) Speed	(J) Speed	Mean Difference (I-J)	Std. Error	Sig.[b]	95% Confidence Interval for Difference[b]	
					Lower Bound	Upper Bound
1	2	.681	.386	.098	-.142	1.505
	3	1.484*	.647	.037	.105	2.864
2	1	-.681	.386	.098	-1.505	.142
	3	.803	.466	.106	-.191	1.797
3	1	-1.484*	.647	.037	-2.864	-.105
	2	-.803	.466	.106	-1.797	.191

Based on estimated marginal means

*. The mean difference is significant at the .05 level.

b. Adjustment for multiple comparisons: Least Significant Difference (equivalent to no adjustments).

Multivariate Tests

	Value	F	Hypothesis df	Error df	Sig.	Partial Eta Squared
Pillai's trace	.261	2.476[a]	2.000	14.000	.120	.261
Wilks' lambda	.739	2.476[a]	2.000	14.000	.120	.261
Hotelling's trace	.354	2.476[a]	2.000	14.000	.120	.261
Roy's largest root	.354	2.476[a]	2.000	14.000	.120	.261

Each F tests the multivariate effect of Speed. These tests are based on the linearly independent pairwise comparisons among the estimated marginal means.

a. Exact statistic

4. System * Speed

Measure: MEASURE_1

System	Speed	Mean	Std. Error	95% Confidence Interval	
				Lower Bound	Upper Bound
1	1	14.719	.483	13.689	15.749
	2	13.844	.506	12.765	14.923
	3	12.788	.398	11.939	13.636
2	1	14.919	.892	13.017	16.821
	2	14.431	.471	13.428	15.435
	3	13.881	.433	12.959	14.803

Profile Plots

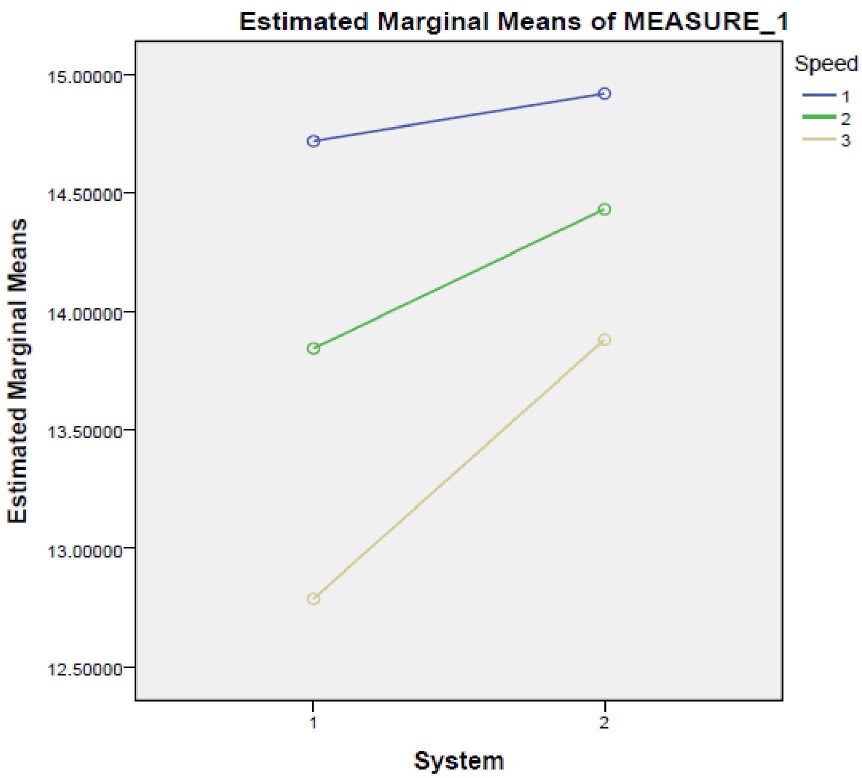
Estimated Marginal Means of MEASURE_1
Speed
1
2
3
15.00000
14.50000
14.00000
13.50000
13.00000
12.50000
Estimated Marginal Means
1
2
System

```
GLM KP_3_M_5 KP_3_M_65 KP_3_M_8 KP_3_ML_5 KP_3_ML_65 KP_3_ML_8
  /WSFACTOR=System 2 Polynomial Speed 3 Polynomial
  /METHOD=SSTYPE(3)
  /PLOT=PROFILE(System*Speed)
  /EMMEANS=TABLES(OVERALL)
  /EMMEANS=TABLES(System) COMPARE ADJ(LSD)
  /EMMEANS=TABLES(Speed) COMPARE ADJ(LSD)
  /EMMEANS=TABLES(System*Speed)
  /PRINT=DESCRIPTIVE ETASQ
  /CRITERIA=ALPHA(.05)
  /WSDESIGN=System Speed System*Speed.
```

General Linear Model

Within-Subjects Factors

Measure: MEASURE_1

System	Speed	Dependent Variable
1	1	KP_3_M_5
	2	KP_3_M_65
	3	KP_3_M_8
2	1	KP_3_ML_5
	2	KP_3_ML_65
	3	KP_3_ML_8

Descriptive Statistics

	Mean	Std. Deviation	N
KP_3_M_5	-1.1487088	.32762721	16
KP_3_M_65	-2.1751394	.59715300	16
KP_3_M_8	-3.71329269	1.234048740	16
KP_3_ML_5	-2.2065493	.48954318	16
KP_3_ML_65	-3.4750889	1.02838098	16
KP_3_ML_8	-5.4599314	1.54138757	16

Multivariate Tests[a]

Effect		Value	F	Hypothesis df	Error df	Sig.	Partial Eta Squared
System	Pillai's Trace	.824	70.198[b]	1.000	15.000	.000	.824
	Wilks' Lambda	.176	70.198[b]	1.000	15.000	.000	.824
	Hotelling's Trace	4.680	70.198[b]	1.000	15.000	.000	.824
	Roy's Largest Root	4.680	70.198[b]	1.000	15.000	.000	.824
Speed	Pillai's Trace	.921	81.170[b]	2.000	14.000	.000	.921
	Wilks' Lambda	.079	81.170[b]	2.000	14.000	.000	.921
	Hotelling's Trace	11.596	81.170[b]	2.000	14.000	.000	.921
	Roy's Largest Root	11.596	81.170[b]	2.000	14.000	.000	.921
System * Speed	Pillai's Trace	.255	2.397[b]	2.000	14.000	.127	.255
	Wilks' Lambda	.745	2.397[b]	2.000	14.000	.127	.255
	Hotelling's Trace	.342	2.397[b]	2.000	14.000	.127	.255
	Roy's Largest Root	.342	2.397[b]	2.000	14.000	.127	.255

a. Design: Intercept
Within Subjects Design: System + Speed + System * Speed

b. Exact statistic

Mauchly's Test of Sphericity[a]

Measure: MEASURE_1

Within Subjects Effect	Mauchly's W	Approx. Chi-Square	df	Sig.	Epsilon[b] Greenhouse-Geisser	Huynh-Feldt	Lower-bound
System	1.000	.000	0	.	1.000	1.000	1.000
Speed	.485	10.127	2	.006	.660	.699	.500
System * Speed	.499	9.742	2	.008	.666	.707	.500

Tests the null hypothesis that the error covariance matrix of the orthonormalized transformed dependent variables is proportional to an identity matrix.

a. Design: Intercept
Within Subjects Design: System + Speed + System * Speed

b. May be used to adjust the degrees of freedom for the averaged tests of significance. Corrected tests are displayed in the Tests of Within-Subjects Effects table.

Tests of Within-Subjects Effects

Measure: MEASURE_1

Source		Type III Sum of Squares	df	Mean Square	F	Sig.	Partial Eta Squared
System	Sphericity Assumed	44.924	1	44.924	70.198	.000	.824
	Greenhouse-Geisser	44.924	1.000	44.924	70.198	.000	.824
	Huynh-Feldt	44.924	1.000	44.924	70.198	.000	.824
	Lower-bound	44.924	1.000	44.924	70.198	.000	.824
Error(System)	Sphericity Assumed	9.599	15	.640			
	Greenhouse-Geisser	9.599	15.000	.640			
	Huynh-Feldt	9.599	15.000	.640			
	Lower-bound	9.599	15.000	.640			
Speed	Sphericity Assumed	137.406	2	68.703	111.783	.000	.882
	Greenhouse-Geisser	137.406	1.320	104.076	111.783	.000	.882
	Huynh-Feldt	137.406	1.398	98.290	111.783	.000	.882
	Lower-bound	137.406	1.000	137.406	111.783	.000	.882
Error(Speed)	Sphericity Assumed	18.438	30	.615			
	Greenhouse-Geisser	18.438	19.804	.931			
	Huynh-Feldt	18.438	20.970	.879			
	Lower-bound	18.438	15.000	1.229			
System * Speed	Sphericity Assumed	1.954	2	.977	3.235	.053	.177
	Greenhouse-Geisser	1.954	1.332	1.466	3.235	.077	.177
	Huynh-Feldt	1.954	1.413	1.382	3.235	.074	.177
	Lower-bound	1.954	1.000	1.954	3.235	.092	.177
Error(System*Speed)	Sphericity Assumed	9.058	30	.302			
	Greenhouse-Geisser	9.058	19.982	.453			
	Huynh-Feldt	9.058	21.197	.427			
	Lower-bound	9.058	15.000	.604			

Tests of Within-Subjects Contrasts

Measure: MEASURE_1

Source	System	Speed	Type III Sum of Squares	df	Mean Square	F	Sig.	Partial Eta Squared
System	Linear		44.924	1	44.924	70.198	.000	.824
Error(System)	Linear		9.599	15	.640			
Speed		Linear	135.395	1	135.395	145.057	.000	.906
		Quadratic	2.011	1	2.011	6.797	.020	.312
Error(Speed)		Linear	14.001	15	.933			
		Quadratic	4.438	15	.296			
System * Speed	Linear	Linear	1.898	1	1.898	4.345	.055	.225
		Quadratic	.056	1	.056	.334	.572	.022
Error(System*Speed)	Linear	Linear	6.552	15	.437			
		Quadratic	2.507	15	.167			

Tests of Between-Subjects Effects

Measure: MEASURE_1

Transformed Variable: Average

Source	Type III Sum of Squares	df	Mean Square	F	Sig.	Partial Eta Squared
Intercept	881.241	1	881.241	276.525	.000	.949
Error	47.803	15	3.187			

Estimated Marginal Means

1. Grand Mean

Measure: MEASURE_1

Mean	Std. Error	95% Confidence Interval	
		Lower Bound	Upper Bound
-3.030	.182	-3.418	-2.641

2. System

Estimates

Measure: MEASURE_1

System	Mean	Std. Error	95% Confidence Interval	
			Lower Bound	Upper Bound
1	-2.346	.145	-2.654	-2.037
2	-3.714	.243	-4.231	-3.197

Pairwise Comparisons

Measure: MEASURE_1

(I) System	(J) System	Mean Difference (I-J)	Std. Error	Sig.[b]	95% Confidence Interval for Difference[b]	
					Lower Bound	Upper Bound
1	2	1.368*	.163	.000	1.020	1.716
2	1	-1.368*	.163	.000	-1.716	-1.020

Based on estimated marginal means

*. The mean difference is significant at the .05 level.

b. Adjustment for multiple comparisons: Least Significant Difference (equivalent to no adjustments).

Multivariate Tests

	Value	F	Hypothesis df	Error df	Sig.	Partial Eta Squared
Pillai's trace	.824	70.198[a]	1.000	15.000	.000	.824
Wilks' lambda	.176	70.198[a]	1.000	15.000	.000	.824
Hotelling's trace	4.680	70.198[a]	1.000	15.000	.000	.824
Roy's largest root	4.680	70.198[a]	1.000	15.000	.000	.824

Each F tests the multivariate effect of System. These tests are based on the linearly independent pairwise comparisons among the estimated marginal means.

a. Exact statistic

3. Speed

Estimates

Measure: MEASURE_1

Speed	Mean	Std. Error	95% Confidence Interval	
			Lower Bound	Upper Bound
1	-1.678	.099	-1.889	-1.466
2	-2.825	.192	-3.235	-2.416
3	-4.587	.302	-5.230	-3.943

Pairwise Comparisons

Measure: MEASURE_1

(I) Speed	(J) Speed	Mean Difference (I-J)	Std. Error	Sig.[b]	95% Confidence Interval for Difference[b]	
					Lower Bound	Upper Bound
1	2	1.147*	.109	.000	.914	1.381
	3	2.909*	.242	.000	2.394	3.424
2	1	-1.147*	.109	.000	-1.381	-.914
	3	1.761*	.212	.000	1.310	2.213
3	1	-2.909*	.242	.000	-3.424	-2.394
	2	-1.761*	.212	.000	-2.213	-1.310

Based on estimated marginal means

*. The mean difference is significant at the .05 level.

b. Adjustment for multiple comparisons: Least Significant Difference (equivalent to no adjustments).

Multivariate Tests

	Value	F	Hypothesis df	Error df	Sig.	Partial Eta Squared
Pillai's trace	.921	81.170[a]	2.000	14.000	.000	.921
Wilks' lambda	.079	81.170[a]	2.000	14.000	.000	.921
Hotelling's trace	11.596	81.170[a]	2.000	14.000	.000	.921
Roy's largest root	11.596	81.170[a]	2.000	14.000	.000	.921

Each F tests the multivariate effect of Speed. These tests are based on the linearly independent pairwise comparisons among the estimated marginal means.

a. Exact statistic

4. System * Speed

Measure: MEASURE_1

System	Speed	Mean	Std. Error	95% Confidence Interval	
				Lower Bound	Upper Bound
1	1	-1.149	.082	-1.323	-.974
	2	-2.175	.149	-2.493	-1.857
	3	-3.713	.309	-4.371	-3.056
2	1	-2.207	.122	-2.467	-1.946
	2	-3.475	.257	-4.023	-2.927
	3	-5.460	.385	-6.281	-4.639

Profile Plots

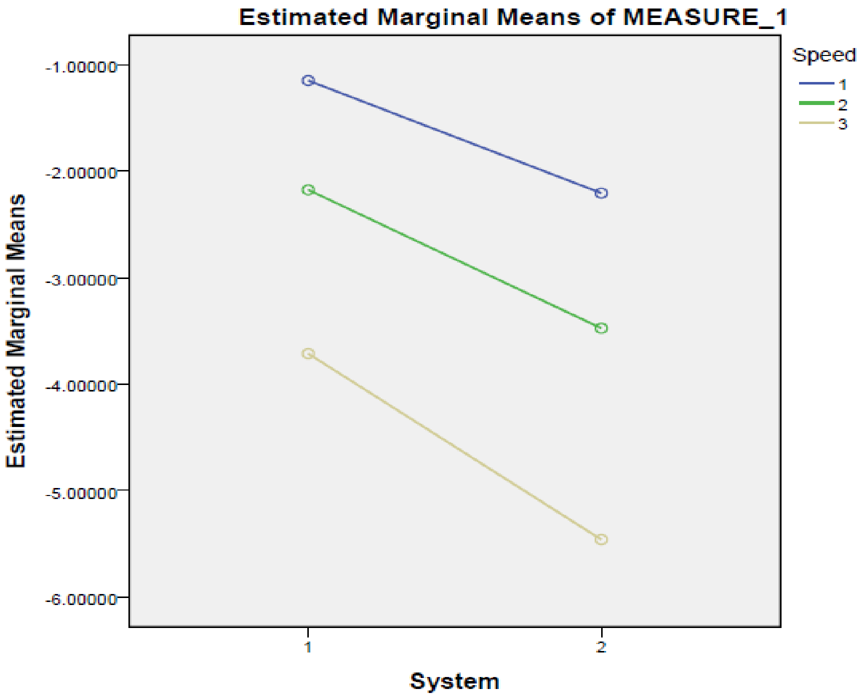


```
GLM KP_3_T_M_5 KP_3_T_M_65 KP_3_T_M_8 KP_3_T_ML_5 KP_3_T_ML_65 KP_3_T_ML_8
  /WSFACTOR=System 2 Polynomial Speed 3 Polynomial
  /METHOD=SSTYPE(3)
  /PLOT=PROFILE(System*Speed)
  /EMMEANS=TABLES(OVERALL)
  /EMMEANS=TABLES(System) COMPARE ADJ(LSD)
  /EMMEANS=TABLES(Speed) COMPARE ADJ(LSD)
  /EMMEANS=TABLES(System*Speed)
  /PRINT=DESCRIPTIVE ETASQ
  /CRITERIA=ALPHA(.05)
  /WSDESIGN=System Speed System*Speed.
```

General Linear Model

Within-Subjects Factors

Measure: MEASURE_1

System	Speed	Dependent Variable
1	1	KP_3_T_M_5
	2	KP_3_T_M_65
	3	KP_3_T_M_8
2	1	KP_3_T_ML_5
	2	KP_3_T_ML_65
	3	KP_3_T_ML_8

Descriptive Statistics

	Mean	Std. Deviation	N
KP_3_T_M_5	39.1562500	3.00088181	16
KP_3_T_M_65	37.0812500	3.23567999	16
KP_3_T_M_8	34.48125000	3.878869036	16
KP_3_T_ML_5	38.6250000	1.88202019	16
KP_3_T_ML_65	36.1437500	2.79140795	16
KP_3_T_ML_8	34.2125000	3.99697803	16

Multivariate Tests[a]

Effect		Value	F	Hypothesis df	Error df	Sig.	Partial Eta Squared
System	Pillai's Trace	.223	4.297[b]	1.000	15.000	.056	.223
	Wilks' Lambda	.777	4.297[b]	1.000	15.000	.056	.223
	Hotelling's Trace	.286	4.297[b]	1.000	15.000	.056	.223
	Roy's Largest Root	.286	4.297[b]	1.000	15.000	.056	.223
Speed	Pillai's Trace	.753	21.351[b]	2.000	14.000	.000	.753
	Wilks' Lambda	.247	21.351[b]	2.000	14.000	.000	.753
	Hotelling's Trace	3.050	21.351[b]	2.000	14.000	.000	.753
	Roy's Largest Root	3.050	21.351[b]	2.000	14.000	.000	.753
System * Speed	Pillai's Trace	.180	1.532[b]	2.000	14.000	.250	.180
	Wilks' Lambda	.820	1.532[b]	2.000	14.000	.250	.180
	Hotelling's Trace	.219	1.532[b]	2.000	14.000	.250	.180
	Roy's Largest Root	.219	1.532[b]	2.000	14.000	.250	.180

a. Design: Intercept
Within Subjects Design: System + Speed + System * Speed

b. Exact statistic

Mauchly's Test of Sphericity[a]

Measure: MEASURE_1

Within Subjects Effect	Mauchly's W	Approx. Chi-Square	df	Sig.	Epsilon[b]		
					Greenhouse-Geisser	Huynh-Feldt	Lower-bound
System	1.000	.000	0	.	1.000	1.000	1.000
Speed	.786	3.375	2	.185	.824	.912	.500
System * Speed	.997	.043	2	.979	.997	1.000	.500

Tests the null hypothesis that the error covariance matrix of the orthonormalized transformed dependent variables is proportional to an identity matrix.

a. Design: Intercept
Within Subjects Design: System + Speed + System * Speed

b. May be used to adjust the degrees of freedom for the averaged tests of significance. Corrected tests are displayed in the Tests of Within-Subjects Effects table.

Tests of Within-Subjects Effects

Measure: MEASURE_1

Source		Type III Sum of Squares	df	Mean Square	F	Sig.	Partial Eta Squared
System	Sphericity Assumed	8.050	1	8.050	4.297	.056	.223
	Greenhouse-Geisser	8.050	1.000	8.050	4.297	.056	.223
	Huynh-Feldt	8.050	1.000	8.050	4.297	.056	.223
	Lower-bound	8.050	1.000	8.050	4.297	.056	.223
Error(System)	Sphericity Assumed	28.100	15	1.873			
	Greenhouse-Geisser	28.100	15.000	1.873			
	Huynh-Feldt	28.100	15.000	1.873			
	Lower-bound	28.100	15.000	1.873			
Speed	Sphericity Assumed	330.331	2	165.166	32.881	.000	.687
	Greenhouse-Geisser	330.331	1.647	200.545	32.881	.000	.687
	Huynh-Feldt	330.331	1.824	181.109	32.881	.000	.687
	Lower-bound	330.331	1.000	330.331	32.881	.000	.687
Error(Speed)	Sphericity Assumed	150.692	30	5.023			
	Greenhouse-Geisser	150.692	24.708	6.099			
	Huynh-Feldt	150.692	27.359	5.508			
	Lower-bound	150.692	15.000	10.046			
System * Speed	Sphericity Assumed	1.816	2	.908	1.693	.201	.101
	Greenhouse-Geisser	1.816	1.994	.911	1.693	.201	.101
	Huynh-Feldt	1.816	2.000	.908	1.693	.201	.101
	Lower-bound	1.816	1.000	1.816	1.693	.213	.101
Error(System*Speed)	Sphericity Assumed	16.094	30	.536			
	Greenhouse-Geisser	16.094	29.908	.538			
	Huynh-Feldt	16.094	30.000	.536			
	Lower-bound	16.094	15.000	1.073			

Tests of Within-Subjects Contrasts

Measure: MEASURE_1

Source	System	Speed	Type III Sum of Squares	df	Mean Square	F	Sig.	Partial Eta Squared
System	Linear		8.050	1	8.050	4.297	.056	.223
Error(System)	Linear		28.100	15	1.873			
Speed		Linear	330.331	1	330.331	45.259	.000	.751
		Quadratic	.001	1	.001	.000	.986	.000
Error(Speed)		Linear	109.479	15	7.299			
		Quadratic	41.213	15	2.748			
System * Speed	Linear	Linear	.276	1	.276	.544	.472	.035
		Quadratic	1.541	1	1.541	2.723	.120	.154
Error(System*Speed)	Linear	Linear	7.604	15	.507			
		Quadratic	8.489	15	.566			

Tests of Between-Subjects Effects

Measure: MEASURE_1

Transformed Variable: Average

Source	Type III Sum of Squares	df	Mean Square	F	Sig.	Partial Eta Squared
Intercept	128714.907	1	128714.907	2635.548	.000	.994
Error	732.570	15	48.838			

Estimated Marginal Means

1. Grand Mean

Measure: MEASURE_1

Mean	Std. Error	95% Confidence Interval	
		Lower Bound	Upper Bound
36.617	.713	35.096	38.137

2. System

Estimates

Measure: MEASURE_1

System	Mean	Std. Error	95% Confidence Interval	
			Lower Bound	Upper Bound
1	36.906	.777	35.251	38.562
2	36.327	.673	34.892	37.762

Pairwise Comparisons

Measure: MEASURE_1

(I) System	(J) System	Mean Difference (I-J)	Std. Error	Sig.[a]	95% Confidence Interval for Difference[a]	
					Lower Bound	Upper Bound
1	2	.579	.279	.056	-.016	1.175
2	1	-.579	.279	.056	-1.175	.016

Based on estimated marginal means

a. Adjustment for multiple comparisons: Least Significant Difference (equivalent to no adjustments).

Multivariate Tests

	Value	F	Hypothesis df	Error df	Sig.	Partial Eta Squared
Pillai's trace	.223	4.297[a]	1.000	15.000	.056	.223
Wilks' lambda	.777	4.297[a]	1.000	15.000	.056	.223
Hotelling's trace	.286	4.297[a]	1.000	15.000	.056	.223
Roy's largest root	.286	4.297[a]	1.000	15.000	.056	.223

Each F tests the multivariate effect of System. These tests are based on the linearly independent pairwise comparisons among the estimated marginal means.

a. Exact statistic

3. Speed

Estimates

Measure: MEASURE_1

Speed	Mean	Std. Error	95% Confidence Interval	
			Lower Bound	Upper Bound
1	38.891	.585	37.643	40.138
2	36.613	.746	35.023	38.202
3	34.347	.970	32.279	36.415

Pairwise Comparisons

Measure: MEASURE_1

(I) Speed	(J) Speed	Mean Difference (I-J)	Std. Error	Sig.[b]	95% Confidence Interval for Difference[b]	
					Lower Bound	Upper Bound
1	2	2.278*	.518	.001	1.174	3.383
	3	4.544*	.675	.000	3.104	5.983
2	1	-2.278*	.518	.001	-3.383	-1.174
	3	2.266*	.466	.000	1.273	3.259
3	1	-4.544*	.675	.000	-5.983	-3.104
	2	-2.266*	.466	.000	-3.259	-1.273

Based on estimated marginal means

*. The mean difference is significant at the .05 level.

b. Adjustment for multiple comparisons: Least Significant Difference (equivalent to no adjustments).

Multivariate Tests

	Value	F	Hypothesis df	Error df	Sig.	Partial Eta Squared
Pillai's trace	.753	21.351[a]	2.000	14.000	.000	.753
Wilks' lambda	.247	21.351[a]	2.000	14.000	.000	.753
Hotelling's trace	3.050	21.351[a]	2.000	14.000	.000	.753
Roy's largest root	3.050	21.351[a]	2.000	14.000	.000	.753

Each F tests the multivariate effect of Speed. These tests are based on the linearly independent pairwise comparisons among the estimated marginal means.

a. Exact statistic

4. System * Speed

Measure: MEASURE_1

System	Speed	Mean	Std. Error	95% Confidence Interval	
				Lower Bound	Upper Bound
1	1	39.156	.750	37.557	40.755
	2	37.081	.809	35.357	38.805
	3	34.481	.970	32.414	36.548
2	1	38.625	.471	37.622	39.628
	2	36.144	.698	34.656	37.631
	3	34.213	.999	32.083	36.342

Profile Plots

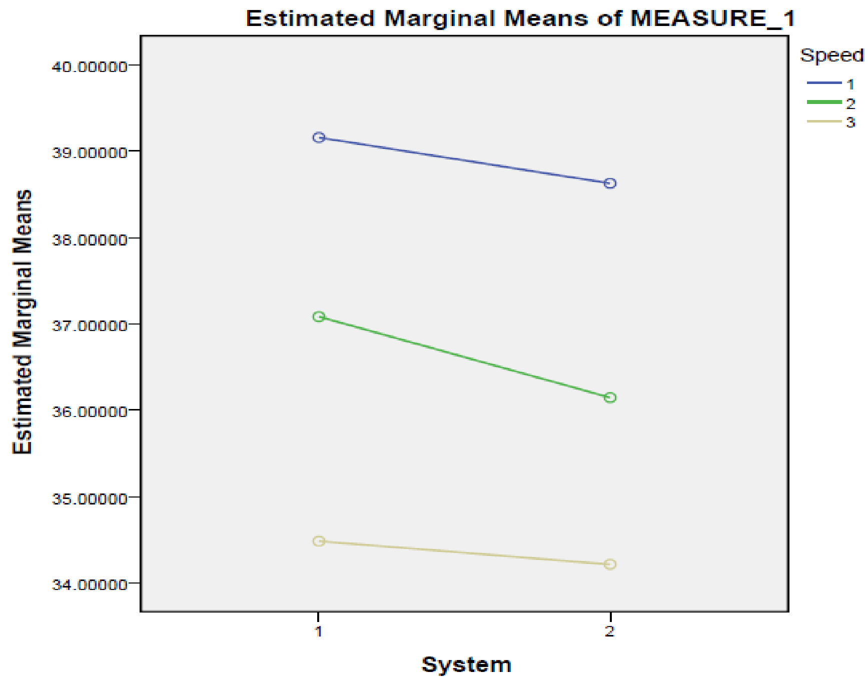


```
GLM KP_4_M_5 KP_4_M_65 KP_4_M_8 KP_4_ML_5 KP_4_ML_65 KP_4_ML_8
  /WSFACTOR=System 2 Polynomial Speed 3 Polynomial
  /METHOD=SSTYPE(3)
  /PLOT=PROFILE(System*Speed)
  /EMMEANS=TABLES(OVERALL)
  /EMMEANS=TABLES(System) COMPARE ADJ(LSD)
  /EMMEANS=TABLES(Speed) COMPARE ADJ(LSD)
  /EMMEANS=TABLES(System*Speed)
  /PRINT=DESCRIPTIVE ETASQ
  /CRITERIA=ALPHA(.05)
  /WSDESIGN=System Speed System*Speed.
```

General Linear Model

Within-Subjects Factors

Measure: MEASURE_1

System	Speed	Dependent Variable
1	1	KP_4_M_5
	2	KP_4_M_65
	3	KP_4_M_8
2	1	KP_4_ML_5
	2	KP_4_ML_65
	3	KP_4_ML_8

Descriptive Statistics

	Mean	Std. Deviation	N
KP_4_M_5	-3.36544850	.702929678	16
KP_4_M_65	-5.04505756	1.132975396	16
KP_4_M_8	-7.357898250	1.947553500	16
KP_4_ML_5	-4.70033206	.940468272	16
KP_4_ML_65	-6.69104088	1.225838624	16
KP_4_ML_8	-9.59726675	2.340462140	16

Multivariate Tests[a]

Effect		Value	F	Hypothesis df	Error df	Sig.	Partial Eta Squared
System	Pillai's Trace	.928	194.685[b]	1.000	15.000	.000	.928
	Wilks' Lambda	.072	194.685[b]	1.000	15.000	.000	.928
	Hotelling's Trace	12.979	194.685[b]	1.000	15.000	.000	.928
	Roy's Largest Root	12.979	194.685[b]	1.000	15.000	.000	.928
Speed	Pillai's Trace	.939	108.013[b]	2.000	14.000	.000	.939
	Wilks' Lambda	.061	108.013[b]	2.000	14.000	.000	.939
	Hotelling's Trace	15.430	108.013[b]	2.000	14.000	.000	.939
	Roy's Largest Root	15.430	108.013[b]	2.000	14.000	.000	.939
System * Speed	Pillai's Trace	.561	8.948[b]	2.000	14.000	.003	.561
	Wilks' Lambda	.439	8.948[b]	2.000	14.000	.003	.561
	Hotelling's Trace	1.278	8.948[b]	2.000	14.000	.003	.561
	Roy's Largest Root	1.278	8.948[b]	2.000	14.000	.003	.561

a. Design: Intercept
Within Subjects Design: System + Speed + System * Speed

b. Exact statistic

Mauchly's Test of Sphericity[a]

Measure: MEASURE_1

Within Subjects Effect	Mauchly's W	Approx. Chi-Square	df	Sig.	Epsilon[b]		
					Greenhouse-Geisser	Huynh-Feldt	Lower-bound
System	1.000	.000	0	.	1.000	1.000	1.000
Speed	.295	17.072	2	.000	.587	.607	.500
System * Speed	.642	6.202	2	.045	.736	.797	.500

Tests the null hypothesis that the error covariance matrix of the orthonormalized transformed dependent variables is proportional to an identity matrix.

a. Design: Intercept
Within Subjects Design: System + Speed + System * Speed

b. May be used to adjust the degrees of freedom for the averaged tests of significance. Corrected tests are displayed in the Tests of Within-Subjects Effects table.

Tests of Within-Subjects Effects

Measure: MEASURE_1

Source		Type III Sum of Squares	df	Mean Square	F	Sig.	Partial Eta Squared
System	Sphericity Assumed	72.669	1	72.669	194.685	.000	.928
	Greenhouse-Geisser	72.669	1.000	72.669	194.685	.000	.928
	Huynh-Feldt	72.669	1.000	72.669	194.685	.000	.928
	Lower-bound	72.669	1.000	72.669	194.685	.000	.928
Error(System)	Sphericity Assumed	5.599	15	.373			
	Greenhouse-Geisser	5.599	15.000	.373			
	Huynh-Feldt	5.599	15.000	.373			
	Lower-bound	5.599	15.000	.373			
Speed	Sphericity Assumed	319.283	2	159.641	106.846	.000	.877
	Greenhouse-Geisser	319.283	1.173	272.125	106.846	.000	.877
	Huynh-Feldt	319.283	1.213	263.203	106.846	.000	.877
	Lower-bound	319.283	1.000	319.283	106.846	.000	.877
Error(Speed)	Sphericity Assumed	44.824	30	1.494			
	Greenhouse-Geisser	44.824	17.599	2.547			
	Huynh-Feldt	44.824	18.196	2.463			
	Lower-bound	44.824	15.000	2.988			
System * Speed	Sphericity Assumed	3.379	2	1.689	8.352	.001	.358
	Greenhouse-Geisser	3.379	1.473	2.294	8.352	.004	.358
	Huynh-Feldt	3.379	1.594	2.119	8.352	.003	.358
	Lower-bound	3.379	1.000	3.379	8.352	.011	.358
Error(System*Speed)	Sphericity Assumed	6.068	30	.202			
	Greenhouse-Geisser	6.068	22.093	.275			
	Huynh-Feldt	6.068	23.915	.254			
	Lower-bound	6.068	15.000	.405			

Tests of Within-Subjects Contrasts

Measure: MEASURE_1

Source	System	Speed	Type III Sum of Squares	df	Mean Square	F	Sig.	Partial Eta Squared
System	Linear		72.669	1	72.669	194.685	.000	.928
Error(System)	Linear		5.599	15	.373			
Speed		Linear	316.085	1	316.085	134.882	.000	.900
		Quadratic	3.198	1	3.198	4.960	.042	.248
Error(Speed)		Linear	35.151	15	2.343			
		Quadratic	9.673	15	.645			
System * Speed	Linear	Linear	3.272	1	3.272	15.280	.001	.505
		Quadratic	.106	1	.106	.558	.467	.036
Error(System*Speed)	Linear	Linear	3.212	15	.214			
		Quadratic	2.855	15	.190			

Tests of Between-Subjects Effects

Measure: MEASURE_1

Transformed Variable: Average

Source	Type III Sum of Squares	df	Mean Square	F	Sig.	Partial Eta Squared
Intercept	3602.881	1	3602.881	372.599	.000	.961
Error	145.044	15	9.670			

Estimated Marginal Means

1. Grand Mean

Measure: MEASURE_1

Mean	Std. Error	95% Confidence Interval	
		Lower Bound	Upper Bound
-6.126	.317	-6.803	-5.450

2. System

Estimates

Measure: MEASURE_1

System	Mean	Std. Error	95% Confidence Interval	
			Lower Bound	Upper Bound
1	-5.256	.295	-5.886	-4.626
2	-6.996	.349	-7.740	-6.252

Pairwise Comparisons

Measure: MEASURE_1

(I) System	(J) System	Mean Difference (I-J)	Std. Error	Sig.[b]	95% Confidence Interval for Difference[b]	
					Lower Bound	Upper Bound
1	2	1.740*	.125	.000	1.474	2.006
2	1	-1.740*	.125	.000	-2.006	-1.474

Based on estimated marginal means

*. The mean difference is significant at the .05 level.

b. Adjustment for multiple comparisons: Least Significant Difference (equivalent to no adjustments).

Multivariate Tests

	Value	F	Hypothesis df	Error df	Sig.	Partial Eta Squared
Pillai's trace	.928	194.685[a]	1.000	15.000	.000	.928
Wilks' lambda	.072	194.685[a]	1.000	15.000	.000	.928
Hotelling's trace	12.979	194.685[a]	1.000	15.000	.000	.928
Roy's largest root	12.979	194.685[a]	1.000	15.000	.000	.928

Each F tests the multivariate effect of System. These tests are based on the linearly independent pairwise comparisons among the estimated marginal means.

a. Exact statistic

3. Speed

Estimates

Measure: MEASURE_1

Speed	Mean	Std. Error	95% Confidence Interval	
			Lower Bound	Upper Bound
1	-4.033	.199	-4.458	-3.608
2	-5.868	.282	-6.469	-5.267
3	-8.478	.526	-9.598	-7.357

Pairwise Comparisons

Measure: MEASURE_1

(I) Speed	(J) Speed	Mean Difference (I-J)	Std. Error	Sig.[b]	95% Confidence Interval for Difference[b]	
					Lower Bound	Upper Bound
1	2	1.835*	.130	.000	1.558	2.112
	3	4.445*	.383	.000	3.629	5.260
2	1	-1.835*	.130	.000	-2.112	-1.558
	3	2.610*	.342	.000	1.881	3.338
3	1	-4.445*	.383	.000	-5.260	-3.629
	2	-2.610*	.342	.000	-3.338	-1.881

Based on estimated marginal means

*. The mean difference is significant at the .05 level.

b. Adjustment for multiple comparisons: Least Significant Difference (equivalent to no adjustments).

Multivariate Tests

	Value	F	Hypothesis df	Error df	Sig.	Partial Eta Squared
Pillai's trace	.939	108.013[a]	2.000	14.000	.000	.939
Wilks' lambda	.061	108.013[a]	2.000	14.000	.000	.939
Hotelling's trace	15.430	108.013[a]	2.000	14.000	.000	.939
Roy's largest root	15.430	108.013[a]	2.000	14.000	.000	.939

Each F tests the multivariate effect of Speed. These tests are based on the linearly independent pairwise comparisons among the estimated marginal means.

a. Exact statistic

4. System * Speed

Measure: MEASURE_1

System	Speed	Mean	Std. Error	95% Confidence Interval	
				Lower Bound	Upper Bound
1	1	-3.365	.176	-3.740	-2.991
	2	-5.045	.283	-5.649	-4.441
	3	-7.358	.487	-8.396	-6.320
2	1	-4.700	.235	-5.201	-4.199
	2	-6.691	.306	-7.344	-6.038
	3	-9.597	.585	-10.844	-8.350

Profile Plots

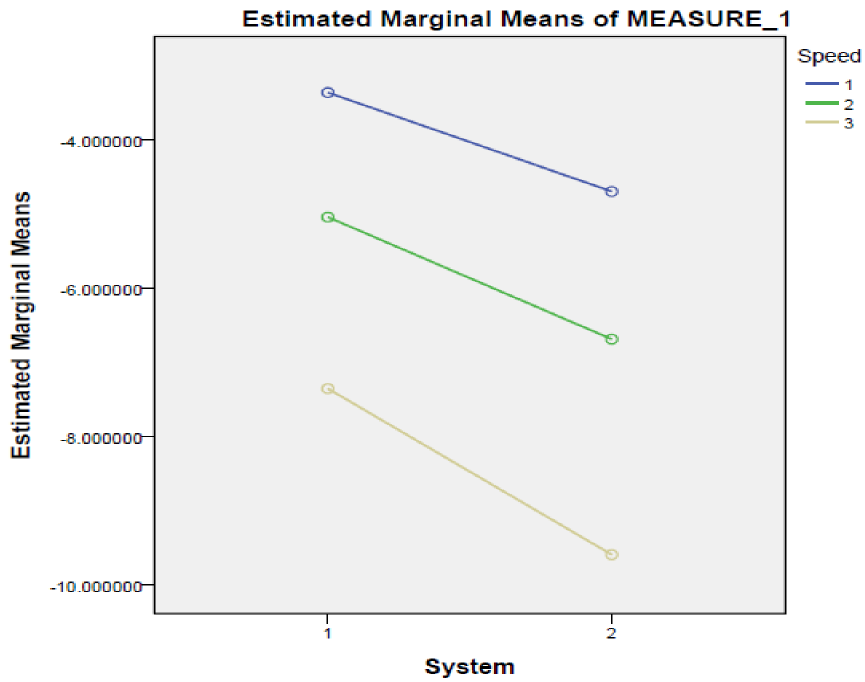


```
GLM KP_4_T_M_5 KP_4_T_M_65 KP_4_T_M_8 KP_4_T_ML_5 KP_4_T_ML_65 KP_4_T_ML_8
  /WSFACTOR=System 2 Polynomial Speed 3 Polynomial
  /METHOD=SSTYPE(3)
  /PLOT=PROFILE(System*Speed)
  /EMMEANS=TABLES(OVERALL)
  /EMMEANS=TABLES(System) COMPARE ADJ(LSD)
  /EMMEANS=TABLES(Speed) COMPARE ADJ(LSD)
  /EMMEANS=TABLES(System*Speed)
  /PRINT=DESCRIPTIVE ETASQ
  /CRITERIA=ALPHA(.05)
  /WSDESIGN=System Speed System*Speed.
```

General Linear Model

Within-Subjects Factors

Measure: MEASURE_1

System	Speed	Dependent Variable
1	1	KP_4_T_M_5
	2	KP_4_T_M_65
	3	KP_4_T_M_8
2	1	KP_4_T_ML_5
	2	KP_4_T_ML_65
	3	KP_4_T_ML_8

Descriptive Statistics

	Mean	Std. Deviation	N
KP_4_T_M_5	63.9000	5.56058	16
KP_4_T_M_65	60.8438	5.69643	16
KP_4_T_M_8	55.9563	5.93947	16
KP_4_T_ML_5	63.5438	5.32816	16
KP_4_T_ML_65	60.7438	5.70169	16
KP_4_T_ML_8	56.8875	5.88794	16

Multivariate Tests[a]

Effect		Value	F	Hypothesis df	Error df	Sig.	Partial Eta Squared
System	Pillai's Trace	.009	.138[b]	1.000	15.000	.716	.009
	Wilks' Lambda	.991	.138[b]	1.000	15.000	.716	.009
	Hotelling's Trace	.009	.138[b]	1.000	15.000	.716	.009
	Roy's Largest Root	.009	.138[b]	1.000	15.000	.716	.009
Speed	Pillai's Trace	.818	31.521[b]	2.000	14.000	.000	.818
	Wilks' Lambda	.182	31.521[b]	2.000	14.000	.000	.818
	Hotelling's Trace	4.503	31.521[b]	2.000	14.000	.000	.818
	Roy's Largest Root	4.503	31.521[b]	2.000	14.000	.000	.818
System * Speed	Pillai's Trace	.144	1.177[b]	2.000	14.000	.337	.144
	Wilks' Lambda	.856	1.177[b]	2.000	14.000	.337	.144
	Hotelling's Trace	.168	1.177[b]	2.000	14.000	.337	.144
	Roy's Largest Root	.168	1.177[b]	2.000	14.000	.337	.144

a. Design: Intercept
Within Subjects Design: System + Speed + System * Speed

b. Exact statistic

Mauchly's Test of Sphericity[a]

Measure: MEASURE_1

Within Subjects Effect	Mauchly's W	Approx. Chi-Square	df	Sig.	Epsilon[b]		
					Greenhouse-Geisser	Huynh-Feldt	Lower-bound
System	1.000	.000	0	.	1.000	1.000	1.000
Speed	.940	.871	2	.647	.943	1.000	.500
System * Speed	.046	43.185	2	.000	.512	.514	.500

Tests the null hypothesis that the error covariance matrix of the orthonormalized transformed dependent variables is proportional to an identity matrix.

a. Design: Intercept
Within Subjects Design: System + Speed + System * Speed

b. May be used to adjust the degrees of freedom for the averaged tests of significance. Corrected tests are displayed in the Tests of Within-Subjects Effects table.

Tests of Within-Subjects Effects

Measure: MEASURE_1

Source		Type III Sum of Squares	df	Mean Square	F	Sig.	Partial Eta Squared
System	Sphericity Assumed	.602	1	.602	.138	.716	.009
	Greenhouse-Geisser	.602	1.000	.602	.138	.716	.009
	Huynh-Feldt	.602	1.000	.602	.138	.716	.009
	Lower-bound	.602	1.000	.602	.138	.716	.009
Error(System)	Sphericity Assumed	65.635	15	4.376			
	Greenhouse-Geisser	65.635	15.000	4.376			
	Huynh-Feldt	65.635	15.000	4.376			
	Lower-bound	65.635	15.000	4.376			
Speed	Sphericity Assumed	863.757	2	431.878	42.021	.000	.737
	Greenhouse-Geisser	863.757	1.886	457.939	42.021	.000	.737
	Huynh-Feldt	863.757	2.000	431.878	42.021	.000	.737
	Lower-bound	863.757	1.000	863.757	42.021	.000	.737
Error(Speed)	Sphericity Assumed	308.330	30	10.278			
	Greenhouse-Geisser	308.330	28.293	10.898			
	Huynh-Feldt	308.330	30.000	10.278			
	Lower-bound	308.330	15.000	20.555			
System * Speed	Sphericity Assumed	7.431	2	3.716	.946	.399	.059
	Greenhouse-Geisser	7.431	1.023	7.261	.946	.348	.059
	Huynh-Feldt	7.431	1.028	7.226	.946	.348	.059
	Lower-bound	7.431	1.000	7.431	.946	.346	.059
Error(System*Speed)	Sphericity Assumed	117.802	30	3.927			
	Greenhouse-Geisser	117.802	15.351	7.674			
	Huynh-Feldt	117.802	15.427	7.636			
	Lower-bound	117.802	15.000	7.853			

Tests of Within-Subjects Contrasts

Measure: MEASURE_1

Source	System	Speed	Type III Sum of Squares	df	Mean Square	F	Sig.	Partial Eta Squared
System	Linear		.602	1	.602	.138	.716	.009
Error(System)	Linear		65.635	15	4.376			
Speed		Linear	852.640	1	852.640	67.238	.000	.818
		Quadratic	11.117	1	11.117	1.412	.253	.086
Error(Speed)		Linear	190.215	15	12.681			
		Quadratic	118.115	15	7.874			
System * Speed	Linear	Linear	6.631	1	6.631	1.076	.316	.067
		Quadratic	.801	1	.801	.474	.502	.031
Error(System*Speed)	Linear	Linear	92.454	15	6.164			
		Quadratic	25.347	15	1.690			

Tests of Between-Subjects Effects

Measure: MEASURE_1

Transformed Variable: Average

Source	Type III Sum of Squares	df	Mean Square	F	Sig.	Partial Eta Squared
Intercept	349209.375	1	349209.375	2163.244	.000	.993
Error	2421.428	15	161.429			

Estimated Marginal Means

1. Grand Mean

Measure: MEASURE_1

Mean	Std. Error	95% Confidence Interval	
		Lower Bound	Upper Bound
60.313	1.297	57.549	63.076

2. System

Estimates

Measure: MEASURE_1

System	Mean	Std. Error	95% Confidence Interval	
			Lower Bound	Upper Bound
1	60.233	1.286	57.493	62.974
2	60.392	1.342	57.531	63.252

Pairwise Comparisons

Measure: MEASURE_1

(I) System	(J) System	Mean Difference (I-J)	Std. Error	Sig.[a]	95% Confidence Interval for Difference[a]	
					Lower Bound	Upper Bound
1	2	-.158	.427	.716	-1.068	.752
2	1	.158	.427	.716	-.752	1.068

Based on estimated marginal means

a. Adjustment for multiple comparisons: Least Significant Difference (equivalent to no adjustments).

Multivariate Tests

	Value	F	Hypothesis df	Error df	Sig.	Partial Eta Squared
Pillai's trace	.009	.138[a]	1.000	15.000	.716	.009
Wilks' lambda	.991	.138[a]	1.000	15.000	.716	.009
Hotelling's trace	.009	.138[a]	1.000	15.000	.716	.009
Roy's largest root	.009	.138[a]	1.000	15.000	.716	.009

Each F tests the multivariate effect of System. These tests are based on the linearly independent pairwise comparisons among the estimated marginal means.

a. Exact statistic

3. Speed

Estimates

Measure: MEASURE_1

Speed	Mean	Std. Error	95% Confidence Interval	
			Lower Bound	Upper Bound
1	63.722	1.350	60.843	66.600
2	60.794	1.419	57.769	63.819
3	56.422	1.360	53.524	59.320

Pairwise Comparisons

Measure: MEASURE_1

(I) Speed	(J) Speed	Mean Difference (I-J)	Std. Error	Sig.[b]	95% Confidence Interval for Difference[b]	
					Lower Bound	Upper Bound
1	2	2.928*	.725	.001	1.383	4.473
	3	7.300*	.890	.000	5.402	9.198
2	1	-2.928*	.725	.001	-4.473	-1.383
	3	4.372*	.780	.000	2.708	6.035
3	1	-7.300*	.890	.000	-9.198	-5.402
	2	-4.372*	.780	.000	-6.035	-2.708

Based on estimated marginal means

*. The mean difference is significant at the .05 level.

b. Adjustment for multiple comparisons: Least Significant Difference (equivalent to no adjustments).

Multivariate Tests

	Value	F	Hypothesis df	Error df	Sig.	Partial Eta Squared
Pillai's trace	.818	31.521[a]	2.000	14.000	.000	.818
Wilks' lambda	.182	31.521[a]	2.000	14.000	.000	.818
Hotelling's trace	4.503	31.521[a]	2.000	14.000	.000	.818
Roy's largest root	4.503	31.521[a]	2.000	14.000	.000	.818

Each F tests the multivariate effect of Speed. These tests are based on the linearly independent pairwise comparisons among the estimated marginal means.

a. Exact statistic

4. System * Speed

Measure: MEASURE_1

System	Speed	Mean	Std. Error	95% Confidence Interval	
				Lower Bound	Upper Bound
1	1	63.900	1.390	60.937	66.863
	2	60.844	1.424	57.808	63.879
	3	55.956	1.485	52.791	59.121
2	1	63.544	1.332	60.705	66.383
	2	60.744	1.425	57.706	63.782
	3	56.888	1.472	53.750	60.025

Profile Plots

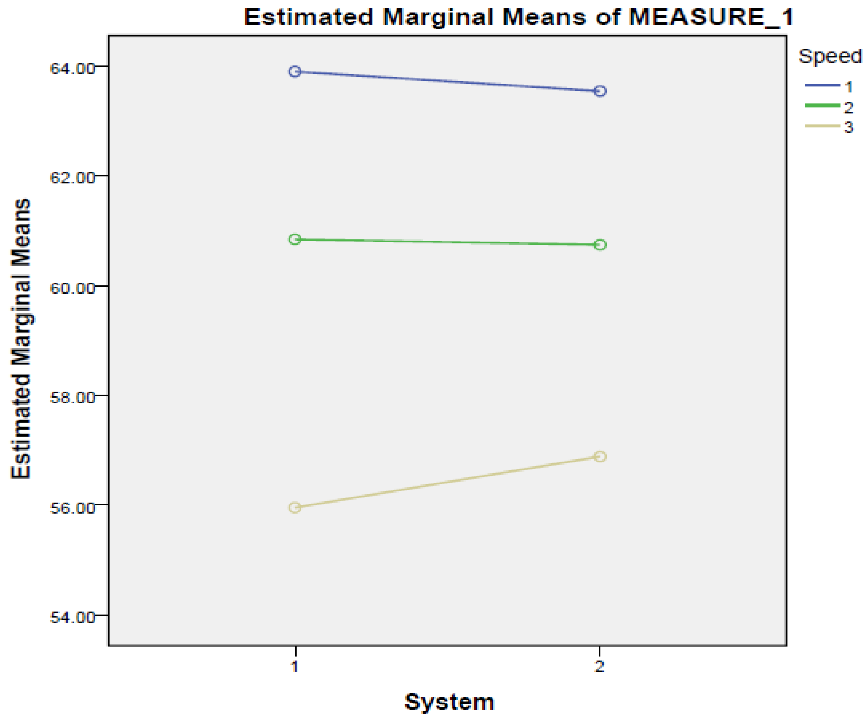


```
GLM KM_2_M_5 KM_2_M_65 KM_2_M_8 KM_2_ML_5 KM_2_ML_65 KM_2_ML_8
  /WSFACTOR=System 2 Polynomial Speed 3 Polynomial
  /METHOD=SSTYPE(3)
  /PLOT=PROFILE(System*Speed Speed*System)
  /EMMEANS=TABLES(OVERALL)
  /EMMEANS=TABLES(System) COMPARE ADJ(LSD)
  /EMMEANS=TABLES(Speed) COMPARE ADJ(LSD)
  /EMMEANS=TABLES(System*Speed)
  /PRINT=DESCRIPTIVE ETASQ
  /CRITERIA=ALPHA(.05)
  /WSDESIGN=System Speed System*Speed.
```

General Linear Model

Within-Subjects Factors

Measure: MEASURE_1

System	Speed	Dependent Variable
1	1	KM_2_M_5
	2	KM_2_M_65
	3	KM_2_M_8
2	1	KM_2_ML_5
	2	KM_2_ML_65
	3	KM_2_ML_8

Descriptive Statistics

	Mean	Std. Deviation	N
KM_2_M_5	-.4952513	.09023758	16
KM_2_M_65	-.61095963	.104910014	16
KM_2_M_8	-.74133212	.125514872	16
KM_2_ML_5	-.7826791	.14230370	16
KM_2_ML_65	-.9527258	.16009008	16
KM_2_ML_8	-1.1741616	.23441179	16

Multivariate Tests[a]

Effect		Value	F	Hypothesis df	Error df	Sig.	Partial Eta Squared
System	Pillai's Trace	.958	342.120[b]	1.000	15.000	.000	.958
	Wilks' Lambda	.042	342.120[b]	1.000	15.000	.000	.958
	Hotelling's Trace	22.808	342.120[b]	1.000	15.000	.000	.958
	Roy's Largest Root	22.808	342.120[b]	1.000	15.000	.000	.958
Speed	Pillai's Trace	.940	109.005[b]	2.000	14.000	.000	.940
	Wilks' Lambda	.060	109.005[b]	2.000	14.000	.000	.940
	Hotelling's Trace	15.572	109.005[b]	2.000	14.000	.000	.940
	Roy's Largest Root	15.572	109.005[b]	2.000	14.000	.000	.940
System * Speed	Pillai's Trace	.740	19.910[b]	2.000	14.000	.000	.740
	Wilks' Lambda	.260	19.910[b]	2.000	14.000	.000	.740
	Hotelling's Trace	2.844	19.910[b]	2.000	14.000	.000	.740
	Roy's Largest Root	2.844	19.910[b]	2.000	14.000	.000	.740

a. Design: Intercept
Within Subjects Design: System + Speed + System * Speed

b. Exact statistic

Mauchly's Test of Sphericity[a]

Measure: MEASURE_1

Within Subjects Effect	Mauchly's W	Approx. Chi-Square	df	Sig.	Epsilon[b]		
					Greenhouse-Geisser	Huynh-Feldt	Lower-bound
System	1.000	.000	0	.	1.000	1.000	1.000
Speed	.628	6.504	2	.039	.729	.788	.500
System * Speed	.653	5.973	2	.050	.742	.805	.500

Tests the null hypothesis that the error covariance matrix of the orthonormalized transformed dependent variables is proportional to an identity matrix.

a. Design: Intercept
Within Subjects Design: System + Speed + System * Speed

b. May be used to adjust the degrees of freedom for the averaged tests of significance. Corrected tests are displayed in the Tests of Within-Subjects Effects table.

Tests of Within-Subjects Effects

Measure: MEASURE_1

Source		Type III Sum of Squares	df	Mean Square	F	Sig.	Partial Eta Squared
System	Sphericity Assumed	3.008	1	3.008	342.120	.000	.958
	Greenhouse-Geisser	3.008	1.000	3.008	342.120	.000	.958
	Huynh-Feldt	3.008	1.000	3.008	342.120	.000	.958
	Lower-bound	3.008	1.000	3.008	342.120	.000	.958
Error(System)	Sphericity Assumed	.132	15	.009			
	Greenhouse-Geisser	.132	15.000	.009			
	Huynh-Feldt	.132	15.000	.009			
	Lower-bound	.132	15.000	.009			
Speed	Sphericity Assumed	1.632	2	.816	87.174	.000	.853
	Greenhouse-Geisser	1.632	1.458	1.119	87.174	.000	.853
	Huynh-Feldt	1.632	1.575	1.036	87.174	.000	.853
	Lower-bound	1.632	1.000	1.632	87.174	.000	.853
Error(Speed)	Sphericity Assumed	.281	30	.009			
	Greenhouse-Geisser	.281	21.873	.013			
	Huynh-Feldt	.281	23.628	.012			
	Lower-bound	.281	15.000	.019			
System * Speed	Sphericity Assumed	.086	2	.043	9.870	.001	.397
	Greenhouse-Geisser	.086	1.484	.058	9.870	.002	.397
	Huynh-Feldt	.086	1.609	.054	9.870	.001	.397
	Lower-bound	.086	1.000	.086	9.870	.007	.397
Error(System*Speed)	Sphericity Assumed	.131	30	.004			
	Greenhouse-Geisser	.131	22.267	.006			
	Huynh-Feldt	.131	24.140	.005			
	Lower-bound	.131	15.000	.009			

Tests of Within-Subjects Contrasts

Measure: MEASURE_1

Source	System	Speed	Type III Sum of Squares	df	Mean Square	F	Sig.	Partial Eta Squared
System	Linear		3.008	1	3.008	342.120	.000	.958
Error(System)	Linear		.132	15	.009			
Speed		Linear	1.626	1	1.626	159.857	.000	.914
		Quadratic	.006	1	.006	.681	.422	.043
Error(Speed)		Linear	.153	15	.010			
		Quadratic	.128	15	.009			
System * Speed	Linear	Linear	.085	1	.085	39.793	.000	.726
		Quadratic	.002	1	.002	.271	.610	.018
Error(System*Speed)	Linear	Linear	.032	15	.002			
		Quadratic	.099	15	.007			

Tests of Between-Subjects Effects

Measure: MEASURE_1
Transformed Variable: Average

Source	Type III Sum of Squares	df	Mean Square	F	Sig.	Partial Eta Squared
Intercept	60.347	1	60.347	606.678	.000	.976
Error	1.492	15	.099			

Estimated Marginal Means

1. Grand Mean

Measure: MEASURE_1

Mean	Std. Error	95% Confidence Interval	
		Lower Bound	Upper Bound
-.793	.032	-.861	-.724

2. System

Estimates

Measure: MEASURE_1

System	Mean	Std. Error	95% Confidence Interval	
			Lower Bound	Upper Bound
1	-.616	.025	-.670	-.562
2	-.970	.040	-1.055	-.884

Pairwise Comparisons

Measure: MEASURE_1

(I) System	(J) System	Mean Difference (I-J)	Std. Error	Sig.[b]	95% Confidence Interval for Difference[b]	
					Lower Bound	Upper Bound
1	2	.354*	.019	.000	.313	.395
2	1	-.354*	.019	.000	-.395	-.313

Based on estimated marginal means

*. The mean difference is significant at the .05 level.

b. Adjustment for multiple comparisons: Least Significant Difference (equivalent to no adjustments).

Multivariate Tests

	Value	F	Hypothesis df	Error df	Sig.	Partial Eta Squared
Pillai's trace	.958	342.120[a]	1.000	15.000	.000	.958
Wilks' lambda	.042	342.120[a]	1.000	15.000	.000	.958
Hotelling's trace	22.808	342.120[a]	1.000	15.000	.000	.958
Roy's largest root	22.808	342.120[a]	1.000	15.000	.000	.958

Each F tests the multivariate effect of System. These tests are based on the linearly independent pairwise comparisons among the estimated marginal means.

a. Exact statistic

3. Speed

Estimates

Measure: MEASURE_1

Speed	Mean	Std. Error	95% Confidence Interval Lower Bound	Upper Bound
1	-.639	.029	-.700	-.578
2	-.782	.030	-.847	-.717
3	-.958	.044	-1.052	-.863

Pairwise Comparisons

Measure: MEASURE_1

(I) Speed	(J) Speed	Mean Difference (I-J)	Std. Error	Sig.[b]	95% Confidence Interval for Difference[b] Lower Bound	Upper Bound
1	2	.143*	.016	.000	.109	.177
	3	.319*	.025	.000	.265	.373
2	1	-.143*	.016	.000	-.177	-.109
	3	.176*	.029	.000	.113	.239
3	1	-.319*	.025	.000	-.373	-.265
	2	-.176*	.029	.000	-.239	-.113

Based on estimated marginal means

*. The mean difference is significant at the .05 level.

b. Adjustment for multiple comparisons: Least Significant Difference (equivalent to no adjustments).

Multivariate Tests

	Value	F	Hypothesis df	Error df	Sig.	Partial Eta Squared
Pillai's trace	.940	109.005[a]	2.000	14.000	.000	.940
Wilks' lambda	.060	109.005[a]	2.000	14.000	.000	.940
Hotelling's trace	15.572	109.005[a]	2.000	14.000	.000	.940
Roy's largest root	15.572	109.005[a]	2.000	14.000	.000	.940

Each F tests the multivariate effect of Speed. These tests are based on the linearly independent pairwise comparisons among the estimated marginal means.

a. Exact statistic

4. System * Speed

Measure: MEASURE_1

System	Speed	Mean	Std. Error	95% Confidence Interval Lower Bound	Upper Bound
1	1	-.495	.023	-.543	-.447
	2	-.611	.026	-.667	-.555
	3	-.741	.031	-.808	-.674
2	1	-.783	.036	-.859	-.707
	2	-.953	.040	-1.038	-.867
	3	-1.174	.059	-1.299	-1.049

Profile Plots

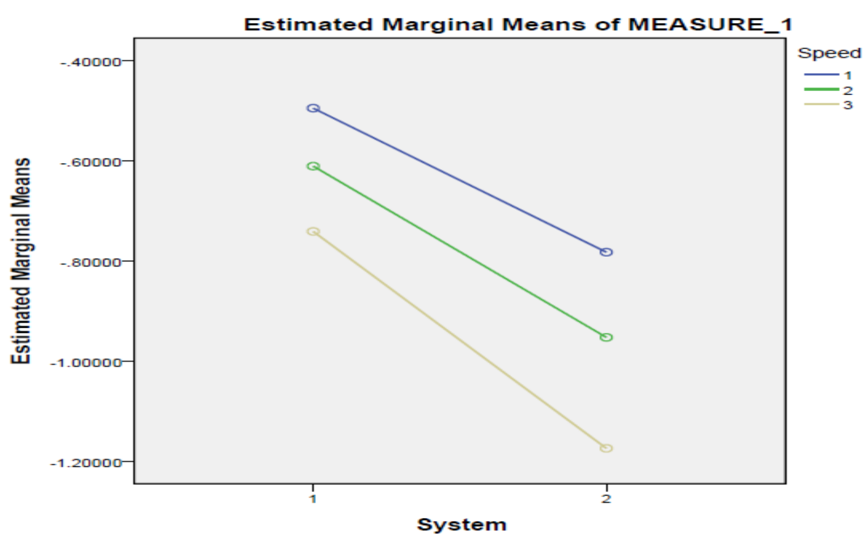

Hip Joint

```
GLM HM_1_M_5 HM_1_M_65 HM_1_M_8 HM_1_ML_5 HM_1_ML_65 HM_1_ML_8
  /WSFACTOR=System 2 Polynomial Speed 3 Polynomial
  /METHOD=SSTYPE(3)
  /PLOT=PROFILE(System*Speed)
  /EMMEANS=TABLES(OVERALL)
  /EMMEANS=TABLES(System) COMPARE ADJ(LSD)
  /EMMEANS=TABLES(Speed) COMPARE ADJ(LSD)
  /EMMEANS=TABLES(System*Speed)
  /PRINT=DESCRIPTIVE ETASQ
  /CRITERIA=ALPHA(.05)
  /WSDESIGN=System Speed System*Speed.
```

General Linear Model

```
[DataSet1] D:\desktop\layout.sav
```

Within-Subjects Factors

Measure: MEASURE_1

System	Speed	Dependent Variable
1	1	HM_1_M_5
	2	HM_1_M_65
	3	HM_1_M_8
2	1	HM_1_ML_5
	2	HM_1_ML_65
	3	HM_1_ML_8

Descriptive Statistics

	Mean	Std. Deviation	N
HM_1_M_5	-1.39308619	.484944126	16
HM_1_M_65	-1.7548584	.49018321	16
HM_1_M_8	-2.210762500	.6484364286	16
HM_1_ML_5	-1.34743588	.429120522	16
HM_1_ML_65	-1.6113832	.49158018	16
HM_1_ML_8	-2.03512906	.694512907	16

Multivariate Tests[a]

Effect		Value	F	Hypothesis df	Error df	Sig.
System	Pillai's Trace	.107	1.788[b]	1.000	15.000	.201
	Wilks' Lambda	.893	1.788[b]	1.000	15.000	.201
	Hotelling's Trace	.119	1.788[b]	1.000	15.000	.201
	Roy's Largest Root	.119	1.788[b]	1.000	15.000	.201
Speed	Pillai's Trace	.736	19.493[b]	2.000	14.000	.000
	Wilks' Lambda	.264	19.493[b]	2.000	14.000	.000
	Hotelling's Trace	2.785	19.493[b]	2.000	14.000	.000
	Roy's Largest Root	2.785	19.493[b]	2.000	14.000	.000
System * Speed	Pillai's Trace	.230	2.087[b]	2.000	14.000	.161
	Wilks' Lambda	.770	2.087[b]	2.000	14.000	.161
	Hotelling's Trace	.298	2.087[b]	2.000	14.000	.161
	Roy's Largest Root	.298	2.087[b]	2.000	14.000	.161

Multivariate Tests[a]

Effect		Partial Eta Squared
System	Pillai's Trace	.107
	Wilks' Lambda	.107
	Hotelling's Trace	.107
	Roy's Largest Root	.107
Speed	Pillai's Trace	.736
	Wilks' Lambda	.736
	Hotelling's Trace	.736
	Roy's Largest Root	.736
System * Speed	Pillai's Trace	.230
	Wilks' Lambda	.230
	Hotelling's Trace	.230
	Roy's Largest Root	.230

a. Design: Intercept
Within Subjects Design: System + Speed + System * Speed

b. Exact statistic

Mauchly's Test of Sphericity[a]

Measure: MEASURE_1

Within Subjects Effect	Mauchly's W	Approx. Chi-Square	df	Sig.	Epsilon[b]
					Greenhouse-Geisser
System	1.000	.000	0	.	1.000
Speed	.319	15.993	2	.000	.595
System * Speed	.826	2.676	2	.262	.852

Mauchly's Test of Sphericity[a]

Measure: MEASURE_1

Within Subjects Effect	Epsilon[b]	
	Huynh-Feldt	Lower-bound
System	1.000	1.000
Speed	.617	.500
System * Speed	.950	.500

Tests the null hypothesis that the error covariance matrix of the orthonormalized transformed dependent variables is proportional to an identity matrix.

a. Design: Intercept
Within Subjects Design: System + Speed + System * Speed

b. May be used to adjust the degrees of freedom for the averaged tests of significance. Corrected tests are displayed in the Tests of Within-Subjects Effects table.

Tests of Within-Subjects Effects

Measure: MEASURE_1

Source		Type III Sum of Squares	df	Mean Square	F
System	Sphericity Assumed	.355	1	.355	1.788
	Greenhouse-Geisser	.355	1.000	.355	1.788
	Huynh-Feldt	.355	1.000	.355	1.788
	Lower-bound	.355	1.000	.355	1.788
Error(System)	Sphericity Assumed	2.976	15	.198	
	Greenhouse-Geisser	2.976	15.000	.198	
	Huynh-Feldt	2.976	15.000	.198	
	Lower-bound	2.976	15.000	.198	
Speed	Sphericity Assumed	9.151	2	4.575	33.419
	Greenhouse-Geisser	9.151	1.190	7.691	33.419
	Huynh-Feldt	9.151	1.234	7.417	33.419
	Lower-bound	9.151	1.000	9.151	33.419
Error(Speed)	Sphericity Assumed	4.107	30	.137	
	Greenhouse-Geisser	4.107	17.847	.230	
	Huynh-Feldt	4.107	18.505	.222	
	Lower-bound	4.107	15.000	.274	
System * Speed	Sphericity Assumed	.073	2	.037	1.953
	Greenhouse-Geisser	.073	1.704	.043	1.953
	Huynh-Feldt	.073	1.900	.039	1.953
	Lower-bound	.073	1.000	.073	1.953
Error(System*Speed)	Sphericity Assumed	.563	30	.019	
	Greenhouse-Geisser	.563	25.553	.022	
	Huynh-Feldt	.563	28.493	.020	
	Lower-bound	.563	15.000	.038	

Tests of Within-Subjects Effects

Measure: MEASURE_1

Source		Sig.	Partial Eta Squared
System	Sphericity Assumed	.201	.107
	Greenhouse-Geisser	.201	.107
	Huynh-Feldt	.201	.107
	Lower-bound	.201	.107
Error(System)	Sphericity Assumed		
	Greenhouse-Geisser		
	Huynh-Feldt		
	Lower-bound		
Speed	Sphericity Assumed	.000	.690
	Greenhouse-Geisser	.000	.690
	Huynh-Feldt	.000	.690
	Lower-bound	.000	.690
Error(Speed)	Sphericity Assumed		
	Greenhouse-Geisser		
	Huynh-Feldt		
	Lower-bound		
System * Speed	Sphericity Assumed	.159	.115
	Greenhouse-Geisser	.167	.115
	Huynh-Feldt	.162	.115
	Lower-bound	.183	.115
Error(System*Speed)	Sphericity Assumed		
	Greenhouse-Geisser		
	Huynh-Feldt		
	Lower-bound		

Tests of Within-Subjects Contrasts

Measure: MEASURE_1

Source	System	Speed	Type III Sum of Squares	df	Mean Square	F
System	Linear		.355	1	.355	1.788
Error(System)	Linear		2.976	15	.198	
Speed		Linear	9.065	1	9.065	37.900
		Quadratic	.086	1	.086	2.482
Error(Speed)		Linear	3.588	15	.239	
		Quadratic	.520	15	.035	
System * Speed	Linear	Linear	.068	1	.068	2.839
		Quadratic	.006	1	.006	.418
Error(System*Speed)	Linear	Linear	.357	15	.024	
		Quadratic	.206	15	.014	

Tests of Within-Subjects Contrasts

Measure: MEASURE_1

Source	System	Speed	Sig.	Partial Eta Squared
System	Linear		.201	.107
Error(System)	Linear			
Speed		Linear	.000	.716
		Quadratic	.136	.142
Error(Speed)		Linear		
		Quadratic		
System * Speed	Linear	Linear	.113	.159
		Quadratic	.527	.027
Error(System*Speed)	Linear	Linear		
		Quadratic		

Tests of Between-Subjects Effects

Measure: MEASURE_1
Transformed Variable: Average

Source	Type III Sum of Squares	df	Mean Square	F	Sig.	Partial Eta Squared
Intercept	285.807	1	285.807	220.823	.000	.936
Error	19.414	15	1.294			

Estimated Marginal Means

1. Grand Mean

Measure: MEASURE_1

Mean	Std. Error	95% Confidence Interval	
		Lower Bound	Upper Bound
-1.725	.116	-1.973	-1.478

2. System

Estimates

Measure: MEASURE_1

System	Mean	Std. Error	95% Confidence Interval	
			Lower Bound	Upper Bound
1	-1.786	.123	-2.049	-1.523
2	-1.665	.126	-1.933	-1.396

Pairwise Comparisons

Measure: MEASURE_1

(I) System	(J) System	Mean Difference (I-J)	Std. Error	Sig.[a]	95% Confidence Interval for Difference[a]	
					Lower Bound	Upper Bound
1	2	-.122	.091	.201	-.315	.072
2	1	.122	.091	.201	-.072	.315

Based on estimated marginal means

a. Adjustment for multiple comparisons: Least Significant Difference (equivalent to no adjustments).

Multivariate Tests

	Value	F	Hypothesis df	Error df	Sig.	Partial Eta Squared
Pillai's trace	.107	1.788[a]	1.000	15.000	.201	.107
Wilks' lambda	.893	1.788[a]	1.000	15.000	.201	.107
Hotelling's trace	.119	1.788[a]	1.000	15.000	.201	.107
Roy's largest root	.119	1.788[a]	1.000	15.000	.201	.107

Each F tests the multivariate effect of System. These tests are based on the linearly independent pairwise comparisons among the estimated marginal means.

a. Exact statistic

3. Speed

Estimates

Measure: MEASURE_1

Speed	Mean	Std. Error	95% Confidence Interval	
			Lower Bound	Upper Bound
1	-1.370	.108	-1.600	-1.141
2	-1.683	.113	-1.925	-1.442
3	-2.123	.157	-2.457	-1.789

Pairwise Comparisons

Measure: MEASURE_1

(I) Speed	(J) Speed	Mean Difference (I-J)	Std. Error	Sig.[b]	95% Confidence Interval for Difference[b]	
					Lower Bound	Upper Bound
1	2	.313*	.053	.000	.201	.425
	3	.753*	.122	.000	.492	1.013
2	1	-.313*	.053	.000	-.425	-.201
	3	.440*	.089	.000	.250	.630
3	1	-.753*	.122	.000	-1.013	-.492
	2	-.440*	.089	.000	-.630	-.250

Based on estimated marginal means

*. The mean difference is significant at the .05 level.

b. Adjustment for multiple comparisons: Least Significant Difference (equivalent to no adjustments).

Multivariate Tests

	Value	F	Hypothesis df	Error df	Sig.	Partial Eta Squared
Pillai's trace	.736	19.493[a]	2.000	14.000	.000	.736
Wilks' lambda	.264	19.493[a]	2.000	14.000	.000	.736
Hotelling's trace	2.785	19.493[a]	2.000	14.000	.000	.736
Roy's largest root	2.785	19.493[a]	2.000	14.000	.000	.736

Each F tests the multivariate effect of Speed. These tests are based on the linearly independent pairwise comparisons among the estimated marginal means.

a. Exact statistic

4. System * Speed

Measure: MEASURE_1

System	Speed	Mean	Std. Error	95% Confidence Interval	
				Lower Bound	Upper Bound
1	1	-1.393	.121	-1.651	-1.135
	2	-1.755	.123	-2.016	-1.494
	3	-2.211	.162	-2.556	-1.865
2	1	-1.347	.107	-1.576	-1.119
	2	-1.611	.123	-1.873	-1.349
	3	-2.035	.174	-2.405	-1.665

Profile Plots

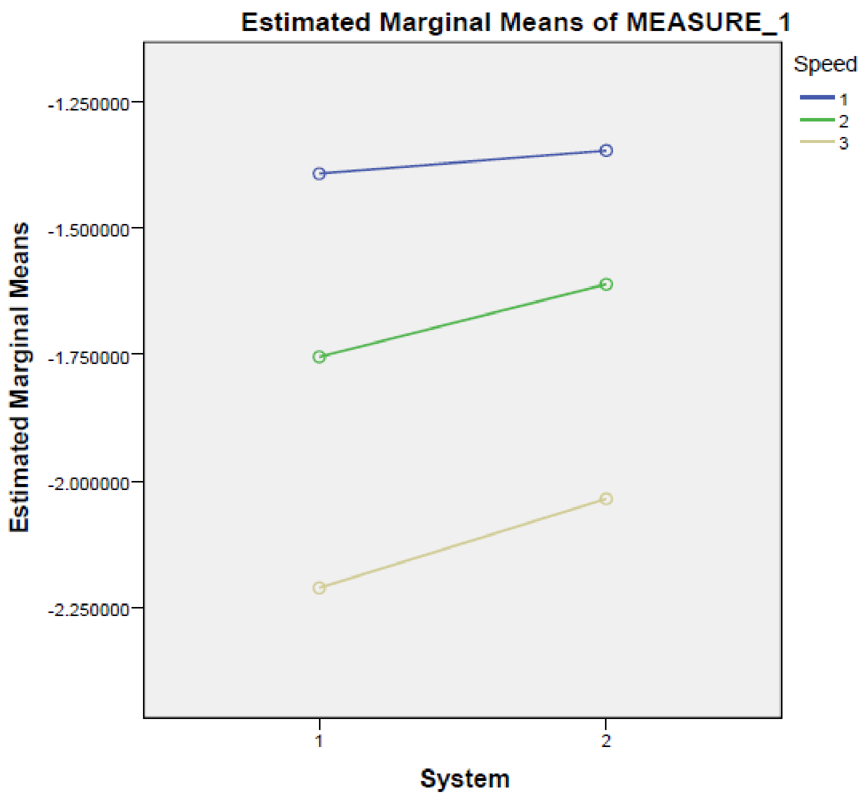

General Linear Model

Within-Subjects Factors

Measure: MEASURE_1

System	Speed	Dependent Variable
1	1	HM_1_T_M_5
	2	HM_1_T_M_65
	3	HM_1_T_M_8
2	1	HM_1_T_ML_5
	2	HM_1_T_ML_65
	3	HM_1_T_ML_8

Descriptive Statistics

	Mean	Std. Deviation	N
HM_1_T_M_5	5.2062500	1.84263172	16
HM_1_T_M_65	3.40625000	.387244539	16
HM_1_T_M_8	3.32500000	.612644541	16
HM_1_T_ML_5	3.62500000	.549545267	16
HM_1_T_ML_65	4.88125000	2.000072915	16
HM_1_T_ML_8	4.59375000	1.654677713	16

Multivariate Tests[a]

Effect		Value	F	Hypothesis df	Error df	Sig.
System	Pillai's Trace	.173	3.140[b]	1.000	15.000	.097
	Wilks' Lambda	.827	3.140[b]	1.000	15.000	.097
	Hotelling's Trace	.209	3.140[b]	1.000	15.000	.097
	Roy's Largest Root	.209	3.140[b]	1.000	15.000	.097
Speed	Pillai's Trace	.157	1.301[b]	2.000	14.000	.303
	Wilks' Lambda	.843	1.301[b]	2.000	14.000	.303
	Hotelling's Trace	.186	1.301[b]	2.000	14.000	.303
	Roy's Largest Root	.186	1.301[b]	2.000	14.000	.303
System * Speed	Pillai's Trace	.614	11.121[b]	2.000	14.000	.001
	Wilks' Lambda	.386	11.121[b]	2.000	14.000	.001
	Hotelling's Trace	1.589	11.121[b]	2.000	14.000	.001
	Roy's Largest Root	1.589	11.121[b]	2.000	14.000	.001

Multivariate Tests[a]

Effect		Partial Eta Squared
System	Pillai's Trace	.173
	Wilks' Lambda	.173
	Hotelling's Trace	.173
	Roy's Largest Root	.173
Speed	Pillai's Trace	.157
	Wilks' Lambda	.157
	Hotelling's Trace	.157
	Roy's Largest Root	.157
System * Speed	Pillai's Trace	.614
	Wilks' Lambda	.614
	Hotelling's Trace	.614
	Roy's Largest Root	.614

a. Design: Intercept
Within Subjects Design: System + Speed + System * Speed

b. Exact statistic

Mauchly's Test of Sphericity[a]

Measure: MEASURE_1

Within Subjects Effect	Mauchly's W	Approx. Chi-Square	df	Sig.	Epsilon[b] Greenhouse-Geisser
System	1.000	.000	0	.	1.000
Speed	.961	.562	2	.755	.962
System * Speed	1.000	.003	2	.999	1.000

Mauchly's Test of Sphericity[a]

Measure: MEASURE_1

Within Subjects Effect	Epsilon[b]	
	Huynh-Feldt	Lower-bound
System	1.000	1.000
Speed	1.000	.500
System * Speed	1.000	.500

Tests the null hypothesis that the error covariance matrix of the orthonormalized transformed dependent variables is proportional to an identity matrix.

a. Design: Intercept
Within Subjects Design: System + Speed + System * Speed

b. May be used to adjust the degrees of freedom for the averaged tests of significance. Corrected tests are displayed in the Tests of Within-Subjects Effects table.

Tests of Within-Subjects Effects

Measure: MEASURE_1

Source		Type III Sum of Squares	df	Mean Square	F
System	Sphericity Assumed	3.604	1	3.604	3.140
	Greenhouse-Geisser	3.604	1.000	3.604	3.140
	Huynh-Feldt	3.604	1.000	3.604	3.140
	Lower-bound	3.604	1.000	3.604	3.140
Error(System)	Sphericity Assumed	17.216	15	1.148	
	Greenhouse-Geisser	17.216	15.000	1.148	
	Huynh-Feldt	17.216	15.000	1.148	
	Lower-bound	17.216	15.000	1.148	
Speed	Sphericity Assumed	3.371	2	1.686	1.121
	Greenhouse-Geisser	3.371	1.924	1.752	1.121
	Huynh-Feldt	3.371	2.000	1.686	1.121
	Lower-bound	3.371	1.000	3.371	1.121
Error(Speed)	Sphericity Assumed	45.132	30	1.504	
	Greenhouse-Geisser	45.132	28.864	1.564	
	Huynh-Feldt	45.132	30.000	1.504	
	Lower-bound	45.132	15.000	3.009	
System * Speed	Sphericity Assumed	46.682	2	23.341	11.964
	Greenhouse-Geisser	46.682	2.000	23.346	11.964
	Huynh-Feldt	46.682	2.000	23.341	11.964
	Lower-bound	46.682	1.000	46.682	11.964
Error(System*Speed)	Sphericity Assumed	58.528	30	1.951	
	Greenhouse-Geisser	58.528	29.994	1.951	
	Huynh-Feldt	58.528	30.000	1.951	
	Lower-bound	58.528	15.000	3.902	

Tests of Within-Subjects Effects

Measure: MEASURE_1

Source		Sig.	Partial Eta Squared
System	Sphericity Assumed	.097	.173
	Greenhouse-Geisser	.097	.173
	Huynh-Feldt	.097	.173
	Lower-bound	.097	.173
Error(System)	Sphericity Assumed		
	Greenhouse-Geisser		
	Huynh-Feldt		
	Lower-bound		
Speed	Sphericity Assumed	.339	.070
	Greenhouse-Geisser	.338	.070
	Huynh-Feldt	.339	.070
	Lower-bound	.307	.070
Error(Speed)	Sphericity Assumed		
	Greenhouse-Geisser		
	Huynh-Feldt		
	Lower-bound		
System * Speed	Sphericity Assumed	.000	.444
	Greenhouse-Geisser	.000	.444
	Huynh-Feldt	.000	.444
	Lower-bound	.004	.444
Error(System*Speed)	Sphericity Assumed		
	Greenhouse-Geisser		
	Huynh-Feldt		
	Lower-bound		

Tests of Within-Subjects Contrasts

Measure: MEASURE_1

Source	System	Speed	Type III Sum of Squares	df	Mean Square	F
System	Linear		3.604	1	3.604	3.140
Error(System)	Linear		17.216	15	1.148	
Speed		Linear	3.331	1	3.331	2.705
		Quadratic	.041	1	.041	.023
Error(Speed)		Linear	18.469	15	1.231	
		Quadratic	26.662	15	1.777	
System * Speed	Linear	Linear	32.490	1	32.490	16.420
		Quadratic	14.192	1	14.192	7.379
Error(System*Speed)	Linear	Linear	29.680	15	1.979	
		Quadratic	28.848	15	1.923	

Tests of Within-Subjects Contrasts

Measure: MEASURE_1

Source	System	Speed	Sig.	Partial Eta Squared
System	Linear		.097	.173
Error(System)	Linear			
Speed		Linear	.121	.153
		Quadratic	.882	.002
Error(Speed)		Linear		
		Quadratic		
System * Speed	Linear	Linear	.001	.523
		Quadratic	.016	.330
Error(System*Speed)	Linear	Linear		
		Quadratic		

Tests of Between-Subjects Effects

Measure: MEASURE_1

Transformed Variable: Average

Source	Type III Sum of Squares	df	Mean Square	F	Sig.	Partial Eta Squared
Intercept	1671.670	1	1671.670	575.958	.000	.975
Error	43.536	15	2.902			

Estimated Marginal Means

1. Grand Mean

Measure: MEASURE_1

Mean	Std. Error	95% Confidence Interval	
		Lower Bound	Upper Bound
4.173	.174	3.802	4.544

2. System

Estimates

Measure: MEASURE_1

System	Mean	Std. Error	95% Confidence Interval	
			Lower Bound	Upper Bound
1	3.979	.180	3.596	4.363
2	4.367	.228	3.881	4.853

Pairwise Comparisons

Measure: MEASURE_1

(I) System	(J) System	Mean Difference (I-J)	Std. Error	Sig.[a]	95% Confidence Interval for Difference[a]	
					Lower Bound	Upper Bound
1	2	-.387	.219	.097	-.854	.079
2	1	.387	.219	.097	-.079	.854

Based on estimated marginal means

a. Adjustment for multiple comparisons: Least Significant Difference (equivalent to no adjustments).

Multivariate Tests

	Value	F	Hypothesis df	Error df	Sig.	Partial Eta Squared
Pillai's trace	.173	3.140[a]	1.000	15.000	.097	.173
Wilks' lambda	.827	3.140[a]	1.000	15.000	.097	.173
Hotelling's trace	.209	3.140[a]	1.000	15.000	.097	.173
Roy's largest root	.209	3.140[a]	1.000	15.000	.097	.173

Each F tests the multivariate effect of System. These tests are based on the linearly independent pairwise comparisons among the estimated marginal means.

a. Exact statistic

3. Speed

Estimates

Measure: MEASURE_1

Speed	Mean	Std. Error	95% Confidence Interval	
			Lower Bound	Upper Bound
1	4.416	.252	3.879	4.953
2	4.144	.269	3.571	4.717
3	3.959	.221	3.487	4.431

Pairwise Comparisons

Measure: MEASURE_1

(I) Speed	(J) Speed	Mean Difference (I-J)	Std. Error	Sig.[a]	95% Confidence Interval for Difference[a]	
					Lower Bound	Upper Bound
1	2	.272	.310	.394	-.389	.932
	3	.456	.277	.121	-.135	1.048
2	1	-.272	.310	.394	-.932	.389
	3	.184	.330	.585	-.520	.888
3	1	-.456	.277	.121	-1.048	.135
	2	-.184	.330	.585	-.888	.520

Based on estimated marginal means

a. Adjustment for multiple comparisons: Least Significant Difference (equivalent to no adjustments).

Multivariate Tests

	Value	F	Hypothesis df	Error df	Sig.	Partial Eta Squared
Pillai's trace	.157	1.301[a]	2.000	14.000	.303	.157
Wilks' lambda	.843	1.301[a]	2.000	14.000	.303	.157
Hotelling's trace	.186	1.301[a]	2.000	14.000	.303	.157
Roy's largest root	.186	1.301[a]	2.000	14.000	.303	.157

Each F tests the multivariate effect of Speed. These tests are based on the linearly independent pairwise comparisons among the estimated marginal means.

a. Exact statistic

4. System * Speed

Measure: MEASURE_1

System	Speed	Mean	Std. Error	95% Confidence Interval Lower Bound	95% Confidence Interval Upper Bound
1	1	5.206	.461	4.224	6.188
	2	3.406	.097	3.200	3.613
	3	3.325	.153	2.999	3.651
2	1	3.625	.137	3.332	3.918
	2	4.881	.500	3.815	5.947
	3	4.594	.414	3.712	5.475

Profile Plots

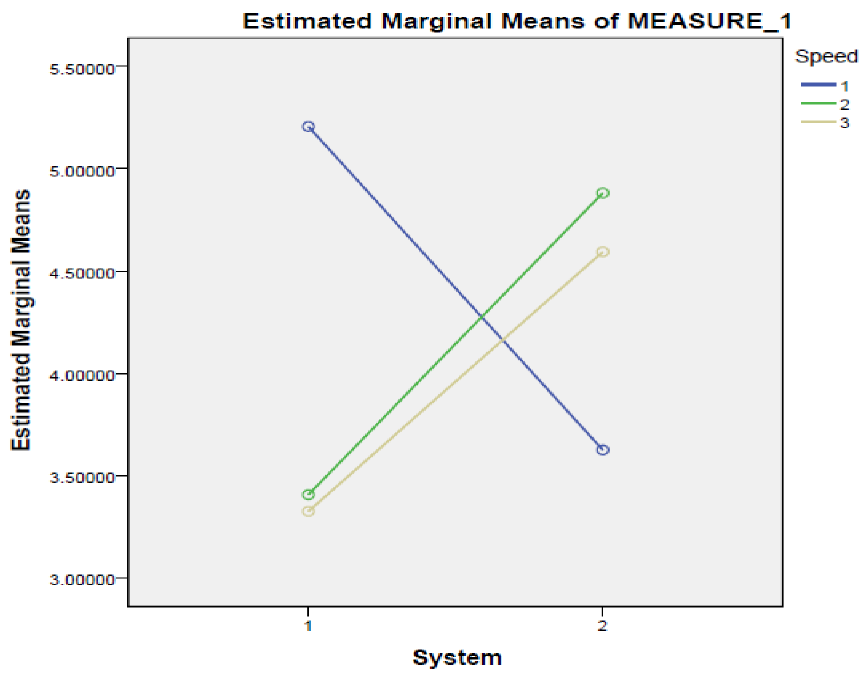

General Linear Model

Within-Subjects Factors

Measure: MEASURE_1

System	Speed	Dependent Variable
1	1	HM_2_M_5
	2	HM_2_M_65
	3	HM_2_M_8
2	1	HM_2_ML_5
	2	HM_2_ML_65
	3	HM_2_ML_8

Descriptive Statistics

	Mean	Std. Deviation	N
HM_2_M_5	.82340838	.193084207	16
HM_2_M_65	1.01161600	.233827433	16
HM_2_M_8	1.4443929	.23196142	16
HM_2_ML_5	1.0626492	.17029565	16
HM_2_ML_65	1.2299021	.29448010	16
HM_2_ML_8	1.7624770	.23893185	16

Multivariate Tests[a]

Effect		Value	F	Hypothesis df	Error df	Sig.	Partial Eta Squared
System	Pillai's Trace	.878	108.365[b]	1.000	15.000	.000	.878
	Wilks' Lambda	.122	108.365[b]	1.000	15.000	.000	.878
	Hotelling's Trace	7.224	108.365[b]	1.000	15.000	.000	.878
	Roy's Largest Root	7.224	108.365[b]	1.000	15.000	.000	.878
Speed	Pillai's Trace	.954	146.721[b]	2.000	14.000	.000	.954
	Wilks' Lambda	.046	146.721[b]	2.000	14.000	.000	.954
	Hotelling's Trace	20.960	146.721[b]	2.000	14.000	.000	.954
	Roy's Largest Root	20.960	146.721[b]	2.000	14.000	.000	.954
System * Speed	Pillai's Trace	.129	1.040[b]	2.000	14.000	.379	.129
	Wilks' Lambda	.871	1.040[b]	2.000	14.000	.379	.129
	Hotelling's Trace	.149	1.040[b]	2.000	14.000	.379	.129
	Roy's Largest Root	.149	1.040[b]	2.000	14.000	.379	.129

a. Design: Intercept
Within Subjects Design: System + Speed + System * Speed

b. Exact statistic

Mauchly's Test of Sphericity[a]

Measure: MEASURE_1

Within Subjects Effect	Mauchly's W	Approx. Chi-Square	df	Sig.	Epsilon[b] Greenhouse-Geisser	Epsilon[b] Huynh-Feldt	Epsilon[b] Lower-bound
System	1.000	.000	0	.	1.000	1.000	1.000
Speed	.712	4.759	2	.093	.776	.849	.500
System * Speed	.659	5.838	2	.054	.746	.809	.500

Tests the null hypothesis that the error covariance matrix of the orthonormalized transformed dependent variables is proportional to an identity matrix.

a. Design: Intercept
Within Subjects Design: System + Speed + System * Speed

b. May be used to adjust the degrees of freedom for the averaged tests of significance. Corrected tests are displayed in the Tests of Within-Subjects Effects table.

Tests of Within-Subjects Effects

Measure: MEASURE_1

Source		Type III Sum of Squares	df	Mean Square	F
System	Sphericity Assumed	1.604	1	1.604	108.365
	Greenhouse-Geisser	1.604	1.000	1.604	108.365
	Huynh-Feldt	1.604	1.000	1.604	108.365
	Lower-bound	1.604	1.000	1.604	108.365
Error(System)	Sphericity Assumed	.222	15	.015	
	Greenhouse-Geisser	.222	15.000	.015	
	Huynh-Feldt	.222	15.000	.015	
	Lower-bound	.222	15.000	.015	
Speed	Sphericity Assumed	7.474	2	3.737	116.766
	Greenhouse-Geisser	7.474	1.553	4.814	116.766
	Huynh-Feldt	7.474	1.699	4.400	116.766
	Lower-bound	7.474	1.000	7.474	116.766
Error(Speed)	Sphericity Assumed	.960	30	.032	
	Greenhouse-Geisser	.960	23.288	.041	
	Huynh-Feldt	.960	25.478	.038	
	Lower-bound	.960	15.000	.064	
System * Speed	Sphericity Assumed	.044	2	.022	1.223
	Greenhouse-Geisser	.044	1.491	.030	1.223
	Huynh-Feldt	.044	1.618	.027	1.223
	Lower-bound	.044	1.000	.044	1.223
Error(System*Speed)	Sphericity Assumed	.543	30	.018	
	Greenhouse-Geisser	.543	22.372	.024	
	Huynh-Feldt	.543	24.277	.022	
	Lower-bound	.543	15.000	.036	

Tests of Within-Subjects Effects

Measure: MEASURE_1

Source		Sig.	Partial Eta Squared
System	Sphericity Assumed	.000	.878
	Greenhouse-Geisser	.000	.878
	Huynh-Feldt	.000	.878
	Lower-bound	.000	.878
Error(System)	Sphericity Assumed		
	Greenhouse-Geisser		
	Huynh-Feldt		
	Lower-bound		
Speed	Sphericity Assumed	.000	.886
	Greenhouse-Geisser	.000	.886
	Huynh-Feldt	.000	.886
	Lower-bound	.000	.886
Error(Speed)	Sphericity Assumed		
	Greenhouse-Geisser		
	Huynh-Feldt		
	Lower-bound		
System * Speed	Sphericity Assumed	.309	.075
	Greenhouse-Geisser	.301	.075
	Huynh-Feldt	.304	.075
	Lower-bound	.286	.075
Error(System*Speed)	Sphericity Assumed		
	Greenhouse-Geisser		
	Huynh-Feldt		
	Lower-bound		

Tests of Within-Subjects Contrasts

Measure: MEASURE_1

Source	System	Speed	Type III Sum of Squares	df	Mean Square	F
System	Linear		1.604	1	1.604	108.365
Error(System)	Linear		.222	15	.015	
Speed		Linear	6.978	1	6.978	283.259
		Quadratic	.496	1	.496	12.596
Error(Speed)		Linear	.370	15	.025	
		Quadratic	.591	15	.039	
System * Speed	Linear	Linear	.025	1	.025	2.192
		Quadratic	.019	1	.019	.781
Error(System*Speed)	Linear	Linear	.170	15	.011	
		Quadratic	.373	15	.025	

Tests of Within-Subjects Contrasts

Measure: MEASURE_1

Source	System	Speed	Sig.	Partial Eta Squared
System	Linear		.000	.878
Error(System)	Linear			
Speed		Linear	.000	.950
		Quadratic	.003	.456
Error(Speed)		Linear		
		Quadratic		
System * Speed	Linear	Linear	.159	.127
		Quadratic	.391	.050
Error(System*Speed)	Linear	Linear		
		Quadratic		

Tests of Between-Subjects Effects

Measure: MEASURE_1

Transformed Variable: Average

Source	Type III Sum of Squares	df	Mean Square	F	Sig.	Partial Eta Squared
Intercept	143.451	1	143.451	704.799	.000	.979
Error	3.053	15	.204			

Estimated Marginal Means

1. Grand Mean

Measure: MEASURE_1

Mean	Std. Error	95% Confidence Interval	
		Lower Bound	Upper Bound
1.222	.046	1.124	1.321

2. System

Estimates

Measure: MEASURE_1

System	Mean	Std. Error	95% Confidence Interval	
			Lower Bound	Upper Bound
1	1.093	.048	.992	1.194
2	1.352	.048	1.250	1.454

Pairwise Comparisons

Measure: MEASURE_1

(I) System	(J) System	Mean Difference (I-J)	Std. Error	Sig.[b]	95% Confidence Interval for Difference[b]	
					Lower Bound	Upper Bound
1	2	-.259*	.025	.000	-.311	-.206
2	1	.259*	.025	.000	.206	.311

Based on estimated marginal means

*. The mean difference is significant at the .05 level.

b. Adjustment for multiple comparisons: Least Significant Difference (equivalent to no adjustments).

Multivariate Tests

	Value	F	Hypothesis df	Error df	Sig.	Partial Eta Squared
Pillai's trace	.878	108.365[a]	1.000	15.000	.000	.878
Wilks' lambda	.122	108.365[a]	1.000	15.000	.000	.878
Hotelling's trace	7.224	108.365[a]	1.000	15.000	.000	.878
Roy's largest root	7.224	108.365[a]	1.000	15.000	.000	.878

Each F tests the multivariate effect of System. These tests are based on the linearly independent pairwise comparisons among the estimated marginal means.

a. Exact statistic

3. Speed

Estimates

Measure: MEASURE_1

Speed	Mean	Std. Error	95% Confidence Interval	
			Lower Bound	Upper Bound
1	.943	.043	.851	1.035
2	1.121	.058	.996	1.245
3	1.603	.055	1.485	1.722

Pairwise Comparisons

Measure: MEASURE_1

(I) Speed	(J) Speed	Mean Difference (I-J)	Std. Error	Sig.[b]	95% Confidence Interval for Difference[b] Lower Bound	Upper Bound
1	2	-.178*	.037	.000	-.257	-.098
	3	-.660*	.039	.000	-.744	-.577
2	1	.178*	.037	.000	.098	.257
	3	-.483*	.055	.000	-.601	-.365
3	1	.660*	.039	.000	.577	.744
	2	.483*	.055	.000	.365	.601

Based on estimated marginal means

*. The mean difference is significant at the .05 level.

b. Adjustment for multiple comparisons: Least Significant Difference (equivalent to no adjustments).

Multivariate Tests

	Value	F	Hypothesis df	Error df	Sig.	Partial Eta Squared
Pillai's trace	.954	146.721[a]	2.000	14.000	.000	.954
Wilks' lambda	.046	146.721[a]	2.000	14.000	.000	.954
Hotelling's trace	20.960	146.721[a]	2.000	14.000	.000	.954
Roy's largest root	20.960	146.721[a]	2.000	14.000	.000	.954

Each F tests the multivariate effect of Speed. These tests are based on the linearly independent pairwise comparisons among the estimated marginal means.

a. Exact statistic

4. System * Speed

Measure: MEASURE_1

System	Speed	Mean	Std. Error	95% Confidence Interval Lower Bound	Upper Bound
1	1	.823	.048	.721	.926
	2	1.012	.058	.887	1.136
	3	1.444	.058	1.321	1.568
2	1	1.063	.043	.972	1.153
	2	1.230	.074	1.073	1.387
	3	1.762	.060	1.635	1.890

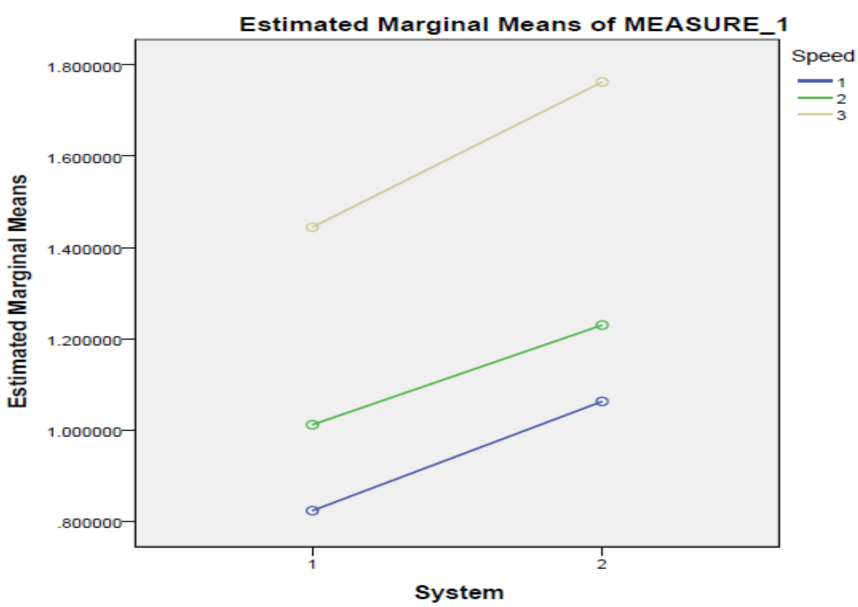

General Linear Model

Within-Subjects Factors

Measure: MEASURE_1

System	Speed	Dependent Variable
1	1	HM_2_T_M_5
	2	HM_2_T_M_65
	3	HM_2_T_M_8
2	1	HM_2_T_ML_5
	2	HM_2_T_ML_65
	3	HM_2_T_ML_8

Descriptive Statistics

	Mean	Std. Deviation	N
HM_2_T_M_5	27.3062500	4.84595622	16
HM_2_T_M_65	28.2937500	5.65195763	16
HM_2_T_M_8	26.0187500	3.88419340	16
HM_2_T_ML_5	34.5500000	4.67232990	16
HM_2_T_ML_65	32.0062500	4.80325844	16
HM_2_T_ML_8	27.9125000	3.46369263	16

Multivariate Tests[a]

Effect		Value	F	Hypothesis df	Error df	Sig.
System	Pillai's Trace	.640	26.695[b]	1.000	15.000	.000
	Wilks' Lambda	.360	26.695[b]	1.000	15.000	.000
	Hotelling's Trace	1.780	26.695[b]	1.000	15.000	.000
	Roy's Largest Root	1.780	26.695[b]	1.000	15.000	.000
Speed	Pillai's Trace	.441	5.532[b]	2.000	14.000	.017
	Wilks' Lambda	.559	5.532[b]	2.000	14.000	.017
	Hotelling's Trace	.790	5.532[b]	2.000	14.000	.017
	Roy's Largest Root	.790	5.532[b]	2.000	14.000	.017
System * Speed	Pillai's Trace	.671	14.283[b]	2.000	14.000	.000
	Wilks' Lambda	.329	14.283[b]	2.000	14.000	.000
	Hotelling's Trace	2.040	14.283[b]	2.000	14.000	.000
	Roy's Largest Root	2.040	14.283[b]	2.000	14.000	.000

Multivariate Tests[a]

Effect		Partial Eta Squared
System	Pillai's Trace	.640
	Wilks' Lambda	.640
	Hotelling's Trace	.640
	Roy's Largest Root	.640
Speed	Pillai's Trace	.441
	Wilks' Lambda	.441
	Hotelling's Trace	.441
	Roy's Largest Root	.441
System * Speed	Pillai's Trace	.671
	Wilks' Lambda	.671
	Hotelling's Trace	.671
	Roy's Largest Root	.671

a. Design: Intercept
Within Subjects Design: System + Speed + System * Speed

b. Exact statistic

Mauchly's Test of Sphericity[a]

Measure: MEASURE_1

Within Subjects Effect	Mauchly's W	Approx. Chi-Square	df	Sig.	Epsilon[b] Greenhouse-Geisser
System	1.000	.000	0	.	1.000
Speed	.971	.413	2	.813	.972
System * Speed	.613	6.845	2	.033	.721

Mauchly's Test of Sphericity[a]

Measure: MEASURE_1

Within Subjects Effect	Epsilon[b]	
	Huynh-Feldt	Lower-bound
System	1.000	1.000
Speed	1.000	.500
System * Speed	.777	.500

Tests the null hypothesis that the error covariance matrix of the orthonormalized transformed dependent variables is proportional to an identity matrix.

a. Design: Intercept
Within Subjects Design: System + Speed + System * Speed

b. May be used to adjust the degrees of freedom for the averaged tests of significance. Corrected tests are displayed in the Tests of Within-Subjects Effects table.

Tests of Within-Subjects Effects

Measure: MEASURE_1

Source		Type III Sum of Squares	df	Mean Square	F
System	Sphericity Assumed	440.327	1	440.327	26.695
	Greenhouse-Geisser	440.327	1.000	440.327	26.695
	Huynh-Feldt	440.327	1.000	440.327	26.695
	Lower-bound	440.327	1.000	440.327	26.695
Error(System)	Sphericity Assumed	247.423	15	16.495	
	Greenhouse-Geisser	247.423	15.000	16.495	
	Huynh-Feldt	247.423	15.000	16.495	
	Lower-bound	247.423	15.000	16.495	
Speed	Sphericity Assumed	282.103	2	141.051	6.915
	Greenhouse-Geisser	282.103	1.944	145.150	6.915
	Huynh-Feldt	282.103	2.000	141.051	6.915
	Lower-bound	282.103	1.000	282.103	6.915
Error(Speed)	Sphericity Assumed	611.907	30	20.397	
	Greenhouse-Geisser	611.907	29.153	20.990	
	Huynh-Feldt	611.907	30.000	20.397	
	Lower-bound	611.907	15.000	40.794	
System * Speed	Sphericity Assumed	118.400	2	59.200	11.216
	Greenhouse-Geisser	118.400	1.442	82.093	11.216
	Huynh-Feldt	118.400	1.555	76.163	11.216
	Lower-bound	118.400	1.000	118.400	11.216
Error(System*Speed)	Sphericity Assumed	158.350	30	5.278	
	Greenhouse-Geisser	158.350	21.634	7.319	
	Huynh-Feldt	158.350	23.318	6.791	
	Lower-bound	158.350	15.000	10.557	

Tests of Within-Subjects Effects

Measure: MEASURE_1

Source		Sig.	Partial Eta Squared
System	Sphericity Assumed	.000	.640
	Greenhouse-Geisser	.000	.640
	Huynh-Feldt	.000	.640
	Lower-bound	.000	.640
Error(System)	Sphericity Assumed		
	Greenhouse-Geisser		
	Huynh-Feldt		
	Lower-bound		
Speed	Sphericity Assumed	.003	.316
	Greenhouse-Geisser	.004	.316
	Huynh-Feldt	.003	.316
	Lower-bound	.019	.316
Error(Speed)	Sphericity Assumed		
	Greenhouse-Geisser		
	Huynh-Feldt		
	Lower-bound		
System * Speed	Sphericity Assumed	.000	.428
	Greenhouse-Geisser	.001	.428
	Huynh-Feldt	.001	.428
	Lower-bound	.004	.428
Error(System*Speed)	Sphericity Assumed		
	Greenhouse-Geisser		
	Huynh-Feldt		
	Lower-bound		

Tests of Within-Subjects Contrasts

Measure: MEASURE_1

Source	System	Speed	Type III Sum of Squares	df	Mean Square	F
System	Linear		440.327	1	440.327	26.695
Error(System)	Linear		247.423	15	16.495	
Speed		Linear	251.222	1	251.222	10.714
		Quadratic	30.880	1	30.880	1.780
Error(Speed)		Linear	351.727	15	23.448	
		Quadratic	260.180	15	17.345	
System * Speed	Linear	Linear	114.490	1	114.490	23.126
		Quadratic	3.910	1	3.910	.698
Error(System*Speed)	Linear	Linear	74.260	15	4.951	
		Quadratic	84.090	15	5.606	

Tests of Within-Subjects Contrasts

Measure: MEASURE_1

Source	System	Speed	Sig.	Partial Eta Squared
System	Linear		.000	.640
Error(System)	Linear			
Speed		Linear	.005	.417
		Quadratic	.202	.106
Error(Speed)		Linear		
		Quadratic		
System * Speed	Linear	Linear	.000	.607
		Quadratic	.417	.044
Error(System*Speed)	Linear	Linear		
		Quadratic		

Tests of Between-Subjects Effects

Measure: MEASURE_1
Transformed Variable: Average

Source	Type III Sum of Squares	df	Mean Square	F	Sig.	Partial Eta Squared
Intercept	82684.820	1	82684.820	1388.060	.000	.989
Error	893.530	15	59.569			

Estimated Marginal Means

1. Grand Mean

Measure: MEASURE_1

Mean	Std. Error	95% Confidence Interval	
		Lower Bound	Upper Bound
29.348	.788	27.669	31.027

2. System

Estimates

Measure: MEASURE_1

System	Mean	Std. Error	95% Confidence Interval	
			Lower Bound	Upper Bound
1	27.206	.923	25.238	29.174
2	31.490	.856	29.666	33.313

Pairwise Comparisons

Measure: MEASURE_1

(I) System	(J) System	Mean Difference (I-J)	Std. Error	Sig.[b]	95% Confidence Interval for Difference[b]	
					Lower Bound	Upper Bound
1	2	-4.283*	.829	.000	-6.050	-2.516
2	1	4.283*	.829	.000	2.516	6.050

Based on estimated marginal means

*. The mean difference is significant at the .05 level.

b. Adjustment for multiple comparisons: Least Significant Difference (equivalent to no adjustments).

Multivariate Tests

	Value	F	Hypothesis df	Error df	Sig.	Partial Eta Squared
Pillai's trace	.640	26.695[a]	1.000	15.000	.000	.640
Wilks' lambda	.360	26.695[a]	1.000	15.000	.000	.640
Hotelling's trace	1.780	26.695[a]	1.000	15.000	.000	.640
Roy's largest root	1.780	26.695[a]	1.000	15.000	.000	.640

Each F tests the multivariate effect of System. These tests are based on the linearly independent pairwise comparisons among the estimated marginal means.

a. Exact statistic

3. Speed

Estimates

Measure: MEASURE_1

Speed	Mean	Std. Error	95% Confidence Interval	
			Lower Bound	Upper Bound
1	30.928	.996	28.804	33.052
2	30.150	1.186	27.622	32.678
3	26.966	.858	25.136	28.795

Pairwise Comparisons

Measure: MEASURE_1

(I) Speed	(J) Speed	Mean Difference (I-J)	Std. Error	Sig.[b]	95% Confidence Interval for Difference[b]	
					Lower Bound	Upper Bound
1	2	.778	1.044	.467	-1.446	3.003
	3	3.963*	1.211	.005	1.382	6.543
2	1	-.778	1.044	.467	-3.003	1.446
	3	3.184*	1.127	.013	.783	5.586
3	1	-3.963*	1.211	.005	-6.543	-1.382
	2	-3.184*	1.127	.013	-5.586	-.783

Based on estimated marginal means

*. The mean difference is significant at the .05 level.

b. Adjustment for multiple comparisons: Least Significant Difference (equivalent to no adjustments).

Multivariate Tests

	Value	F	Hypothesis df	Error df	Sig.	Partial Eta Squared
Pillai's trace	.441	5.532[a]	2.000	14.000	.017	.441
Wilks' lambda	.559	5.532[a]	2.000	14.000	.017	.441
Hotelling's trace	.790	5.532[a]	2.000	14.000	.017	.441
Roy's largest root	.790	5.532[a]	2.000	14.000	.017	.441

Each F tests the multivariate effect of Speed. These tests are based on the linearly independent pairwise comparisons among the estimated marginal means.

a. Exact statistic

4. System * Speed

Measure: MEASURE_1

System	Speed	Mean	Std. Error	95% Confidence Interval	
				Lower Bound	Upper Bound
1	1	27.306	1.211	24.724	29.888
	2	28.294	1.413	25.282	31.305
	3	26.019	.971	23.949	28.088
2	1	34.550	1.168	32.060	37.040
	2	32.006	1.201	29.447	34.566
	3	27.912	.866	26.067	29.758

Profile Plots

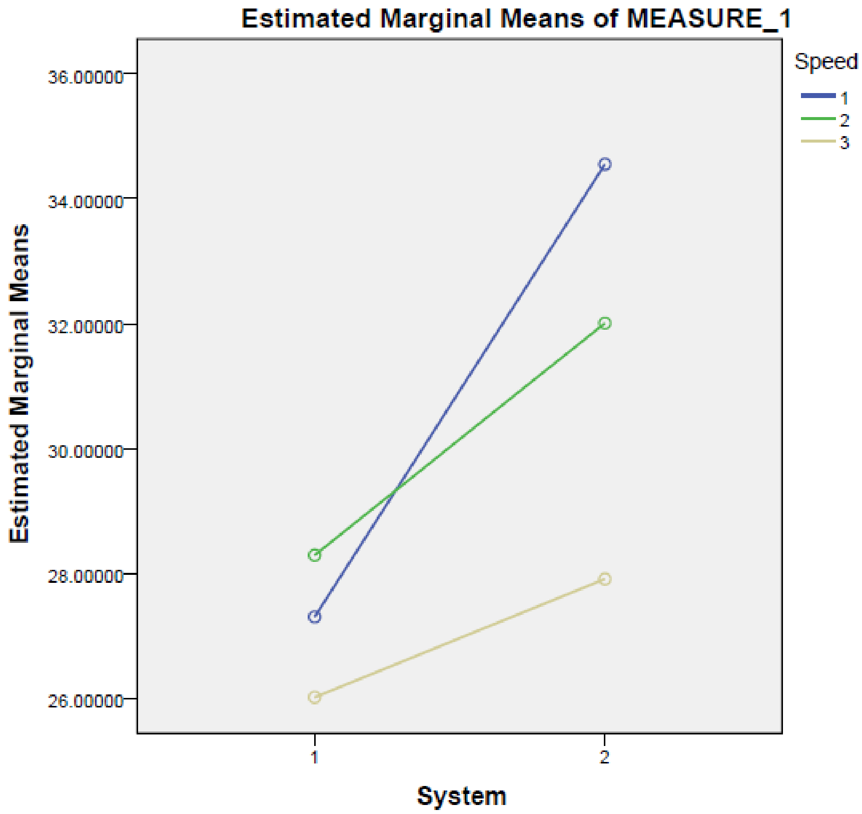

General Linear Model

Within-Subjects Factors

Measure: MEASURE_1

System	Speed	Dependent Variable
1	1	HM_3_M_5
	2	HM_3_M_65
	3	HM_3_M_8
2	1	HM_3_ML_5
	2	HM_3_ML_65
	3	HM_3_ML_8

Descriptive Statistics

	Mean	Std. Deviation	N
HM_3_M_5	-.885155	.1927389	16
HM_3_M_65	-1.1196659	.23102337	16
HM_3_M_8	-1.4179094	.29095781	16
HM_3_ML_5	-1.5020399	.30370353	16
HM_3_ML_65	-1.7274430	.45738559	16
HM_3_ML_8	-2.1424128	.77950861	16

Multivariate Tests[a]

Effect		Value	F	Hypothesis df	Error df	Sig.
System	Pillai's Trace	.870	100.194[b]	1.000	15.000	.000
	Wilks' Lambda	.130	100.194[b]	1.000	15.000	.000
	Hotelling's Trace	6.680	100.194[b]	1.000	15.000	.000
	Roy's Largest Root	6.680	100.194[b]	1.000	15.000	.000
Speed	Pillai's Trace	.803	28.536[b]	2.000	14.000	.000
	Wilks' Lambda	.197	28.536[b]	2.000	14.000	.000
	Hotelling's Trace	4.077	28.536[b]	2.000	14.000	.000
	Roy's Largest Root	4.077	28.536[b]	2.000	14.000	.000
System * Speed	Pillai's Trace	.038	.279[b]	2.000	14.000	.761
	Wilks' Lambda	.962	.279[b]	2.000	14.000	.761
	Hotelling's Trace	.040	.279[b]	2.000	14.000	.761
	Roy's Largest Root	.040	.279[b]	2.000	14.000	.761

Multivariate Tests[a]

Effect		Partial Eta Squared
System	Pillai's Trace	.870
	Wilks' Lambda	.870
	Hotelling's Trace	.870
	Roy's Largest Root	.870
Speed	Pillai's Trace	.803
	Wilks' Lambda	.803
	Hotelling's Trace	.803
	Roy's Largest Root	.803
System * Speed	Pillai's Trace	.038
	Wilks' Lambda	.038
	Hotelling's Trace	.038
	Roy's Largest Root	.038

a. Design: Intercept
Within Subjects Design: System + Speed + System * Speed

b. Exact statistic

Mauchly's Test of Sphericity[a]

Measure: MEASURE_1

Within Subjects Effect	Mauchly's W	Approx. Chi-Square	df	Sig.	Epsilon[b] Greenhouse-Geisser
System	1.000	.000	0	.	1.000
Speed	.423	12.054	2	.002	.634
System * Speed	.674	5.533	2	.063	.754

Mauchly's Test of Sphericity[a]

Measure: MEASURE_1

Within Subjects Effect	Epsilon[b]	
	Huynh-Feldt	Lower-bound
System	1.000	1.000
Speed	.666	.500
System * Speed	.820	.500

Tests the null hypothesis that the error covariance matrix of the orthonormalized transformed dependent variables is proportional to an identity matrix.

a. Design: Intercept
Within Subjects Design: System + Speed + System * Speed

b. May be used to adjust the degrees of freedom for the averaged tests of significance. Corrected tests are displayed in the Tests of Within-Subjects Effects table.

Tests of Within-Subjects Effects

Measure: MEASURE_1

Source		Type III Sum of Squares	df	Mean Square	F
System	Sphericity Assumed	10.131	1	10.131	100.194
	Greenhouse-Geisser	10.131	1.000	10.131	100.194
	Huynh-Feldt	10.131	1.000	10.131	100.194
	Lower-bound	10.131	1.000	10.131	100.194
Error(System)	Sphericity Assumed	1.517	15	.101	
	Greenhouse-Geisser	1.517	15.000	.101	
	Huynh-Feldt	1.517	15.000	.101	
	Lower-bound	1.517	15.000	.101	
Speed	Sphericity Assumed	5.590	2	2.795	19.949
	Greenhouse-Geisser	5.590	1.268	4.409	19.949
	Huynh-Feldt	5.590	1.332	4.198	19.949
	Lower-bound	5.590	1.000	5.590	19.949
Error(Speed)	Sphericity Assumed	4.204	30	.140	
	Greenhouse-Geisser	4.204	19.020	.221	
	Huynh-Feldt	4.204	19.977	.210	
	Lower-bound	4.204	15.000	.280	
System * Speed	Sphericity Assumed	.067	2	.034	.399
	Greenhouse-Geisser	.067	1.508	.045	.399
	Huynh-Feldt	.067	1.640	.041	.399
	Lower-bound	.067	1.000	.067	.399
Error(System*Speed)	Sphericity Assumed	2.536	30	.085	
	Greenhouse-Geisser	2.536	22.617	.112	
	Huynh-Feldt	2.536	24.597	.103	
	Lower-bound	2.536	15.000	.169	

Tests of Within-Subjects Contrasts

Measure: MEASURE_1

Source	System	Speed	Type III Sum of Squares	df	Mean Square	F
System	Linear		10.131	1	10.131	100.194
Error(System)	Linear		1.517	15	.101	
Speed		Linear	5.505	1	5.505	33.407
		Quadratic	.086	1	.086	.741
Error(Speed)		Linear	2.472	15	.165	
		Quadratic	1.732	15	.115	
System * Speed	Linear	Linear	.046	1	.046	.594
		Quadratic	.021	1	.021	.232
Error(System*Speed)	Linear	Linear	1.169	15	.078	
		Quadratic	1.367	15	.091	

Tests of Within-Subjects Contrasts

Measure: MEASURE_1

Source	System	Speed	Sig.	Partial Eta Squared
System	Linear		.000	.870
Error(System)	Linear			
Speed		Linear	.000	.690
		Quadratic	.403	.047
Error(Speed)		Linear		
		Quadratic		
System * Speed	Linear	Linear	.453	.038
		Quadratic	.637	.015
Error(System*Speed)	Linear	Linear		
		Quadratic		

Tests of Between-Subjects Effects

Measure: MEASURE_1

Transformed Variable: Average

Source	Type III Sum of Squares	df	Mean Square	F	Sig.	Partial Eta Squared
Intercept	206.255	1	206.255	386.394	.000	.963
Error	8.007	15	.534			

Estimated Marginal Means

1. Grand Mean

Measure: MEASURE_1

Mean	Std. Error	95% Confidence Interval	
		Lower Bound	Upper Bound
-1.466	.075	-1.625	-1.307

2. System

Estimates

Measure: MEASURE_1

System	Mean	Std. Error	95% Confidence Interval	
			Lower Bound	Upper Bound
1	-1.141	.056	-1.261	-1.021
2	-1.791	.100	-2.004	-1.577

Pairwise Comparisons

Measure: MEASURE_1

(I) System	(J) System	Mean Difference (I-J)	Std. Error	Sig.[b]	95% Confidence Interval for Difference[b]	
					Lower Bound	Upper Bound
1	2	.650*	.065	.000	.511	.788
2	1	-.650*	.065	.000	-.788	-.511

Based on estimated marginal means

*. The mean difference is significant at the .05 level.

b. Adjustment for multiple comparisons: Least Significant Difference (equivalent to no adjustments).

Multivariate Tests

	Value	F	Hypothesis df	Error df	Sig.	Partial Eta Squared
Pillai's trace	.870	100.194[a]	1.000	15.000	.000	.870
Wilks' lambda	.130	100.194[a]	1.000	15.000	.000	.870
Hotelling's trace	6.680	100.194[a]	1.000	15.000	.000	.870
Roy's largest root	6.680	100.194[a]	1.000	15.000	.000	.870

Each F tests the multivariate effect of System. These tests are based on the linearly independent pairwise comparisons among the estimated marginal means.

a. Exact statistic

3. Speed

Estimates

Measure: MEASURE_1

Speed	Mean	Std. Error	95% Confidence Interval	
			Lower Bound	Upper Bound
1	-1.194	.060	-1.322	-1.065
2	-1.424	.075	-1.583	-1.264
3	-1.780	.127	-2.052	-1.509

Pairwise Comparisons

Measure: MEASURE_1

(I) Speed	(J) Speed	Mean Difference (I-J)	Std. Error	Sig.[b]	95% Confidence Interval for Difference[b]	
					Lower Bound	Upper Bound
1	2	.230*	.049	.000	.126	.334
	3	.587*	.101	.000	.370	.803
2	1	-.230*	.049	.000	-.334	-.126
	3	.357*	.117	.008	.108	.605
3	1	-.587*	.101	.000	-.803	-.370
	2	-.357*	.117	.008	-.605	-.108

Based on estimated marginal means

*. The mean difference is significant at the .05 level.

b. Adjustment for multiple comparisons: Least Significant Difference (equivalent to no adjustments).

Multivariate Tests

	Value	F	Hypothesis df	Error df	Sig.	Partial Eta Squared
Pillai's trace	.803	28.536[a]	2.000	14.000	.000	.803
Wilks' lambda	.197	28.536[a]	2.000	14.000	.000	.803
Hotelling's trace	4.077	28.536[a]	2.000	14.000	.000	.803
Roy's largest root	4.077	28.536[a]	2.000	14.000	.000	.803

Each F tests the multivariate effect of Speed. These tests are based on the linearly independent pairwise comparisons among the estimated marginal means.

a. Exact statistic

4. System * Speed

Measure: MEASURE_1

System	Speed	Mean	Std. Error	95% Confidence Interval	
				Lower Bound	Upper Bound
1	1	-.885	.048	-.988	-.782
	2	-1.120	.058	-1.243	-.997
	3	-1.418	.073	-1.573	-1.263
2	1	-1.502	.076	-1.664	-1.340
	2	-1.727	.114	-1.971	-1.484
	3	-2.142	.195	-2.558	-1.727

Profile Plots

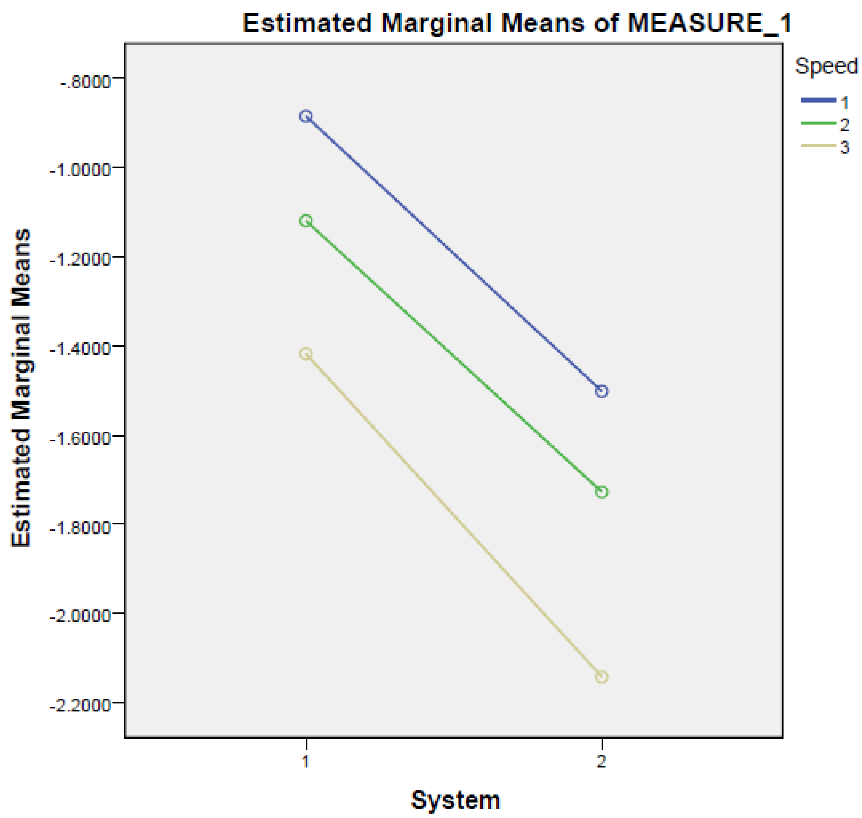

General Linear Model

Within-Subjects Factors

Measure: MEASURE_1

System	Speed	Dependent Variable
1	1	HM_3_T_M_5
	2	HM_3_T_M_65
	3	HM_3_T_M_8
2	1	HM_3_T_ML_5
	2	HM_3_T_ML_65
	3	HM_3_T_ML_8

Descriptive Statistics

	Mean	Std. Deviation	N
HM_3_T_M_5	68.1125000	6.31958596	16
HM_3_T_M_65	64.5187500	6.53495409	16
HM_3_T_M_8	59.73750000	6.719114525	16
HM_3_T_ML_5	69.1187500	5.88288124	16
HM_3_T_ML_65	65.6437500	5.95896733	16
HM_3_T_ML_8	60.2187500	5.93960927	16

Multivariate Tests[a]

Effect		Value	F	Hypothesis df	Error df	Sig.
System	Pillai's Trace	.221	4.262[b]	1.000	15.000	.057
	Wilks' Lambda	.779	4.262[b]	1.000	15.000	.057
	Hotelling's Trace	.284	4.262[b]	1.000	15.000	.057
	Roy's Largest Root	.284	4.262[b]	1.000	15.000	.057
Speed	Pillai's Trace	.821	32.187[b]	2.000	14.000	.000
	Wilks' Lambda	.179	32.187[b]	2.000	14.000	.000
	Hotelling's Trace	4.598	32.187[b]	2.000	14.000	.000
	Roy's Largest Root	4.598	32.187[b]	2.000	14.000	.000
System * Speed	Pillai's Trace	.039	.287[b]	2.000	14.000	.755
	Wilks' Lambda	.961	.287[b]	2.000	14.000	.755
	Hotelling's Trace	.041	.287[b]	2.000	14.000	.755
	Roy's Largest Root	.041	.287[b]	2.000	14.000	.755

Multivariate Tests[a]

Effect		Partial Eta Squared
System	Pillai's Trace	.221
	Wilks' Lambda	.221
	Hotelling's Trace	.221
	Roy's Largest Root	.221
Speed	Pillai's Trace	.821
	Wilks' Lambda	.821
	Hotelling's Trace	.821
	Roy's Largest Root	.821
System * Speed	Pillai's Trace	.039
	Wilks' Lambda	.039
	Hotelling's Trace	.039
	Roy's Largest Root	.039

a. Design: Intercept
Within Subjects Design: System + Speed + System * Speed

b. Exact statistic

Mauchly's Test of Sphericity[a]

Measure: MEASURE_1

Within Subjects Effect	Mauchly's W	Approx. Chi-Square	df	Sig.	Epsilon[b] Greenhouse-Geisser
System	1.000	.000	0	.	1.000
Speed	.801	3.107	2	.212	.834
System * Speed	.571	7.837	2	.020	.700

Mauchly's Test of Sphericity[a]

Measure: MEASURE_1

Within Subjects Effect	Epsilon[b] Huynh-Feldt	Epsilon[b] Lower-bound
System	1.000	1.000
Speed	.926	.500
System * Speed	.750	.500

Tests the null hypothesis that the error covariance matrix of the orthonormalized transformed dependent variables is proportional to an identity matrix.

a. Design: Intercept
Within Subjects Design: System + Speed + System * Speed

b. May be used to adjust the degrees of freedom for the averaged tests of significance. Corrected tests are displayed in the Tests of Within-Subjects Effects table.

Tests of Within-Subjects Effects

Measure: MEASURE_1

Source		Type III Sum of Squares	df	Mean Square	F
System	Sphericity Assumed	18.200	1	18.200	4.262
	Greenhouse-Geisser	18.200	1.000	18.200	4.262
	Huynh-Feldt	18.200	1.000	18.200	4.262
	Lower-bound	18.200	1.000	18.200	4.262
Error(System)	Sphericity Assumed	64.056	15	4.270	
	Greenhouse-Geisser	64.056	15.000	4.270	
	Huynh-Feldt	64.056	15.000	4.270	
	Lower-bound	64.056	15.000	4.270	
Speed	Sphericity Assumed	1206.828	2	603.414	45.825
	Greenhouse-Geisser	1206.828	1.668	723.504	45.825
	Huynh-Feldt	1206.828	1.852	651.696	45.825
	Lower-bound	1206.828	1.000	1206.828	45.825
Error(Speed)	Sphericity Assumed	395.036	30	13.168	
	Greenhouse-Geisser	395.036	25.020	15.789	
	Huynh-Feldt	395.036	27.777	14.221	
	Lower-bound	395.036	15.000	26.336	
System * Speed	Sphericity Assumed	1.878	2	.939	.413
	Greenhouse-Geisser	1.878	1.400	1.341	.413
	Huynh-Feldt	1.878	1.500	1.252	.413
	Lower-bound	1.878	1.000	1.878	.413
Error(System*Speed)	Sphericity Assumed	68.146	30	2.272	
	Greenhouse-Geisser	68.146	20.998	3.245	
	Huynh-Feldt	68.146	22.498	3.029	
	Lower-bound	68.146	15.000	4.543	

Tests of Within-Subjects Effects

Measure: MEASURE_1

Source		Sig.	Partial Eta Squared
System	Sphericity Assumed	.057	.221
	Greenhouse-Geisser	.057	.221
	Huynh-Feldt	.057	.221
	Lower-bound	.057	.221
Error(System)	Sphericity Assumed		
	Greenhouse-Geisser		
	Huynh-Feldt		
	Lower-bound		
Speed	Sphericity Assumed	.000	.753
	Greenhouse-Geisser	.000	.753
	Huynh-Feldt	.000	.753
	Lower-bound	.000	.753
Error(Speed)	Sphericity Assumed		
	Greenhouse-Geisser		
	Huynh-Feldt		
	Lower-bound		
System * Speed	Sphericity Assumed	.665	.027
	Greenhouse-Geisser	.595	.027
	Huynh-Feldt	.609	.027
	Lower-bound	.530	.027
Error(System*Speed)	Sphericity Assumed		
	Greenhouse-Geisser		
	Huynh-Feldt		
	Lower-bound		

Tests of Within-Subjects Contrasts

Measure: MEASURE_1

Source	System	Speed	Type III Sum of Squares	df	Mean Square	F
System	Linear		18.200	1	18.200	4.262
Error(System)	Linear		64.056	15	4.270	
Speed		Linear	1193.702	1	1193.702	63.363
		Quadratic	13.125	1	13.125	1.751
Error(Speed)		Linear	282.587	15	18.839	
		Quadratic	112.448	15	7.497	
System * Speed	Linear	Linear	1.102	1	1.102	.345
		Quadratic	.775	1	.775	.577
Error(System*Speed)	Linear	Linear	47.998	15	3.200	
		Quadratic	20.148	15	1.343	

Tests of Within-Subjects Contrasts

Measure: MEASURE_1

Source	System	Speed	Sig.	Partial Eta Squared
System	Linear		.057	.221
Error(System)	Linear			
Speed		Linear	.000	.809
		Quadratic	.206	.105
Error(Speed)		Linear		
		Quadratic		
System * Speed	Linear	Linear	.566	.022
		Quadratic	.459	.037
Error(System*Speed)	Linear	Linear		
		Quadratic		

Tests of Between-Subjects Effects

Measure: MEASURE_1
Transformed Variable: Average

Source	Type III Sum of Squares	df	Mean Square	F	Sig.	Partial Eta Squared
Intercept	400106.727	1	400106.727	2020.367	.000	.993
Error	2970.550	15	198.037			

Estimated Marginal Means

1. Grand Mean

Measure: MEASURE_1

Mean	Std. Error	95% Confidence Interval	
		Lower Bound	Upper Bound
64.558	1.436	61.497	67.620

2. System

Estimates

Measure: MEASURE_1

System	Mean	Std. Error	95% Confidence Interval	
			Lower Bound	Upper Bound
1	64.123	1.552	60.815	67.431
2	64.994	1.344	62.130	67.858

Pairwise Comparisons

Measure: MEASURE_1

(I) System	(J) System	Mean Difference (I-J)	Std. Error	Sig.[a]	95% Confidence Interval for Difference[a] Lower Bound	Upper Bound
1	2	-.871	.422	.057	-1.770	.028
2	1	.871	.422	.057	-.028	1.770

Based on estimated marginal means

a. Adjustment for multiple comparisons: Least Significant Difference (equivalent to no adjustments).

Multivariate Tests

	Value	F	Hypothesis df	Error df	Sig.	Partial Eta Squared
Pillai's trace	.221	4.262[a]	1.000	15.000	.057	.221
Wilks' lambda	.779	4.262[a]	1.000	15.000	.057	.221
Hotelling's trace	.284	4.262[a]	1.000	15.000	.057	.221
Roy's largest root	.284	4.262[a]	1.000	15.000	.057	.221

Each F tests the multivariate effect of System. These tests are based on the linearly independent pairwise comparisons among the estimated marginal means.

a. Exact statistic

3. Speed

Estimates

Measure: MEASURE_1

Speed	Mean	Std. Error	95% Confidence Interval Lower Bound	Upper Bound
1	68.616	1.515	65.387	71.844
2	65.081	1.549	61.779	68.384
3	59.978	1.522	56.734	63.223

Pairwise Comparisons

Measure: MEASURE_1

(I) Speed	(J) Speed	Mean Difference (I-J)	Std. Error	Sig.[b]	95% Confidence Interval for Difference[b] Lower Bound	Upper Bound
1	2	3.534*	.854	.001	1.715	5.354
	3	8.637*	1.085	.000	6.325	10.950
2	1	-3.534*	.854	.001	-5.354	-1.715
	3	5.103*	.750	.000	3.504	6.702
3	1	-8.637*	1.085	.000	-10.950	-6.325
	2	-5.103*	.750	.000	-6.702	-3.504

Based on estimated marginal means

*. The mean difference is significant at the .05 level.

b. Adjustment for multiple comparisons: Least Significant Difference (equivalent to no adjustments).

Multivariate Tests

	Value	F	Hypothesis df	Error df	Sig.	Partial Eta Squared
Pillai's trace	.821	32.187[a]	2.000	14.000	.000	.821
Wilks' lambda	.179	32.187[a]	2.000	14.000	.000	.821
Hotelling's trace	4.598	32.187[a]	2.000	14.000	.000	.821
Roy's largest root	4.598	32.187[a]	2.000	14.000	.000	.821

Each F tests the multivariate effect of Speed. These tests are based on the linearly independent pairwise comparisons among the estimated marginal means.

a. Exact statistic

4. System * Speed

Measure: MEASURE_1

System	Speed	Mean	Std. Error	95% Confidence Interval	
				Lower Bound	Upper Bound
1	1	68.113	1.580	64.745	71.480
	2	64.519	1.634	61.037	68.001
	3	59.738	1.680	56.157	63.318
2	1	69.119	1.471	65.984	72.254
	2	65.644	1.490	62.468	68.819
	3	60.219	1.485	57.054	63.384

Profile Plots

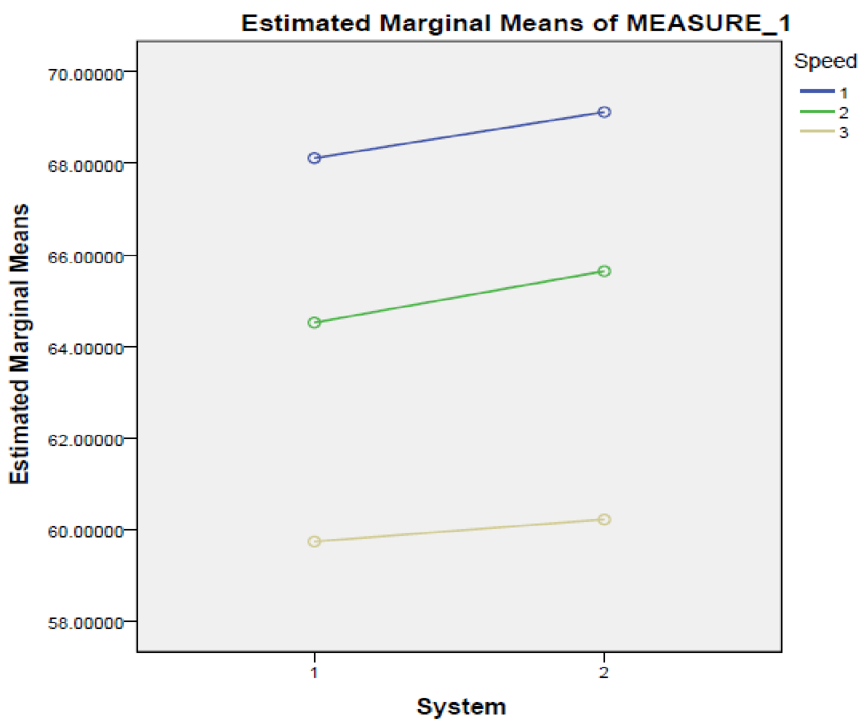

General Linear Model

Within-Subjects Factors

Measure: MEASURE_1

System	Speed	Dependent Variable
1	1	HP_1_M_5
	2	HP_1_M_65
	3	HP_1_M_8
2	1	HP_1_ML_5
	2	HP_1_ML_65
	3	HP_1_ML_8

Descriptive Statistics

	Mean	Std. Deviation	N
HP_1_M_5	-2.2151	1.04631	16
HP_1_M_65	-3.4416	1.56314	16
HP_1_M_8	-5.5900	3.30353	16
HP_1_ML_5	-2.1132	.98725	16
HP_1_ML_65	-3.5495	1.62613	16
HP_1_ML_8	-5.3766	1.96070	16

Multivariate Tests[a]

Effect		Value	F	Hypothesis df	Error df	Sig.
System	Pillai's Trace	.004	.060[b]	1.000	15.000	.809
	Wilks' Lambda	.996	.060[b]	1.000	15.000	.809
	Hotelling's Trace	.004	.060[b]	1.000	15.000	.809
	Roy's Largest Root	.004	.060[b]	1.000	15.000	.809
Speed	Pillai's Trace	.798	27.598[b]	2.000	14.000	.000
	Wilks' Lambda	.202	27.598[b]	2.000	14.000	.000
	Hotelling's Trace	3.943	27.598[b]	2.000	14.000	.000
	Roy's Largest Root	3.943	27.598[b]	2.000	14.000	.000
System * Speed	Pillai's Trace	.074	.556[b]	2.000	14.000	.586
	Wilks' Lambda	.926	.556[b]	2.000	14.000	.586
	Hotelling's Trace	.079	.556[b]	2.000	14.000	.586
	Roy's Largest Root	.079	.556[b]	2.000	14.000	.586

Multivariate Tests[a]

Effect		Partial Eta Squared
System	Pillai's Trace	.004
	Wilks' Lambda	.004
	Hotelling's Trace	.004
	Roy's Largest Root	.004
Speed	Pillai's Trace	.798
	Wilks' Lambda	.798
	Hotelling's Trace	.798
	Roy's Largest Root	.798
System * Speed	Pillai's Trace	.074
	Wilks' Lambda	.074
	Hotelling's Trace	.074
	Roy's Largest Root	.074

a. Design: Intercept
Within Subjects Design: System + Speed + System * Speed

b. Exact statistic

Mauchly's Test of Sphericity[a]

Measure: MEASURE_1

Within Subjects Effect	Mauchly's W	Approx. Chi-Square	df	Sig.	Epsilon[b] Greenhouse-Geisser
System	1.000	.000	0	.	1.000
Speed	.374	13.773	2	.001	.615
System * Speed	.325	15.754	2	.000	.597

Mauchly's Test of Sphericity[a]

Measure: MEASURE_1

Within Subjects Effect	Epsilon[b] Huynh-Feldt	Epsilon[b] Lower-bound
System	1.000	1.000
Speed	.642	.500
System * Speed	.619	.500

Tests the null hypothesis that the error covariance matrix of the orthonormalized transformed dependent variables is proportional to an identity matrix.

a. Design: Intercept
Within Subjects Design: System + Speed + System * Speed

b. May be used to adjust the degrees of freedom for the averaged tests of significance. Corrected tests are displayed in the Tests of Within-Subjects Effects table.

Tests of Within-Subjects Effects

Measure: MEASURE_1

Source		Type III Sum of Squares	df	Mean Square	F
System	Sphericity Assumed	.115	1	.115	.060
	Greenhouse-Geisser	.115	1.000	.115	.060
	Huynh-Feldt	.115	1.000	.115	.060
	Lower-bound	.115	1.000	.115	.060
Error(System)	Sphericity Assumed	28.509	15	1.901	
	Greenhouse-Geisser	28.509	15.000	1.901	
	Huynh-Feldt	28.509	15.000	1.901	
	Lower-bound	28.509	15.000	1.901	
Speed	Sphericity Assumed	178.571	2	89.285	24.979
	Greenhouse-Geisser	178.571	1.230	145.188	24.979
	Huynh-Feldt	178.571	1.284	139.089	24.979
	Lower-bound	178.571	1.000	178.571	24.979
Error(Speed)	Sphericity Assumed	107.231	30	3.574	
	Greenhouse-Geisser	107.231	18.449	5.812	
	Huynh-Feldt	107.231	19.258	5.568	
	Lower-bound	107.231	15.000	7.149	
System * Speed	Sphericity Assumed	.426	2	.213	.189
	Greenhouse-Geisser	.426	1.194	.357	.189
	Huynh-Feldt	.426	1.239	.344	.189
	Lower-bound	.426	1.000	.426	.189
Error(System*Speed)	Sphericity Assumed	33.756	30	1.125	
	Greenhouse-Geisser	33.756	17.906	1.885	
	Huynh-Feldt	33.756	18.578	1.817	
	Lower-bound	33.756	15.000	2.250	

Tests of Within-Subjects Effects

Measure: MEASURE_1

Source		Sig.	Partial Eta Squared
System	Sphericity Assumed	.809	.004
	Greenhouse-Geisser	.809	.004
	Huynh-Feldt	.809	.004
	Lower-bound	.809	.004
Error(System)	Sphericity Assumed		
	Greenhouse-Geisser		
	Huynh-Feldt		
	Lower-bound		
Speed	Sphericity Assumed	.000	.625
	Greenhouse-Geisser	.000	.625
	Huynh-Feldt	.000	.625
	Lower-bound	.000	.625
Error(Speed)	Sphericity Assumed		
	Greenhouse-Geisser		
	Huynh-Feldt		
	Lower-bound		
System * Speed	Sphericity Assumed	.829	.012
	Greenhouse-Geisser	.712	.012
	Huynh-Feldt	.721	.012
	Lower-bound	.670	.012
Error(System*Speed)	Sphericity Assumed		
	Greenhouse-Geisser		
	Huynh-Feldt		
	Lower-bound		

Tests of Within-Subjects Contrasts

Measure: MEASURE_1

Source	System	Speed	Type III Sum of Squares	df	Mean Square	F
System	Linear		.115	1	.115	.060
Error(System)	Linear		28.509	15	1.901	
Speed		Linear	176.274	1	176.274	34.816
		Quadratic	2.297	1	2.297	1.101
Error(Speed)		Linear	75.946	15	5.063	
		Quadratic	31.285	15	2.086	
System * Speed	Linear	Linear	.050	1	.050	.029
		Quadratic	.376	1	.376	.733
Error(System*Speed)	Linear	Linear	26.061	15	1.737	
		Quadratic	7.694	15	.513	

Tests of Within-Subjects Contrasts

Measure: MEASURE_1

Source	System	Speed	Sig.	Partial Eta Squared
System	Linear		.809	.004
Error(System)	Linear			
Speed		Linear	.000	.699
		Quadratic	.311	.068
Error(Speed)		Linear		
		Quadratic		
System * Speed	Linear	Linear	.868	.002
		Quadratic	.405	.047
Error(System*Speed)	Linear	Linear		
		Quadratic		

Tests of Between-Subjects Effects

Measure: MEASURE_1

Transformed Variable: Average

Source	Type III Sum of Squares	df	Mean Square	F	Sig.	Partial Eta Squared
Intercept	1324.440	1	1324.440	124.769	.000	.893
Error	159.227	15	10.615			

Estimated Marginal Means

1. Grand Mean

Measure: MEASURE_1

Mean	Std. Error	95% Confidence Interval Lower Bound	95% Confidence Interval Upper Bound
-3.714	.333	-4.423	-3.006

2. System

Estimates

Measure: MEASURE_1

System	Mean	Std. Error	95% Confidence Interval Lower Bound	95% Confidence Interval Upper Bound
1	-3.749	.413	-4.630	-2.868
2	-3.680	.300	-4.319	-3.041

Pairwise Comparisons

Measure: MEASURE_1

(I) System	(J) System	Mean Difference (I-J)	Std. Error	Sig.[a]	95% Confidence Interval for Difference[a] Lower Bound	Upper Bound
1	2	-.069	.281	.809	-.669	.531
2	1	.069	.281	.809	-.531	.669

Based on estimated marginal means

a. Adjustment for multiple comparisons: Least Significant Difference (equivalent to no adjustments).

Multivariate Tests

	Value	F	Hypothesis df	Error df	Sig.	Partial Eta Squared
Pillai's trace	.004	.060[a]	1.000	15.000	.809	.004
Wilks' lambda	.996	.060[a]	1.000	15.000	.809	.004
Hotelling's trace	.004	.060[a]	1.000	15.000	.809	.004
Roy's largest root	.004	.060[a]	1.000	15.000	.809	.004

Each F tests the multivariate effect of System. These tests are based on the linearly independent pairwise comparisons among the estimated marginal means.

a. Exact statistic

3. Speed

Estimates

Measure: MEASURE_1

Speed	Mean	Std. Error	95% Confidence Interval Lower Bound	Upper Bound
1	-2.164	.221	-2.635	-1.693
2	-3.496	.375	-4.296	-2.695
3	-5.483	.604	-6.772	-4.195

Pairwise Comparisons

Measure: MEASURE_1

(I) Speed	(J) Speed	Mean Difference (I-J)	Std. Error	Sig.[b]	95% Confidence Interval for Difference[b] Lower Bound	Upper Bound
1	2	1.331*	.216	.000	.871	1.792
	3	3.319*	.563	.000	2.120	4.518
2	1	-1.331*	.216	.000	-1.792	-.871
	3	1.988*	.554	.003	.807	3.169
3	1	-3.319*	.563	.000	-4.518	-2.120
	2	-1.988*	.554	.003	-3.169	-.807

Based on estimated marginal means

*. The mean difference is significant at the .05 level.

b. Adjustment for multiple comparisons: Least Significant Difference (equivalent to no adjustments).

Multivariate Tests

	Value	F	Hypothesis df	Error df	Sig.	Partial Eta Squared
Pillai's trace	.798	27.598[a]	2.000	14.000	.000	.798
Wilks' lambda	.202	27.598[a]	2.000	14.000	.000	.798
Hotelling's trace	3.943	27.598[a]	2.000	14.000	.000	.798
Roy's largest root	3.943	27.598[a]	2.000	14.000	.000	.798

Each F tests the multivariate effect of Speed. These tests are based on the linearly independent pairwise comparisons among the estimated marginal means.

a. Exact statistic

4. System * Speed

Measure: MEASURE_1

System	Speed	Mean	Std. Error	95% Confidence Interval Lower Bound	Upper Bound
1	1	-2.215	.262	-2.773	-1.658
	2	-3.442	.391	-4.275	-2.609
	3	-5.590	.826	-7.350	-3.830
2	1	-2.113	.247	-2.639	-1.587
	2	-3.550	.407	-4.416	-2.683
	3	-5.377	.490	-6.421	-4.332

Profile Plots

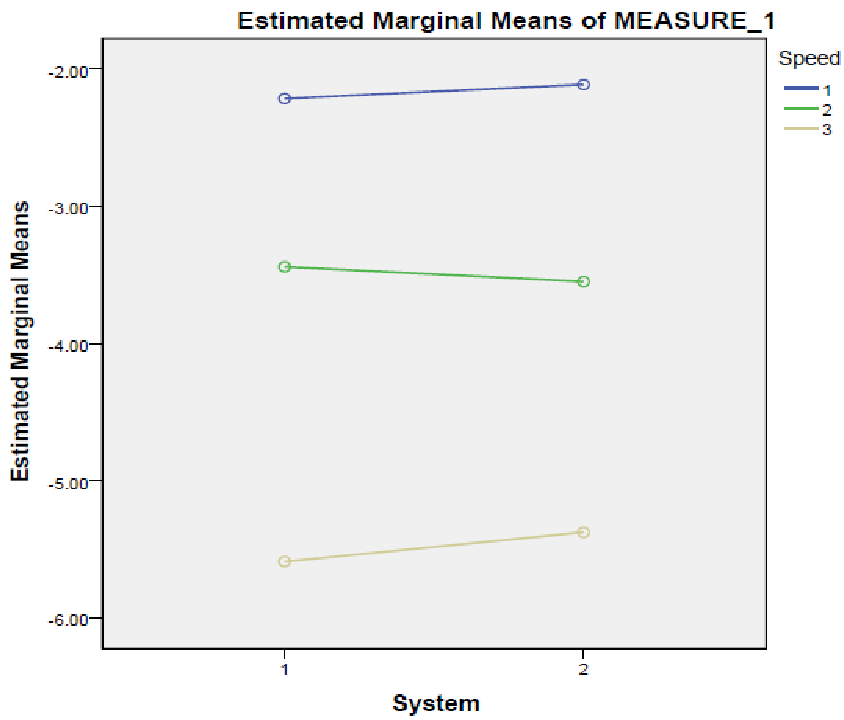

General Linear Model

Within-Subjects Factors

Measure: MEASURE_1

System	Speed	Dependent Variable
1	1	HP_1_T_M_5
	2	HP_1_T_M_65
	3	HP_1_T_M_8
2	1	HP_1_T_ML_5
	2	HP_1_T_ML_65
	3	HP_1_T_ML_8

Descriptive Statistics

	Mean	Std. Deviation	N
HP_1_T_M_5	19.3000	3.82936	16
HP_1_T_M_65	18.1750	3.66433	16
HP_1_T_M_8	17.556250	4.3130760	16
HP_1_T_ML_5	23.2812	2.84376	16
HP_1_T_ML_65	20.9125	2.90078	16
HP_1_T_ML_8	18.75625000	2.670572660	16

Multivariate Tests[a]

Effect		Value	F	Hypothesis df	Error df	Sig.
System	Pillai's Trace	.722	38.897[b]	1.000	15.000	.000
	Wilks' Lambda	.278	38.897[b]	1.000	15.000	.000
	Hotelling's Trace	2.593	38.897[b]	1.000	15.000	.000
	Roy's Largest Root	2.593	38.897[b]	1.000	15.000	.000
Speed	Pillai's Trace	.543	8.310[b]	2.000	14.000	.004
	Wilks' Lambda	.457	8.310[b]	2.000	14.000	.004
	Hotelling's Trace	1.187	8.310[b]	2.000	14.000	.004
	Roy's Largest Root	1.187	8.310[b]	2.000	14.000	.004
System * Speed	Pillai's Trace	.421	5.080[b]	2.000	14.000	.022
	Wilks' Lambda	.579	5.080[b]	2.000	14.000	.022
	Hotelling's Trace	.726	5.080[b]	2.000	14.000	.022
	Roy's Largest Root	.726	5.080[b]	2.000	14.000	.022

Multivariate Tests[a]

Effect		Partial Eta Squared
System	Pillai's Trace	.722
	Wilks' Lambda	.722
	Hotelling's Trace	.722
	Roy's Largest Root	.722
Speed	Pillai's Trace	.543
	Wilks' Lambda	.543
	Hotelling's Trace	.543
	Roy's Largest Root	.543
System * Speed	Pillai's Trace	.421
	Wilks' Lambda	.421
	Hotelling's Trace	.421
	Roy's Largest Root	.421

a. Design: Intercept
Within Subjects Design: System + Speed + System * Speed

b. Exact statistic

Mauchly's Test of Sphericity[a]

Measure: MEASURE_1

Within Subjects Effect	Mauchly's W	Approx. Chi-Square	df	Sig.	Epsilon[b] Greenhouse-Geisser
System	1.000	.000	0	.	1.000
Speed	.443	11.410	2	.003	.642
System * Speed	.564	8.017	2	.018	.696

Mauchly's Test of Sphericity[a]

Measure: MEASURE_1

Within Subjects Effect	Epsilon[b]	
	Huynh-Feldt	Lower-bound
System	1.000	1.000
Speed	.676	.500
System * Speed	.745	.500

Tests the null hypothesis that the error covariance matrix of the orthonormalized transformed dependent variables is proportional to an identity matrix.

a. Design: Intercept
Within Subjects Design: System + Speed + System * Speed

b. May be used to adjust the degrees of freedom for the averaged tests of significance. Corrected tests are displayed in the Tests of Within-Subjects Effects table.

Tests of Within-Subjects Effects

Measure: MEASURE_1

Source		Type III Sum of Squares	df	Mean Square	F
System	Sphericity Assumed	167.218	1	167.218	38.897
	Greenhouse-Geisser	167.218	1.000	167.218	38.897
	Huynh-Feldt	167.218	1.000	167.218	38.897
	Lower-bound	167.218	1.000	167.218	38.897
Error(System)	Sphericity Assumed	64.484	15	4.299	
	Greenhouse-Geisser	64.484	15.000	4.299	
	Huynh-Feldt	64.484	15.000	4.299	
	Lower-bound	64.484	15.000	4.299	
Speed	Sphericity Assumed	157.878	2	78.939	9.644
	Greenhouse-Geisser	157.878	1.284	122.937	9.644
	Huynh-Feldt	157.878	1.352	116.750	9.644
	Lower-bound	157.878	1.000	157.878	9.644
Error(Speed)	Sphericity Assumed	245.566	30	8.186	
	Greenhouse-Geisser	245.566	19.263	12.748	
	Huynh-Feldt	245.566	20.284	12.106	
	Lower-bound	245.566	15.000	16.371	
System * Speed	Sphericity Assumed	31.056	2	15.528	5.010
	Greenhouse-Geisser	31.056	1.393	22.298	5.010
	Huynh-Feldt	31.056	1.491	20.833	5.010
	Lower-bound	31.056	1.000	31.056	5.010
Error(System*Speed)	Sphericity Assumed	92.987	30	3.100	
	Greenhouse-Geisser	92.987	20.892	4.451	
	Huynh-Feldt	92.987	22.361	4.158	
	Lower-bound	92.987	15.000	6.199	

Tests of Within-Subjects Effects

Measure: MEASURE_1

Source		Sig.	Partial Eta Squared
System	Sphericity Assumed	.000	.722
	Greenhouse-Geisser	.000	.722
	Huynh-Feldt	.000	.722
	Lower-bound	.000	.722
Error(System)	Sphericity Assumed		
	Greenhouse-Geisser		
	Huynh-Feldt		
	Lower-bound		
Speed	Sphericity Assumed	.001	.391
	Greenhouse-Geisser	.004	.391
	Huynh-Feldt	.003	.391
	Lower-bound	.007	.391
Error(Speed)	Sphericity Assumed		
	Greenhouse-Geisser		
	Huynh-Feldt		
	Lower-bound		
System * Speed	Sphericity Assumed	.013	.250
	Greenhouse-Geisser	.026	.250
	Huynh-Feldt	.023	.250
	Lower-bound	.041	.250
Error(System*Speed)	Sphericity Assumed		
	Greenhouse-Geisser		
	Huynh-Feldt		
	Lower-bound		

Tests of Within-Subjects Contrasts

Measure: MEASURE_1

Source	System	Speed	Type III Sum of Squares	df	Mean Square	F
System	Linear		167.218	1	167.218	38.897
Error(System)	Linear		64.484	15	4.299	
Speed		Linear	157.189	1	157.189	11.665
		Quadratic	.689	1	.689	.238
Error(Speed)		Linear	202.134	15	13.476	
		Quadratic	43.432	15	2.895	
System * Speed	Linear	Linear	30.941	1	30.941	7.566
		Quadratic	.115	1	.115	.055
Error(System*Speed)	Linear	Linear	61.341	15	4.089	
		Quadratic	31.646	15	2.110	

Tests of Within-Subjects Contrasts

Measure: MEASURE_1

Source	System	Speed	Sig.	Partial Eta Squared
System	Linear		.000	.722
Error(System)	Linear			
Speed		Linear	.004	.437
		Quadratic	.633	.016
Error(Speed)		Linear		
		Quadratic		
System * Speed	Linear	Linear	.015	.335
		Quadratic	.819	.004
Error(System*Speed)	Linear	Linear		
		Quadratic		

Tests of Between-Subjects Effects

Measure: MEASURE_1
Transformed Variable: Average

Source	Type III Sum of Squares	df	Mean Square	F	Sig.	Partial Eta Squared
Intercept	37118.868	1	37118.868	854.127	.000	.983
Error	651.874	15	43.458			

Estimated Marginal Means

1. Grand Mean

Measure: MEASURE_1

		95% Confidence Interval	
Mean	Std. Error	Lower Bound	Upper Bound
19.664	.673	18.229	21.098

2. System

Estimates

Measure: MEASURE_1

			95% Confidence Interval	
System	Mean	Std. Error	Lower Bound	Upper Bound
1	18.344	.786	16.668	20.020
2	20.983	.614	19.675	22.292

Pairwise Comparisons

Measure: MEASURE_1

(I) System	(J) System	Mean Difference (I-J)	Std. Error	Sig.[b]	95% Confidence Interval for Difference[b] Lower Bound	Upper Bound
1	2	-2.640*	.423	.000	-3.542	-1.737
2	1	2.640*	.423	.000	1.737	3.542

Based on estimated marginal means

*. The mean difference is significant at the .05 level.

b. Adjustment for multiple comparisons: Least Significant Difference (equivalent to no adjustments).

Multivariate Tests

	Value	F	Hypothesis df	Error df	Sig.	Partial Eta Squared
Pillai's trace	.722	38.897[a]	1.000	15.000	.000	.722
Wilks' lambda	.278	38.897[a]	1.000	15.000	.000	.722
Hotelling's trace	2.593	38.897[a]	1.000	15.000	.000	.722
Roy's largest root	2.593	38.897[a]	1.000	15.000	.000	.722

Each F tests the multivariate effect of System. These tests are based on the linearly independent pairwise comparisons among the estimated marginal means.

a. Exact statistic

3. Speed

Estimates

Measure: MEASURE_1

Speed	Mean	Std. Error	95% Confidence Interval Lower Bound	Upper Bound
1	21.291	.790	19.607	22.974
2	19.544	.787	17.867	21.220
3	18.156	.792	16.469	19.844

Pairwise Comparisons

Measure: MEASURE_1

(I) Speed	(J) Speed	Mean Difference (I-J)	Std. Error	Sig.[b]	95% Confidence Interval for Difference[b] Lower Bound	Upper Bound
1	2	1.747*	.425	.001	.841	2.653
	3	3.134*	.918	.004	1.178	5.090
2	1	-1.747*	.425	.001	-2.653	-.841
	3	1.387	.715	.072	-.137	2.912
3	1	-3.134*	.918	.004	-5.090	-1.178
	2	-1.387	.715	.072	-2.912	.137

Based on estimated marginal means

*. The mean difference is significant at the .05 level.

b. Adjustment for multiple comparisons: Least Significant Difference (equivalent to no adjustments).

Multivariate Tests

	Value	F	Hypothesis df	Error df	Sig.	Partial Eta Squared
Pillai's trace	.543	8.310[a]	2.000	14.000	.004	.543
Wilks' lambda	.457	8.310[a]	2.000	14.000	.004	.543
Hotelling's trace	1.187	8.310[a]	2.000	14.000	.004	.543
Roy's largest root	1.187	8.310[a]	2.000	14.000	.004	.543

Each F tests the multivariate effect of Speed. These tests are based on the linearly independent pairwise comparisons among the estimated marginal means.

a. Exact statistic

4. System * Speed

Measure: MEASURE_1

System	Speed	Mean	Std. Error	95% Confidence Interval Lower Bound	Upper Bound
1	1	19.300	.957	17.259	21.341
	2	18.175	.916	16.222	20.128
	3	17.556	1.078	15.258	19.855
2	1	23.281	.711	21.766	24.797
	2	20.912	.725	19.367	22.458
	3	18.756	.668	17.333	20.179

Profile Plots

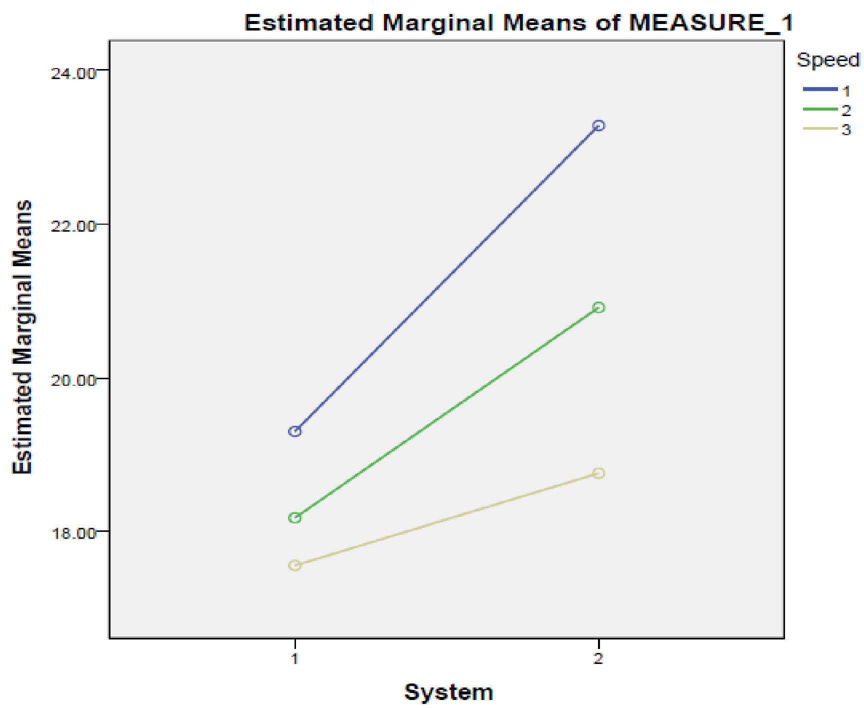

General Linear Model

Within-Subjects Factors

Measure: MEASURE_1

System	Speed	Dependent Variable
1	1	HP_2_M_5
	2	HP_2_M_65
	3	HP_2_M_8
2	1	HP_2_ML_5
	2	HP_2_ML_65
	3	HP_2_ML_8

Descriptive Statistics

	Mean	Std. Deviation	N
HP_2_M_5	1.58861038	.411947523	16
HP_2_M_65	2.70286925	.615321751	16
HP_2_M_8	4.4851254	1.27035689	16
HP_2_ML_5	3.44688175	.732485274	16
HP_2_ML_65	5.06355825	1.052438082	16
HP_2_ML_8	8.20341938	1.777414771	16

Multivariate Tests[a]

Effect		Value	F	Hypothesis df	Error df	Sig.	Partial Eta Squared
System	Pillai's Trace	.913	157.929[b]	1.000	15.000	.000	.913
	Wilks' Lambda	.087	157.929[b]	1.000	15.000	.000	.913
	Hotelling's Trace	10.529	157.929[b]	1.000	15.000	.000	.913
	Roy's Largest Root	10.529	157.929[b]	1.000	15.000	.000	.913
Speed	Pillai's Trace	.953	142.149[b]	2.000	14.000	.000	.953
	Wilks' Lambda	.047	142.149[b]	2.000	14.000	.000	.953
	Hotelling's Trace	20.307	142.149[b]	2.000	14.000	.000	.953
	Roy's Largest Root	20.307	142.149[b]	2.000	14.000	.000	.953
System * Speed	Pillai's Trace	.587	9.935[b]	2.000	14.000	.002	.587
	Wilks' Lambda	.413	9.935[b]	2.000	14.000	.002	.587
	Hotelling's Trace	1.419	9.935[b]	2.000	14.000	.002	.587
	Roy's Largest Root	1.419	9.935[b]	2.000	14.000	.002	.587

a. Design: Intercept
Within Subjects Design: System + Speed + System * Speed

b. Exact statistic

Mauchly's Test of Sphericity[a]

Measure: MEASURE_1

Within Subjects Effect	Mauchly's W	Approx. Chi-Square	df	Sig.	Epsilon[b] Greenhouse-Geisser	Epsilon[b] Huynh-Feldt	Epsilon[b] Lower-bound
System	1.000	.000	0	.	1.000	1.000	1.000
Speed	.706	4.869	2	.088	.773	.845	.500
System * Speed	.718	4.639	2	.098	.780	.854	.500

Tests the null hypothesis that the error covariance matrix of the orthonormalized transformed dependent variables is proportional to an identity matrix.

a. Design: Intercept
Within Subjects Design: System + Speed + System * Speed

b. May be used to adjust the degrees of freedom for the averaged tests of significance. Corrected tests are displayed in the Tests of Within-Subjects Effects table.

Tests of Within-Subjects Effects

Measure: MEASURE_1

Source		Type III Sum of Squares	df	Mean Square	F
System	Sphericity Assumed	168.000	1	168.000	157.929
	Greenhouse-Geisser	168.000	1.000	168.000	157.929
	Huynh-Feldt	168.000	1.000	168.000	157.929
	Lower-bound	168.000	1.000	168.000	157.929
Error(System)	Sphericity Assumed	15.957	15	1.064	
	Greenhouse-Geisser	15.957	15.000	1.064	
	Huynh-Feldt	15.957	15.000	1.064	
	Lower-bound	15.957	15.000	1.064	
Speed	Sphericity Assumed	240.679	2	120.339	158.350
	Greenhouse-Geisser	240.679	1.546	155.687	158.350
	Huynh-Feldt	240.679	1.690	142.431	158.350
	Lower-bound	240.679	1.000	240.679	158.350
Error(Speed)	Sphericity Assumed	22.799	30	.760	
	Greenhouse-Geisser	22.799	23.189	.983	
	Huynh-Feldt	22.799	25.347	.899	
	Lower-bound	22.799	15.000	1.520	
System * Speed	Sphericity Assumed	14.814	2	7.407	12.841
	Greenhouse-Geisser	14.814	1.560	9.496	12.841
	Huynh-Feldt	14.814	1.708	8.672	12.841
	Lower-bound	14.814	1.000	14.814	12.841
Error(System*Speed)	Sphericity Assumed	17.305	30	.577	
	Greenhouse-Geisser	17.305	23.400	.740	
	Huynh-Feldt	17.305	25.624	.675	
	Lower-bound	17.305	15.000	1.154	

Tests of Within-Subjects Effects

Measure: MEASURE_1

Source		Sig.	Partial Eta Squared
System	Sphericity Assumed	.000	.913
	Greenhouse-Geisser	.000	.913
	Huynh-Feldt	.000	.913
	Lower-bound	.000	.913
Error(System)	Sphericity Assumed		
	Greenhouse-Geisser		
	Huynh-Feldt		
	Lower-bound		
Speed	Sphericity Assumed	.000	.913
	Greenhouse-Geisser	.000	.913
	Huynh-Feldt	.000	.913
	Lower-bound	.000	.913
Error(Speed)	Sphericity Assumed		
	Greenhouse-Geisser		
	Huynh-Feldt		
	Lower-bound		
System * Speed	Sphericity Assumed	.000	.461
	Greenhouse-Geisser	.000	.461
	Huynh-Feldt	.000	.461
	Lower-bound	.003	.461
Error(System*Speed)	Sphericity Assumed		
	Greenhouse-Geisser		
	Huynh-Feldt		
	Lower-bound		

Tests of Within-Subjects Contrasts

Measure: MEASURE_1

Source	System	Speed	Type III Sum of Squares	df	Mean Square	F
System	Linear		168.000	1	168.000	157.929
Error(System)	Linear		15.957	15	1.064	
Speed		Linear	234.277	1	234.277	265.060
		Quadratic	6.402	1	6.402	10.065
Error(Speed)		Linear	13.258	15	.884	
		Quadratic	9.541	15	.636	
System * Speed	Linear	Linear	13.839	1	13.839	20.313
		Quadratic	.975	1	.975	2.064
Error(System*Speed)	Linear	Linear	10.219	15	.681	
		Quadratic	7.086	15	.472	

Tests of Within-Subjects Contrasts

Measure: MEASURE_1

Source	System	Speed	Sig.	Partial Eta Squared
System	Linear		.000	.913
Error(System)	Linear			
Speed		Linear	.000	.946
		Quadratic	.006	.402
Error(Speed)		Linear		
		Quadratic		
System * Speed	Linear	Linear	.000	.575
		Quadratic	.171	.121
Error(System*Speed)	Linear	Linear		
		Quadratic		

Tests of Between-Subjects Effects

Measure: MEASURE_1
Transformed Variable: Average

Source	Type III Sum of Squares	df	Mean Square	F	Sig.	Partial Eta Squared
Intercept	1732.703	1	1732.703	536.747	.000	.973
Error	48.422	15	3.228			

Estimated Marginal Means

1. Grand Mean

Measure: MEASURE_1

Mean	Std. Error	95% Confidence Interval	
		Lower Bound	Upper Bound
4.248	.183	3.858	4.639

2. System

Estimates

Measure: MEASURE_1

System	Mean	Std. Error	95% Confidence Interval	
			Lower Bound	Upper Bound
1	2.926	.166	2.571	3.280
2	5.571	.248	5.042	6.101

Pairwise Comparisons

Measure: MEASURE_1

(I) System	(J) System	Mean Difference (I-J)	Std. Error	Sig.[b]	95% Confidence Interval for Difference[b] Lower Bound	Upper Bound
1	2	-2.646*	.211	.000	-3.094	-2.197
2	1	2.646*	.211	.000	2.197	3.094

Based on estimated marginal means

*. The mean difference is significant at the .05 level.

b. Adjustment for multiple comparisons: Least Significant Difference (equivalent to no adjustments).

Multivariate Tests

	Value	F	Hypothesis df	Error df	Sig.	Partial Eta Squared
Pillai's trace	.913	157.929[a]	1.000	15.000	.000	.913
Wilks' lambda	.087	157.929[a]	1.000	15.000	.000	.913
Hotelling's trace	10.529	157.929[a]	1.000	15.000	.000	.913
Roy's largest root	10.529	157.929[a]	1.000	15.000	.000	.913

Each F tests the multivariate effect of System. These tests are based on the linearly independent pairwise comparisons among the estimated marginal means.

a. Exact statistic

3. Speed

Estimates

Measure: MEASURE_1

Speed	Mean	Std. Error	95% Confidence Interval Lower Bound	Upper Bound
1	2.518	.120	2.262	2.773
2	3.883	.176	3.508	4.259
3	6.344	.321	5.660	7.028

Pairwise Comparisons

Measure: MEASURE_1

(I) Speed	(J) Speed	Mean Difference (I-J)	Std. Error	Sig.[b]	95% Confidence Interval for Difference[b] Lower Bound	Upper Bound
1	2	-1.365*	.150	.000	-1.684	-1.047
	3	-3.827*	.235	.000	-4.327	-3.326
2	1	1.365*	.150	.000	1.047	1.684
	3	-2.461*	.255	.000	-3.004	-1.918
3	1	3.827*	.235	.000	3.326	4.327
	2	2.461*	.255	.000	1.918	3.004

Based on estimated marginal means

*. The mean difference is significant at the .05 level.

b. Adjustment for multiple comparisons: Least Significant Difference (equivalent to no adjustments).

Multivariate Tests

	Value	F	Hypothesis df	Error df	Sig.	Partial Eta Squared
Pillai's trace	.953	142.149[a]	2.000	14.000	.000	.953
Wilks' lambda	.047	142.149[a]	2.000	14.000	.000	.953
Hotelling's trace	20.307	142.149[a]	2.000	14.000	.000	.953
Roy's largest root	20.307	142.149[a]	2.000	14.000	.000	.953

Each F tests the multivariate effect of Speed. These tests are based on the linearly independent pairwise comparisons among the estimated marginal means.

a. Exact statistic

4. System * Speed

Measure: MEASURE_1

System	Speed	Mean	Std. Error	95% Confidence Interval Lower Bound	95% Confidence Interval Upper Bound
1	1	1.589	.103	1.369	1.808
	2	2.703	.154	2.375	3.031
	3	4.485	.318	3.808	5.162
2	1	3.447	.183	3.057	3.837
	2	5.064	.263	4.503	5.624
	3	8.203	.444	7.256	9.151

Profile Plots

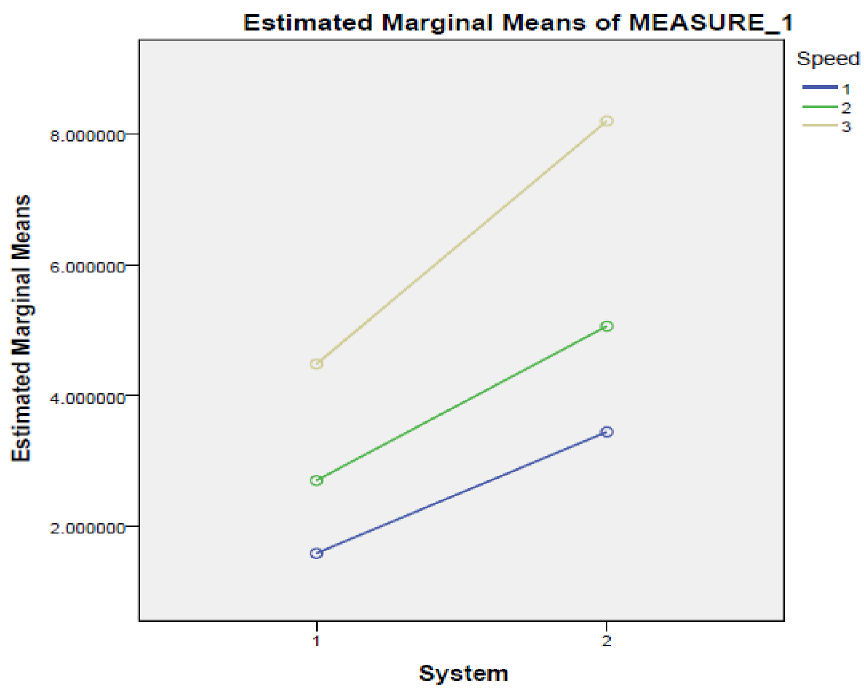

General Linear Model

Within-Subjects Factors

Measure: MEASURE_1

System	Speed	Dependent Variable
1	1	HP_2_T_M_5
	2	HP_2_T_M_65
	3	HP_2_T_M_8
2	1	HP_2_T_ML_5
	2	HP_2_T_ML_65
	3	HP_2_T_ML_8

Descriptive Statistics

	Mean	Std. Deviation	N
HP_2_T_M_5	38.58125000	4.565554913	16
HP_2_T_M_65	36.8625	4.24890	16
HP_2_T_M_8	34.0875	5.16241	16
HP_2_T_ML_5	38.944	3.7942	16
HP_2_T_ML_65	37.0625	4.02275	16
HP_2_T_ML_8	34.7375	4.03202	16

Multivariate Tests[a]

Effect		Value	F	Hypothesis df	Error df	Sig.
System	Pillai's Trace	.085	1.396[b]	1.000	15.000	.256
	Wilks' Lambda	.915	1.396[b]	1.000	15.000	.256
	Hotelling's Trace	.093	1.396[b]	1.000	15.000	.256
	Roy's Largest Root	.093	1.396[b]	1.000	15.000	.256
Speed	Pillai's Trace	.749	20.898[b]	2.000	14.000	.000
	Wilks' Lambda	.251	20.898[b]	2.000	14.000	.000
	Hotelling's Trace	2.985	20.898[b]	2.000	14.000	.000
	Roy's Largest Root	2.985	20.898[b]	2.000	14.000	.000
System * Speed	Pillai's Trace	.047	.349[b]	2.000	14.000	.711
	Wilks' Lambda	.953	.349[b]	2.000	14.000	.711
	Hotelling's Trace	.050	.349[b]	2.000	14.000	.711
	Roy's Largest Root	.050	.349[b]	2.000	14.000	.711

Multivariate Tests[a]

Effect		Partial Eta Squared
System	Pillai's Trace	.085
	Wilks' Lambda	.085
	Hotelling's Trace	.085
	Roy's Largest Root	.085
Speed	Pillai's Trace	.749
	Wilks' Lambda	.749
	Hotelling's Trace	.749
	Roy's Largest Root	.749
System * Speed	Pillai's Trace	.047
	Wilks' Lambda	.047
	Hotelling's Trace	.047
	Roy's Largest Root	.047

a. Design: Intercept
Within Subjects Design: System + Speed + System * Speed

b. Exact statistic

Mauchly's Test of Sphericity[a]

Measure: MEASURE_1

Within Subjects Effect	Mauchly's W	Approx. Chi-Square	df	Sig.	Epsilon[b] Greenhouse-Geisser
System	1.000	.000	0	.	1.000
Speed	.789	3.321	2	.190	.826
System * Speed	.913	1.279	2	.528	.920

Mauchly's Test of Sphericity[a]

Measure: MEASURE_1

Within Subjects Effect	Epsilon[b] Huynh-Feldt	Lower-bound
System	1.000	1.000
Speed	.915	.500
System * Speed	1.000	.500

Tests the null hypothesis that the error covariance matrix of the orthonormalized transformed dependent variables is proportional to an identity matrix.

a. Design: Intercept
Within Subjects Design: System + Speed + System * Speed

b. May be used to adjust the degrees of freedom for the averaged tests of significance. Corrected tests are displayed in the Tests of Within-Subjects Effects table.

Tests of Within-Subjects Effects

Measure: MEASURE_1

Source		Type III Sum of Squares	df	Mean Square	F
System	Sphericity Assumed	3.920	1	3.920	1.396
	Greenhouse-Geisser	3.920	1.000	3.920	1.396
	Huynh-Feldt	3.920	1.000	3.920	1.396
	Lower-bound	3.920	1.000	3.920	1.396
Error(System)	Sphericity Assumed	42.113	15	2.808	
	Greenhouse-Geisser	42.113	15.000	2.808	
	Huynh-Feldt	42.113	15.000	2.808	
	Lower-bound	42.113	15.000	2.808	
Speed	Sphericity Assumed	305.760	2	152.880	21.284
	Greenhouse-Geisser	305.760	1.651	185.162	21.284
	Huynh-Feldt	305.760	1.829	167.130	21.284
	Lower-bound	305.760	1.000	305.760	21.284
Error(Speed)	Sphericity Assumed	215.483	30	7.183	
	Greenhouse-Geisser	215.483	24.770	8.699	
	Huynh-Feldt	215.483	27.442	7.852	
	Lower-bound	215.483	15.000	14.366	
System * Speed	Sphericity Assumed	.831	2	.415	.287
	Greenhouse-Geisser	.831	1.839	.452	.287
	Huynh-Feldt	.831	2.000	.415	.287
	Lower-bound	.831	1.000	.831	.287
Error(System*Speed)	Sphericity Assumed	43.426	30	1.448	
	Greenhouse-Geisser	43.426	27.591	1.574	
	Huynh-Feldt	43.426	30.000	1.448	
	Lower-bound	43.426	15.000	2.895	

Tests of Within-Subjects Effects

Measure: MEASURE_1

Source		Sig.	Partial Eta Squared
System	Sphericity Assumed	.256	.085
	Greenhouse-Geisser	.256	.085
	Huynh-Feldt	.256	.085
	Lower-bound	.256	.085
Error(System)	Sphericity Assumed		
	Greenhouse-Geisser		
	Huynh-Feldt		
	Lower-bound		
Speed	Sphericity Assumed	.000	.587
	Greenhouse-Geisser	.000	.587
	Huynh-Feldt	.000	.587
	Lower-bound	.000	.587
Error(Speed)	Sphericity Assumed		
	Greenhouse-Geisser		
	Huynh-Feldt		
	Lower-bound		
System * Speed	Sphericity Assumed	.753	.019
	Greenhouse-Geisser	.735	.019
	Huynh-Feldt	.753	.019
	Lower-bound	.600	.019
Error(System*Speed)	Sphericity Assumed		
	Greenhouse-Geisser		
	Huynh-Feldt		
	Lower-bound		

Tests of Within-Subjects Contrasts

Measure: MEASURE_1

Source	System	Speed	Type III Sum of Squares	df	Mean Square	F
System	Linear		3.920	1	3.920	1.396
Error(System)	Linear		42.113	15	2.808	
Speed		Linear	302.760	1	302.760	33.695
		Quadratic	3.000	1	3.000	.558
Error(Speed)		Linear	134.780	15	8.985	
		Quadratic	80.703	15	5.380	
System * Speed	Linear	Linear	.331	1	.331	.181
		Quadratic	.500	1	.500	.468
Error(System*Speed)	Linear	Linear	27.379	15	1.825	
		Quadratic	16.046	15	1.070	

Tests of Within-Subjects Contrasts

Measure: MEASURE_1

Source	System	Speed	Sig.	Partial Eta Squared
System	Linear		.256	.085
Error(System)	Linear			
Speed		Linear	.000	.692
		Quadratic	.467	.036
Error(Speed)		Linear		
		Quadratic		
System * Speed	Linear	Linear	.676	.012
		Quadratic	.505	.030
Error(System*Speed)	Linear	Linear		
		Quadratic		

Tests of Between-Subjects Effects

Measure: MEASURE_1

Transformed Variable: Average

Source	Type III Sum of Squares	df	Mean Square	F	Sig.	Partial Eta Squared
Intercept	129389.535	1	129389.535	1401.602	.000	.989
Error	1384.732	15	92.315			

Estimated Marginal Means

1. Grand Mean

Measure: MEASURE_1

Mean	Std. Error	95% Confidence Interval	
		Lower Bound	Upper Bound
36.713	.981	34.622	38.803

2. System

Estimates

Measure: MEASURE_1

System	Mean	Std. Error	95% Confidence Interval	
			Lower Bound	Upper Bound
1	36.510	1.064	34.242	38.779
2	36.915	.921	34.951	38.879

Pairwise Comparisons

Measure: MEASURE_1

(I) System	(J) System	Mean Difference (I-J)	Std. Error	Sig.[a]	95% Confidence Interval for Difference[a]	
					Lower Bound	Upper Bound
1	2	-.404	.342	.256	-1.133	.325
2	1	.404	.342	.256	-.325	1.133

Based on estimated marginal means

a. Adjustment for multiple comparisons: Least Significant Difference (equivalent to no adjustments).

Multivariate Tests

	Value	F	Hypothesis df	Error df	Sig.	Partial Eta Squared
Pillai's trace	.085	1.396[a]	1.000	15.000	.256	.085
Wilks' lambda	.915	1.396[a]	1.000	15.000	.256	.085
Hotelling's trace	.093	1.396[a]	1.000	15.000	.256	.085
Roy's largest root	.093	1.396[a]	1.000	15.000	.256	.085

Each F tests the multivariate effect of System. These tests are based on the linearly independent pairwise comparisons among the estimated marginal means.

a. Exact statistic

3. Speed

Estimates

Measure: MEASURE_1

Speed	Mean	Std. Error	95% Confidence Interval	
			Lower Bound	Upper Bound
1	38.763	1.014	36.601	40.924
2	36.963	1.005	34.820	39.105
3	34.413	1.138	31.987	36.838

Pairwise Comparisons

Measure: MEASURE_1

(I) Speed	(J) Speed	Mean Difference (I-J)	Std. Error	Sig.[b]	95% Confidence Interval for Difference[b]	
					Lower Bound	Upper Bound
1	2	1.800*	.736	.027	.230	3.370
	3	4.350*	.749	.000	2.753	5.947
2	1	-1.800*	.736	.027	-3.370	-.230
	3	2.550*	.493	.000	1.499	3.601
3	1	-4.350*	.749	.000	-5.947	-2.753
	2	-2.550*	.493	.000	-3.601	-1.499

Based on estimated marginal means

*. The mean difference is significant at the .05 level.

b. Adjustment for multiple comparisons: Least Significant Difference (equivalent to no adjustments).

Multivariate Tests

	Value	F	Hypothesis df	Error df	Sig.	Partial Eta Squared
Pillai's trace	.749	20.898[a]	2.000	14.000	.000	.749
Wilks' lambda	.251	20.898[a]	2.000	14.000	.000	.749
Hotelling's trace	2.985	20.898[a]	2.000	14.000	.000	.749
Roy's largest root	2.985	20.898[a]	2.000	14.000	.000	.749

Each F tests the multivariate effect of Speed. These tests are based on the linearly independent pairwise comparisons among the estimated marginal means.

a. Exact statistic

4. System * Speed

Measure: MEASURE_1

System	Speed	Mean	Std. Error	95% Confidence Interval Lower Bound	Upper Bound
1	1	38.581	1.141	36.148	41.014
	2	36.863	1.062	34.598	39.127
	3	34.088	1.291	31.337	36.838
2	1	38.944	.949	36.922	40.966
	2	37.063	1.006	34.919	39.206
	3	34.738	1.008	32.589	36.886

Profile Plots

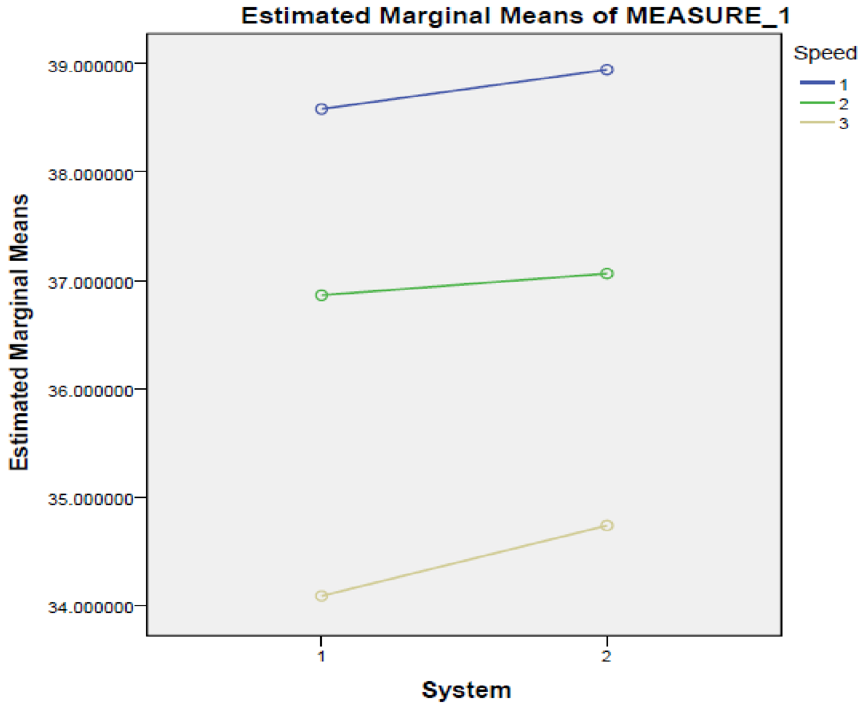

General Linear Model

Within-Subjects Factors

Measure: MEASURE_1

System	Speed	Dependent Variable
1	1	HP_3_M_5
	2	HP_3_M_65
	3	HP_3_M_8
2	1	HP_3_ML_5
	2	HP_3_ML_65
	3	HP_3_ML_8

Descriptive Statistics

	Mean	Std. Deviation	N
HP_3_M_5	1.33000669	.499644904	16
HP_3_M_65	2.2390678	.93513272	16
HP_3_M_8	3.9604166	2.26127498	16
HP_3_ML_5	2.27147475	.853247813	16
HP_3_ML_65	3.4324837	1.20502048	16
HP_3_ML_8	5.6538667	2.53571264	16

Multivariate Tests[a]

Effect		Value	F	Hypothesis df	Error df	Sig.
System	Pillai's Trace	.734	41.440[b]	1.000	15.000	.000
	Wilks' Lambda	.266	41.440[b]	1.000	15.000	.000
	Hotelling's Trace	2.763	41.440[b]	1.000	15.000	.000
	Roy's Largest Root	2.763	41.440[b]	1.000	15.000	.000
Speed	Pillai's Trace	.778	24.515[b]	2.000	14.000	.000
	Wilks' Lambda	.222	24.515[b]	2.000	14.000	.000
	Hotelling's Trace	3.502	24.515[b]	2.000	14.000	.000
	Roy's Largest Root	3.502	24.515[b]	2.000	14.000	.000
System * Speed	Pillai's Trace	.288	2.833[b]	2.000	14.000	.093
	Wilks' Lambda	.712	2.833[b]	2.000	14.000	.093
	Hotelling's Trace	.405	2.833[b]	2.000	14.000	.093
	Roy's Largest Root	.405	2.833[b]	2.000	14.000	.093

Multivariate Tests[a]

Effect		Partial Eta Squared
System	Pillai's Trace	.734
	Wilks' Lambda	.734
	Hotelling's Trace	.734
	Roy's Largest Root	.734
Speed	Pillai's Trace	.778
	Wilks' Lambda	.778
	Hotelling's Trace	.778
	Roy's Largest Root	.778
System * Speed	Pillai's Trace	.288
	Wilks' Lambda	.288
	Hotelling's Trace	.288
	Roy's Largest Root	.288

a. Design: Intercept
Within Subjects Design: System + Speed + System * Speed

b. Exact statistic

Mauchly's Test of Sphericity[a]

Measure: MEASURE_1

Within Subjects Effect	Mauchly's W	Approx. Chi-Square	df	Sig.	Epsilon[b] Greenhouse-Geisser
System	1.000	.000	0	.	1.000
Speed	.269	18.368	2	.000	.578
System * Speed	.846	2.349	2	.309	.866

Mauchly's Test of Sphericity[a]

Measure: MEASURE_1

Within Subjects Effect	Epsilon[b]	
	Huynh-Feldt	Lower-bound
System	1.000	1.000
Speed	.596	.500
System * Speed	.969	.500

Tests the null hypothesis that the error covariance matrix of the orthonormalized transformed dependent variables is proportional to an identity matrix.

a. Design: Intercept
Within Subjects Design: System + Speed + System * Speed

b. May be used to adjust the degrees of freedom for the averaged tests of significance. Corrected tests are displayed in the Tests of Within-Subjects Effects table.

Tests of Within-Subjects Effects

Measure: MEASURE_1

Source		Type III Sum of Squares	df	Mean Square	F
System	Sphericity Assumed	39.083	1	39.083	41.440
	Greenhouse-Geisser	39.083	1.000	39.083	41.440
	Huynh-Feldt	39.083	1.000	39.083	41.440
	Lower-bound	39.083	1.000	39.083	41.440
Error(System)	Sphericity Assumed	14.147	15	.943	
	Greenhouse-Geisser	14.147	15.000	.943	
	Huynh-Feldt	14.147	15.000	.943	
	Lower-bound	14.147	15.000	.943	
Speed	Sphericity Assumed	149.291	2	74.645	34.145
	Greenhouse-Geisser	149.291	1.156	129.190	34.145
	Huynh-Feldt	149.291	1.191	125.344	34.145
	Lower-bound	149.291	1.000	149.291	34.145
Error(Speed)	Sphericity Assumed	65.584	30	2.186	
	Greenhouse-Geisser	65.584	17.334	3.784	
	Huynh-Feldt	65.584	17.866	3.671	
	Lower-bound	65.584	15.000	4.372	
System * Speed	Sphericity Assumed	2.344	2	1.172	3.615
	Greenhouse-Geisser	2.344	1.732	1.353	3.615
	Huynh-Feldt	2.344	1.938	1.209	3.615
	Lower-bound	2.344	1.000	2.344	3.615
Error(System*Speed)	Sphericity Assumed	9.727	30	.324	
	Greenhouse-Geisser	9.727	25.986	.374	
	Huynh-Feldt	9.727	29.077	.335	
	Lower-bound	9.727	15.000	.648	

Tests of Within-Subjects Effects

Measure: MEASURE_1

Source		Sig.	Partial Eta Squared
System	Sphericity Assumed	.000	.734
	Greenhouse-Geisser	.000	.734
	Huynh-Feldt	.000	.734
	Lower-bound	.000	.734
Error(System)	Sphericity Assumed		
	Greenhouse-Geisser		
	Huynh-Feldt		
	Lower-bound		
Speed	Sphericity Assumed	.000	.695
	Greenhouse-Geisser	.000	.695
	Huynh-Feldt	.000	.695
	Lower-bound	.000	.695
Error(Speed)	Sphericity Assumed		
	Greenhouse-Geisser		
	Huynh-Feldt		
	Lower-bound		
System * Speed	Sphericity Assumed	.039	.194
	Greenhouse-Geisser	.047	.194
	Huynh-Feldt	.041	.194
	Lower-bound	.077	.194
Error(System*Speed)	Sphericity Assumed		
	Greenhouse-Geisser		
	Huynh-Feldt		
	Lower-bound		

Tests of Within-Subjects Contrasts

Measure: MEASURE_1

Source	System	Speed	Type III Sum of Squares	df	Mean Square	F
System	Linear		39.083	1	39.083	41.440
Error(System)	Linear		14.147	15	.943	
Speed		Linear	144.615	1	144.615	40.537
		Quadratic	4.676	1	4.676	5.810
Error(Speed)		Linear	53.512	15	3.567	
		Quadratic	12.071	15	.805	
System * Speed	Linear	Linear	2.262	1	2.262	5.951
		Quadratic	.082	1	.082	.306
Error(System*Speed)	Linear	Linear	5.701	15	.380	
		Quadratic	4.026	15	.268	

Tests of Within-Subjects Contrasts

Measure: MEASURE_1

Source	System	Speed	Sig.	Partial Eta Squared
System	Linear		.000	.734
Error(System)	Linear			
Speed		Linear	.000	.730
		Quadratic	.029	.279
Error(Speed)		Linear		
		Quadratic		
System * Speed	Linear	Linear	.028	.284
		Quadratic	.588	.020
Error(System*Speed)	Linear	Linear		
		Quadratic		

Tests of Between-Subjects Effects

Measure: MEASURE_1
Transformed Variable: Average

Source	Type III Sum of Squares	df	Mean Square	F	Sig.	Partial Eta Squared
Intercept	951.282	1	951.282	107.083	.000	.877
Error	133.254	15	8.884			

Estimated Marginal Means

1. Grand Mean

Measure: MEASURE_1

Mean	Std. Error	95% Confidence Interval	
		Lower Bound	Upper Bound
3.148	.304	2.500	3.796

2. System

Estimates

Measure: MEASURE_1

System	Mean	Std. Error	95% Confidence Interval	
			Lower Bound	Upper Bound
1	2.510	.281	1.911	3.109
2	3.786	.355	3.030	4.542

Pairwise Comparisons

Measure: MEASURE_1

(I) System	(J) System	Mean Difference (I-J)	Std. Error	Sig.[b]	95% Confidence Interval for Difference[b]	
					Lower Bound	Upper Bound
1	2	-1.276*	.198	.000	-1.699	-.854
2	1	1.276*	.198	.000	.854	1.699

Based on estimated marginal means

*. The mean difference is significant at the .05 level.

b. Adjustment for multiple comparisons: Least Significant Difference (equivalent to no adjustments).

Multivariate Tests

	Value	F	Hypothesis df	Error df	Sig.	Partial Eta Squared
Pillai's trace	.734	41.440[a]	1.000	15.000	.000	.734
Wilks' lambda	.266	41.440[a]	1.000	15.000	.000	.734
Hotelling's trace	2.763	41.440[a]	1.000	15.000	.000	.734
Roy's largest root	2.763	41.440[a]	1.000	15.000	.000	.734

Each F tests the multivariate effect of System. These tests are based on the linearly independent pairwise comparisons among the estimated marginal means.

a. Exact statistic

3. Speed

Estimates

Measure: MEASURE_1

Speed	Mean	Std. Error	95% Confidence Interval	
			Lower Bound	Upper Bound
1	1.801	.154	1.472	2.129
2	2.836	.253	2.297	3.375
3	4.807	.571	3.589	6.025

Pairwise Comparisons

Measure: MEASURE_1

(I) Speed	(J) Speed	Mean Difference (I-J)	Std. Error	Sig.[b]	95% Confidence Interval for Difference[b]	
					Lower Bound	Upper Bound
1	2	-1.035*	.159	.000	-1.374	-.696
	3	-3.006*	.472	.000	-4.013	-2.000
2	1	1.035*	.159	.000	.696	1.374
	3	-1.971*	.402	.000	-2.828	-1.115
3	1	3.006*	.472	.000	2.000	4.013
	2	1.971*	.402	.000	1.115	2.828

Based on estimated marginal means

*. The mean difference is significant at the .05 level.

b. Adjustment for multiple comparisons: Least Significant Difference (equivalent to no adjustments).

Multivariate Tests

	Value	F	Hypothesis df	Error df	Sig.	Partial Eta Squared
Pillai's trace	.778	24.515[a]	2.000	14.000	.000	.778
Wilks' lambda	.222	24.515[a]	2.000	14.000	.000	.778
Hotelling's trace	3.502	24.515[a]	2.000	14.000	.000	.778
Roy's largest root	3.502	24.515[a]	2.000	14.000	.000	.778

Each F tests the multivariate effect of Speed. These tests are based on the linearly independent pairwise comparisons among the estimated marginal means.

a. Exact statistic

4. System * Speed

Measure: MEASURE_1

System	Speed	Mean	Std. Error	95% Confidence Interval Lower Bound	Upper Bound
1	1	1.330	.125	1.064	1.596
	2	2.239	.234	1.741	2.737
	3	3.960	.565	2.755	5.165
2	1	2.271	.213	1.817	2.726
	2	3.432	.301	2.790	4.075
	3	5.654	.634	4.303	7.005

Profile Plots

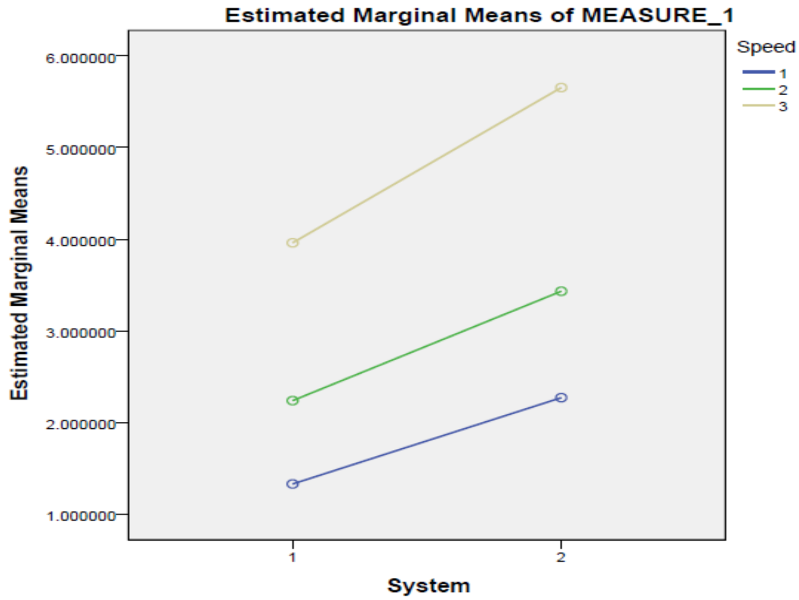

General Linear Model

Within-Subjects Factors

Measure: MEASURE_1

System	Speed	Dependent Variable
1	1	HP_3_T_M_5
	2	HP_3_T_M_65
	3	HP_3_T_M_8
2	1	HP_3_T_ML_5
	2	HP_3_T_ML_65
	3	HP_3_T_ML_8

Descriptive Statistics

	Mean	Std. Deviation	N
HP_3_T_M_5	65.31250	5.653421	16
HP_3_T_M_65	63.8688	6.21779	16
HP_3_T_M_8	59.9250	6.13715	16
HP_3_T_ML_5	62.7500	4.24154	16
HP_3_T_ML_65	59.5687	4.36879	16
HP_3_T_ML_8	58.8313	5.21354	16

Multivariate Tests[a]

Effect		Value	F	Hypothesis df	Error df	Sig.	Partial Eta Squared
System	Pillai's Trace	.365	8.618[b]	1.000	15.000	.010	.365
	Wilks' Lambda	.635	8.618[b]	1.000	15.000	.010	.365
	Hotelling's Trace	.575	8.618[b]	1.000	15.000	.010	.365
	Roy's Largest Root	.575	8.618[b]	1.000	15.000	.010	.365
Speed	Pillai's Trace	.503	7.086[b]	2.000	14.000	.007	.503
	Wilks' Lambda	.497	7.086[b]	2.000	14.000	.007	.503
	Hotelling's Trace	1.012	7.086[b]	2.000	14.000	.007	.503
	Roy's Largest Root	1.012	7.086[b]	2.000	14.000	.007	.503
System * Speed	Pillai's Trace	.384	4.369[b]	2.000	14.000	.034	.384
	Wilks' Lambda	.616	4.369[b]	2.000	14.000	.034	.384
	Hotelling's Trace	.624	4.369[b]	2.000	14.000	.034	.384
	Roy's Largest Root	.624	4.369[b]	2.000	14.000	.034	.384

a. Design: Intercept
Within Subjects Design: System + Speed + System * Speed

b. Exact statistic

Mauchly's Test of Sphericity[a]

Measure: MEASURE_1

Within Subjects Effect	Mauchly's W	Approx. Chi-Square	df	Sig.	Epsilon[b] Greenhouse-Geisser	Epsilon[b] Huynh-Feldt	Epsilon[b] Lower-bound
System	1.000	.000	0	.	1.000	1.000	1.000
Speed	.283	17.654	2	.000	.583	.601	.500
System * Speed	.590	7.390	2	.025	.709	.762	.500

Tests the null hypothesis that the error covariance matrix of the orthonormalized transformed dependent variables is proportional to an identity matrix.

a. Design: Intercept
Within Subjects Design: System + Speed + System * Speed

b. May be used to adjust the degrees of freedom for the averaged tests of significance. Corrected tests are displayed in the Tests of Within-Subjects Effects table.

Tests of Within-Subjects Effects

Measure: MEASURE_1

Source		Type III Sum of Squares	df	Mean Square	F
System	Sphericity Assumed	168.805	1	168.805	8.618
	Greenhouse-Geisser	168.805	1.000	168.805	8.618
	Huynh-Feldt	168.805	1.000	168.805	8.618
	Lower-bound	168.805	1.000	168.805	8.618
Error(System)	Sphericity Assumed	293.810	15	19.587	
	Greenhouse-Geisser	293.810	15.000	19.587	
	Huynh-Feldt	293.810	15.000	19.587	
	Lower-bound	293.810	15.000	19.587	
Speed	Sphericity Assumed	346.429	2	173.215	13.393
	Greenhouse-Geisser	346.429	1.165	297.346	13.393
	Huynh-Feldt	346.429	1.203	288.011	13.393
	Lower-bound	346.429	1.000	346.429	13.393
Error(Speed)	Sphericity Assumed	388.011	30	12.934	
	Greenhouse-Geisser	388.011	17.476	22.202	
	Huynh-Feldt	388.011	18.043	21.505	
	Lower-bound	388.011	15.000	25.867	
System * Speed	Sphericity Assumed	41.216	2	20.608	1.977
	Greenhouse-Geisser	41.216	1.418	29.061	1.977
	Huynh-Feldt	41.216	1.524	27.052	1.977
	Lower-bound	41.216	1.000	41.216	1.977
Error(System*Speed)	Sphericity Assumed	312.764	30	10.425	
	Greenhouse-Geisser	312.764	21.274	14.701	
	Huynh-Feldt	312.764	22.854	13.685	
	Lower-bound	312.764	15.000	20.851	

Tests of Within-Subjects Effects

Measure: MEASURE_1

Source		Sig.	Partial Eta Squared
System	Sphericity Assumed	.010	.365
	Greenhouse-Geisser	.010	.365
	Huynh-Feldt	.010	.365
	Lower-bound	.010	.365
Error(System)	Sphericity Assumed		
	Greenhouse-Geisser		
	Huynh-Feldt		
	Lower-bound		
Speed	Sphericity Assumed	.000	.472
	Greenhouse-Geisser	.001	.472
	Huynh-Feldt	.001	.472
	Lower-bound	.002	.472
Error(Speed)	Sphericity Assumed		
	Greenhouse-Geisser		
	Huynh-Feldt		
	Lower-bound		
System * Speed	Sphericity Assumed	.156	.116
	Greenhouse-Geisser	.171	.116
	Huynh-Feldt	.169	.116
	Lower-bound	.180	.116
Error(System*Speed)	Sphericity Assumed		
	Greenhouse-Geisser		
	Huynh-Feldt		
	Lower-bound		

Tests of Within-Subjects Contrasts

Measure: MEASURE_1

Source	System	Speed	Type III Sum of Squares	df	Mean Square	F
System	Linear		168.805	1	168.805	8.618
Error(System)	Linear		293.810	15	19.587	
Speed		Linear	346.425	1	346.425	14.556
		Quadratic	.004	1	.004	.002
Error(Speed)		Linear	356.992	15	23.799	
		Quadratic	31.018	15	2.068	
System * Speed	Linear	Linear	8.629	1	8.629	1.007
		Quadratic	32.588	1	32.588	2.653
Error(System*Speed)	Linear	Linear	128.489	15	8.566	
		Quadratic	184.275	15	12.285	

Tests of Within-Subjects Contrasts

Measure: MEASURE_1

Source	System	Speed	Sig.	Partial Eta Squared
System	Linear		.010	.365
Error(System)	Linear			
Speed		Linear	.002	.492
		Quadratic	.965	.000
Error(Speed)		Linear		
		Quadratic		
System * Speed	Linear	Linear	.331	.063
		Quadratic	.124	.150
Error(System*Speed)	Linear	Linear		
		Quadratic		

Tests of Between-Subjects Effects

Measure: MEASURE_1

Transformed Variable: Average

Source	Type III Sum of Squares	df	Mean Square	F	Sig.	Partial Eta Squared
Intercept	365572.508	1	365572.508	3441.035	.000	.996
Error	1593.587	15	106.239			

Estimated Marginal Means

1. Grand Mean

Measure: MEASURE_1

Mean	Std. Error	95% Confidence Interval	
		Lower Bound	Upper Bound
61.709	1.052	59.467	63.952

2. System

Estimates

Measure: MEASURE_1

System	Mean	Std. Error	95% Confidence Interval	
			Lower Bound	Upper Bound
1	63.035	1.350	60.158	65.913
2	60.383	.894	58.478	62.289

4. System * Speed

Measure: MEASURE_1

System	Speed	Mean	Std. Error	95% Confidence Interval	
				Lower Bound	Upper Bound
1	1	65.313	1.413	62.300	68.325
	2	63.869	1.554	60.556	67.182
	3	59.925	1.534	56.655	63.195
2	1	62.750	1.060	60.490	65.010
	2	59.569	1.092	57.241	61.897
	3	58.831	1.303	56.053	61.609

Profile Plots

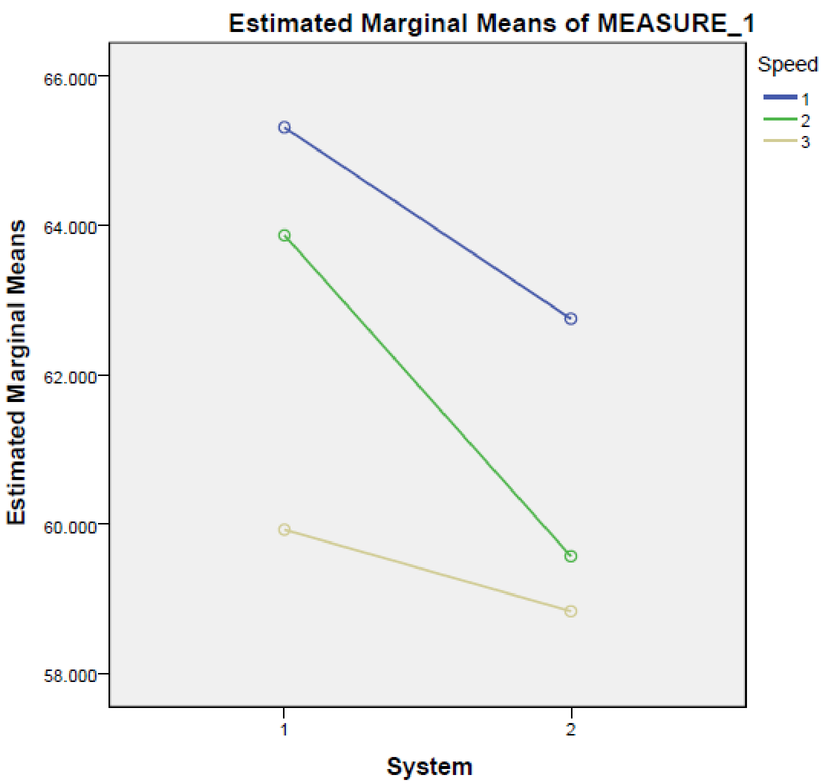

Pairwise Comparisons

Measure: MEASURE_1

(I) System	(J) System	Mean Difference (I-J)	Std. Error	Sig.[b]	95% Confidence Interval for Difference[b]	
					Lower Bound	Upper Bound
1	2	2.652*	.903	.010	.727	4.578
2	1	-2.652*	.903	.010	-4.578	-.727

Based on estimated marginal means

*. The mean difference is significant at the .05 level.

b. Adjustment for multiple comparisons: Least Significant Difference (equivalent to no adjustments).

Multivariate Tests

	Value	F	Hypothesis df	Error df	Sig.	Partial Eta Squared
Pillai's trace	.365	8.618[a]	1.000	15.000	.010	.365
Wilks' lambda	.635	8.618[a]	1.000	15.000	.010	.365
Hotelling's trace	.575	8.618[a]	1.000	15.000	.010	.365
Roy's largest root	.575	8.618[a]	1.000	15.000	.010	.365

Each F tests the multivariate effect of System. These tests are based on the linearly independent pairwise comparisons among the estimated marginal means.

a. Exact statistic

3. Speed

Estimates

Measure: MEASURE_1

Speed	Mean	Std. Error	95% Confidence Interval	
			Lower Bound	Upper Bound
1	64.031	.916	62.080	65.983
2	61.719	1.148	59.271	64.166
3	59.378	1.404	56.385	62.371

Pairwise Comparisons

Measure: MEASURE_1

(I) Speed	(J) Speed	Mean Difference (I-J)	Std. Error	Sig.[b]	95% Confidence Interval for Difference[b]	
					Lower Bound	Upper Bound
1	2	2.313*	.736	.007	.744	3.881
	3	4.653*	1.220	.002	2.054	7.253
2	1	-2.313*	.736	.007	-3.881	-.744
	3	2.341*	.629	.002	.999	3.682
3	1	-4.653*	1.220	.002	-7.253	-2.054
	2	-2.341*	.629	.002	-3.682	-.999

Based on estimated marginal means

*. The mean difference is significant at the .05 level.

b. Adjustment for multiple comparisons: Least Significant Difference (equivalent to no adjustments).

Multivariate Tests

	Value	F	Hypothesis df	Error df	Sig.	Partial Eta Squared
Pillai's trace	.503	7.086[a]	2.000	14.000	.007	.503
Wilks' lambda	.497	7.086[a]	2.000	14.000	.007	.503
Hotelling's trace	1.012	7.086[a]	2.000	14.000	.007	.503
Roy's largest root	1.012	7.086[a]	2.000	14.000	.007	.503

Each F tests the multivariate effect of Speed. These tests are based on the linearly independent pairwise comparisons among the estimated marginal means.

a. Exact statistic

Spatial Parameter Mapping Results of Two-way Repeated Measure ANOVA

MATLAB Codes:

Two-way repeated measure ANOVA

```
clear;  clc
Y = xlsread("Hip power.xlsx");
A = xlsread("Systems.xlsx");
B = xlsread("Speeds.xlsx");
SUBJ = xlsread("SUBJ.xlsx");

%(1) Conduct SPM analysis:
spmlist   = spm1d.stats.anova2onerm(Y, A, B, SUBJ);
spmilist  = spmlist.inference(0.05);
disp_summ(spmilist)
close all
spmilist.plot();

%(2) Plot:
close all
spmilist.plot('plot_threshold_label',false, 'plot_p_values',true, 'autoset_ylim',true);
```

Simple linear regression:

```
%simple linear regression analysis;
clear;  clc
y = xlsread("leg COM&hip moment.xlsx");
x = xlsread("Parameters.xlsx");

% %(0a) Create region(s) of interest (ROI):
% roi = false( 1, size(y,2) );
% roi(40:56) = true;


%(1) Conduct test using spm1d:
spm = spm1d.stats.regress(y,x);
spmi = spm.inference(0.05, 'two_tailed', true);
% disp(spmi)
% r = spm.r
% r2 = spm.r.^2;
% r=r';
% r2=r2';

%(2) Plot:
close all
spmi.plot();
spmi.plot_threshold_label();
spmi.plot_p_values();

% filename = 'Ankle joint moment_r.xlsx';
% xlrange1 = 'A1:A101';
% xlrange2 = 'B1:B101';
% xlswrite(filename, r, xlrange1);
% xlswrite(filename, r2, xlrange2);
```

SPM MATLAB codes sources for different statistical analysis came from:https://spm1d.org/Downloads.html

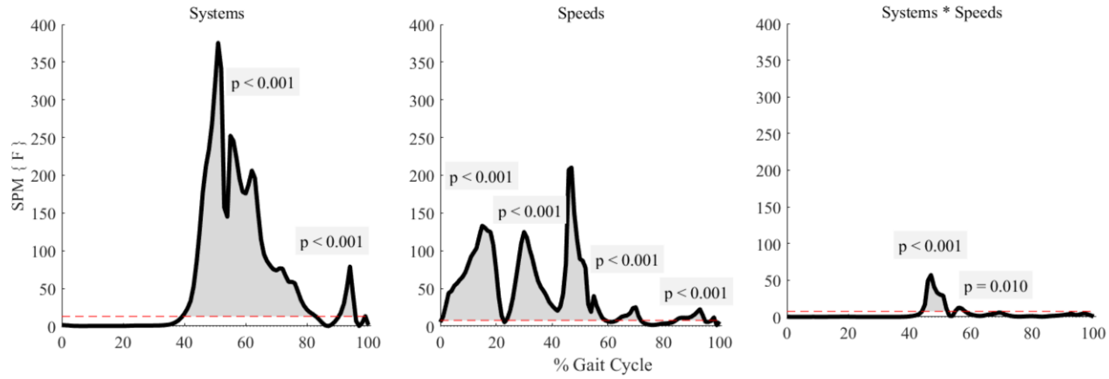

Figure 1. SPM results of repeated measure ANOVA of ankle joint moment

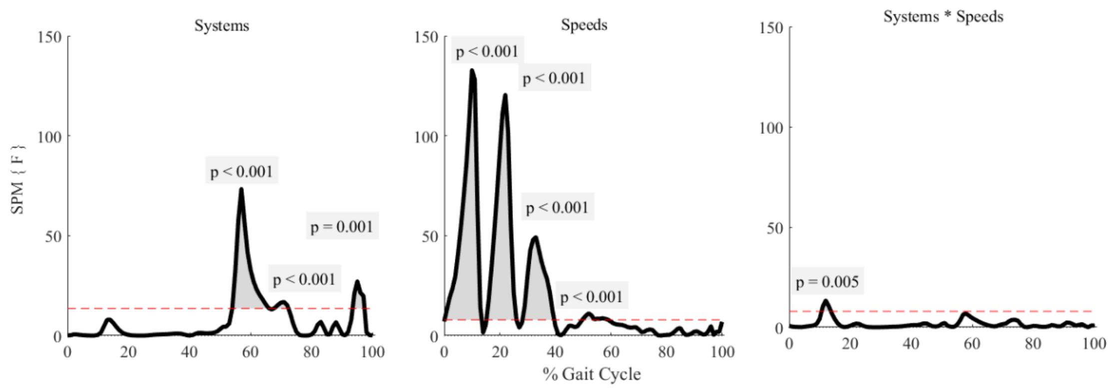

Figure 2. SPM results of repeated measure ANOVA of ankle joint power

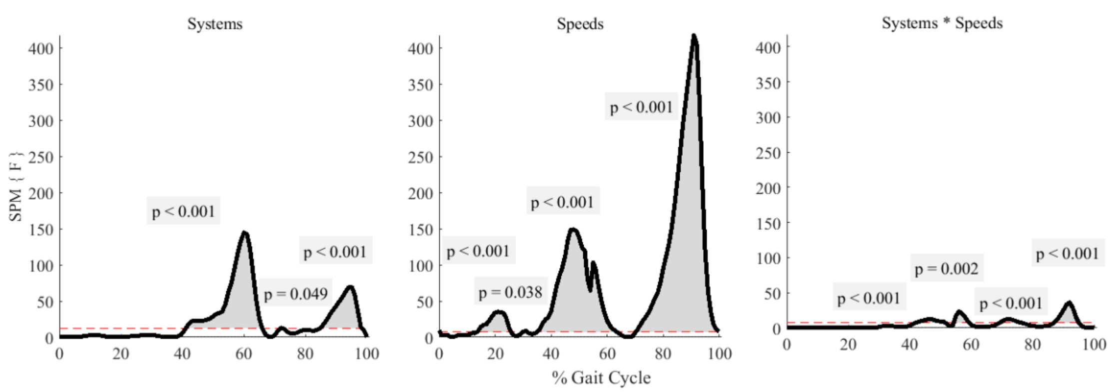

Figure 3. SPM results of repeated measure ANOVA of knee joint moment

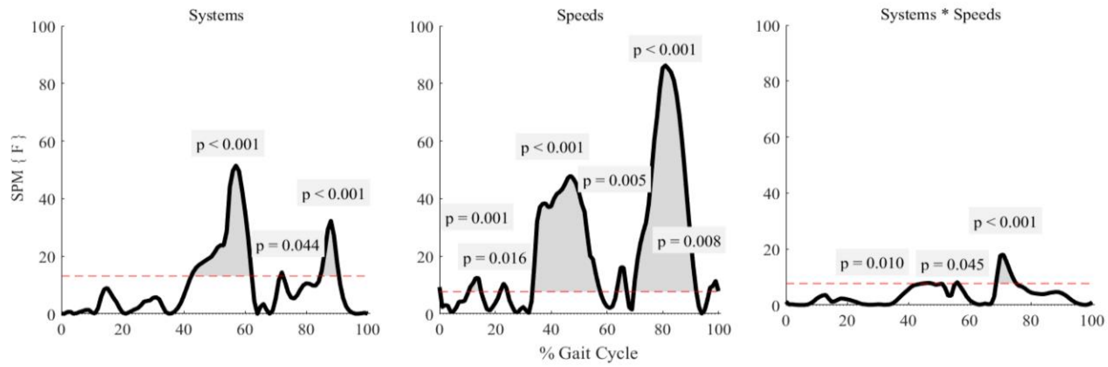

Figure 4. SPM results of repeated measure ANOVA of knee joint power

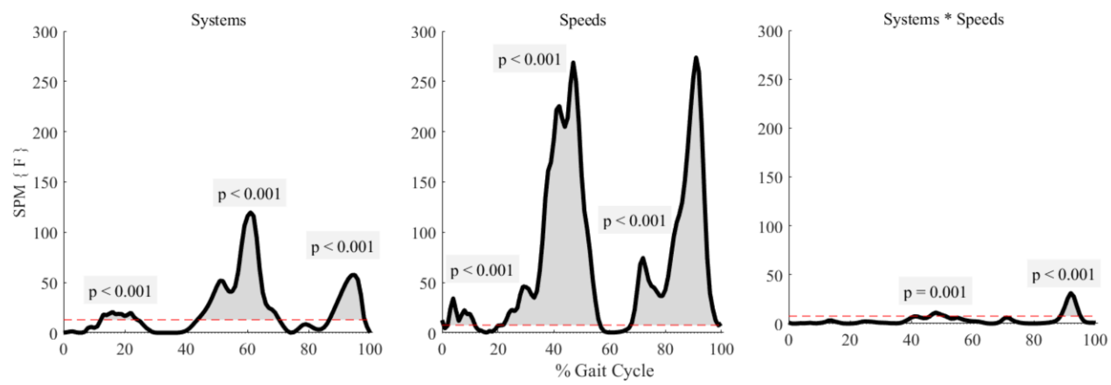

Figure 5. SPM results of repeated measure ANOVA of hip moment

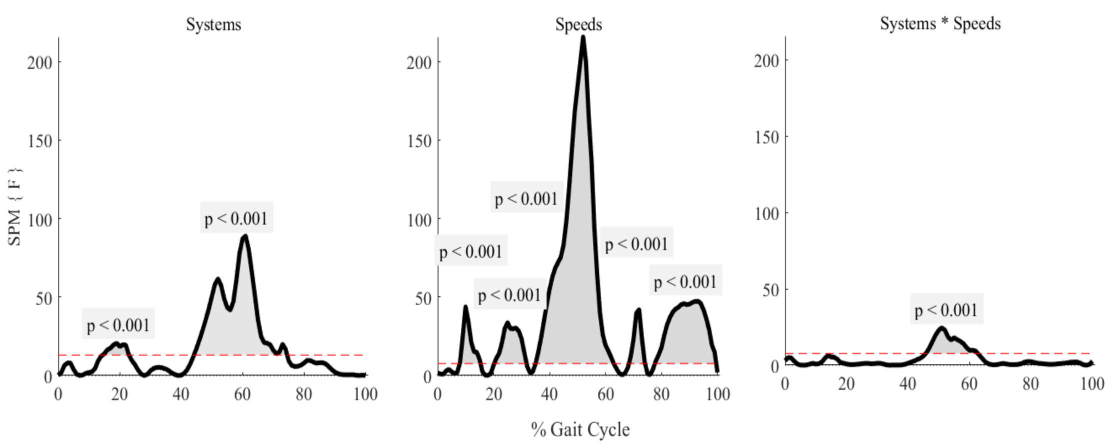

Figure 6. SPM results of repeated measure ANOVA of hip power

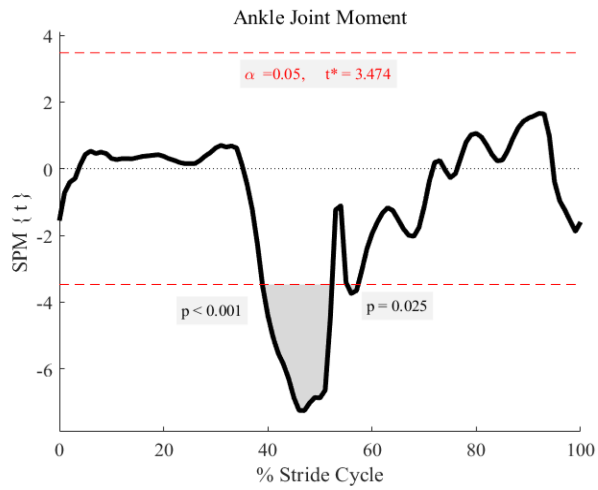

Figure 7. SPM results of simple linear regression of ankle joint moment

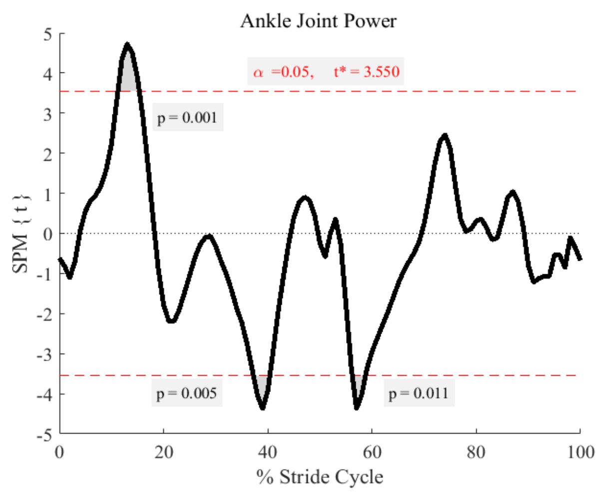

Figure 8. SPM results of simple linear regression of ankle joint power

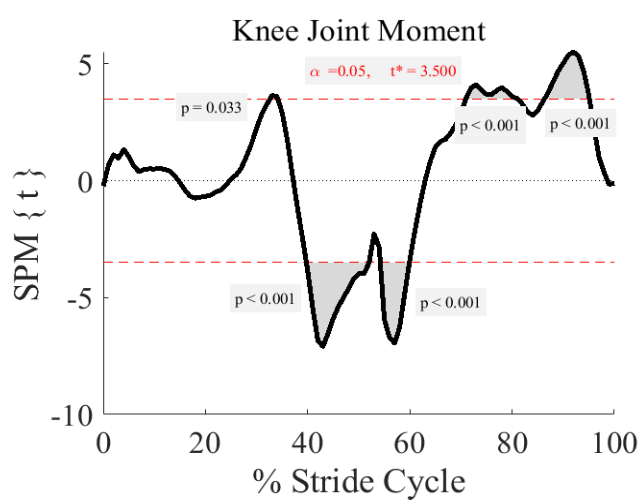

Figure 9. SPM results of simple linear regression of knee joint moment

Figure 10. SPM results of simple linear regression of knee joint power

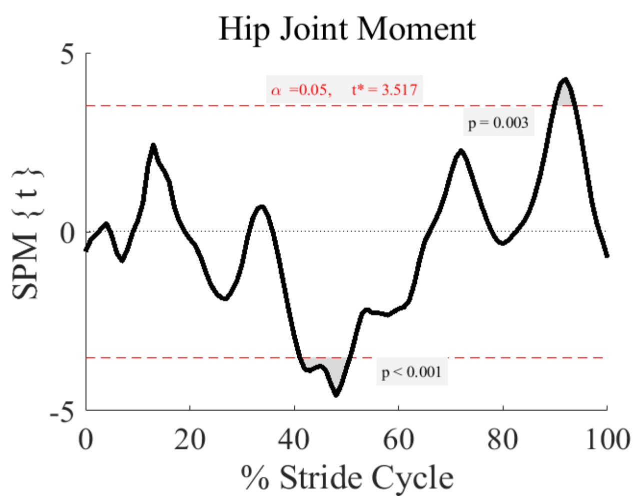

Figure 11. SPM results of simple linear regression of hip joint moment

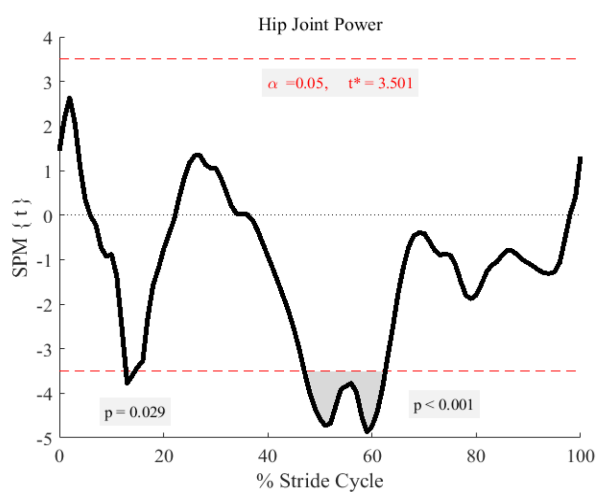

Figure 12. SPM results of simple linear regression of hip joint power

APPENDIX D

INSTITUTIONAL REVIEW BOARD

GEORGIA SOUTHERN UNIVERSITY

RESEARCH INTEGRITY

Institutional Review Board (IRB)

Application for Research Approval – Expedited/Full Board

For Office Use Only: Protocol ID ______________

Please submit this protocol to IRB@georgiasouthern.edu in a single email; scanned signatures and official Adobe electronic signatures are accepted. Applications may also be submitted via mail to the Research Integrity office, PO Box 8005.

Principal Investigator	
PI's Name: Hui Tang	Phone: 912-582-1607
Email: ht01253@georgiasouthern.edu (Note: Georgia Southern email addresses will be used for all correspondence.)	Department: Health Sciences & Kinesiology College: WCHPWCHP
Primary Campus: ☒ Statesboro Campus ☐ Armstrong Campus ☐ Liberty Campus	
☐ Faculty ☐ Doctoral ☐ Specialist ☒ Masters ☐ Undergraduate ☐ Other:	
Georgia Southern Co-Investigator(s)	
Co-I's Name(s): Benjamin Paquette (M), Petra Kis (M), Li Li (F) (By each name indicate: F(Faculty), D(Doctoral), S(Specialist), M(Masters), U(Undergraduate), O(Other))	Email: bp11854@georgiasouthern.edu; pk03815@georgiasouthern.edu; lili@georgiasouthern.edu (Note: Georgia Southern email addresses will be used for all correspondence.)
Personnel and/or Institutions Outside of Georgia Southern University involved in this research:	
	☐ Training Attached ☐ IRB Approval Attached ☐ intent to rely on GS
	☐ Training Attached ☐ IRB Approval Attached ☐ intent to rely on GS

Project Information	
Title: Concurrent Assessment of Gait Biomechanics Using Markerless and Marker-based Motion Capture Systems	
Number of Subjects (Maximum) : 40	
Will you be using monetary incentives (cash and/or gift cards)? ☐ Yes X No	
☒ Self-funded/non-funded ☐ Internal Georgia Southern Internal Source:	☐ External Funding (*You are responsible for duplicate or additional approval submissions required by funders.*) Funding Source: ☐ Federal ☐ State ☐ Private ☐ Contract Funding Agency: Grant Number: 39G Grant Title: ☐ Same as above Enter here: ☐ Funding application scope of work attached
Compliance Information	
Do you or any investigator on this project have a financial interest in the subjects, study outcome, or project sponsor? (A disclosed conflict of interest will not preclude approval. An undisclosed conflict of interest will result in disciplinary action.). ☐ Yes ☒ No (If yes attach disclosure form)	

Certifications

I certify that the statements made in this request are accurate and complete, and if I receive IRB approval for this project, I agree to inform the IRB in writing of any emergent problems or proposed procedural changes. I agree not to proceed with the project until the problems have been resolved or the IRB has reviewed and approved the changes. It is the explicit responsibility of the researchers and supervising faculty/staff to ensure the well-being of human participants. At the conclusion of the project, I will submit a report. A report must be submitted no later than 12 months after project initiation.

Hui Tang ______________ | April 28th, 2022
Signature of Primary Investigator | Date

______________ | April 28th, 2022
Signature of Co-Investigator(s) | Date

By signing this cover page, I acknowledge that I have reviewed and approved this protocol for scientific merit, rationale, and significance. I further acknowledge that I approve the ethical basis for the study.

If faculty project, please have department chair sign; if student project, please have research advisor sign:

Li Li		April 28th , 2022
Typed/Printed Name	Signature	Date

Compliance Information	
Please indicate which of the following will be used in your research: (applications may be submitted simultaneously)	
☒ Human Subjects ☐ Care and Use of Vertebrate Animals (Submit IACUC Application) ☐ Biohazards (Submit IBC Application)	
Please indicate if the following are included in the study (Check all that apply):	
☒ Recruitment delivered to georgiasouthern.edu email addresses ☐ Deception ☐ Prisoners ☐ Children ☐ Individuals with impaired decision-making capacity, or economically or educationally disadvantaged persons	☐ Video or Audio Recordings ☐ Human Subjects Incentives ☒ Medical Procedures, including exercise, administering drugs/dietary supplements, and other procedures, or ingestion of any substance
Is your project a research study in which one or more human subjects are prospectively assigned to one or more interventions (which may include placebo or other control) to evaluate the effects of those interventions on health-related biomedical or behavioral outcomes. See the IRB FAQ for help with the definition above. ☐ Yes ☒ No If yes, attach Good Clinical Practice (GCP) CITI training appropriate to the project.	

Instructions: Please respond to the following as clearly as possible. The application should include a step by step plan of how you will obtain your subjects, conduct the research, and analyze the data. Make sure the application clearly explains aspects of the methodology that provide protections for your human subjects. Your application should be written to be read and understood by a general audience who does not have prior knowledge of your research and by committee members who may not be expert in your specific field of research. Your reviewers will only have the information you provide in your application. Explain any technical terms, jargon or acronyms.

DO NOT REMOVE THE QUESTIONS/PROMPTS.

1. Personnel
A. *Please list ALL individuals who will be conducting research on this study. This includes the principal investigator, co-investigators, and any additional personnel. Please describe the level of involvement in the process and the access to information/data that each may have.*
a. Hui Tang: Hui is responsible for participant recruitment, data collection, and interpretation. Hui has access to all data. Deidentified data will be stored in a password-protected computer in the lab.

b. Benjamin Paquette: Benjamin is the Co-Investigator and is responsible for participant recruitment and data collection. Benjamin has access to all data. Deidentified data will be stored in a password-protected computer in the lab.
c. Petra Kis: Petra will help the parrticipants recruitment and data collection. Petra has access to all data. Deidentified data will be stored in a password-protected computer in the lab.
d. Li Li, Ph.D.: Co-Investigator and advisor. Dr. Li will assist with participant recruitment, data collection, and interpretation. Dr. Li has access to all data. Informed consent and corresponding participating code will be stored in a locked cabinet in Dr. Li's office.

e. *Please detail the experience of each researcher. Please include any credentials, training, or education that directly relate to the procedures in this research. Specifically, address any experience or knowledge that will help mitigate any risks associated with this research.*

Hui has been working in the biomechanical lab for over one year and is familiar with biomechanical equipment such as motion capture systems and force-plate embedded treadmill. She has conducted whole-body motion capture experiments safely and successfully.

Benjamin has been working in the biomechanical lab and the athletic training department for one year. He is familiar with clinical biomechanics applications.

Petra has been working in the biomechanical lab for about a year and is familiar with biomechanical equipment such as motion capture systems, and force plates. She has conducted a lower body motion capture experiment safely and successfully.

Dr. Li has been working in the biomechanics field for over thirty years. The experiment design will be repeatedly supervised. We have been piloting the protocol, adjusting the fastest running speed to 8 miles/h for recreational athletes and healthy participants, without any adverse events.

2. Purpose

A. *Briefly describe in one or two sentences the purpose of your research.*

The aim of this research is to validate a markerless motion capture system for measuring biomechanical features during treadmill running at three different speeds.

B. *What questions are you trying to answer in this project? Please include your research question in this section. The jurisdiction of the IRB requires that we ensure the appropriateness of research. It is unethical to put participants at risk without the possibility of sound scientific result. For this reason, you should be very clear about how participants and others will benefit from knowledge gained in this project.*

This investigation asks: a) how the markerless compared to the marker-based motion capture system (gold standard) in gait biomechanical study; b) how time series affect the accuracy of the markerless system in gait kinematics and kinetics. We hypothesize that: a) calculated kinematic and kinetic parameters from the markerless system would be accurate and consistent with the marker-based system; b) the markerless system will be more accurate as time series.

A better understanding of the markerless motion capture system will help researchers resolve the time-consuming and limit size issues in motion capture studies. The improvements in the application of this technology will provide participants with an easy way to cooperate with researchers with effectiveness and efficiency.

C. *Provide a brief description of how this study fits into the current literature. Have the research procedures been used before? How were similar risks controlled for and documented in the literature? Have your instruments been validated with this audience? Include citations in the description. Do not include dissertation or thesis chapters.*

Researchers and clinicians use three-dimensional (3D) motion capture systems to analyze the biomechanics of human movement. While marker-based motion capture systems are considered as the non-invasive gold standard of motion analysis, it is time-consuming to set up and process data (1), limiting their use in large studies (2). Newly developed markerless motion capture has the potential to alleviate some of the technical and practical issues of marker-based motion analysis by replacing physical palpation and skin surface marker tracking of bony landmarks with probabilistic estimation of landmark positions using trained neural networks (3-4). However, the dispute about the reliability and validity of a markerless system is constant.

According to previous literature, markerless motion capture can provide reliable kinematic analysis in gait studies (5-7) where kinematic analysis has been focused on lower limb joint poses and angles. For example, Sandau et al. (2014) applied highly detailed 3D reconstructions to compare the poses of the hip, knee, and ankle joints during walking overground. Kan et al. (2021) investigated the lower limb segment pose and joint angles of walking gaits on the treadmill (3).

However, there is no study probing the comparisons of gait kinematics and kinetics of different running speeds using markerless and marker-based motion capture systems. To better understand how reliable the markerless system in both gait kinematics and kinetics in a clinical setting is, this project will apply the speed-varied running protocol in gait biomechanical studies. Risk management was prepared for this research by performing pre-running warm-up and post-running relaxation.

References:

1. S.G. McLean, K. Walker, K.R. Ford, G.D. Myer, T.E. Hewett, A.J. van den Bogert, Evaluation of a two dimensional analysis method as a screening and evaluation tool for anterior cruciate ligament injury, BJSM 39 (2005) 355–362.
2. Perrott, M. A., Pizzari, T., Cook, J., & McClelland, J. A. (2017). Comparison of lower limb and trunk kinematics between markerless and marker-based motion capture systems. Gait & posture, 52, 57-61.
3. Kanko, R. M., Laende, E. K., Davis, E. M., Selbie, W. S., & Deluzio, K. J. (2021). Concurrent assessment of gait kinematics using marker-based and markerless motion capture. Journal of biomechanics, 127, 110665.
4. Mathis, A., Mamidanna, P., Cury, K. M., Abe, T., Murthy, V. N., Mathis, M. W., & Bethge, M. (2018). DeepLabCut: markerless pose estimation of user-defined body parts with deep learning. Nature neuroscience, 21(9), 1281-1289.
5. Sandau, M., Koblauch, H., Moeslund, T. B., Aanæs, H., Alkjær, T., & Simonsen, E. B. (2014). Markerless motion capture can provide reliable 3D gait kinematics in the extension/flexion and frontal plane. Medical engineering & physics, 36(9), 1168-1175.
6. Ong, A., Harris, I. S., & Hamill, J. (2017). The efficacy of a video-based marker-less tracking system for gait analysis. Computer methods in biomechanics and biomedical engineering, 20(10), 1089-1095.
7. Ceseracciu, E., Sawacha, Z., & Cobelli, C. (2014). Comparison of markerless and marker-based motion capture technologies through simultaneous data collection during gait: proof of concept. PloS one, 9(3), e87640.

3. Outcome

Please state what results you expect to achieve. Who will benefit from this study? How will the participants benefit (if at all)? Remember that the participants do not necessarily have to benefit directly. The results of your study may have broadly stated outcomes for a large number of people or society in general.

In this project, we expect to see: a) calculated kinematic and kinetic parameters from the markerless system would be accurate and consistent with the marker-based system; b) the markerless system becomes more reliable over time. The outcome of this project will directly propel the development of motion-based biomechanical studies. The markerless motion capture system will help researchers to resolve the time-consuming and limiting size problems in biomechanical studies. The validity of a markerless system will provide researchers with a better understanding when applying this technology.

Participants in this study may not have direct benefits. However, more people will benefit from the convenience of the markerless system if it is proven to be as good as the marker system.

4. Describe Your Subjects

A. *Maximum number of participants*

40

B. *Briefly describe the study population.*

This study will recruit healthy, recreationally active individuals of all genders between the age of 18 and 30 years old.

C. *Applicable inclusion or exclusion requirements (ages, gender requirements, allergies, etc.)*

The project includes healthy, recreationally active college students (between 18 to 30 years old) of all genders. Participants who answered “No” to all the PAR-Q questions, and did not check any boxes in the Present/Past History section of the Health History Questionnaire, will be defined as “healthy”. Participants are “recreationally active” are the ones who answered “Yes” to the first two questions of the Activity History section of the Health History Questionnaire. Exclusion criteria: participants who are screened by the EIM Health History Questionnaire (attached) with present/past history of “seizures”, “muscle or joint problems (e.g., back, knee)”, “pain, discomfort in the chest, neck, jaw, arms, or other areas”, “unusual fatigue or shortness of breath at rest or with light activity”, “temporary loss of clear vision or speech or short- term numbness or weakness in one side, arm, or leg of your body”, “intermittent claudication (calf cramping)” will be excluded from participation. People who answered "Yes" for any of the PAR-Q questions will also be excluded from participation.

D. *How long will each subject be involved in the project? (Number of occasions and duration)*

Each participant will visit the lab once for about 60 minutes. The lab visit will consist of 15 minutes guided warm-up exercise and three 2-minute-running sessions with different speeds (5, 6.5, and 8 miles/hour).

5. Recruitment

Describe how subjects will be recruited. (Attach a copy of recruitment emails, flyers, social media posts, etc.) DO NOT state that subjects will not be recruited.

Participants will be recruited from kinesiology courses offered on campus, such as Biomechanical Analysis of Movement (KINS 50453), Physiological Aspects of Exercise (KINS 50442), and Data Acquisition of Biomechanics (KINS 51699). The investigators will go to the classes with the instructors' permission and then distribute the recruitment flyers (attached) to the class. Potential questions will be discussed after the flyer distribution. Researchers' email addresses are provided on the flyer. Potential participants will contact the PI via their Georgia Southern email address. Future communication regarding the project will be conducted using Georgia Southern emails.

6. Incentives

A. *Are you compensating your subjects with money, course credit, extra credit, or other incentives?*

☐ Yes ☒ No

B. *If yes, indicate how much and how they will be distributed.*

C. *Describe if and how you will compensate subjects who withdraw from the project before it ends and any exclusion criteria from compensation.*

Not applicable

7. Research Procedures and Timeline

A. *Which statement best describes the procedures in this protocol (including recruitment, consent, interventions, etc,)?*

☐ This data is being collected without ANY in person interactions with participants (ie. online surveys, virtual interviews, etc.)

☐ This data is being collected in person with participants but without any direct physical contact (ie. in person interviews, in person focus groups, etc.). **Safety Plan REQUIRED**

☒ This data requires direct physical contact with participants (ie. placing sensors on a participant, etc.) **Safety Plan REQUIRED**

B. *Outline step-by-step what will happen to participants in this study (including what kind of experimental manipulations you will use, what kinds of questions or recording of behavior you will use, the location of these interactions). Focus on the interactions you will have with the human subjects. Specify tasks given as attachments to this document.*

The participants will receive PAR-Q and EIM-Health History Questionnaire through email communication (attacheed). They will be instructed to fill out these two questionnaires and send back to the experimenters. All participants' eligibility will be confirmed by experimenters after checking their filled questionnaires. PAR-Q is a 7-step questionnaire for use with persons of all ages that has been validated in many previous studies (1-3). It screens for evidence of risk factors during moderate physical activity and reviews family history and disease severity. If a potential participant answers yes to one or more questions, the individual may not be eligible for participation. EIM-Health-History Questionnaire is provided and validated by the American College of Sports Medicine (ACSM) and the American Medical Association (AMA) co-launched Exercise is Medicine (EIM) (4). By using this questionnaire, investigators can assess potential participants' level of physical activity by screening their past and current family and personal medical history. Before the first lab visit, eligible participants will be asked to read and sign the Informed Consent Form through email. All questions regarding the project will be answered satisfactorily.

Participants visit the Biomechanics Lab at Georgia Southern University at a scheduled time. Before the visit, participants will be advised to wear athletic attire and refrain from pre-workout in advance.

Each participant will be required to run on the instrumented treadmill (AMTI force-sensing tandem treadmill; MA, USA) in the balanced order: slow (5 miles/h), intermediate (6.5 miles/h), and fast (8 miles/h) running speeds. An eight high-speed camera system (Vue, Vicon, Oxford, UK) will be used to record motion video and sampling rate at 100 Hz. Another eight-camera motion capture system (Vero, Vicon, Oxford, UK) will be used to record the coordination of markers and sampling rate at 100 Hz. The instrumented treadmill will be used to record force data and sampling rate at 1000 Hz. The Nexus lock+ system (Vicon, Oxford, UK) will be used to synchronize. The data collection will use the Nexus system (Vicon, Oxford, UK).

Preparations for motion capture include:

1) Participants will change to minimal, skin-tight clothing and lab running shoes.
2) The researcher will record anthropometric measurements of each participant, such as body mass and height.
3) A set of retroreflective markers and tracking clusters are affixed to relevant anatomical landmarks and body segments (Figure 1).
4) Participants will perform 10 minutes warm-up exercises guided by researchers.
5) Participants will familiarize the running protocol on the treadmill guided by one researcher.
6) Each participant is required to stand still on the force-plate embedded treadmill with arms crossed for 2 seconds for the marker-based Vicon system to calibrate. However, the Thia system does not require calibration.

The running speed starts from slow (5 m/h) to fast (8 m/h). Two researchers will help the participant to accomplish the running motion capture process in the following steps:

1) With the verbal instruction, "Capture started", one investigator will help to increase to target speed (slow-5 miles/h, intermediate-6.5 miles/h, fast 8 miles/h). Meanwhile, the participant will transition from walking to running. When the participant reaches a steady speed and run for 2 minutes, the other investigator will record data for 30 seconds. Then, one

investigator will inform the participant to slow down and adjust the treadmill speed. The participant can stop and step out of the treadmill after hearing "Capture Ended".

2) To avoid fatigue, the participant will rest for 5 minutes between each running condition.
3) The participant will perform some relaxation guided by the investigator.

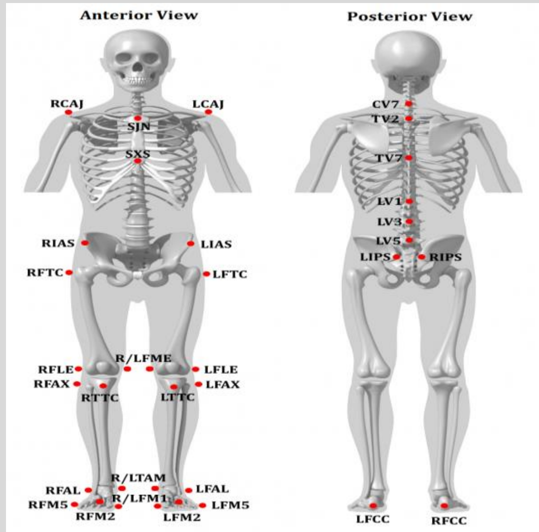

Figure 1. IOR Full-Body Model.

References:
1. Shephard, R. J. (1988). PAR-Q, Canadian Home Fitness Test and exercise screening alternatives. Sports medicine, 5(3), 185-195.
2. Adams, R. (1999). Revised Physical Activity Readiness Questionnaire. Canadian Family Physician, 45, 992.
3. Warburton, D. E., Bredin, S. S., Jamnik, V. K., & Gledhill, N. (2011). Validation of the PAR-Q+ and ePARmed-X+. The Health & Fitness Journal of Canada, 4(2), 38-46.
4. Exercise is Medicine, American College of Sports Medicine. https://www.exerciseismedicine.org/about-eim/

C. *Identify any activity included in the research description that will occur without modification regardless of the research effort. (E.g., A class exercise that is part of the normal course activities that is not altered for the research about which you will collect data or a team warm-up exercise session that is not altered for the study about which you will collect data.)* Answer "N/A" if this does not apply.

N/A

D. *Describe how legally effective informed consent will be obtained. (Also, attach a copy of the consent form(s).)*

A signed informed consent form will be collected through email communication after all questions are answered satisfactorily and before data collection.

E. *If minors are to be used describe procedures used to gain consent of their parent (s), guardian (s), or legal representative (s), and gain assent of the minor.*

☒ N/A or Explain:

F. *Describe all study instruments and whether they are validated. Attach copies of questionnaires, surveys, and/or interview questions used, labeled accordingly.*

Potential participant eligibility will be accessed using PAR-Q and EIM-Health-History questionnaire (attached). PAR-Q is a 7-step questionnaire for screening the risks of participating in physical activity by researchers and teachers worldwide for a long time. If a potential participant answers yes to one or more questions, the individual may not be eligible for participation. EIM-Health-History Questionnaire is prepared by the American College of Sports Medicine (ACSM) and the American Medical Association (AMA) co-launched Exercise is Medicine (EIM) which is more detailed than the PAR-Q. Investigators can assess potential participants' vulnerabilities in participating physical activity by screening family and personal medical history.

This study will use an eight high-speed camera system (Vue, Vicon, Oxford, UK) and another eight-camera motion capture system (Vero, Vicon, Oxford, UK) to capture running movement. The instrumented treadmill will be used to record force data. The Vicon motion capture system is considered as gold standard in the motion capture (1-3). The instrumented treadmill (AMTI force-sensing tandem treadmill; MA, USA) used in this study is reliable and safe equipment for kinetics data collection. It has been applied in both children (4) and older adults (5).

1. Miranda, D. L., Schwartz, J. B., Loomis, A. C., Brainerd, E. L., Fleming, B. C., & Crisco, J. J. (2011). Static and dynamic error of a biplanar videoradiography system using marker-based and markerless tracking techniques.

2. Ganguly, A., Rashidi, G., & Mombaur, K. (2021). Comparison of the Performance of the Leap Motion ControllerTM with a Standard Marker-Based Motion Capture System. Sensors, 21(5), 1750.
3. Rodrigues, T. B., Catháin, C. Ó., Devine, D., Moran, K., O'Connor, N. E., & Murray, N. (2019, June). An evaluation of a 3D multimodal marker-less motion analysis system. In Proceedings of the 10th ACM Multimedia Systems Conference (pp. 213-221).
4. Rozumalski, A., Novacheck, T. F., Griffith, C. J., Walt, K., & Schwartz, M. H. (2015). Treadmill vs. overground running gait during childhood: A qualitative and quantitative analysis. Gait & posture, 41(2), 613-618.
5. Harada, N. D., Chiu, V., & Stewart, A. L. (1999). Mobility-related function in older adults: assessment with a 6-minute walk test. Archives of physical medicine and rehabilitation, 80(7), 837-841.

G. *Describe how you will protect the privacy of study participants.*

Participants' privacy will be protected confidentially. They will be deidentified with ID numbers with all collected data. The copies of signed informed consent forms stored in Dr. Li's office will be the only documentation linking the participants' identities to their research ID numbers. All research-specific data will be stored in password-protected computers within lock-protected offices. Only Hui Tang, Benjamin Paquette, Petra Kis, and Dr. Li Li have access to these data.

4) Data Analysis

A. *Briefly describe how you will analyze and report the collected data.*

The video streaming from Thia system (Theia markerless, Inc., Kingston Ontario, Canada) will be used for pre-processing. The Nexus system will be used to pre-process the marker position. Then, Visual 3D will be utilized to calculate biomechanical parameters, such as joint angle, moment, and power of the lower limb.

We will assess the concurrent validity of the biomechanical features from a markerless and marker-based (gold standard) motion capture system for 90 strides (30 strides for each speed). Mean RMSD will be calculated for the time-normalized for each outcome variable at each speed. For the time series analysis, the relative difference will be calculated as the coefficient of variation of RMSD relative to the mean of the gold standard. Intraclass correlation coefficients (ICC2,1) and Bland–Altman plot metrics (markerless system measurement bias, 95% limits of agreement) will be computed to examine consistency and agreement between outcomes. Additionally, we will evaluate the validity of the biomechanical features from the markerless system and gold standard at different time epochs. Here, mean RMSD will be calculated for the time-normalized for each outcome variable at each speed at three different epochs (first, middle, and last five strides). The rest analysis method is the same as the aforementioned.

B. *What will you do with the results of your study (e.g. contributing to generalizable knowledge, publishing sharing at a conference, etc.)?*

The results of this project will be disseminated through professional conferences and peer-reviewed journals.

C. *Include an explanation of how will the data be maintained after the study is complete. Specify where and how it will be stored (room number, password-protected file, etc.)*

The data will be stored in Dr. Li's password-protected office computer. The office is located in Room 1070C, Water College of Health Professions, Hollis Building, Georgia Southern University.

D. *If this research is externally funded (funded by non-Georgia Southern funds), student researchers must specify which faculty or staff member will be responsible for records after you have left the university. The person listed below must be included in the personnel section of this application.*

Responsible Party:

☒ **N/A**

E. *Anticipated destruction date or method used to render data anonymous for future use. Please make sure this in consistent with your informed consent.*

☐ Destroyed 3 Years after conclusion of research (minimum required for all PIs)

☐ Other timeframe (min 3 years):

☒ Maintained for future use in a deidentified fashion. Method used to render it anonymous for future use:

Note: Your data may be subject to other retention regulations (i.e. American Psychology Association, etc.)

Special Conditions

5) Risk

Even minor discomfort in answering questions on a survey may pose some risk to subjects. Carefully consider how the subjects will react and address ANY potential risks.

A. *Is there greater than minimal risk from physical, mental, or social discomfort?*

☐ No

If no, Do not simply state that no risk exists. If risk is no greater than risk associated with daily life experiences, state risk in these terms.

☒ Yes

If yes, describe the risks and the steps taken to minimize them. Justify the risk undertaken by outlining any benefits that might result from the study, both on a participant and societal level.

In clinical settings, treadmill running is used to inform gait retraining strategies for performance enhancement, injury prevention, and rehabilitation. During rehabilitation, it is also used to commence running in a controlled environment (1). Therefore, the risk of running on a treadmill is even smaller than overground running. In addition, the eligible participants are recreationally active and should run for a long distance. Given the running duration in this project is only 2 and half minutes for each trial, the risks of possible fatigue and ankle sprain can hardly be more significant than their daily life experiences.

1. Van Hooren, B., Fuller, J. T., Buckley, J. D., Miller, J. R., Sewell, K., Rao, G., ... & Willy, R. W. (2020). Is motorized treadmill running biomechanically comparable to overground running? A systematic review and meta-analysis of cross-over studies. Sports medicine, 50(4), 785-813.

B. Will you be carrying out procedures or asking questions that might disturb your subjects emotionally or produce stress or anxiety? If yes, describe your plans for providing appropriate resources for subjects.

No.

6) Research Involving Minors

A. Will minors be involved in your research?

☐ Yes ☒ No

B. If yes, describe how the details of your study will be communicated to parents/guardians. Please provide both parental consent letters and child assent letters (or processes for children too young to read).

C. Will the research take part in a school (elementary, middle, or high school)?

☐ Yes ☒ No

D. If yes, describe how permission will be obtained from school officials/teachers, and indicate whether the study will be a part of the normal curriculum/school process.

☐ Part of the normal curriculum/school process

☒ Not part of the normal curriculum/school process

7) Deception

A. Will you use deception in your research?

☒ No Deception

☐ Passive Deception

☐ Active Deception

B. If yes, describe the deception and how the subject will be debriefed. Include a copy of any debriefing materials. Make sure the debriefing process is listed in your timeline in the Procedures section.

C. Address the rationale for using deception.

Be sure to review the deception disclaimer language required in the informed consent. Note: All research in which active deception will be used is required to be reviewed by the full Institutional Review Board. Passive deception may receive expedited review.

8) Medical Procedures

A. Does your research procedures involve any of the following procedures:

☒ Low expenditures of physical effort unlikely to lead to physical injury

☐High expenditures of physical effort that could lead to physical injury

☐ Ingesting, injecting, or absorbing any substances into the body or through the skin

☐ Inserting any objects into bodies through orifices or otherwise

☐ Handling of blood or other bodily fluids

☐Other Medical Procedures

☒ No Medical Procedures Involved

B. Describe your procedures, including safeguards. If appropriate, briefly describe the necessity for employing a medical procedure in this study. Be sure to review the medical disclaimer language required in the informed consent.

To avoid minimal potential running injuries, sufficient warm-up and after-running relaxation exercises guided by researchers are applied. To discourage the onset of fatigue and discomforts caused by running, participants are allowed to take sufficient rest between different running speeds.

C.	*Describe a medical emergency plan if the research involves any physical risk beyond the most minimal kind. The medical research plan should include, but not necessarily be limited to: emergency equipment appropriate for the risks involved, first rescuer actions to address the most likely physical risk of the protocol, further actions necessary for the likely risks.*
	If any physical risk beyond the most minimal kind happened, experimenters will contact Georgia Southern Health Service at 912-478-5641 immediately and allow the professional health providers to handle the injuries.

Reminder: No research can be undertaken until your proposal has been approved by the IRB.

CERTIFICATION OF INVESTIGATOR RESPONSIBILITIES

By signing the cover page, I agree/certify that:

1. I have reviewed this protocol submission in its entirety and I state that I am fully cognizant of, and in agreement with, all submitted statements and that all statements are truthful.
2. This application, if funded by an extramural source, accurately reflects all procedures involving human participants described in the proposal to the funding agency previously noted.
3. I will conduct this research study in strict accordance with all submitted statements except where a change may be necessary to eliminate an apparent immediate hazard to a given research subject.
   a. I will notify the IRB promptly of any change in the research procedures necessitated in the interest of the safety of a given research subject.
   b. I will request and obtain IRB approval of any proposed modification to the research protocol or informed consent document(s) prior to implementing such modifications.
4. I will ensure that all co-investigators, and other personnel assisting in the conduct of this research study have been provided a copy of the entire current version of the research protocol and are fully informed of the current (a) study procedures (including procedure modifications); (b) informed consent requirements and process; (c) anonymity and/or confidentiality assurances promised when securing informed consent (d) potential risks associated with the study participation and the steps to be taken to prevent or minimize these potential risks; (e) adverse event reporting requirements; (f) data and record-keeping requirements; and (g) the current IRB approval status of the research study.
5. I will not enroll any individual into this research study: (a) until such time that the conduct of the study has been approved in writing by the IRB; (b) during any period wherein IRB renewal approval of this research study has lapsed; (c) during any period wherein IRB approval of the research study or research study enrollment has been suspended, or wherein the sponsor has suspended research study enrollment; or (d) following termination of IRB approval of the research study or following sponsor/principal investigator termination of research study enrollment.
6. I will respond promptly to all requests for information or materials solicited by the IRB or IRB Office.
7. I will submit the research study in a timely manner for IRB renewal approval.
8. I will not enroll any individual into this research study until such time that I obtain his/her written informed consent, or, if applicable, the written informed consent of his/her authorized representative (i.e., unless the IRB has granted a waiver of the requirement to obtain written informed consent).
9. I will employ and oversee an informed consent process that ensures that potential research subjects understand fully the purpose of the research study, the nature of the research procedures they are being asked to undergo, the potential risks of these research procedures, and their rights as a research study volunteer.
10. I will ensure that research subjects are kept fully informed of any new information that may affect their willingness to continue to participate in the research study.
11. I will maintain adequate, current, and accurate records of research data, outcomes, and adverse events to permit an ongoing assessment of the risks/benefit ratio of research study participation.
12. I am cognizant of, and will comply with, current federal regulations and IRB requirements governing human subject research including adverse event reporting requirements.
13. I will notify the IRB within 24 hours regarding any unexpected study results or adverse events that injure or cause harm to human participants.
14. I will make a reasonable effort to ensure that subjects who have suffered an adverse event associated with research participation receive adequate care to correct or alleviate the consequences of the adverse event to the extent possible.
15. I will notify the IRB prior to any change made to this protocol or consent form (if applicable).
16. I will notify the IRB office within 30 days of a change in the PI or the closure of the study.

***Faculty signature on the first page indicates that he/she has reviewed the application and attests to its completeness and accuracy**

APPENDIX

1. CITI HUMAN SUBJECTS TRAINING
2. INFORMED CONSENT
3. INSTRUMENT 1: PAR-Q SURVEY
4. INSTRUMENT 2: EIM-HEALTH-HISTORY QUESTIONNAIRE
5. RECRUITMENT FLYER
6. RECRUITMENT EMAIL SAMPLE

CITI PROGRAM

Completion Date 09-Aug-2021
Expiration Date 08-Aug-2024
Record ID 44118951

This is to certify that:

Hui Tang

Has completed the following CITI Program course:

Not valid for renewal of certification through CME.

Human Subjects-Social & Behavioral Research - Basic/Refresher
(Curriculum Group)
Human Subjects-Social & Behavioral Research - Basic/Refresher
(Course Learner Group)
1 - Basic Course
(Stage)

Under requirements set by:

Georgia Southern University

CITI
Collaborative Institutional Training Initiative

Verify at www.citiprogram.org/verify/?w26210e2d-3575-413e-bfd0-2645f08e28f1-44118951

CITI PROGRAM

Completion Date 09-Nov-2021
Expiration Date 08-Nov-2024
Record ID 45971559

This is to certify that:

Hui Tang

Has completed the following CITI Program course:

Not valid for renewal of certification through CME.

GCP for Clinical Investigations of Devices
(Curriculum Group)
GCP for Clinical Investigations of Devices
(Course Learner Group)
1 - GCP
(Stage)

Under requirements set by:

Georgia Southern University

CITI
Collaborative Institutional Training Initiative

Verify at www.citiprogram.org/verify/?we583778d-29ef-48f3-b577-8adf7fd95d3d-45971559

CITI PROGRAM

Completion Date 12-Aug-2021
Expiration Date 11-Aug-2024
Record ID 44170709

This is to certify that:

Benjamin Paquette

Has completed the following CITI Program course:

Not valid for renewal of certification through CME.

Human Subjects-Social & Behavioral Research - Basic/Refresher
(Curriculum Group)
Human Subjects-Social & Behavioral Research - Basic/Refresher
(Course Learner Group)
1 - Basic Course
(Stage)

Under requirements set by:

Georgia Southern University

CITI
Collaborative Institutional Training Initiative

Verify at www.citiprogram.org/verify/?w956d2e8a-d17b-474a-a259-fcb67d6e4f4c-44170709

CITI PROGRAM

Completion Date 12-Aug-2021
Expiration Date 11-Aug-2024
Record ID 44190400

This is to certify that:

Petra Kis

Has completed the following CITI Program course:

Not valid for renewal of certification through CME.

Human Subjects-Social & Behavioral Research - Basic/Refresher
(Curriculum Group)
Human Subjects-Social & Behavioral Research - Basic/Refresher
(Course Learner Group)
1 - Basic Course
(Stage)

Under requirements set by:

Georgia Southern University

CITI
Collaborative Institutional Training Initiative

Verify at www.citiprogram.org/verify/?wafd14f3b-0769-4e6e-9e0e-691cc893f29f-44190400

Completion Date 16-Aug-2019
Expiration Date 15-Aug-2022
Record ID 31431761

This is to certify that:

Li Li

Has completed the following CITI Program course:

IRB Members - Basic/Refresher	(Curriculum Group)
IRB Members - Basic/Refresher	(Course Learner Group)
3 - Refresher Course	(Stage)

Under requirements set by:

Georgia Southern University

Collaborative Institutional Training Initiative

Verify at www.citiprogram.org/verify/?w3fbe178b-3cc9-4b75-a00e-bc3bcf03aea2-31431761

WATERS COLLEGE OF HEALTH PROFESSIONS

DEPARTMENT OF HEALTH SCIENCES AND KINESIOLOGY

Informed Consent

Concurrent Assessment of Gait Biomechanics Using Markerless and Marker-based Motion Capture Systems

You are being invited to participate in the study of the **Concurrent Assessment of Gait Biomechanics Using Markerless and Marker-based Motion Capture Systems**. The primary investigator is Hui Tang who is currently a Master's student at Georgia Southern University. The purpose of this research is to validate a markerless motion capture system for measuring biomechanical features during treadmill running at three different speeds.

To participate, you must be between the ages of 18-30, have regular physical activity habits, and meet all of the following criteria: be healthy (answered "No" to all the PAR-Q questions, and did not check any boxes in the Present/Past History section of the Health History Questionnaire), and be "recreationally active" (answered "Yes" to the first two questions of the Activity History section of the Health History Questionnaire). You wear athletic outfits and your preferred athletic, non-high top shoes during testing. After reporting to the Kinesiology laboratory, we take your forehead temperature and screen your COVID symptoms. After signing the consent document (if you failed to sign it electronically) , the data collection is in the Biomechanical Lab 2.

We test your gait kinematics and kinetics under slow, intermediate, and fast running on the force-plate embedded treadmill using both markerless and marker-based motion capture systems. Your eligibility will be confirmed by completing PAR-Q and health history questionnaires via email. Once confirmed, you will visit the Biomechanical lab at a pre-scheduled appointment time. The visit starts with familiazing the lab environment, followed by a three-trial testing protocol. The protocol has three running trials that require slow (5 miles/hour), intermediate (6.5 miles/ hour), and fast (8 miles/hour) speeds, respectively. Each running trial will be recorded by both markerless and marker-based motion capture systems simultaneously. To obtain sufficient and steady speed gait cycles for further analysis, the running duration for each speed is 2 minutes. The duration of the scheduled lab visit is 60 minutes at most, including 1) 25 minutes of marker-based motion capture preparation, 2) 10 minutes pre-running warm-up exercises and familiarization; 3) 15 minutes of motion capture testing, 4) 10 minutes post-running relaxation.

In preparation for marker-based motion capture testing, we place a set of retroreflective markers and tracking clusters on your skin. We may ask you to change to the lab-provided tight clothing and running shoes for quality control. All provided tights and shoes are thoroughly washed using laundry detergent and sanitizer and dried with scent booster to ensure the tidy and odor-free before applying to each participant.

You follow the researcher's guidance to perform 10 minutes of pre-running warm-up exercises. You familiarize yourself with running on the instrumented treadmill. You then stand still on the instrumented treadmill with arms crossed over for 2 seconds for marker-based motion capture calibration. After the static standing, two investigators will help you accomplish the running protocol. With the verbal instruction, "Capture started", one investigator will help you to adjust the speed to 5 miles/h. Meanwhile, you will transition from walking to running. You keep running for 2 minutes for the otherinvestigator to record the data. Then, one investigator will inform you to slow down and start to adjust the treadmill speed for you. You will stop and step out of the treadmill after hearing "Capture Ended". You rest for 5 minutes before you initiate the second running trial. The process is identical to the previous one except for the running speed set as 6.5 miles/hour. Before proceeding to the fast running speed, you may rest sufficiently. The fast speed running trial is the same as the previous ones except for the speed set as 8 miles/hour. Upon completing all running trials, you follow the researcher's guidance to do post-running stretching and relaxation.

The risk of this study includes the possible COVID-19 transmission. However, precautions will be taken with current Georgia Southern policies to reduce the spread, including encouraging experimenters and participants wearing masks (except for performing running protocols), and having fully vaccinated experimenters. In addition, the risk of the experimental protocol is no greater than risks associated with daily life experiences. Running on the force-plate embedded treadmill in clinical settings is safer than overground running. Before being tested for different running speeds, researchers will guide warm-up exercises to minimize the potential running-related discomforts and muscle injuries. To reduce the possible discomforts caused by running, you will perform the post-running relaxation exercise guided by researchers. Your request to stop the procedure will be honored during the test if you feel uncomfortable. You understand that medical care is available in the unlikely event of injury resulting from research. We would contact Georgia Southern University Health Service at 912-478-5641 immediately if any injury were to happen.

You understand that although there is no direct benefit for you to participate in this study, however, the project results can help the community and enhance scientific understanding of the motion capture technology. Additionally, more people will benefit from the convenience of the markerless system if it is proven to be as good as the marker system.

You understand that all personal information and data are only open to the principal and co-investigator. Your privacy is protected confidentially. Your name is deidentified with ID numbers with all collected data. All research-specific data are stored in password-protected computers within lock-protected offices located in Room 1070C, Hollis Building, Georgia Southern University (Dr. Li's office).

You have the right to ask questions and have those questions answered. If you have questions about this study, please get in touch with the researchers named above, whose contact information is located at the end of this document. For questions concerning your rights as a research participant, contact Georgia Southern University Institutional Review Board at 912-478-5465.

Please understand that your participation is voluntary. You may discontinue your participation at any time. Additionally, the researchers reserve the right to terminate your participation in the study without your consent.

If you consent to participate in this research study and the terms above, please sign your name and indicate the date below.

You will be given a copy of this consent form to keep for your records. This project has been reviewed and approved by the GS Institutional Review Board under tracking number H _22372_.

Title of Project: Concurrent Assessment of Gait Biomechanics Using Markerless and Marker-based Motion Capture Systems

Principal Investigator:

Hui Tang, M.S. Student

Email: ht01253@georgiasouthern.edu

Ph: 912-582-1607

Co-Investigator:

Benjamin Paquette, M.S. Student

Email: bp11854@georgiasouthern.edu

Petra Kis, M.S. Student

Email: pk03815@georgiasouthern.edu

Li Li, PhD.

Email: lili@georgiasouthern.edu

Ph: 912-478-0200

If you consent to participate in this research study and to the terms above, please sign your name and indicate the date below:

____________________________________ ____________________

Participant Signature Date

Health History Questionnaire

Exercise is Medicine | AMERICAN COLLEGE of SPORTS MEDICINE

Name: ______________________________ Date of birth: ____________ Date: ____________

Address: ____

City: ______________________________ State: __________________ Zip: _____________

Phone (Cell): _____________ (Work): ________________ Email address:

In case of emergency, whom may we contact?

Name: ____ Relationship: ___________________________________

(Home): ______________________________________

~~Phone (Cell):~~ ____

Health Care Provider: ____

Name: ______________________________ Phone: _________________ Fax:

Present/Past History

Have you had, or do you presently have any of the following? (Check if yes.)

- ☐ Heart attack
- ☐ Any kind of heart disease or heart surgery
- ☐ Diabetes
- ☐ Prediabetes
- ☐ High blood pressure
- ☐ Low blood pressure ☐ Kidney disease
- ☐ High Cholesterol
- ☐ Lung disease
- ☐ Seizures
- ☐ Cancer
- ☐ Rheumatic fever
- ☐ Recent operation
- ☐ Other (please describe):

□ Fainting or dizziness

□ Chest pains

□ Palpitations or tachycardia (unusually strong or rapid heartbeat)

□ Known heart murmur

□ Muscle or joint problems (e.g., back, knee)

□ Edema (swelling of ankles)

□ Pain, discomfort in the chest, neck, jaw, arms, or other areas

□ Unusual fatigue or shortness of breath at rest or with light activity

□ Temporary loss of clear vision or speech or short-term numbness or weakness in one side, arm, or leg of your body

□ Shortness of breath while lying down, at night or that comes on suddenly

□ Intermittent claudication (calf cramping)

Family History

Have any of your first-degree relatives (parent, sibling, or child) experienced the following conditions? (Check if yes.) In addition, please identify at what age the condition occurred.

□ Heart attack

□ Heart surgery

□ Congenital heart disease

□ Diabetes

□ High blood pressure

□ Other major illness:

□ High cholesterol Explain checked items:

Activity History

1. Why have you decided to seek exercise guidance at this time? (Please be specific.)
2. Were you referred to this program? □ Yes By whom:
3. Have you ever worked with a personal trainer before? □ Yes □ No
4. Date of your last physical examination performed by a physician:
5. Do you participate in a regular exercise program currently? □ Yes □ No If yes, briefly describe:
6. Can you currently walk 2 miles briskly without fatigue? □ Yes □ No
7. Have you ever performed strength training exercises in the past? □ Yes □ No
8. Do you have injuries (bone/muscle disabilities) that may interfere with exercising? □ Yes □ No If yes, briefly describe:
9. Do you smoke? □ Yes □ No

If yes, how much per day and what was your age when you started?

10. What is your body weight now? What was it one year ago? At age 21?
11. How tall are you?
12. Do you follow, or have you recently followed any specific dietary intake plan and, in general, how do you feel about your nutritional habits?
13. List the medications you are presently taking.
14. What are your personal health or fitness goals?

Georgia Southern University

Physical Activity Readiness Questionnaire (PAR-Q)

Please check “Yes” or “No” for each of the following questions

1. Has your doctor ever said that you have a heart condition and that you should only do physical activity recommended by a doctor?
A. Yes; B. No.

2. Do you feel pain in your chest when you do physical activity?
A. Yes; B. No.

3. In the past month, have you had chest pain when you were not doing physical activity?
A. Yes; B. No.

4. Do you lose your balance because of dizziness or do you ever lose consciousness?
A. Yes; B. No.

5. Do you have a bone or joint problem that could be made worse by a change in your physical activity?
A. Yes; B. No.

6. Is your doctor currently prescribing drugs (for example, water pills) for your blood pressure or heart condition?
A. Yes; B. No.

7. Do you know of any other reason why you should not do physical activity?
A. Yes; B. No.

RECRUITMENT EMAIL SAMPLE:

Ask for professors' permission to recruit participants in class:

Dear Dr. XXX,

I am Hui Tang, a graduate student from the Department of Health Sciences & Kinesiology. I am writing to ask for permission to recruit potential participants for my project supervised by Dr. Li Li from your class during class time.

The project "*Concurrent Assessment of Gait Biomechanics Using Markerless and Marker-based Motion Capture Systems* " aims to validate a markerless motion capture system for measuring biomechanical features during treadmill running at three different speeds. The project needs a maximal amount of 40 healthy, recreationally active young adults aged from 18 to 30 years old. This project involves three running trials that require different speeds (slow, intermediate, and fast). Students who take kinesiology courses may be familiar with those procedures and be eligible for participation. Therefore, I hope I can recruit some students in your class.

I would be grateful if you could allow me to use 5 to 10 minutes of your class time to send out recruitment flyers and deliver a brief introduction of the project. Please let me know if you have any other concerns.

I am looking forward to hearing from you soon.

Regards,

Hui Tang

Graduate Assistant,

Department of Health Sciences and Kinesiology,

Georgia Southern University

Reply for potential participants:

Dear XXXX,

Thank you for reaching out and being interested in our project.

Before officially participating in our project, we need you to complete two surveys, namely PAR-Q and EIM-Health History Questionnaire. The primary purpose of completing these two surveys is to screen for evidence of risk factors during participation. Upon completion, we will inform you within 3 days about your eligibility. If you are eligible, we will schedule the testing date for your lab visit.

Please let me know if you have any concerns or questions, and I would be more than happy to answer.

Best,

Hui Tang,

Graduate Assistant,

Department of Health Sciences and Kinesiology,

Georgia Southern University

Waters College of Health Professions
Department of Health Sciences & Kinesiology

Volunteers Needed for Research Study on Gait Biomechanics.

We would like to have you in our project, *Concurrent Assessment of Gait Biomechanics Using Markerless and Marker-based Motion Capture Systems*

This project seeks to investigate the discrepancy between markerless system (Thia) and marker-based motion capture system (Vicon) in gait kinematics and kinetics under different running speeds in the recreationally active healthy population.

You May Qualify If You

- Are aged between 18 and 30
- Have physical activity habits
- Do not have recent knee or ankle injuries
- Do not have cardiovascular diseases

Location

Biomechanical Lab, Hanner Fieldhouse, 590 Herty Dr, Statesboro, GA, 30458.

Participation Involves

- One testing visit to Biomechanics Lab
- Running at three different speeds for the lab visit
- The lab visit will last for 60 minutes

FOR MORE INFORMATION

Please contact Hui Tang at 912-582-1607, email ht01253@georgiasouthern.edu